1191

TRANSPORTATION RESEARCH RECORD

Culverts and Tiebacks

TRANSPORTATION RESEARCH BOARD
NATIONAL RESEARCH COUNCIL
WASHINGTON, D.C. 1988

Transportation Research Record 1191
Price: $25.00
Editor: Alison Tobias

modes
1 highway transportation
3 rail transportation

subject areas
25 structures design and performance
62 soil foundations
63 soil and rock mechanics

Transportation Research Board publications are available by ordering directly from TRB. They may also be obtained on a regular basis through organizational or individual affiliation with TRB; affiliates or library subscribers are eligible for substantial discounts. For further information, write to the Transportation Research Board, National Research Council, 2101 Constitution Avenue, N.W., Washington, D.C. 20418.

Printed in the United States of America

Library of Congress Cataloging-in-Publication Data
National Research Council. Transportation Research Board.

Culverts and tiebacks.
p. cm.—(Transportation research record, ISSN 0361-1981 ; 1191)
ISBN 0-309-04802-8
1. Culverts. 2. Retaining walls. I. National Research Council (U.S.). Transportation Research Board. II. Series.
TE7.H5 no. 1191
[TE213] 89-38439
CIP

Sponsorship of Transportation Research Record 1191

GROUP 2—DESIGN AND CONSTRUCTION OF TRANSPORTATION FACILITIES
Chairman: David S. Gedney, Harland Bartholomew & Associates

Structures Section
Chairman: John M. Hanson, Wiss Janney, Elstner & Associates, Inc.

Committee on Culverts and Hydraulic Structures
Chairman: L. R. Lawrence, Federal Highway Administration
Gordon A. Alison, James D. Arnoult, A. E. Bacher, Kenneth J. Boedecker, Jr., Thomas K. Breitfuss, Dennis L. Bunke, Bernard E. Butler, James E. Cowgill, William D. Drake, J. M. Duncan, Sam S. Gillespie, James B. Goddard, Frank J. Heger, James J. Hill, Carl M. Hirsch, Iraj I. Kaspar, Michael G. Katona, A. P. Moser, Russell B. Preuit, Jr., Norman H. Rognlie, Harold R. Sandberg, R. S. Standley, Robert P. Walker, Jr.

Soil Mechanics Section
Chairman: Raymond A. Forsyth, California Department of Transportation

Committee on Subsurface Soil-Structure Interaction
Chairman: Michael G. Katona, TRW Ballistic Missiles Division
George Abdel-Sayed, Baidar Bakht, Sangchul Bang, Timothy J. Beach, Mike Bealey, C. S. Desai, J. M. Duncan, Lester H. Gabriel, John Owen Hurd, J. Neil Kay, Raymond J. Krizek, Richard W. Lautensleger, L. R. Lawrence, G. A. Leonards, Donald Ray McNeal, Michael C. McVay, A. P. Moser, Samuel C. Musser, Thomas D. O'Rourke, Raymond B. Seed, Ernest T. Selig, H. J. Siriwardane, Mehdi S. Zarghamee

G. P. Jayaprakash and George W. Ring III, Transportation Research Board staff

Sponsorship is indicated by a footnote at the end of each paper. The organizational units, officers, and members are as of December 31, 1987.

TRANSPORTATION RESEARCH BOARD
National Research Council

ERRATA
TRB Publications
(through May 1990)

Transportation Research Record 1191

page 130

Figure 14 was printed incorrectly. The correct Figure 14 is given below.

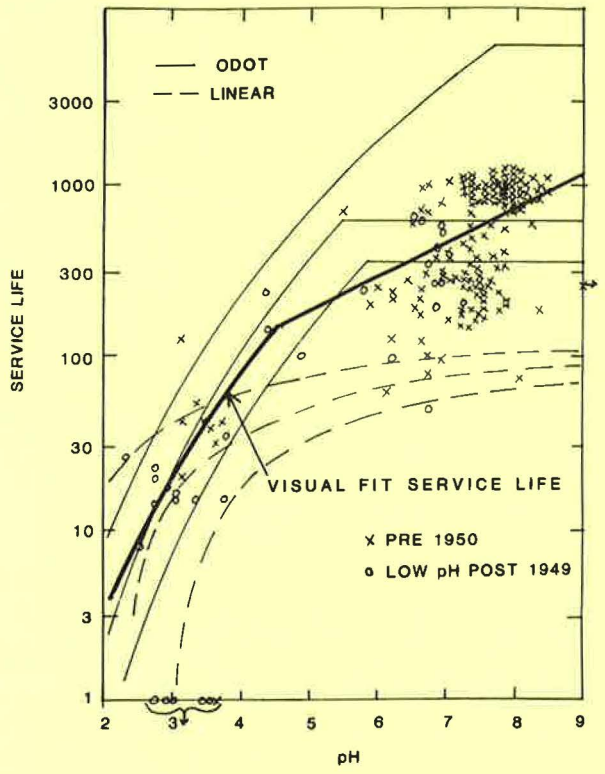

FIGURE 14 Linear projected visual fit service life for inspected culverts.

page 131

Figure 15 was printed incorrectly. The correct Figure 15 is given below.

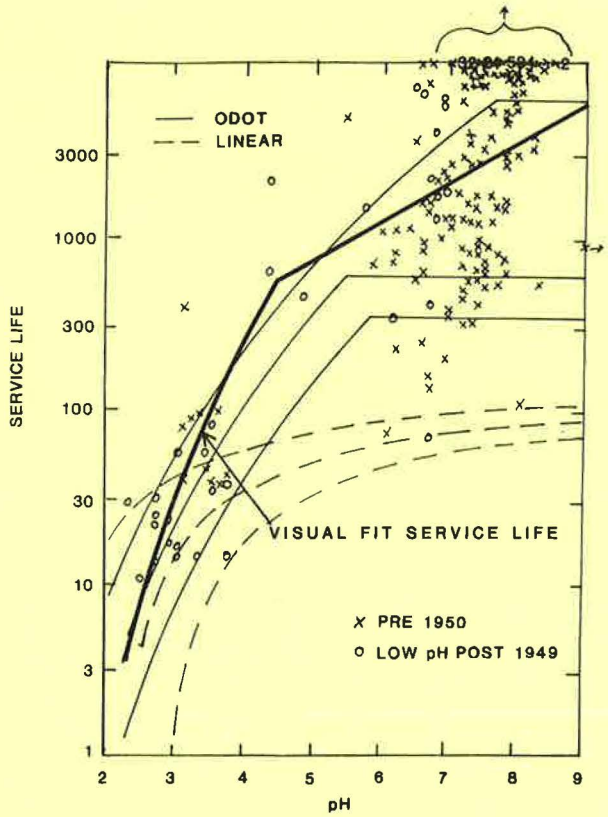

FIGURE 15 Log-linear projected visual fit service life for inspected culverts.

Transportation Research Record 1210

page 12

Change item (c) in the abstract to "(c) the overwhelming majority of children involved in accidents were unaccompanied. . . ."

Transportation Research Record 1215

page 80

Replace Figure 5 with the following:

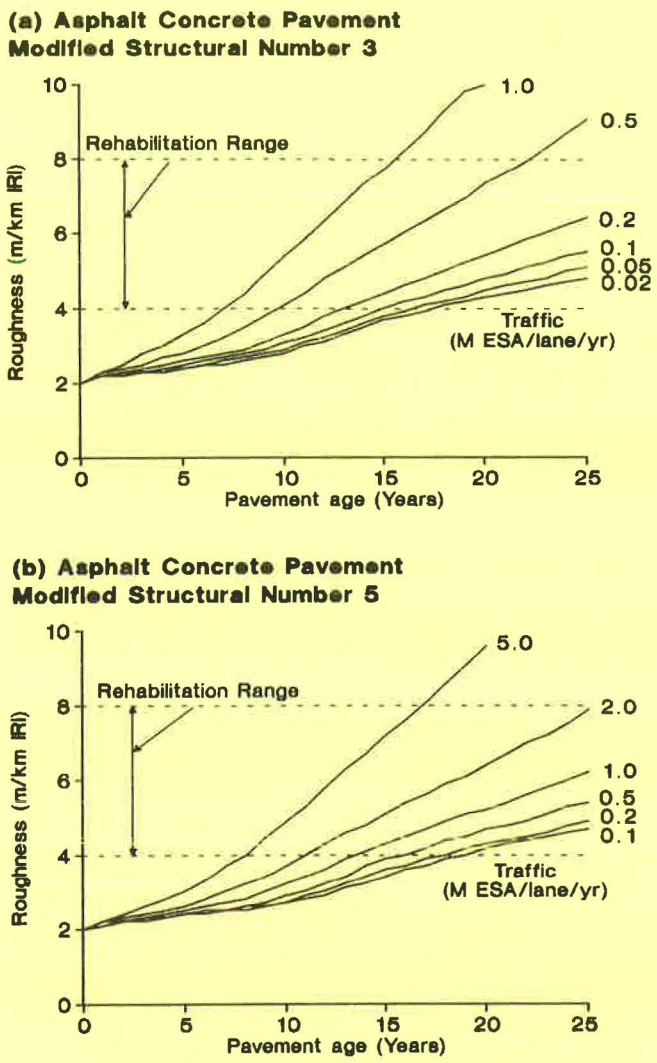

Note: Maintenance comprised patching of all potholes in the year in which they appeared.
Source: Equation (3) applied through Road Deterioration and Maintenance Submodel of HDM-III.

FIGURE 5 Roughness progression prediction curves for a maintenance policy of patching all potholes.

Transportation Research Record 1231

See the attachment to these errata.

Transportation Research Circular 352

Pages 5 and 6 are reversed.

NCHRP Report 311

page 17, second complete paragraph, last sentence

Insert "below" after "15 dB."

page 20

Figure 8(a) shows only one road (interrupted flow); Figure 8(b) shows two roads (interrupted plus cruise).

page 25

Figure 18(a) is for two roads (both interrupted); Figure 18(b) is for four roads (two interrupted, two cruise).

page 32, Table 7

Table is incorrect; substitute values from Table C–5 on page 88 for those published in Table 7.

In the second footnote, add "(or the end of the queue for unsignalized intersections)" after "point of stop."

page 87, Table C-4

Add "Multiplier" after "AZOI" in the heading of the third column.

page 88, Table C-5

In the second footnote, add "(or the end of the queue for unsignalized intersections)" after "point of stop."

page 88, Table C-6

Change the MT speed for ZOI(2) for the 0 to 55 mph case (sixth row, ninth column) from 40 to 49.

NCHRP Report 325

pages 52 and 53

Tables are reversed (table headings are correct). Material noted under Table 25.3.1A heading (page 52) for *natural rubber* should be Table 25.3.1B (*neoprene*), and material provided under Table 25.3.1B heading (page 53) should be Table 25.3.1A.

Attachment

Transportation Research Record 1231

The third discussion of the paper by Potter and Ulery was omitted. The discussion appears below.

DISCUSSION

JOHN O. HURD

Ohio Department of Transportation, 25 South Front St., Columbus, Ohio 43215.

I commend the author for providing heretofore unpublished information on the structural performance of corrugated steel pipe and reinforced concrete pipe subjected to large vehicle live loads. However, additional elaboration on the structural performance and failure modes of corrugated steel pipe and reinforced concrete pipe is required for the reader to fully benefit from the information provided. The elaboration is given here.

The author cites only deflection as a failure mode for corrugated steel pipe. Because it was not clearly indicated, the reader must assume that the measured deflections were due to elliptical deformation, as in accepted deflection theory (*1*). This failure mode methodology would not be applicable if deformation were not elliptical. Deflection is actually but one of four failure modes that must be checked (*2,3*). The others are wall crushing, buckling, and seam failure.

For thin-walled, small-diameter pipes with well-compacted select side fill, seam strength is of much greater concern than deflection (*4*). Because no measurements of strains or stresses in the wall around the seams were reported, the reader cannot know what factor of safety existed for seam failure. The reader cannot assume that the large factor of safety against failure implied by the measured deflections is the factor of safety against failure in some other failure mode that might be governing.

If seam failure was not imminent, it appears that the test installation covers are reasonable minimums for properly installed corrugated steel pipe for the loading condition. This assumes that the reported roadway surface condition measured above the pipe is acceptable to the users of the facility.

The author cites cracking as the accepted criterion for failure of reinforced concrete pipe. This criterion is only for testing—not performance. In reinforced concrete structure design it is not intended that the concrete carry tension loads. This is the requirement of the reinforcing steel (*5*). In the case of reinforced concrete pipe, failure might occur when the reinforcing steel can no longer withstand the tensile stresses created by bending moments in the pipe wall. A hairline crack in the pipe wall indicates that the tensile stresses have surpassed the tensile strength of the concrete and that the steel is carrying all of the tensile load. The rather wide 0.01-in. crack used to define reinforced concrete pipe strength in the three-edge bearing test occurs at much less than the ultimate load-carrying capacity of the pipe in both the test and in service. The Ohio Department of Transportation requires that the ultimate strength of Class IV reinforced concrete pipe in the test be at least 1.5 times the load that produces the 0.01-in. crack (*6*). Cracks much larger than 0.01 in. can occur before a reinforced concrete structure is judged to have failed (*7*).

In the paper, it was reported that a "barely visible" crack was observed in the 18-in. concrete pipe and that "hairline" cracks were observed in the 24-in. concrete pipe. However, it does not appear that the actual widths of the cracks were measured or estimated or that measurements of reinforcing steel strains were taken. No attempt was made to correlate the loads at crack inception, and subsequently larger cracks, with the ultimate load-carrying capacity of the pipe during laboratory tests. Therefore, the reader cannot know how close the field-tested reinforced concrete pipes were to actual "failure." Based on the description of cracks given in the report, it appears that the pipes were loaded to less than one-half the load to cause failure.

Placing pipes on a flat bedding, as done in this study, is not recommended for either corrugated steel pipe or reinforced concrete pipe (*8,9*). However, because of the bending moment induced failure mode of reinforced concrete pipe, the use of this type of bedding has a more severe effect on the structural performance of that material. The concrete pipe design bedding factor for a flat bedding is 1.1, whereas that for the recommended shaped bedding is 1.9. The use of a flat bedding reduces the load-carrying capacity of the concrete pipe to 58 percent of that of a properly bedded pipe.

Based on these observations, I can see no justification for the minimum cover for properly installed reinforced concrete pipe to be increased (as recommended by Table 5) to greater than the test installation covers for the loading condition.

Considering the installation methods, the reported condition of the roadway surface, and the pipes, both types of pipe material appear to have performed acceptably.

REFERENCES

1. M. G. Spangler. *Soil Engineering*. International Textbook Co., 1960.
2. Section 12—Soil Corrugated Metal Structure Interaction Systems. In *Standard Specifications for Highway Bridges*. AASHTO, Washington, D.C., 1983.
3. *Handbook of Steel Drainage and Highway Construction Products*. American Iron and Steel Institute, Washington, D.C., 1983.
4. D. G. Meacham, C. L. Foley, and E. U. Blackwell. *Structural Design Criteria for Corrugated Steel Culverts*. Ohio Department of Highways, Columbus, Ohio, 1971.
5. C. K. Wang and C. G. Salmon. *Reinforced Concrete Design*. Harper and Row, New York, N.Y., 1985.
6. *Construction and Material Specifications*. Ohio Department of Transportation, Columbus, Ohio, 1989.
7. T. J. Beach. Load Test Report and Evaluation of a Precast Concrete Arch Culvert. In *Transportation Research Record 1191*, TRB, National Research Council, Washington, D.C., 1988, pp. 12–21.
8. Section 23—Construction and Installation of Soil Metal Plate Structure Interaction Systems. In *Standard Specifications for Highway Bridges*. AASHTO, Washington, D.C., 1983.
9. *Concrete Pipe Handbook*. American Concrete Pipe Association, Vienna, Va., 1980.

Transportation Research Record 1191

Contents

Foreword

This Record is of interest to highway engineers, particularly those interested in drainage structures. Papers 1 through 17 included in this record are on laboratory and field testing of buried conduits, design of concrete drainage structures, and life-cycle costs of drainage structures. Paper 18 is on cast-in-drilled-hole piles, and the last two papers are on tieback retaining walls.

Rogers presents data on a full-scale experiment conducted to study the response of flexible pipes to surface loading. He found significant deviations from an elliptical deformation that is generally assumed in both theoretical and experimental work. Beach reports the results of a full-scale load test performed on a Con/Span culvert. He used CANDE, the finite element program, for the detailed analysis of the structure and found good correlation between the performance of the culvert and the results of the analysis. Seed and Raines present the results of finite element analyses of three full-scale field cases involving culvert failures under exceptional live loads. Katona provides fill height tables and graphs that give the maximum allowable burial depth of corrugated polyethylene pipes of standard sizes. Katona compares the design solutions determined using the CANDE program with the laboratory test data. Hurd and Sargand report on the findings of an evaluation study of 39 corrugated aluminum and 10 corrugated steel rib stiffened box culverts in Ohio, and Degler, Cowherd, and Hurd report on a study of 890 pipe-arch structures in Ohio. The objective of Degler's study was to determine the causes of the problems experienced by the pipe-arch structures. Moore, Selig, and Haggag describe the use of continuum theory to evaluate the buckling strength of buried flexible culverts and compare the results with those of existing codes.

Tadros, Belina, and Meyer present the state of the art in the design of reinforced concrete box culverts. They provide information on field measurements and the results of a survey on design practices. Frederick, Ardis, Tarhini, and Koo present an overview of an investigation conducted in Ohio to determine the structural behavior of ASTM *C*850 box culvert section under live loads. They give results of theoretical analyses, and field and model testing. Rowekamp, Hill, and Krauthammer give a summary of the results of a structural analysis of elliptical precast concrete arch structures and circular arches conducted in Minnesota. Bacher, Kirkland, and Seyed present data on evaluations of precast thin wall reinforced concrete arches constructed using the dimension ratio design concept. They conclude that substantial future savings are possible if significant reduction is made in the wall thickness of reinforced concrete arch semicircular arch design. McGrath, Tigue, and Heger present microcomputer versions of PIPECAR and BOXCAR, the computer programs for reinforced concrete pipe and box sections.

Potter and Schindler present data on life-cycle cost analyses of drainage structures for determining the relative economic rating of design alternatives. Wonsiewicz discusses the selection of discount rates and the inflation factor in using the life-cycle cost techniques. Hurd reports on an Ohio study conducted to verify two service life models for concrete pipe culverts. Kurdziel reviews the culvert condition rating systems used in durability studies conducted by various agencies. He proposes a new material durability rating system for both concrete and metal pipe. In the next paper, Kurdziel discusses the contents and operation of the American Pipe Association's Least Cost (Life Cycle) Analysis microcomputer program.

Shen, Bang, DeSalvatore, and Poran report on the results of a study of an instrumented model test pile conducted to investigate the behavior of cast-in-drilled-hole pile. Fragaszy, Ali, Denby, and Kilian present the findings of a study on the seismic response of permanent tieback walls. Carpenter reviews methods for analyzing the overall stability of tieback structures, and discusses the capabilities of STABL5 and PCSTABL5, which are limiting equilibrium slope stability programs.

Some Observations on Flexible Pipe Response to Load

C. D. F. ROGERS

The response of 160-mm-diameter shallow-buried unplasticized polyvinylchloride pipes to surface loading has been investigated in full-scale experiments in a reinforced box. Standard installation and loading conditions were adopted. Measurements of pipe-wall strain and pipe deformation were taken to determine the influence of the surrounding soil on the mode of pipe deformation. The shape of the pipes when deformed varied with the stiffness of the soil at each level within the trench. Pipe deformation in soils offering little support was roughly elliptical, whereas in stiffer soil configurations the deformation deviated markedly from elliptical. In addition, the deviation from an ellipse was far more pronounced under static loading, subsequent cyclic loading causing an additive component of elliptical deformation. Four deformation modes have been isolated and data from other researchers have been included to confirm the observations. A clear relationship between pipe-wall strain and vertical diametral strain was found, indicating that inference of deformation from strain gauge measurements is possible if care is used. The assumption of elliptical pipe deformation in both theoretical and experimental work on flexible pipes should be avoided and allowance for significant deviations from an ellipse should be made in predictions of deformation measurement.

Pipelines are currently used for transportation, communications, and the supply and removal of fluids on a vast scale. A large quantity of new pipeline is being installed and, perhaps more pertinently, a considerable amount of existing pipeline is being replaced annually, thus emphasizing the need to understand fully the behavior of such pipelines in use. This in turn provides the information required to successfully design and construct a suitable infrastructure for future generations.

The fundamental engineering requirement of a pipeline is that it should retain a suitable size, shape, direction, and degree of integrity for as long as it is in use. This requirement can be met by relatively rigid pipes that have inherent strength and require only a suitable bedding layer, or by relatively flexible pipes that deform under load and thereby derive support by composite action with the surrounding soil. The distinction between rigid and flexible pipes has become less important with the advent of pipes of intermediate flexibility and greater attention is being paid to the fill materials used to surround pipes. Pipeline design therefore requires an appreciation of the composite response of the pipe and soil, and various design methods of varying sophistication have been proposed to account for this.

Prediction of flexible pipe performance has presented a challenge ever since Spangler (*1*) presented his classic work on deformation prediction. In the development of his theory, Spangler assumed the deformed shape of a flexible pipe to be elliptical, based on observations of large-diameter corrugated steel culverts. This assumption has recurred in many subsequent theories of behavior, either explicitly or implicitly, and has resulted in vertical deformation, or vertical diametral strain (VDS), being the critical performance parameter to be measured in experimental work. A number of researchers have recorded a deviation from elliptical behavior under certain circumstances, notably Howard (*2*), who refers to rectangular deformation.

A program of full-scale experiments was conducted at the University of Nottingham on 160-mm-diameter shallow-buried unplasticized polyvinylchloride (uPVC) pipe under conditions simulative of building drainage. As part of this program, instigated and sponsored by the British Plastics Federation, a series of experiments was conducted in a reinforced box to determine the influence of the surrounding soil on the magnitude and mode of pipe deformation. In particular, measurements were taken of pipe-wall strain and the deformation profile of the pipe under load. The aim of this paper is to examine the cause of deviation of the deformed profiles from an ellipse, based on the findings of these experiments and confirmed by research data published in the literature.

The terminology shown in Figure 1 is used when discussing the experimental results. Diametral strain is defined as the change in the diametral measurement divided by the original diameter.

PREVIOUS OBSERVATIONS OF SHAPE OF DEFORMATION

Howard (*2*) reports the results of experiments in a 2-m cubic box in which unlined steel pipes of various diameter and wall thickness were buried in clay at different densities and were subject to uniform surface pressures. Elliptical deformation, characterized by plastic hinges developing at 90 and 270 degrees (the pipe springings), tended to occur in the stiffer pipes, whereas more flexible pipes deformed rectangularly with plastic hinges developing at 45, 135, 225, and 315 degrees. The ratio of horizontal to VDS (diametral strain ratio) for elliptical pipe deformation was in the range 0.8 to 0.9 (a perfect ellipse would give 0.91) and for rectangular deflection was between 0.6 and 0.8. The deflected form was predicted from strain gauge readings, which showed high compressive strains on the internal surface at the critical points.

Loughborough University of Technology, Loughborough, Leicestershire LE11 3TU, England.

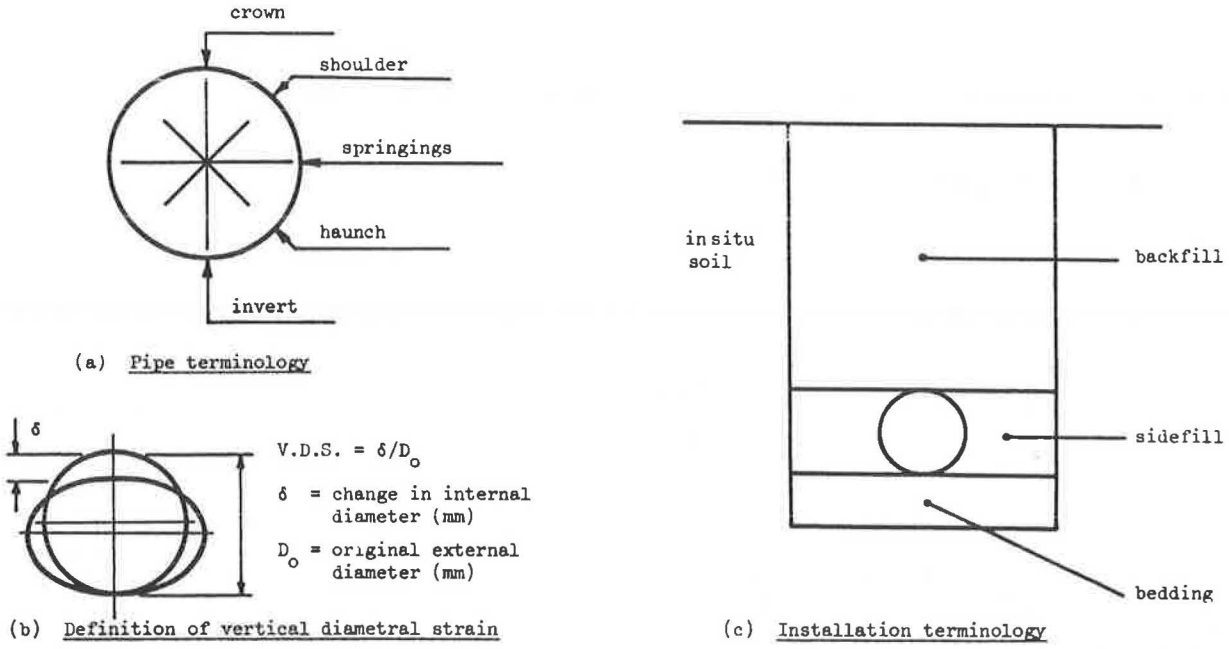

FIGURE 1 Terminology and definitions.

This series of tests was extended to include plastic pipes and is reported by Howard (*3*). For uPVC pipe, the diametral strain ratio implied a departure from purely elliptical deformation at an early stage of the test. This was verified by the internal pipe-wall strain profiles, from which Howard describes the deformation as semielliptical.

In a later paper, Howard (*4*) reiterates the variation in deformed shape and associates rectangular deformation with large ratios of soil to pipe stiffness. When pipes have deformed rectangularly, the horizontal diametral strain is found to be much less than the VDS. Howard considers that elliptical deformations may be expected for dumped and lightly compacted sidefills, but that the deformed shape of pipes in moderate or highly compacted sidefill will depend on the stiffness of the pipe.

Broere (*5*) reports experiments on uPVC pressure pipes in practice. Eight 500-mm-diameter uPVC pipes were buried under distinctly different conditions and deformation was measured using 36 strain gauges equidistantly spaced around the external circumference of the pipe. Broere describes the deformation of the pipe in uncompacted sand as being elliptical in the upper half of the pipe and that corresponding to deformation between two flat plates in the lower half. He ascribes this behavior to the hard trench bottom's providing a linear support to the pipe, which produces an exaggerated peak stress at the invert. The pipe deformed more in the lower half than the upper half of the pipe. Little deformation occurred in compacted sand. In compacted clay, the strain gauge pattern is described as elliptical in both the upper and lower halves, though with more deformation above the springings. In uncompacted clay, deformation is described as elliptical in the upper half and somewhere between elliptical and flat plate deformation in the lower half (the trench bottom was relatively soft). Greater deformation occurred below the springings because the soil was considered to be looser around the haunches than the shoulders.

Soini (*6*) describes field measurements of plastic pipes using a pipe cruiser to describe the deformed profile. In order to calculate the tangential strain in the pipe wall from the measured ring deformation, a factor (k) is applied to account for the shape of the deformed pipe. Where deformation is elliptical the value of k will be 3.0, and values for pipes in general use have been thought by Scandinavian researchers to range from 3.0 to 6.0 because of variations in deformed shape. Results obtained by the Pipe-Cruiser indicate that this variation in shape is considerably greater than supposed, with values of k ranging from 2.85 to more than 10. However, no description of the variation in shape is given.

EXPERIMENTAL PROGRAM

The aim of the experimental program was to investigate the performance of small-diameter uPVC pipes when buried at shallow depth in a 500-mm-wide trench. Surface load was applied to simulate the passage of site construction traffic. The main series of experiments was conducted in a large pit and these have been described by Rogers (*7*). A further test was conducted in which a line load was applied across the pipe. A second series of experiments was conducted in a reinforced box, having constant boundary conditions, in order to gain comparative data, and these are reported herein.

The box was 750 mm long, 500 mm wide, and 550 mm deep, with a depth of cover to the pipe of 250 mm. Load was applied to the surface of the backfill through a 480-mm-diameter rigid platen, which represented the load caused by the rear wheel arrangement of a construction truck passing approximately 500 mm above the pipe crown. This loading condition was more severe than that of the main program of tests and was adopted to produce significant deformations in the pipes. Over the surface of the clay not covered by the platen, a dead load was applied to simulate 500 mm of soil

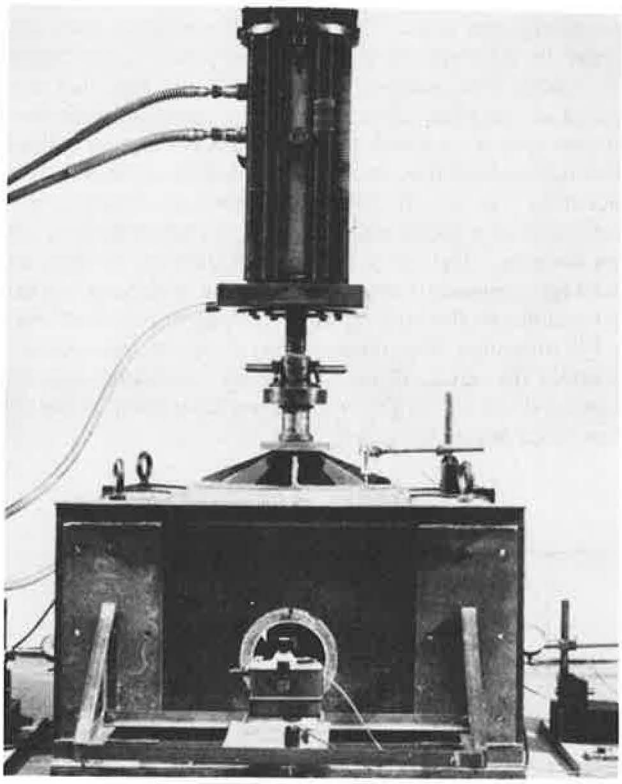

FIGURE 2 The test box.

cover. This equipment is shown in Figure 2 with the dead load removed for clarity.

Howard (*2*) showed that where a trench-width-to-pipe-diameter ratio of 4.67 was used for his experiments, the pressure cell readings on the box wall on the horizontal axis of the pipe were the same as those 600 mm above the horizontal axis. This implied that the box walls had no influence on the behavior of the pipe. When a ratio of 3.50 was used, the lower pressure cell consistently recorded higher stresses on the horizontal axis, indicating an external influence. Dezsenyi (*8*) quotes a limiting ratio of 5.0 beyond which the container walls have no influence. In the experiments quoted herein, the ratio was 3.2, which implies that the box walls do influence pipe behavior. This should be taken into consideration when attempting to measure absolute, as opposed to comparative, performance from the results.

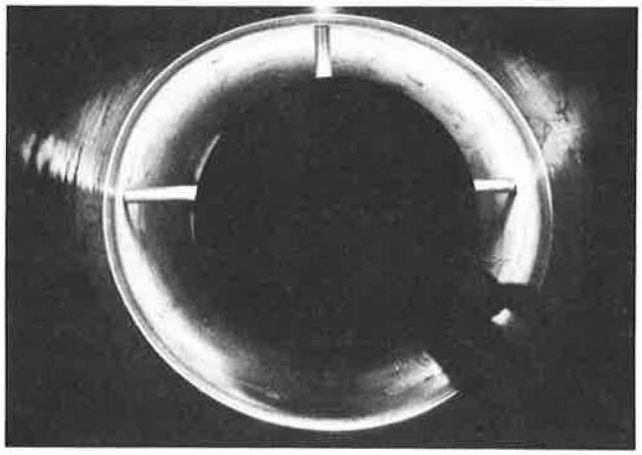

FIGURE 3 A ring flash photograph.

The deformed shape of the pipe was recorded throughout each test using a ring flash camera developed at the Transport and Road Research Laboratory. The ring flash head was mounted on a boom and inserted into the pipe below the load platen. The head, which appears as a silhouette to provide a datum measurement, produced a thin band of light, which was recorded photographically (Figure 3). Diametral change and shape of deformation were measured from the sequence of photographs. Vertical diametral change was also recorded by a linear potentiometer mounted on a sledge. Internal pipe-

TABLE 1 DETAILS OF EXPERIMENTAL INSTALLATIONS IN THE BOX

Reference	Bedding Type	Bedding Thickness (mm)	Sidefill Type	Sidefill Compaction	Comments
1	Pea gravel	100	Pea gravel	None	Standard practice
2	Pea gravel	50	Pea gravel	None	
3	None	0	Pea gravel	None	
4	Pea gravel	50	Pea gravel to springings, silty clay above	None None	Support to mid-height of pipe only
5	None	0	Pea gravel to springings, silty clay above	None; thorough	Split sidefill
6	None	0	Silty clay to springings, pea gravel above	Thorough; none	Split sidefill
7	None	0	Silty clay to crown, pea gravel 50 mm above	Thorough; none	Arching layer over 9
8A and 8B	None	0	Silty clay to springings, pea gravel to 50 mm above pipe crown	Thorough; none	Arching layer over 6; 8*A* had low water content, 8*B* high
9	None	0	Silty clay	Thorough	
10	None	0	Silty clay	Thorough	Compacted in 2 layers
11	None	0	Silty clay	Light	
12	Pea gravel	100	Silty clay	Thorough	
13	None	0	Concrete ballast	Light	
14	None	0	Concrete ballast	None	
15	None	0	Reject sand	Light	
16	None	0	Reject sand	None	

wall strains were measured in the circumferential direction by eight equally spaced single active strain gauges glued directly to the wall of the pipes.

Keuper marl (a silty clay having a liquid limit of 32 percent and a plastic limit of 19 percent) was used as backfill, the side fill and bedding consisting of distinctly different soils (Table 1). In addition to standard installation configurations, relatively good (pea gravel) and poor (silty clay) soils were juxtaposed around the pipe in order to isolate the critical areas of soil support. Pea gravel is a uniform rounded 10-mm gravel, concrete ballast is a well-graded aggregate of medium sand to medium gravel, and reject sand is a well-graded silty sand. Grading curves for these soils are given by Rogers (*7*). The pipes were 160-mm diameter with a standard dimension ratio (diameter-wall thickness) of 41 and were manufactured to the British Standard.

Silty clay was compacted to form a flat trench bottom at the appropriate level. The bedding layer, when used, was spread to the required depth and the pipe was positioned. The sidefill was carefully placed beside the pipe and compacted as specified. Three levels of compaction were used: no compaction, in which the material was dumped and leveled; light compaction, in which the sidefill was carefully compacted by foot after leveling; and thorough compaction by two passes of a pneumatic tamper with a single head of 125-mm diameter. The box was then backfilled in one layer and thorough compaction was applied to the surface of the clay 250 mm above the pipe crown. Readings of pipe-wall strain and deformation were taken at every stage of installation to ascertain the effects of the installation procedure, including negative diametral strain, or diametral elongation, as soil was compacted beside the pipe.

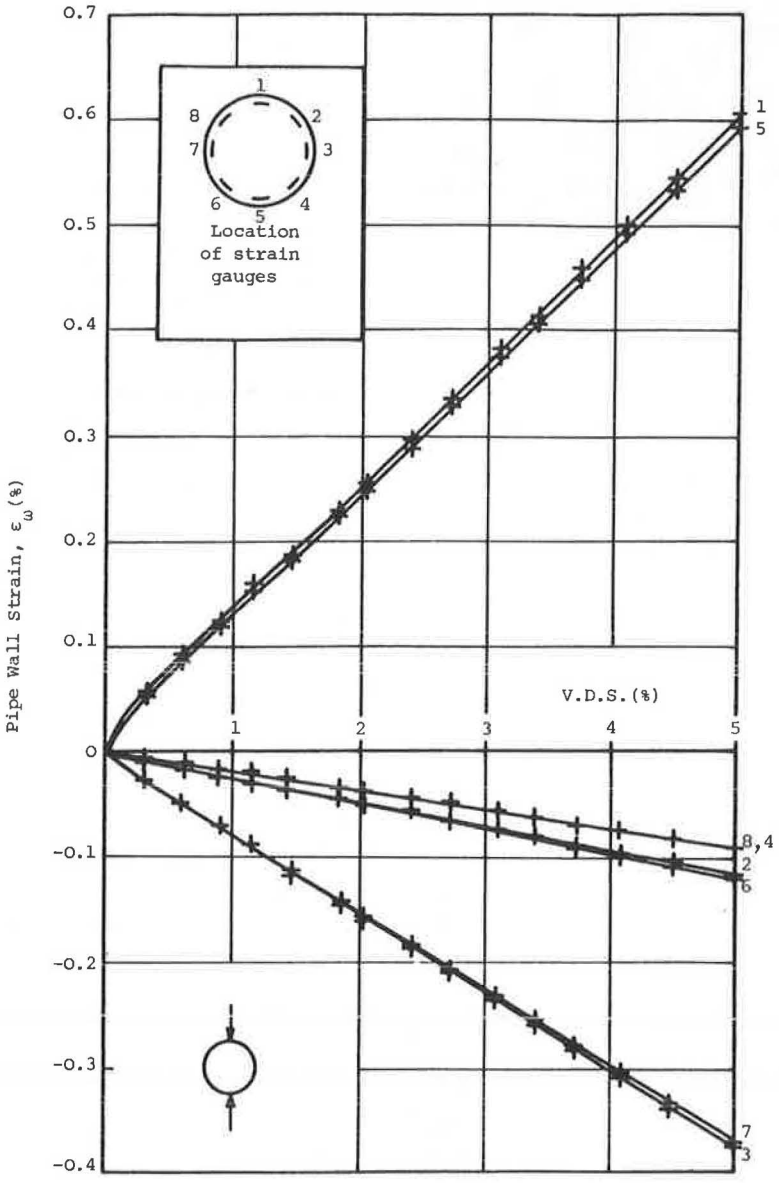

FIGURE 4 Graph of pipe-wall strain against VDS for unconfined line load test.

Surface loads of 5.5 and 7.0 tonnes were applied both statically and cyclically to each experimental installation. The lower load was applied statically for 30 min, was removed for 45 min, and was then cycled 150 times at approximately 12 cycles/min. After 150 cycles of load, the pipe deformation was found to have stabilized. The installation was allowed to recover for 2 hr before the process was repeated with the higher load, the final recovery period being at least 18 hr. Readings were taken throughout the loading sequences and recovery periods. In cases where excessive deformation occurred during the loading sequence, the test was prematurely terminated to avoid equipment damage.

EXPERIMENTAL RESULTS

Although many readings were taken during the test program, only those relating to pipe-wall strain and deformation will be presented herein. Further information is given in Rogers (*7*) and Rogers et al. (*9*). Circumferential strain was measured at 45-degree intervals around the internal surface of the pipe. These data have been presented in either linear or circular plots of the strain profile. Where comparisons have been made between installations, the data have been extrapolated to those that would occur at 5 percent VDS, assuming a linear relationship, and an average strain was taken for linear plots, assuming symmetry about the vertical axis. The sign convention adopted throughout this paper is that tensile strains are positive and compressive strains are negative.

The relationship between pipe-wall strain and vertical diametric strain (VDS) in the unconfined line load test (Figure 4) was linear for each gauge up to 5 percent VDS. Pipe-wall strain profiles at integer percentages of VDS during this test are plotted on a circular axis in Figure 5, from which their elliptical nature can clearly be seen. When the same data were averaged and plotted on a linear axis (Figure 6), a clearer description of the relative magnitudes of strain was apparent. It may be concluded, therefore, that the deformed shape of the pipe was an ellipse, as expected. In addition, the deformed shape of the pipe could be predicted from the strain profiles.

The influence of surrounding the pipe in various soils and applying surface load (Tests 3, 10, 13, and 15) is shown in Figure 7, in which the permanent strains at the end of the test have had the somewhat variable installation effects removed before extrapolation to those that would occur at 5 percent VDS. The tests using the clay and sand sidefills were terminated after the 70 kN static load and the 55 kN cyclic load sequences, respectively. In general, compaction of the sidefill caused diametral elongation of an approximately elliptical nature, the precise shape depending on the level at which the compaction was applied. The effects of diametral elongation on deformation are discussed by Rogers (*7*).

All four curves conformed to the same approximate pattern, with high tensile strain in the pipe crown and equal and opposite strains at the springings (compressive) and invert. The curve for pea gravel exhibited the greatest deviation from the V-shaped pattern, with the highest pipe crown and shoulder strains and the lowest strain at the haunches. Howard (*3*) demonstrated that elliptical deformation is associated with a V-shaped, rather than elliptical, pipe-wall strain profile when the pipe is buried because of the resistance to movement of the side of the pipe. It can be concluded from these data, therefore, that the deformation of the pipes at the end of the tests was approximately elliptical, with the pipe in pea gravel showing a tendency to flatten at the crown and bulge slightly at the shoulders. It should be noted at this point that the amount of deformation of the pipe associated with these profiles is between 5 and 11 percent and the deviations from an

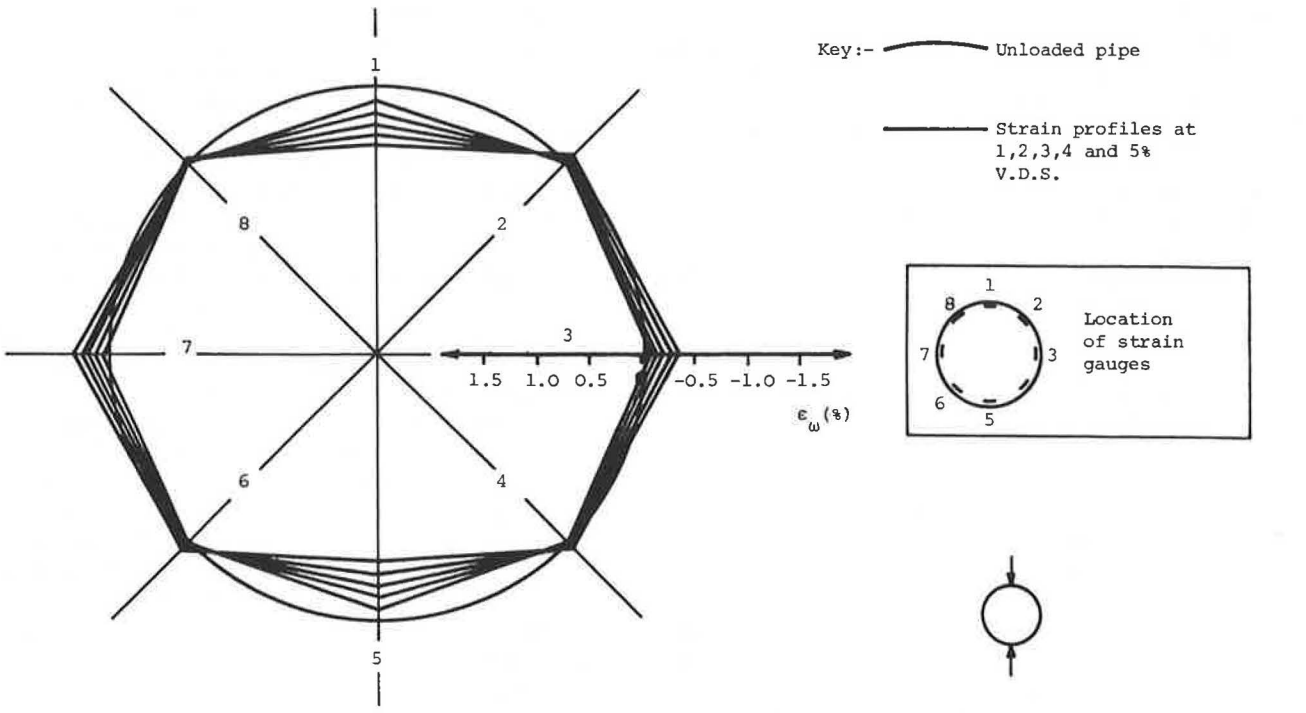

FIGURE 5 Circular pipe-wall strain profiles for unconfined line load test.

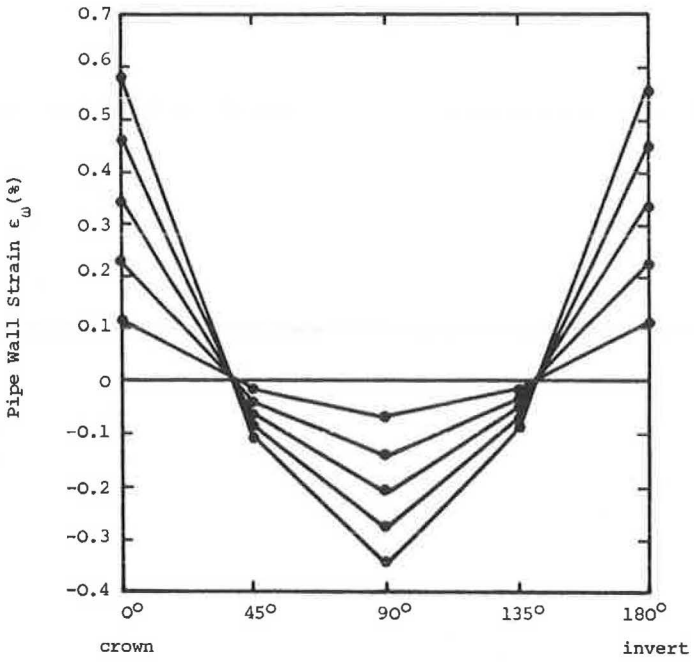

FIGURE 6 Linear pipe-wall strain profiles for unconfined line load test.

ellipse are hardly discernible from the ring flash photographs. The descriptions of flattened crowns and bulging shoulders are, therefore, greatly exaggerated and are solely used to distinguish marginal changes in shape.

In contrast, the extrapolated pipe-wall strain profiles for the same tests after the 55 kN static load had been applied for 30 min (Figure 8) show a considerable difference in behavior. The curve for pea gravel was indicative of considerable action to relieve pressure in the top section of the pipe and consistently good support around the pipe. Similar, though less exaggerated, behavior was apparent in the concrete ballast installation, with greater movement at the haunches and invert reflecting a lack of compaction at these points. The strain profile for the silty clay installation is of a near perfect V form indicating purely elliptical behavior under load, the more competent reject sand conforming to approximately elliptical behavior.

These two figures show that the pipe deformed in an elliptical manner under load when surrounded by a poor material and application of further loads, whether static or cyclic, did not change this pattern. When surrounded by a material that provided good support, however, deformation under load was considerably different from an ellipse and totally dependent on the character of the surrounding soil. Application of the remaining load sequences caused the distortions from an ellipse to become so much less evident that the curves for distinctly different materials took the same form.

Corresponding curves for the four tests using uncompacted pea gravel (UCPG) and well-compacted silty clay (WCSC) in different configurations around the pipe (Tests 3, 5, 6, and 7) are shown in Figures 9 and 10. All four soil configurations provided good support to the pipe. As before, the greatest difference in pipe-wall strain profiles occurred under static load (Figure 10). The profile under load for full depth UCPG exhibited flattening of the crown and bulging of the shoulders, with little movement around the haunches and invert. The curve for WCSC over UCPG showed similar behavior, although with negligible strain at the springings. In this case the relief of pressure concentrations above the pipe was largely affected in the WCSC, though with flattening occurring at both the crown and the invert and bulging at both the shoulders and haunches. The arching layer diverted the area of most action to the lower section of the pipe, resulting in the lowest crown and shoulder strains and highest strains at the haunches (bulging) and invert (flattening). Similar, though less pronounced, behavior occurred where a split sidefill of UCPG overlying WCSC was used.

These tests indicated that most deformation occurred where the support was poorest. The curves at the end of the tests retained the characteristics of those when under load while reverting to a more uniform pattern consistent with elliptical deformation (Figure 9). Retention of strains developed under load was greatest in areas associated with clay surrounds, which indicated a lower degree of elastic recovery and was consistent with the soil properties. A detailed study of recovery on removal of the static load confirmed this observation.

In order to illustrate the behavior under static and cyclic loads, the strain profiles at various stages of the test using a full-depth UCPG sidefill (Test 3) is shown in Figure 11. The effects of installation were small. The profile under the 55 kN static load exhibited large crown and shoulder strains, which increased marginally as the load was held for 30 min. On removal of the load, significant elastic recovery occurred. Application of the cyclic load caused large increases in strain at the crown, springings, and invert, but had a negligible influence on behavior at the shoulders and haunches. Application of the 70 kN static load caused similar large strain increments to those of the lower static load, the pipe exhib-

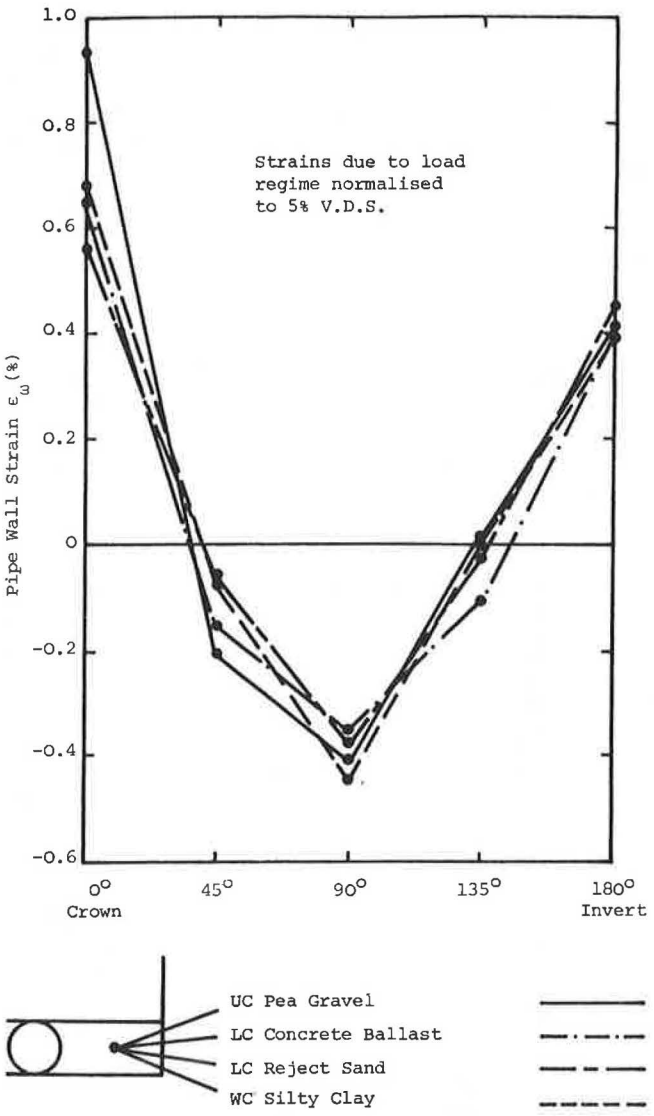

FIGURE 7 Pipe-wall strain profiles at end of tests using four sidefill materials.

iting little creep behavior. On removal of this load, nearly all of the additional strain was lost. The higher cyclic load produced the same results as the lower one.

It is clear from this analysis that, when buried in a competent sidefill, the pipe exhibited distortional behavior under load, with little creep movement and considerable elastic recovery. Application of the cyclic loads produced almost perfect elliptical behavior, thus reducing the distortional influence on the final strain profile.

It has been stated in the literature by Broere (*5*) and others that the deformed shape of a flexible pipe can be obtained when the circumferential pipe-wall strain distribution is known. This was shown to be true for uPVC pipes in the case of unconfined line load test. When the pipe was confined in a good sidefill, the shape of the strain profile differed significantly from an ellipse, and a component of hoop compression would have been expected.

These phenomena are illustrated in Figure 12, which shows a graph of pipe-wall strain against VDS for a full-depth UCPG sidefill (Test 3), in which distortional profiles were produced. At each point around the circumference except the invert, the pipe-wall strain measurements under the static load show higher compressive, or lower tensile, strain than the corresponding values after the cyclic load had been applied, indicating that a compressive component of hoop strain was induced under load. The gauges on the horizontal and vertical axes exhibited a discernible linear relationship through the origin despite this effect. The cyclic load sequences produced a slightly curved relationship for the pipe crown strain. Strain in the gauges on the springings was remarkably similar and also slightly curved. The relationships for the gauges at the shoulders and haunches were of similar type, with large compressive components under static and a slightly curved, though approximately horizontal, line under cyclic load. This reflected distortional behavior under load followed by elliptical behav-

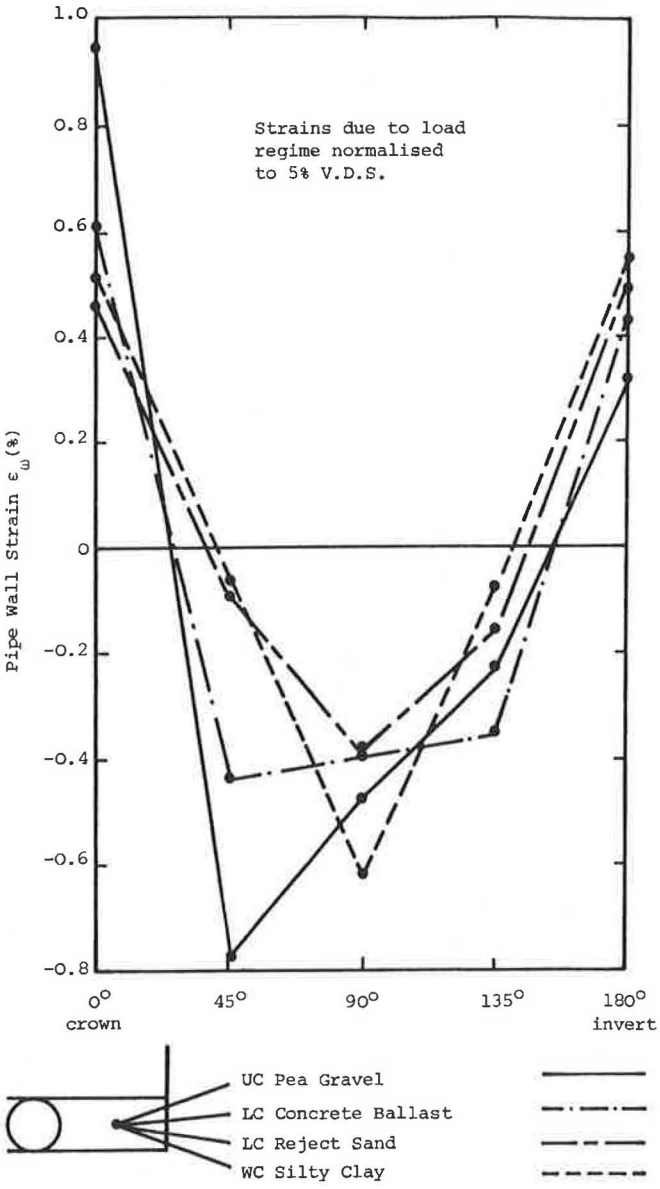

FIGURE 8 Pipe-wall strain profiles under 55 kN static load using four sidefill materials.

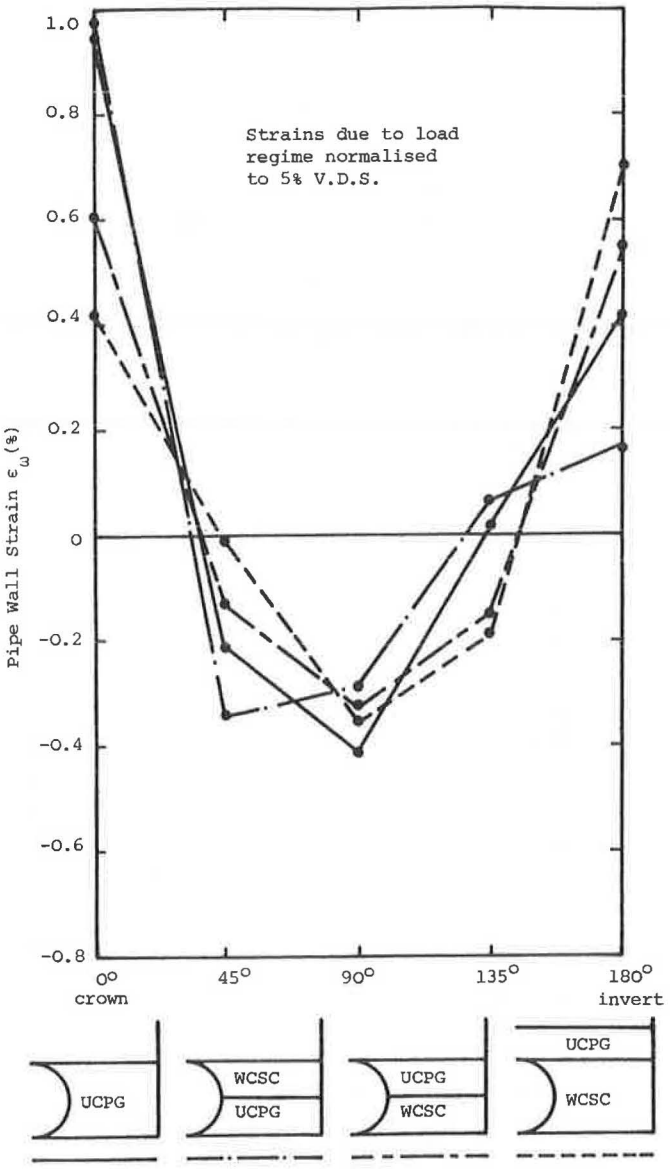

FIGURE 9 Pipe-wall strain profiles at the end of tests using four combinations of gravel and clay.

ior, in which little change in strain was experienced at these points, when the load was cycled.

Considering Figure 12, it can be concluded that the shape of deformation can be deduced from the strain profiles if care is used. When analyzing such data, it should be remembered that the correlation sought ought to have been that between pipe-wall strain and the change in curvature of the wall, or relative movement of the point toward (or away from) the center of the pipe. The good correlation of strain with VDS on both horizontal and vertical axes was encouraging, therefore, and the behavior at the shoulders and haunches was explicable.

The results previously quoted lead to the following working hypotheses of pipe behavior. When a circular pipe is subjected to a line load across its vertical axis but is otherwise unloaded, it will deform elliptically. The pipe-wall strain profile will be elliptical also. When surrounded by a relatively poor soil and load is applied to the soil, the pipe will again deform approximately elliptically, but the pipe-wall strain profile will tend to a V shape (Figure 13*a*). This is caused by the lateral restraint of the soil, or passive pressure developed therein, which induces a greater compressive strain in the pipe springings. Where a buried pipe is bedded in a good quality stiff soil up to at least its horizontal axis and a vertical load is applied to the soil surface, the pipe will tend to deform to a heart shape, in which the pipe crown flattens and the shoulders become relatively more curved with a roughly even change in curvature below this (Figure 13*b*). Such a deformation is accompanied by high tensile wall strain at the pipe crown and high compressive strains at the shoulders. Diametrically opposite behavior can occur in cases where the soil around the haunches is poor and that above it is of good quality (Figure 13*c*). In cases in which exceptionally good lateral restraint is provided at the pipe springings, deformation will tend to be square shaped, in which the pipe and invert flatten and the

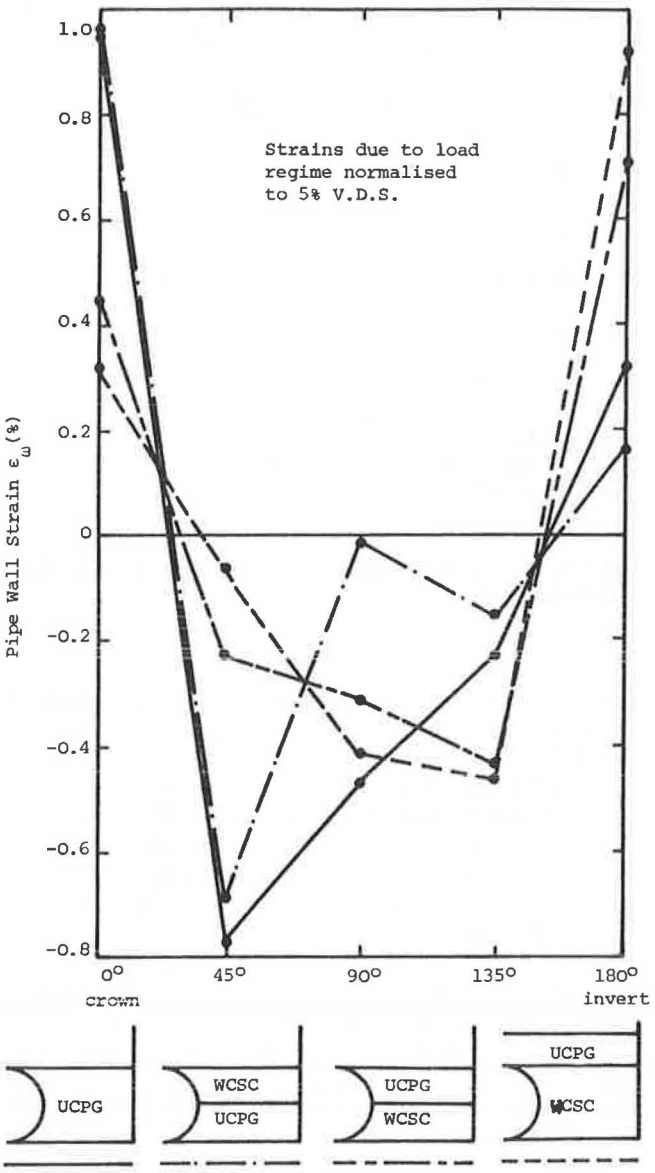

FIGURE 10 Pipe-wall strain profiles under 55 kN static load using four combinations of gravel and clay.

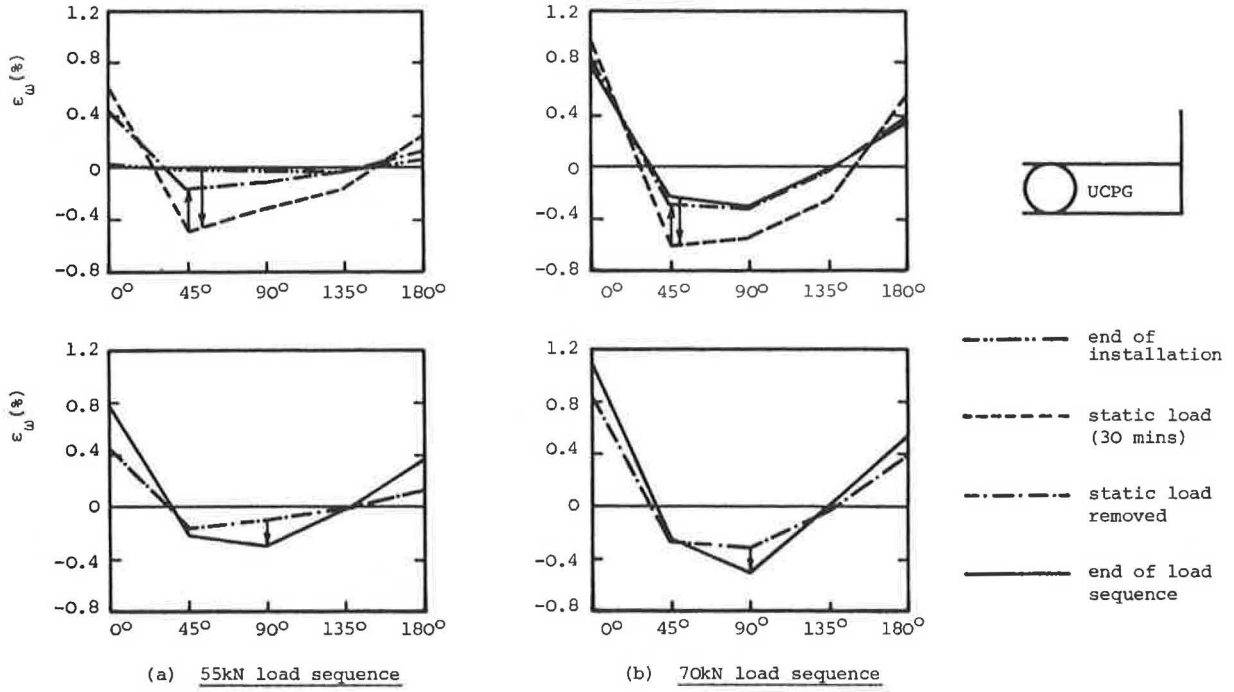

FIGURE 11 Development of pipe-wall strains in pea gravel.

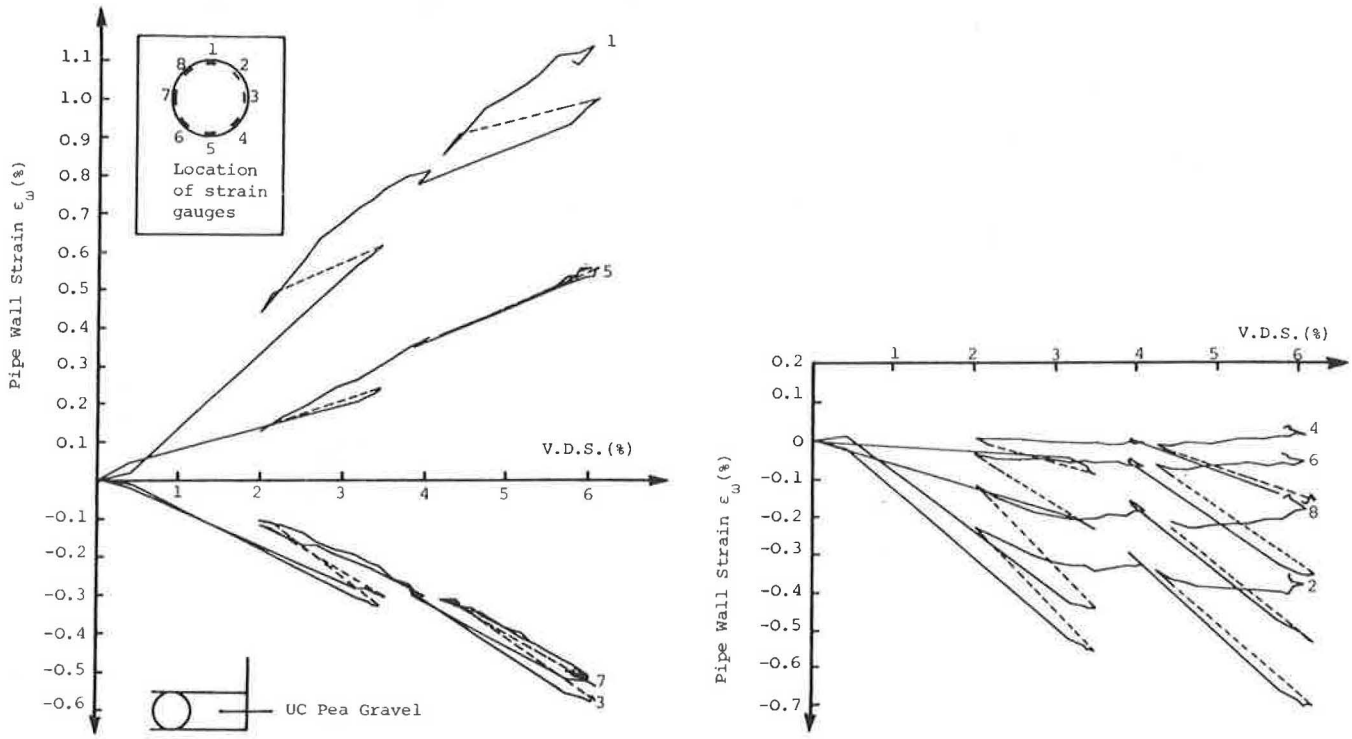

FIGURE 12 Graph of pipe-wall strain against VDS for a pea-gravel installation.

shoulders and haunches take up a smaller radius of curvature, the springings remaining largely unstrained (Figure 13*d*). This behavior typically occurs only in cases in which thorough compaction is applied to the sidefill at the level of the pipe springings, thereby creating a locally stiff medium.

The behavior described as semielliptical by Howard (*3*) is consistent with the inverted-heart-shaped profiles already described, although in a less exaggerated form. The description by Howard (*2*) of rectangular deflection is consistent with the square-shaped deflection referred to previously. In this respect, rectangular is perhaps a better description because the pipe undergoes flattening at the crown and invert, with

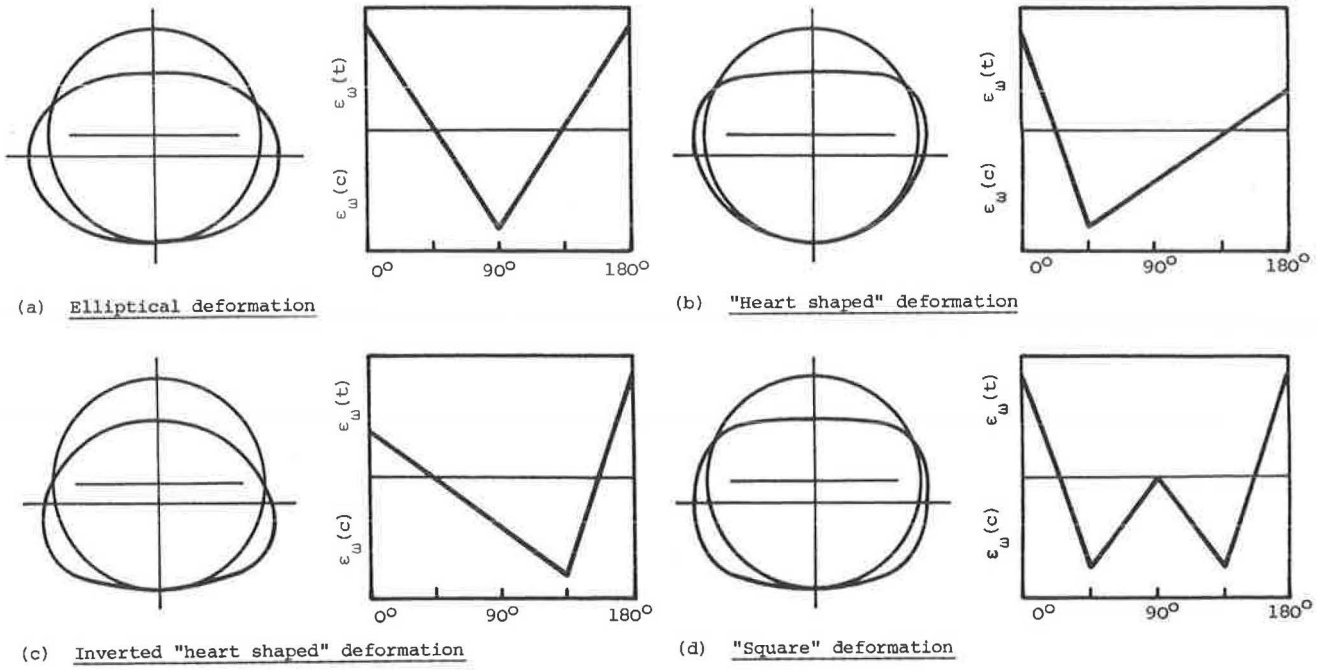

FIGURE 13 Types of deformation and associated strain profiles.

no change in curvature (i.e., negligible strain) at the springings. The V-shaped strain profile associated with elliptical deformation was confirmed by the experimental results.

Where Broere (*5*) refers to flattening, as between two plates, in the lower half of the pipe buried in uncompacted sand, he is referring to the tendency of the pipe to adopt an inverted-heart shape. He confirms this by stating that the pipe deformed more in the lower half of the pipe than in the upper half. The pipe in compacted clay also showed a tendency to an inverted-heart shape.

CONCLUSION

An unconfined pipe produced an elliptical pipe-wall strain profile when loaded, the strains being proportional to VDS at each point around the circumference. This was consistent with the expected elliptical deformation of the pipe. When buried, elliptical deformation was accompanied by a V-shaped pipe-wall strain profile and such behavior was only found with poor sidefills such as silty clay and reject sand. Distortional behavior, consistent with the character of the sidefill, occurred under static load in pipes that were given good support, behavior being essentially elliptical under cyclic loads. Elastic recovery of static load deformation was greatest in soils of highest elasticity and in cases in which pipe support was best. The arching behavior of granular soils was important. The deformed shape of a buried pipe was deduced from the pipe-wall strain profiles, the relationship of the latter being consistent with VDS measurements.

The assumption of elliptical deformation in methods of prediction of pipe deformation is likely to be valid in cases where the pipe is subject to predominantly cyclic load or where the surrounding soil is not relatively stiff. Where applied load is predominantly static, the assumption could prove to be greatly in error. The assumption of elliptical deformation in experimental work should be avoided and measurement of pipe-wall strain or wall movement, or both, should be made all around the circumference rather than solely across the vertical and horizontal axes.

ACKNOWLEDGMENTS

The research described herein was carried out in the Civil Engineering Department of the University of Nottingham under a contract with the British Plastics Federation, whose help and guidance is gratefully acknowledged. The author is grateful to P. S. Pell, head of the Civil Engineering Department, for providing the necessary facilities and particularly to S. F. Brown, who both supervised and contributed greatly to the work. The author also wishes to acknowledge the help of M. P. O'Reilly and his colleagues at the Transport and Road Research Laboratory.

REFERENCES

1. M. G. Spangler. *The Structural Design of Flexible Pipe Culverts.* Bulletin 153, Engineering Experiment Station, Iowa State College (now the University of Northern Iowa), Cedar Falls, 1941.
2. A. K. Howard. Laboratory Load Tests on Buried Flexible Pipe. *Journal of American Water Works Association*, Vol. 64, Oct. 1972.
3. A. K. Howard. *Laboratory Load Tests on Buried Flexible Pipe.* Progress Report No. 5: GRP, PE, and PVC. USBR Report No. REC-ERC-73-16, Bureau of Reclamation (now Water and Power Resources Service), Denver, Colo., July 1973.
4. A. K. Howard. Diametral Elongation of Buried Flexible Pipe. In *Proc., International Conference on Underground Plastic Pipe*, New Orleans, La., March 30–April 1, 1981.
5. J. J. Broere. *The Behavior of PVC Water Mains under Practical Conditions.* (In Dutch.) H2O, Vol. 17, No. 9, The Netherlands, Sept. 1984.

6. R. Soini. Interaction Between Thermoplastic Pipes and Soft Soil. In *Proc., Europipe '82 Conference,* Basle, Switzerland, Jan. 1982.
7. C. D. F. Rogers. *Influence of Surrounding Soil on Flexible Pipe Performance.* Paper presented at 66th Annual Meeting of the Transportation Research Board, Washington, D.C., Jan. 1987.
8. I. Dezsenyi. *Plastic Sewers—Calculating Deformation.* Building Research and Practice, Leyden Publishing Co., Ltd., London, England, Sept. 1975, pp. 278–288.
9. C. D. F. Rogers, S. F. Brown, and G. Boyle. The Influence of Bedding and Sidefill on the Response of uPVC Pipes to Surface Loading. In *Proc., 6th International Plastics Pipe Conference,* University of York, England, March 1985.

Publication of this paper sponsored by Committee on Subsurface Soil-Structure Interaction

Load Test Report and Evaluation of a Precast Concrete Arch Culvert

TIMOTHY J. BEACH

A report on and an evaluation of a full-scale load test performed on a Con/Span culvert are presented in this paper. Because of its intended use, it was important that this three-sided box-arch shape's field performance be evaluated extensively, in addition to rigorous theoretical analysis. A load test procedure was devised to evaluate the structural integrity of this unit and to examine to what extent its field performance compared with its predicted behavior. The finite element program CANDE was used for the detailed analysis of the structure. CANDE is a program especially written for the evaluation of soil-structure interaction conditions, and is ideally suited to evaluate the effect of the conditions that exist in field testing. The evaluation revealed a good correlation between the performance of the culvert and the finite element analysis used. Perhaps more impressive was the culvert's capacity to sustain an extreme overload.

Con/Span culverts were developed to meet a need for precast reinforced concrete culverts with large cross-sectional areas for water conveyance at sites with limited vertical clearance. Because of their great width compared with their height and because of the inherent durability characteristics of concrete, these culverts provide an economical design solution for short-span bridge replacements. The box-arch culvert can be made in a number of span and rise combinations. The geometric properties of the 19-ft span culvert studied is shown in Figure 1.

DESCRIPTION

The unique combination of vertical sidewalls and the arch top not only enhance the hydraulic and aesthetic values of the culvert but also greatly increase its load-carrying capacity. This increase in load-carrying capacity is perhaps most effectively shown by examining Figure 2.

In the arch-box when the culvert begins to deflect, thrust is developed by the passive pressure of the earth backfill counteracting the efforts of the applied loads to deflect the top of the structure. In a state of extreme overload, the arch-box cannot collapse without pushing the block of soil behind the sidewalls far enough to allow the arch to collapse. Hinges will form in the culvert but the units will still be a viable structure with the pressure from the backfill providing the necessary support. The dependence on the backfill is not nearly so critical under normal design conditions. For an actual installation, the units are designed according to American Association of State Highway and Transportation Officials (AASHTO) specifications, which require that the culvert be loaded using ultimate loads and the reinforcing steel not be permitted to yield. Based on this practice and the structure's inherent strength, it is easy to see the large reserve capacity built into these culverts.

Another significant contribution to the structural advantages of the box-arch shape is its resistance to shear. Because of the thrust and the arch shape, shear from the vertical loading is greatly reduced in a section. This allows the unit to maintain its standard 10-in. thickness under much deeper fills than normally considered for such a lightweight section. This issue is illustrated in Figure 3.

A flat slab with the same span and loading would have a shear value ($V = WL/2$). Obviously the effectiveness of this shear reduction relies on the radius of the arch, but even with a flat arch the reduced shear values and thinner sections are quite advantageous.

The behavior of the culvert is therefore dependent to a limited degree on its interaction with the surrounding backfill. The backfill restrains the tendency of the sides of the culvert to flex outward. This restraint develops a thrust in the curved top of the unit that creates arch action to increase its capacity to carry vertical loads. This interaction of the structure and soil can be simulated with a computer model to allow a reliable and realistic basis for design.

The design of the reinforced concrete culvert is based on the concept of soil-structure interaction and is modeled by using the finite element method of analysis. The finite element computer program called CANDE (Culvert Analysis and Design) provides the computer model to analyze the behavior of the arch structure during various loading situations. CANDE permits analysis of the culvert beyond conventional elastic analysis into the plastic range. The analysis is performed in an iterative manner, beginning with the structure resting on its foundation with no backfill. Placement of the first layer of backfill alongside the culvert is modeled by adding the first layer of soil elements and loads to the finite element mesh. Through their interaction, the soil elements load the structure. Subsequent steps of the analysis are performed in the same way, adding one layer of elements at a time, simulating the process of backfilling around and over the culvert. After the final layer of fill has been placed over the top of the structure, loads are applied to the surface of the fill to simulate vehicular traffic loads.

Purpose

The purpose of the load test was to verify the validity of the modified CANDE computer program of analysis to model the actual behavior of field-installed box-arch culverts.

Con/Span Culvert Systems, 1563 East Dorothy Lane, Dayton, Ohio 45429.

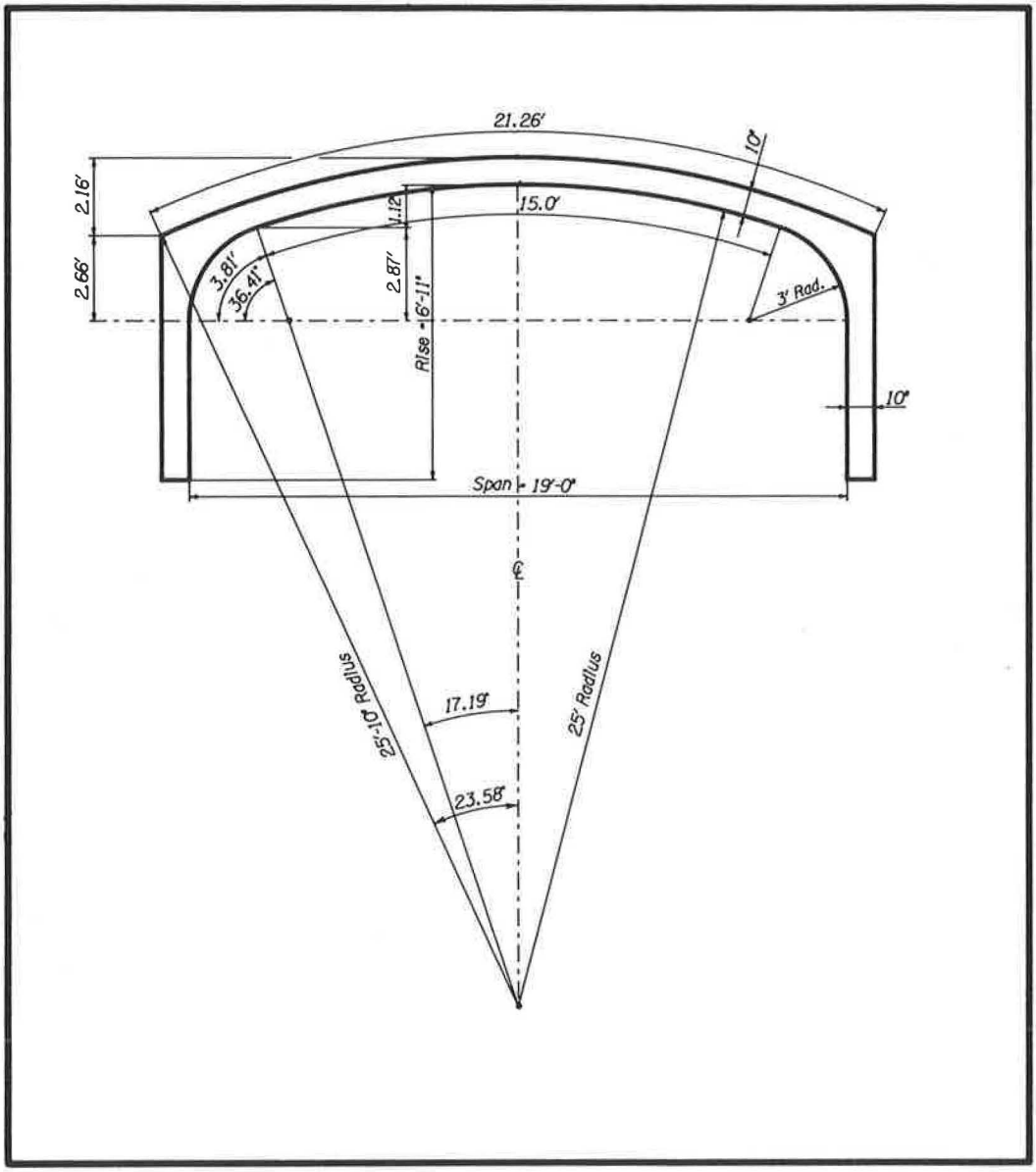

FIGURE 1 Culvert dimensions.

Scope

The test involved installing three 8-ft laying length culverts on a cast-in-place slab. After the backfilling process was complete, the middle culvert was tested. The test culvert was instrumented with deflection gauges. External loads were applied evenly (at mid-span) across the 8-ft laying length of the test culvert. As loads were applied, deflection readings were recorded. The loads applied were as much as five times the HS20 design service loading without impact.

By applying loads that greatly exceed the design loading, appreciable deflections and cracks occurred. After the test was complete, the test unit's actual section properties (com-

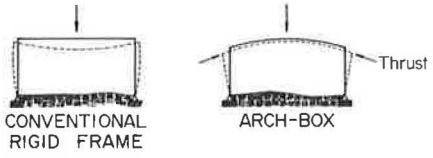

FIGURE 2 Theoretical deflected shapes.

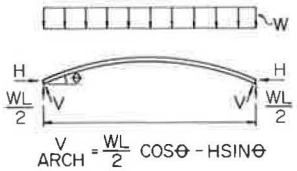

FIGURE 3 Mechanics of arch shape.

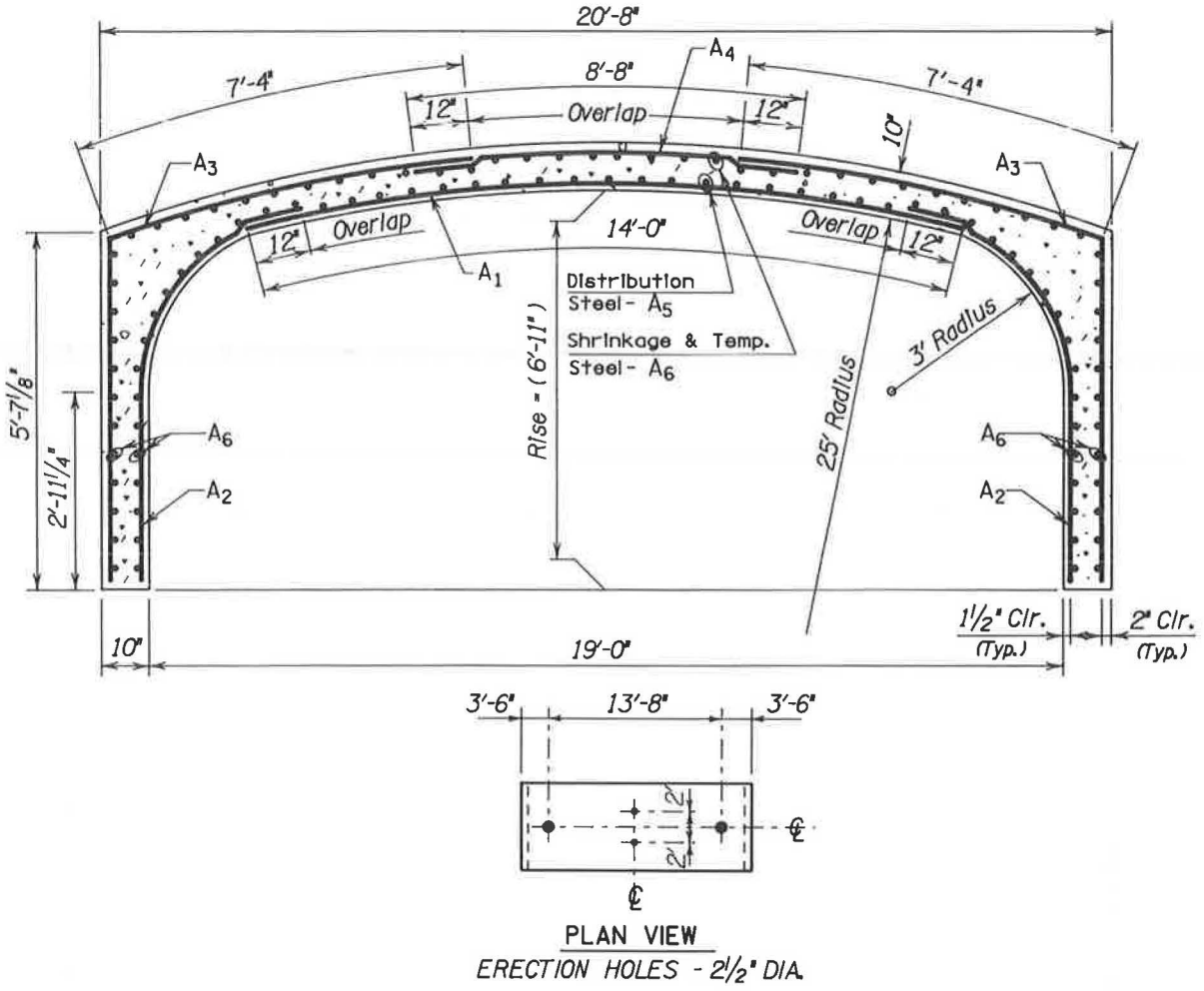

FIGURE 4 Cross section of test unit.

TABLE 1 REINFORCING AREAS FOR TEST UNITS

SPAN: (19'-0") RISE: (6'-11") COVER: (1'-0")

Sheet No.	Area Req'd. (in^2/ft)	Mesh Size	Length (ft)	Area Supl'd. (in^2/ft)
1	A_1 - .62	2x4 - W10.5xW5.0	14'-0"	.63
2	A_2 - .155	2x8 - W2.5xW2.5	8'-8"	.15
3	A_3 - .32	2x8 - W5.5xW2.5	12'-8"	.33
4	A_4 - .125	2x8 - W2.5xW2.5	8'-8"	.15
5	A_5 - .125	Provided by #1 Transverse steel	7'-8"	.15
6	A_6 - .125	#3(s) @ 12"c.c. GR. 60	7'-8"	.15
Design Loading: HS20				

pressive strength, steel areas, etc.) were determined and used as input for the CANDE computer analysis. The evaluation of the computer model's deflection and crack behavior output and the actual field test data is the subject of this report.

Load Test Installation and Procedure

For the load test, a standard 8-ft laying length of a 19-ft span by 6-ft 11-in. rise culvert was used. The test culvert was made according to the manufacturer's specifications (*1*) and the 19-ft by 6-ft 1-in. box-arch shop drawing (Figure 4) with the steel areas called for in Table 1.

As shown in Figures 5 and 6, three culverts were installed end to end on a cast-in-place base slab. The width of the excavation between the culvert leg cast-in-place base slab. The width of the excavation between the culvert leg and the existing soil was a minimum of 3 ft. After the culverts were plumbed and leveled on shims, the space between the bottom of the culvert's legs and the footer was grouted with a cement grout. A 12-in.-wide strip of filter fabric was placed over the joints. The connection plates normally installed between the units were omitted to allow the test unit to function independently.

With the culvert units set, the backfilling process began. The backfill material met the requirements of the Ohio Department of Transportation (ODOT) 310.02 Grading *B* and was constructed according to the manufacturer's specifications (*1*). This required compaction of soil determined per standard proctor that was 95 percent of the maximum laboratory dry weight. Compaction tests were performed by ODOT's Bureau of Testing to ensure proper compaction. The difference in the backfill elevation on each side of the culvert during placement did not exceed 1 ft. The backfill process was to proceed until 1 ft of cover above the outside of the unit at the centerline of the span was achieved.

After the backfilling was complete, the deflection test frame was attached. Deflection gauges supplied by CTL Testing Laboratory were mounted on the frame. The gauges were zeroed before the application of the load.

The test load was applied by the use of a 100-ton hydraulic hand-operated jack supplied by CTL Testing Laboratory. A calibration chart correlating the hydraulic pressure to the load increments was developed by CTL and is included in the CTL report (*2*). The hydraulic jack reacted between a beam tied to the base slab and a beam centered on the culvert that distributed the load uniformly across its length.

FIGURE 5 Box-arch culvert load test, August 1986.

FIGURE 6 External view of test unit.

Loadings were applied to the culvert in multiples of an AASHTO HS-20 service load. The load to be applied was determined as follows:

Cover = 1 ft,
S (span) = 19 ft,
P (single wheel load) = 16 kips,

Per Section 3.24.3.2 AASHTO specifications:

E = distribution width for 1 wheel load,
$E = 4 + 0.06S = 4 + 0.06\ (19) = 5.14$ ft,
W = live load/unit length, and
$W = P/E = 16.0/5.14 = 3.1$ kips/ft of width.

Therefore, on an 8-ft width of culvert:

Design service load = 3.10 (8) = 24.8 kips.

Actual load increments were 25 percent of a full service load multiple, or a 6.2 kip jack reaction.

On August 7, 1986, the first phase of the load test was performed. The culvert was loaded until the 6.2 kips were applied. After the load was stabilized, the CTL testing engineer recorded the deflection readings. In time periods of approximately 3 to 4 min, the load was increased to the next load increment and deflections were recorded. The last load increment was 49.6 kips, which represents two times the design load. After this load was stabilized for a period of 3 min, the deflection readings were recorded. The load was removed and the deflections were again recorded. The deflections that occurred during the first phase of the load test are shown in Table 2. Maximum deflections were less than 1/16 in., and the structure rebounded to nearly its original position.

On August 12, 1986, the jack and the deflection gauges were reinstalled. Once the gauges were zeroed, the load was gradually applied in increments of 6.2 kips in time intervals of 3 to 4 min. Deflections were recorded for each load incre-

TABLE 2 19-FT SPAN LOAD TEST, PHASE 1: ACTUAL DEFLECTIONS

Load (kips)	Gauge Readings (in.)									
	No. 1	No. 3	No. 5	No. 7	No. 0	No. 8	No. 6	No. 4	No. 2	No. 9
6.2	0.001	0.001	0.0015	0.000	0.000	0.001	0.002	0.002	0.000	0.000
12.4	0.002	0.003	0.005	0.003	0.000	0.004	0.006	0.004	0.001	0.000
18.6	0.004	0.005	0.008	0.005	0.000	0.006	0.009	0.007	0.002	0.000
24.8	0.004	0.008	0.013	0.008	0.001	0.008	0.014	0.009	0.003	0.000
31.0	0.008	0.010	0.019	0.011	0.001	0.012	0.020	0.012	0.007	0.000
37.2	0.010	0.014	0.025	0.015	0.001	0.015	0.026	0.016	0.009	0.001
43.4	0.013	0.018	0.032	0.019	0.001	0.018	0.033	0.019	0.012	0.001
49.6	0.017	0.022	0.041	0.023	0.001	0.022	0.041	0.023	0.015	0.002

ment. The load increments and the associated deflections are shown in Table 3. The test culvert was loaded until the maximum load was obtained.

The results of the second phase of the load test are included in a CTL Engineering, Inc., report (*2*). The following are the written remarks by CTL included in their report (taken directly from CTL's report dated August 19, 1986).

II. Results

The loading progressed for 21 increments up to a loading of 133,500 lbs (133.5 kips). At this point the concrete span was loaded more than five (5) times the design load. At this loading, operating the 100-ton jack could only produce the constant loading, but the dial indicators began a constant movement indicating the concrete span was in a failure mode. The constant movement of the concrete surface continued to about a 2¾-inch deflection when it suddenly broke through the 8-foot span in the center of the arch and through the two drilled 2½-inch diameter holes made for passage of the two threaded bars for the loading system.

During the test, two of the dial indicators (# 1 and # 2) had withdrawn from contact with the concrete span. This indicated the span was belling out sideways while the span top was being compressed. Additional material was added to the steel test frame to remount these dial indicators. During this interval of time, about 25 minutes, the load was sustained at 133.5 kips. Once the dial indicators were remounted (at 12:55 p.m.) and pumping the jack continued normally again, the failure mode continued until the major break occurred at 1:02 p.m.

It should be noted that the first hairline cracks appeared at 55.8 kips loading, which was more than twice the design load of 24.8 kips.

Additional hairline cracking continued to appear at 66.0 kips, 68.2 kips, 74.4 kips, and the original hairline cracks became noticeably larger. At 80.6 kips, the original cracks had enlarged to about 1/64 inch. At about 111.6 kips, the cracks had increased to 1/32 inch and passed through the 2½-inch drilled holes for the thread bars. At 130.2 kips, the original cracks had enlarged to 1/16 inch.

At failure, 133.5 kips, the major cracks were about ⅜ inch wide all the way across the concrete span, passing through both drilled 2½-inch diameter holes. Some fallout of material, of course, made wider spots.

Most cracks appeared within about a 4-foot width across the span with the most concentration within about a 1-foot width.

The sideways or north-south movement of the span mainly occurred on the north side, where it remained deflected about 1¼ inch after the failure occurred. This was the side to which the deflection gauge frame was fastened.

TABLE 3 19-FT SPAN LOAD TEST: ACTUAL AND PREDICTED DEFLECTIONS

Load (kips)	Actual Gauge Readings (in.)										Predicted Values (in.)			
	No. 1	No. 2	No. 5	No. 7	No. 0	No. 8	No. 6	No. 4	No. 2	No. 9	No. 1	No. 3	No. 5	No. 0
6.2	0	0	0.002	0.001	0	0.002	0.003	0.002	0.001	0	0.001	0.001	0.000	0
12.4	0.001	0.002	0.006	0.004	0	0.004	0.0065	0.004	0.002	0	0.005	0.010	0.008	0.001
18.6	0.003	0.004	0.011	0.006	0	0.0065	0.011	0.007	0.004	0	0.007	0.015	0.015	0.002
24.8	0.005	0.007	0.017	0.010	0	0.010	0.017	0.010	0.006	0	0.010	0.019	0.023	0.003
31.0	0.007	0.010	0.023	0.013	0	0.014	0.022	0.013	0.008	0	0.013	0.024	0.027	0.004
37.2	0.010	0.013	0.029	0.016	0	0.018	0.027	0.016	0.010	0	0.017	0.029	0.038	0.005
43.4	0.013	0.017	0.036	0.020	0.001	0.021	0.034	0.020	0.013	0.0005	0.020	0.035	0.046	0.006
49.6	0.015	0.020	0.043	0.024	0.001	0.023	0.041	0.023	0.015	0.0005	0.023	0.040	0.054	0.007
55.8	0.019	0.024	0.051	0.028	0.0015	0.028	0.050	0.027	0.019	0.001	0.027	0.046	0.063	0.008
62.0	N/A	0.029	0.064	0.033	0.002	0.050	0.062	0.032	0.024	0.001	0.030	0.051	0.072	0.009
68.2	N/A	0.037	0.080	0.041	0.002	0.048	0.078	0.039	0.030	0.0015		0.060	0.082	0.010
74.4	N/A	0.044	0.093	0.048	0.0025	0.049	0.091	0.045	0.034	0.002		0.073	0.098	0.012
80.6	N/A	0.051	0.108	0.056	0.003	0.055	0.105	0.051	N/A	0.0025		0.094	0.120	0.015
86.8	N/A	0.098	0.188	0.107	0.0035	0.105	0.190	0.095	N/A	0.004		0.115	0.154	0.017
93.0	N/A	0.114	0.217	0.124	0.004	0.120	0.219	0.110	N/A	0.005		0.136	0.187	0.020
99.2	N/A	N/A	N/A	N/A	N/A	N/A	N/A	N/A	N/A	N/A		0.157	0.221	0.023
105.4	N/A	0.131	0.258	0.143	0.005	0.138	0.252	0.128	N/A	0.006		0.184	0.254	0.026
111.6	N/A	0.149	0.289	0.161	0.007	0.156	0.282	0.144	N/A	0.007		0.244	0.296	0.031
117.8	N/A	0.171	0.332	0.186	0.010	0.177	0.322	0.165	N/A	0.008		0.308	0.397	0.035
124.0	N/A	0.240	0.449	0.251	0.015	0.241	0.438	0.229	N/A	0.012		0.391	0.502	0.058
130.2	N/A	0.390	0.735	0.434	0.026	0.417	0.720	0.378	N/A	0.012		0.478	0.621	0.070
133.5	N/A	0.816	1.616	0.924	0.031	0.889	1.604	0.795	N/A	0.012		0.568	0.747	0.080

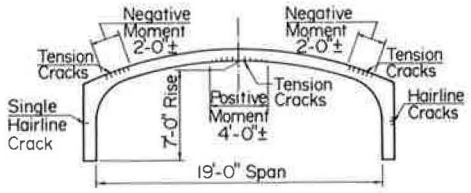

FIGURE 7 Crack patterns.

OBSERVATIONS FOLLOWING TEST

Wide cracks had opened up in the ground surface above both culvert legs indicating horizontal movement of the backfill. Mounding the fill over the culvert in place of complete burial reduced the capacity of the soil to resist the horizontal thrusts. This mounding is apparent in Figures 5 and 6.

Approximately 5 days after the load test, the backfill was removed and the test culvert was exposed. Considerable tension cracking (¼ in. to ⅜ in. wide) occurred in the span at the edge of the haunch section where the wall thickness is 10 in. (see Figure 7 for crack pattern sketches). The backfill at the base of the legs was cleaned away. The grout between the precast leg and the top of the footer was inspected. On the exterior side of the legs, the grout did not crack. No horizontal movement of the precast legs could be detected. The maximum deflection recorded at 1 ft above the foundation was 0.03 in. The precast legs appeared to rotate on the footer.

The tension steel at each of the major cracks was exposed and inspected. At every location the individual wires had elongated, necked down, and cracked. At the mid-span, positive moment area, this feature was characteristic across the full 8-ft cross section. In no instance did the compression face of each high moment area show any signs of distress.

With respect to the load test, the following items are concluded:

1. When the test culvert failed, three distinct hinges formed: two at the haunches and one at the mid-span. At all three locations the tension steel yielded and failed.
2. The legs of the test culvert rotated on top of the footer. The passive pressure resistance of the backfill and the resisting friction force kept the legs from moving horizontally. A pinned connection at the base of the legs can be assumed.
3. After the test culvert formed, three hinges and the tension steel failed at the three hinges, the test unit continued to support the 133.5-kip load. It appeared that the backfill's pressure against the back of the culvert's legs provided the necessary support to sustain this load.

After the testing was complete, the test culvert's actual material properties were determined and used as input for the computer analysis of the test section (Table 4). Samples of the welded wire fabric representative of the steel used in the test unit were submitted to the ODOT Bureau of Testing. A concrete core from the test unit was obtained and submitted to CTL for testing. Samples of the backfill material were also submitted to CTL to determine the density, sieve analysis, and the California bearing ratio value of the granular backfill. The mesh layout (Figure 8) for the computer model was revised to simulate the actual ground surface.

COMPARISON OF ACTUAL AND PREDICTED DEFLECTIONS

As stated, the primary purpose of the test was to compare results obtained from the load test with the results predicted from a CANDE computer analysis. Shown in Figure 9 is a graph of center-line deflections from the load test and the corresponding values determined from the analysis using the actual material properties as input for the program. Also shown is a single curve representing the predicted mid-span deflection based on the original design specifications.

TABLE 4 MATERIAL PROPERTIES

		Actual	Original Specifications
Concrete compressive strength (f'_c)		7,275 lb/in^2	4,000 lb/in^2
Steel yield stress (fy)	*W*5.5	78,610 lb/in^2	60,000 lb/in^2
	*W*10.0	71,360 lb/in^2[a]	60,000 lb/in^2
Steel areas	*W*5.5	0.32 in^2/ft[b]	0.33 in^2/ft
	*W*10.0	0.62 in^2/ft	0.63 in^2/ft
Backfill material			
Compaction		95 percent maximum dry weight	
Classification		*GW, GP*	
"*d*" distance from centroid of the steel reinforcement to the compressive surface			
	*W*5.5	7.75 in.	8.0 in.
	*W*10.0	8.25 in.	8.5 in.

[a] Value used as input for analysis.
[b] Because the *W*5.5 mesh has a higher yield stress than the *W*10.0, the steel area was increased to 0.36 in./ft to compensate for the use of the lower yield stress as the input value in the analysis.

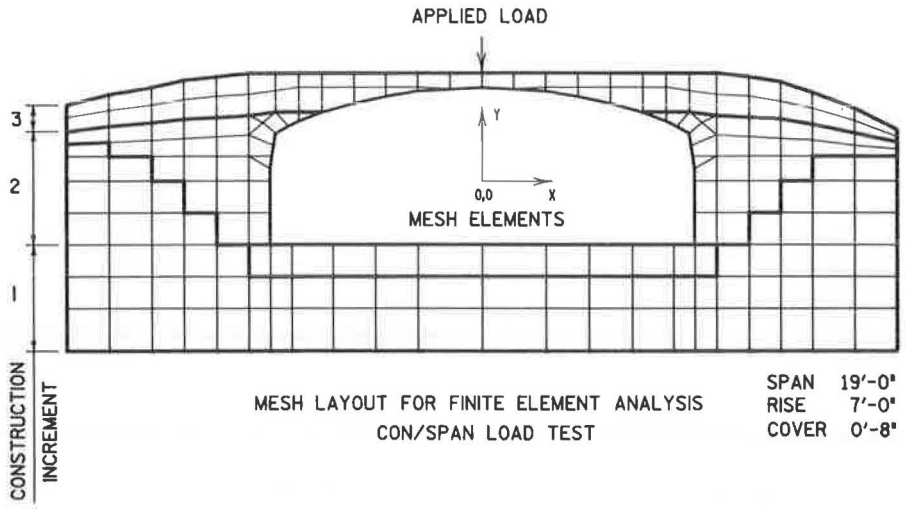

FIGURE 8 Mesh layout for finite element analysis: Con/Span load test.

The comparative values of deflection are in good correlation with each other, although the theoretical values are slightly larger. These larger theoretical deflections result from initial differences in the stiffness of an uncracked section and cracking strain. The theoretical value used for the cracking strain is based on the American Concrete Institute (ACI) recommendation for the tensile rupture strength equal to $7.5\ f'_c$. Of all the parameters, the concrete cracking strain influences the shape of the load-deformation curve the most significantly. The actual value of the tensile rupture strength is normally higher, which would have resulted in a closer correlation through the elastic range.

The sharp deflection occurring at 3½ times the service load on the actual deflection curves is the transfer of loading from the concrete to the steel as the cracking propagates throughout the section. The analysis models the cracking, progressing gradually through the section and producing a smooth stress-strain curve. Also causing this sudden deflection would be the initial cracking at the section just above the haunch, which theoretically occurs two load steps earlier. However, the pattern has been that the theoretical action occurred slightly before the actual action and would have occurred almost simultaneously if a higher value for the cracking strain had been used.

The CANDE analysis assumes plastic flow occurs when the stress in the steel is equal to its yield strength, and the analysis does not identify ultimate tensile or rupture strength of the steel. The actual stress in the steel can increase above the yield stress to its ultimate tensile strength. This is evident from the test in the area of 4 times the service load. The theoretical load-deformation curve flattens out when yielding occurs at midspan, indicating the beginning of the plastic range. The actual curve does not flatten out until two load increments later, indicating its additional load-carrying capacity above initial yield. The test culvert stopped taking additional load once the steel reached its ultimate tensile strength, and the load test was stopped when the steel necked down and cracked, producing excessive deflections. This point on the theoretical curve cannot be identified because the analysis cannot predict the steel's ultimate strain.

A CANDE analysis was run using the same loading on the culvert without backfill or cover. Its load-deformation curve was nearly identical until the loading reached 4½ times the service load, at which time the effects of the support from the backfill were realized. This comparison reveals the inherent strength in the unit itself.

The deflections predicted for the original specifications also predict a substantial capacity above and beyond the required ultimate strength. Although the CANDE analysis does not clearly indicate a load limit, it can be said that the ultimate load is reached when the slopes of the load-deflection curves approach a flat line. Based on this, it appears that the load-carrying capacity of the culvert would have exceeded the required ultimate strength by 50 percent at approximately 4¼ times the design service load, had it been built according to the original specifications.

COMPARISON OF CANDE ANALYSIS WITH CONVENTIONAL ANALYSIS

A comparison was made of moments at mid-span of the culvert using a conventional stress analysis and the CANDE analysis both with backfill and without. The conventional analysis was used, first, with the culvert legs considered restrained (pin-pin), and second, with horizontal movement allowed (pin-roller) as shown in Figure 10. Assuming a conventional elastic analysis, the maximum load carried by the pin-roller structure would be approximately 48 kips. At this point, using conventional concrete design, the steel would yield at mid-span and no further increase in capacity could be mobilized. The conventional analysis for the pin-pin condition would permit a capacity of approximately 65 kips. At this point the steel yields near the haunches. Some increased loading could be sustained but cannot be predicted by an elastic analysis.

The CANDE analysis uses a more sophisticated method of computing the actual section capacity than the standard Whitney rectangular stress distribution block method used in conventional design. This, together with consideration of the benefits of the extra capacity resulting from the axial compression on the section, yields a higher limit to the elastic range than in conventional design. Beyond this point CANDE analysis continues to model the structural response through the in-

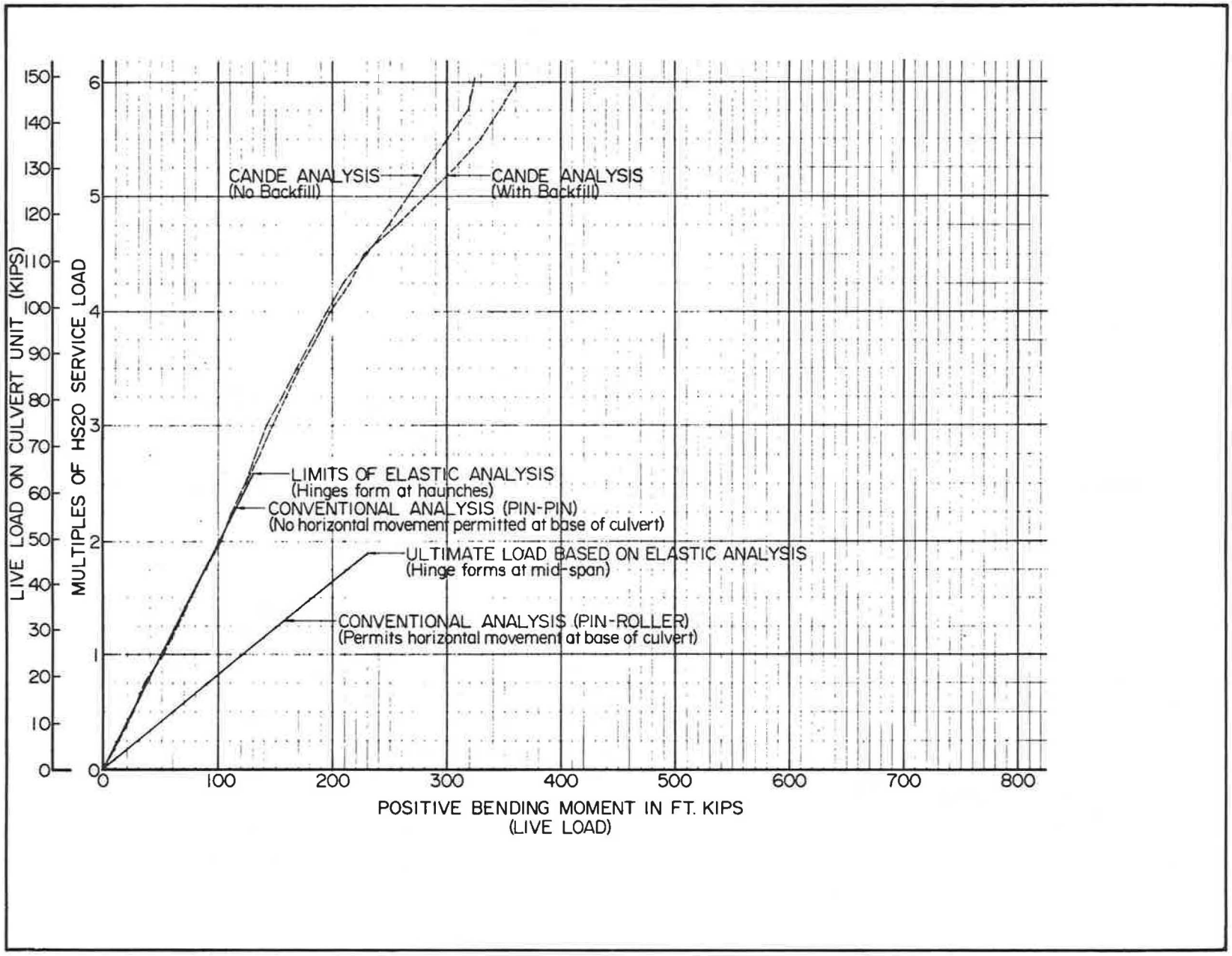

FIGURE 10 Precast box-arch load test: comparison of analyses.

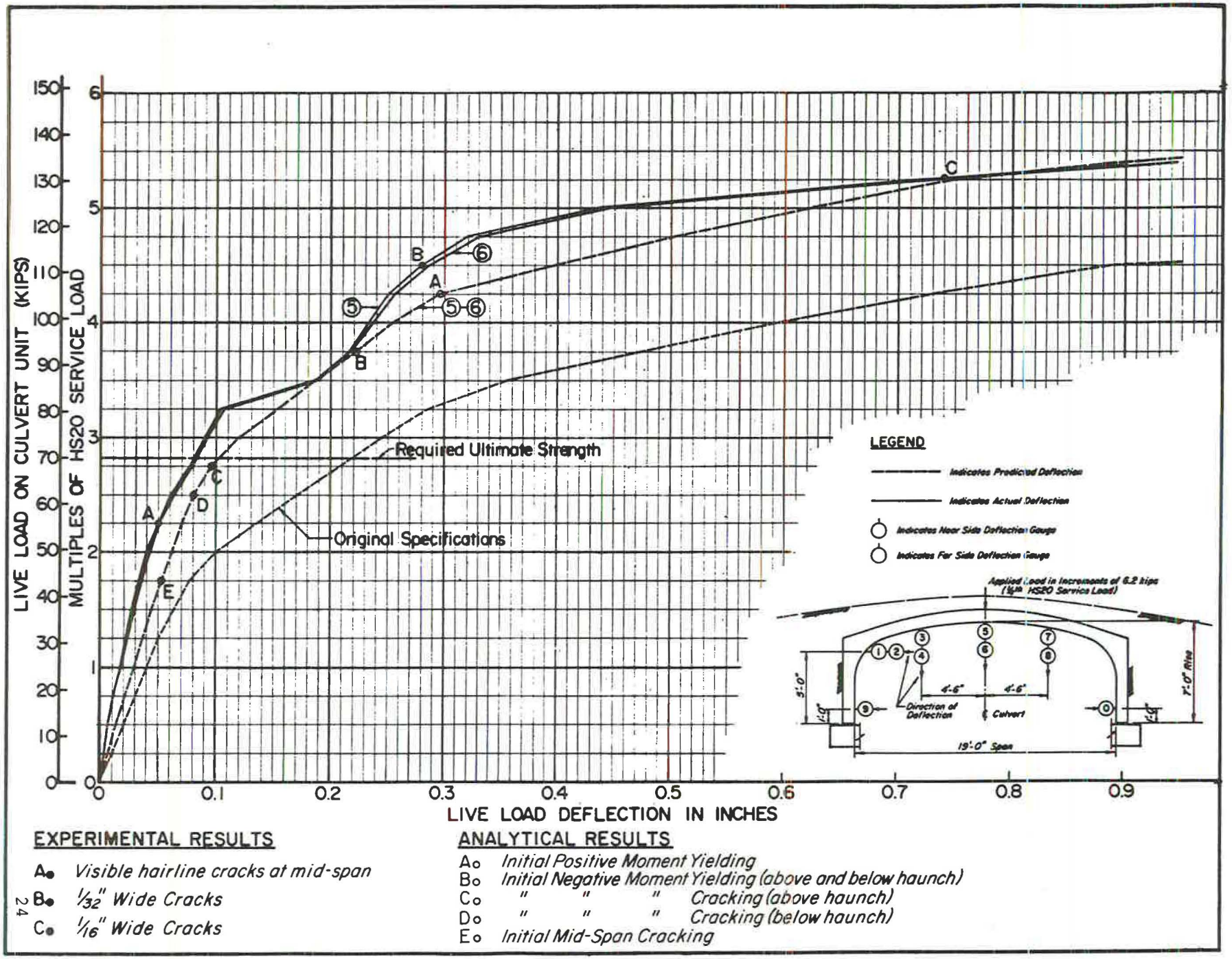

FIGURE 9 Precast box-arch load test: actual and predicted deflections.

Failure of Flexible Long-Span Culverts Under Exceptional Live Loads

RAYMOND B. SEED AND JEFFREY R. RAINES

Despite recent advances in the ability of nonlinear finite element analysis methods to model soil-structure interaction phenomena associated with buried flexible culverts, there are currently few published full-scale field data available for evaluation of the accuracy and reliability with which nonlinear finite element methods model the influence of live vehicle loads on culvert stability. Presented in this paper are the results of finite element analyses of three full-scale field cases involving culvert failure under exceptional live (vehicle) loads. Field evidence in all three cases suggests that the live loadings applied only barely exceeded the structural capacities of the culvert systems so that these three case studies provide a good basis for evaluation of the accuracy and reliability of the finite element analysis methods employed in these studies. A new empirical procedure is employed in these studies to develop equivalent line loads used to provide a representative plane strain modeling of actual discrete vehicle wheel loads. The results of these case studies provide good support for the accuracy and reliability of the analytical procedures used in these studies.

The past 15 years have seen steady improvement in the ability of nonlinear finite element analysis methods (FEM) to model and analyze soil-structure interaction phenomena associated with buried flexible culvert structures. Full-scale case studies and observed long-term successful performance of culvert designs based on such analysis methods suggest that incremental FEM are now able to model backfill loading and compaction-induced stresses with good accuracy for many types of culvert and backfill configurations and conditions.

Unfortunately, however, there are few published data currently available on the ability of nonlinear FEM to correctly model the influence of surficial live (vehicle) loads on culvert stability. This stems, in part, from the large expense associated with performance of meaningful full-scale live load tests to failure or near-failure conditions, as well as from the understandable reluctance of engineers and culvert manufacturers to disseminate information on field cases involving live-load-induced culvert distress or failure, or both. The study of such field cases involving distress or failure would represent an excellent basis for evaluation of the ability of FEM to accurately model live load effects on culvert stability.

Presented in this paper are the results of finite element analyses of three field cases involving culvert distress or failure resulting from inadvertent application of exceptional live loads, where exceptional live loads are vehicle loads considerably in excess of allowable design loading. Two of the cases considered involve long-span flexible pipe arch culverts, and the third case involves a 15-ft span flexible box culvert structure. All three of these cases are of particular interest because field evidence suggests that the live loadings applied only barely exceeded the structural capacities of the culvert systems. Back-analysis of these cases, therefore, provides an excellent basis for evaluation of the accuracy and reliability of the nonlinear FEM used to model these live load effects.

R. B. Seed, Department of Civil Engineering, University of California, Berkeley, Calif. 94720. J. R. Raines, Department of Civil Engineering, Stanford University, Stanford, Calif. 94305.

COOPER CITY PIPE ARCH CULVERT STRUCTURES

The first two case studies involve a pair of long-span corrugated aluminum pipe arch culverts near Cooper City, Florida, that were damaged by exceptional live loads during construction in 1985 and 1986. Both structures have since been repaired and have performed well under design live loading conditions.

28-Ft Span Pipe Arch

Shown in Figure 1(*a*) is a schematic cross-section of a long-span pipe arch culvert that was damaged by exceptional live loading in September of 1985. The structure is a corrugated aluminum pipe arch culvert with a span of 28 ft 5 in. and a rise of 17 ft 10 in. installed to provide a canal overpass. The culvert consists of 0.15-in.-thick 9- × 2 1/2-in. corrugated aluminum plate with Type IV aluminum stiffening ribs spaced at 54 in. on center across the crown. The structure was designed to support HS-20 live traffic loads (32 kips on a single axle) at the final backfill configuration, which would consist of 4 ft of backfill cover over the crown with a concrete relieving slab occurring immediately above the crown of the culvert.

Conditions at the time of culvert damage are illustrated in Figure 1(*a*). The backfill was only partially completed, and had not yet reached the crown of the structure. At this stage of backfill placement, long-span culverts were vulnerable to damage by large vehicle loads occurring above the culvert crown with shallow soil cover, and such large vehicle loads were thus disallowed by design specifications for backfill placement and compaction procedures. Nonetheless, early on the morning of September 3, 1985, a large 16-yd^3 dump truck carrying backfill arrived at the project before routine backfill operations began and passed close alongside the structure, depositing its material. Photographic evidence of tire tracks indicate that the closest rear wheel of the truck travelled parallel to the culvert at a lateral distance of approximately 2 ft from the exposed structure, as indicated in Figure 1(*a*).

elastic range, revealing its true reserve capacity beyond the first incidence of steel yielding.

CONCLUSIONS

The objectives of the load test were to validate the structural integrity of the box-arch culvert section and to verify that the computer model generated by the modified CANDE program provided a valid representation of the structural behavior of the buried culvert.

The structure greatly exceeded all performance requirements for highway loading. It carried a load greater than 5 times an HS20 design service load without impact and sustained the load through succeeding deformations imposed by the loading jack. The required ultimate capacity, including impact, was 2.8 times the service load. Material tests indicated that actual steel and concrete strengths were somewhat higher than the values used in the design. Correcting the analysis for the effect of these higher strength materials still resulted in a conservative design.

The CANDE program has been demonstrated by many others to be a reliable method to use to model the performance of buried structures. Because of the relatively high stiffness of the culvert, the predominant effect in this test was the structural behavior of the precast unit. The soil-structure interaction would have increasing and earlier effects for longer spans, higher fills, and level ground surfaces above the structure.

ACKNOWLEDGMENTS

The author wishes to acknowledge the help of the following: John Hurd, hydraulics research engineer, Ohio Department of Transportation; Philip Colflesh, sales engineer, Universal Concrete Products, Inc., Columbus, Ohio; and Manooch Zoghi, assistant professor, University of Dayton, Ohio.

REFERENCES

1. *Con/Span Specifications for Manufacture and Installation of Con/Span Culverts*. Con/Span Culvert Systems, Dayton, Ohio, August, 1986.
2. *Con/Span Culvert Load Testing Report*. CTL Engineering, Inc., Columbus, Ohio, Aug. 19, 1986.
3. M. G. Katona, P. D. Vittes, C. H. Lee, and H. T. Hoc. *CANDE 1980: Box Culverts and Soil Models*. Report FWA/RD-80/172, Federal Highway Administration, U.S. Department of Transportation, May 1981.
4. M. G. Katona, J. M. Smith, R.S. Odello, and J. R. Allgood. *CANDE—A Modern Approach for the Structural Design and Analysis of Buried Culverts*. FHWA Report RD-77-5, Oct. 1976.

Publication of this paper is sponsored by Committee on Subsurface Soil-Structure Interaction.

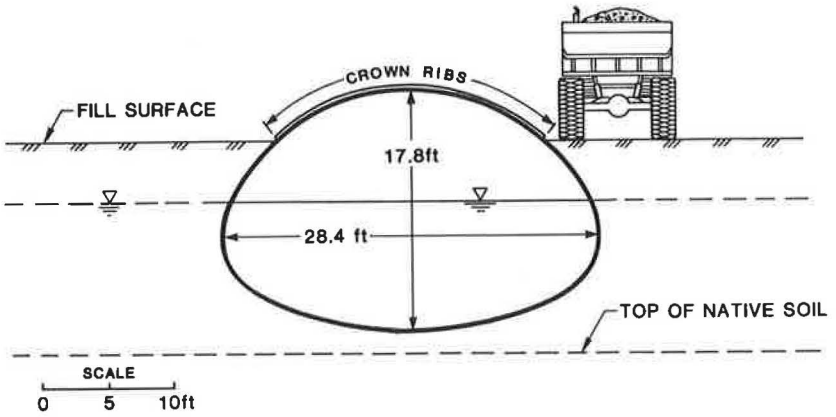

(a) Schematic Cross-Section Showing Backfill Configuration and Critical Live Vehicle Loading at Failure Conditions

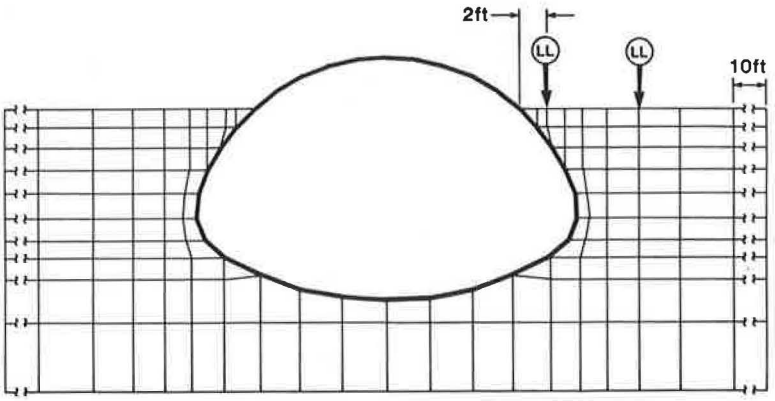

(b) Finite Element Mesh Representing Conditions at Failure

FIGURE 1 Twenty-eight-ft span pipe-arch culvert structure near Cooper City, Florida (a) Schematic cross-section showing backfill configuration and critical live vehicle loading at failure conditions, (b) Finite element mesh representing conditions at failure.

This resulted in inward flexural failure of the upper quarter region of the culvert along a length of approximately 40 ft of the culvert (whose total length was approximately 200 ft), as illustrated schematically in Figure 2. This "failure" was neither rapid nor catastrophic in nature, as the truck drove off the fill without difficulty and the deformations of the buckled zone did not lead to full culvert collapse with the vehicle loading thus removed. This, along with observations made during subsequent excavation and repair (by plate replacement) of the damaged culvert region, suggests that this exceptional live loading barely induced failure. As a result, this failure represents an excellent opportunity to evaluate the ability of finite element analyses to correctly model live load effects on culverts.

Figure 2 is a schematic illustration of the observed deformation modes of the failed culvert region. The large live load in close proximity to the structure resulted in inward flexure of the upper quarter-point region of the culvert, with formation of two plastic hinges representing failure in flexure at Points *A* and *B*. These hinges were manifested as clearly visible creases in the corrugated structural plate. Careful inspection of the structure revealed no additional plastic hinge in the region between Point *A* and the crown of the structure; instead, deformations in this upper region were related to smoother curvature spread more evenly over the rib-reinforced crown. There was no sign of flexural failure in this upper crown region.

Finite element analyses were performed to model this failure using the program SSCOMP (*1*), a plane strain finite element code for incremental nonlinear analysis of soil-structure interaction. The finite element mesh used for these analyses is shown in Figure 1(*b*). Soil elements were modeled with four node isoparametric elements and the culvert structure was modeled with piecewise linear beam elements. Nonlinear stress-strain and volumetric strain soil behavior was modeled using the familiar hyperbolic formulation proposed by Duncan et al. (*2*), as modified by Seed and Duncan (*3*), and structural behavior was modeled as linear elastic. Nodal points at the base boundary were fixed against translation, and nodal points at the right and left boundaries were fixed against lateral translation but were free to translate vertically. The analyses were performed in steps or increments, incrementally modeling layerwise placement of backfill and then, ultimately, the application of live loads representing the 16-yd^3 dump truck.

The backfill material was a loosely dumped gravel (GW)

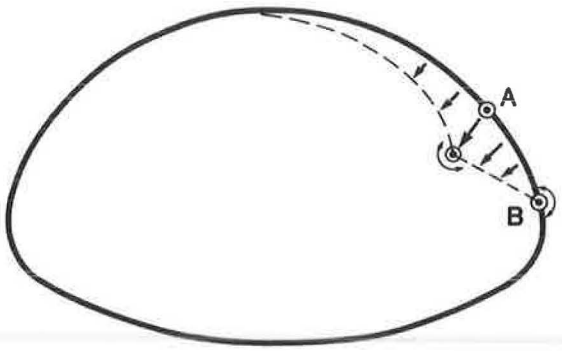

FIGURE 2 Schematic representation of observed failure mode of 28-ft span pipe-arch culvert near Cooper City, Florida.

below the water table, and a fine silty sand (SM) compacted to a minimum of 90 percent relative compation (modified AASHTO, ASTM D1557) above the water table. The foundation soil was a partially cemented silty clayey sand (SM), which was judged to have properties similar to the upper compacted backfill zone. Listed in Table 1 are the hyperbolic soil model parameters used to model the foundation soils and the upper and lower backfill zones. All parameters are effective stress parameters, and water table effects were modeled by using buoyant unit weights below the water table.

Listed in Table 2 are the properties used to model the various components of the culvert structure. Elastic section moduli for the corrugated aluminum plate sections are based on large-scale flexural test data. Section moduli of the ribbed crown section were modeled as intermediate between the theoretical value for the crown plate and ribs functioning as a composite beam and the theoretical value for the ribs and crown plate each functioning independently. This is again based on large-scale flexural test data and represents the effects of shear slippage at the plate and rib connections. The ultimate plastic moment capacities listed in Table 2 are also based on large-scale flexural test data.

The dashed line in Figure 3 shows the calculated bending moments around the perimeter of the culvert structure resulting from placement of backfill up to the elevation shown in Figure 1, but without additional live load application. The maximum calculated bending moments in the crown and upper haunch (shoulder) regions are approximately 0.92 kip-ft/ft and 0.98 ft/ft, representing factors of safety (FS) of approximately

TABLE 1 HYPERBOLIC SOIL MODEL PARAMETERS USED TO MODEL COOPER CITY CULVERT BACKFILL AND FOUNDATION SOILS

	Foundation Soil	Backfill Below Water Table	Backfill Above Water Table
γ(lb/ft^3)	63	78	125
K	450	400	450
n	0.25	0.4	0.25
R_f	0.7	0.7	0.7
K_b	350	120	350
m	0	0.2	0
c	0	0	0
ϕ	34°	36°	34°
$\Delta\phi$	6°	4°	6°

TABLE 2 STRUCTURAL PROPERTIES USED TO MODEL 28-FT-SPAN COOPER CITY PIPE-ARCH CULVERT STRUCTURE

Structural Component	Modulus: E (kip/ft^2)	Area (ft^2/ft)	I ($\times 10^{-4}$) (ft^4/ft)	Plastic Moment Capacity: M_p (kip-ft/ft)
Crown with ribs	1,468,800	0.018	1.86	6.82
Invert and haunches	1,468,800	0.015	0.72	3.18

FS $\approx$ 7.4 and FS $\approx$ 3.2 with respect to flexural failure in these two regions, respectively, at this stage of backfill placement.

The plane strain finite element formulation used for these analyses requires that the actual discrete vehicle wheel loads be represented by one or more equivalent (plane strain) line loads. A number of procedures have been employed for developing such representative line loads, but none has gained universal acceptance. The procedure used in this study to develop equivalent line loads providing representative plane strain modeling of discrete vehicle wheel loads is a slightly modified version of an equivalent line load estimation procedure proposed by Duncan and Drawsky (*4*).

Duncan and Drawsky proposed that the equivalent line load used to model a wheel or an axle with several wheels should be the line load that provides the same maximum vertical stress beneath the wheel(s) on a plane at the depth of the top of the culvert crown as would the actual three-dimensional wheel loading, based on Boussinesq (*5*) linear elastic vertical stress distribution analysis. This approach is inherently slightly conservative because it provides a line load producing this peak stress along the full length of the culvert, whereas discrete wheel loads provide this stress only beneath the actual wheels, with lesser stresses away from the wheel loading points. This inherent conservatism is minimized, however, in corrugated culverts, which do not have significant flexural stiffness longitudinally along the culvert and which are, therefore, vulnerable to localized overstressing directly beneath discrete wheel loads.

Duncan and Drawsky developed a simple equation and tabulated solution expressing their equivalent line load estimation procedure as

$$LL = AL/K4 \quad (1)$$

where

LL = equivalent line load (kips/ft),
AL = total axle load (kips), and
$K4$ = load factor (ft).

Presented in Table 3 are the $K4$ values developed by Duncan and Drawsky based on Boussinesq elastic analyses for various depths of soil cover, where depth of soil cover (Hc) is defined as the vertical distance from the base of the wheel(s) to the top of the culvert.

This equivalent base of the wheel(s) to the top of the culvert.

This equivalent line load estimation procedure was modified in this study by defining equivalent depth of soil cover (Hc) as the shortest radial distance from the base of a wheel load to the culvert plate, and then by using the same $K4$ values as shown in Table 3. This modification provides improved

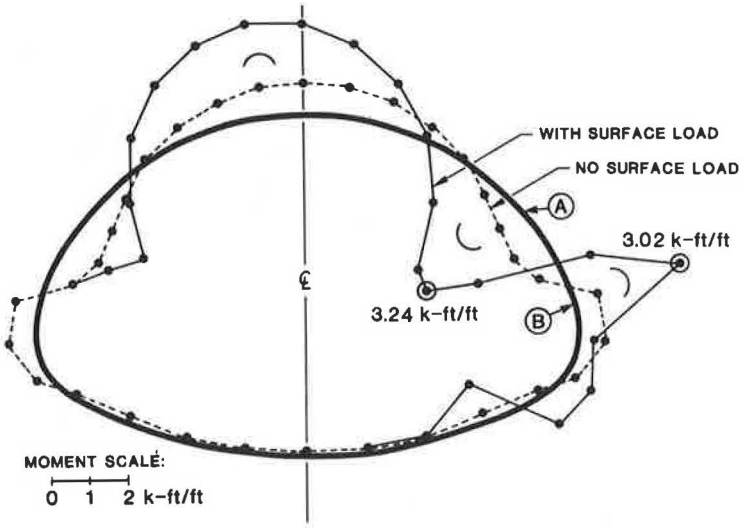

FIGURE 3 Calculated bending moments with and without live load application: 28-ft span pipe-arch culvert.

modeling of live loads not centrally located above the culvert crown.

The fully loaded 16-yd³ dump truck that precipitated the first Cooper City culvert failure had a rear axle load of approximately 46 kips. Allowing for several inches of observed rutting or tire indentation into the backfill surface, the equivalent depth of cover for the rear wheel of the truck closest to the culvert was approximately 2 ft, corresponding to a value of $K4 = 5.3$ ft. This rear wheel was therefore modeled with an equivalent line load of LL $\approx$ 46 kips/5.3 ft = 8.68 kips/ft applied at a lateral distance of 2 ft from the culvert at the fill surface, as shown in Figure 1(*b*). The front and right-hand side wheels of the truck were sufficiently far from the loading region of interest to have had a negligible additional effect on culvert stresses in the region of interest (this was verified by means of additional three-dimensional stress distribution analyses considering all four wheels).

The solid line in Figure 3 indicates the calculated bending moments around the perimeter of the culvert following modeling of application of an equivalent surface line load of 8.68 kip-ft/ft 2 ft from the culvert, as shown in Figure 1(*b*). This live load application caused a large increase in bending moments in the upper haunch (shoulder) and crown regions, as shown in Figure 3, and resulted in a calculated moment of 3.24 kip-ft/ft at a point in the upper haunch region shortly below the crown stiffening ribs. This barely exceeds the plastic moment capacity of 3.18 kip-ft/ft at this point (as listed in Table 2) and would be expected to result in formation of a plastic hinge. The location of this hinge closely corresponds to the actual observed hinge location at Point *A* in Figure 2. A second large bending moment occurs approximately at the location of the second observed plastic hinge at Point *B*.

The calculated factor of safety (FS) at this location is $\approx$ 3.18/3.02 = 1.05, and this would appear to provide satisfactory agreement with field observations, suggesting that flexural failure barely occurred. The maximum calculated crown moment is 2.64 kip-ft/ft, and thus represents a FS $\approx$ 6.82/2.64 = 2.6 in the rib-reinforced crown region, and so agrees with the observation of some bending but no plastic hinge formation in this region.

These analyses provide surprisingly good agreement with field observations inasmuch as (a) they correctly predict the approximate location and occurrence of the two observed plastic hinges at Points *A* and *B*, (b) they correctly predict no third plastic hinge formation in the crown region, and (c) they concur with field observations that the distressed culvert region barely failed. Nonlinear finite element analyses employing the modified Duncan-type live load modelling assumption thus appear to provide excellent prediction of observed field behavior for this case study.

Subsequent to this live-load-induced failure, the pipe-arch culvert structure was excavated and the damaged corrugated structural plate was replaced. The remaining backfill and relieving slab were then placed. The structure has since performed successfully under its original design live loading conditions, including overpassage by the same type of fully loaded 16-yd³ dump trucks as those that caused the initial culvert distress.

TABLE 3 VALUES OF K_4 FOR CALCULATION OF EQUIVALENT LINE LOADS REPRESENTING SURFACE VEHICLE LOADS (after Duncan and Drawsky, 1983)

Cover Depth H_c (ft.)	Values of K_4 (ft.)		
	2 Wheels/Axle	4 Wheels/Axle	8 Wheels/Axle
1	4.3	5.0	8.5
2	5.3	6.4	9.2
3	7.9	8.7	10.6
5	12.3	12.5	13.5
7	14.4	14.5	14.6
10	16.0	16.0	16.0
20	28.0	28.0	28.0

27-Ft Span Pipe Arch

A second, similar pipe-arch culvert structure also in a canal near Cooper City, Florida, was damaged by inadvertent exceptional live loading in August 1986. A schematic cross-section of this second culvert is shown in Figure 4(*a*). The

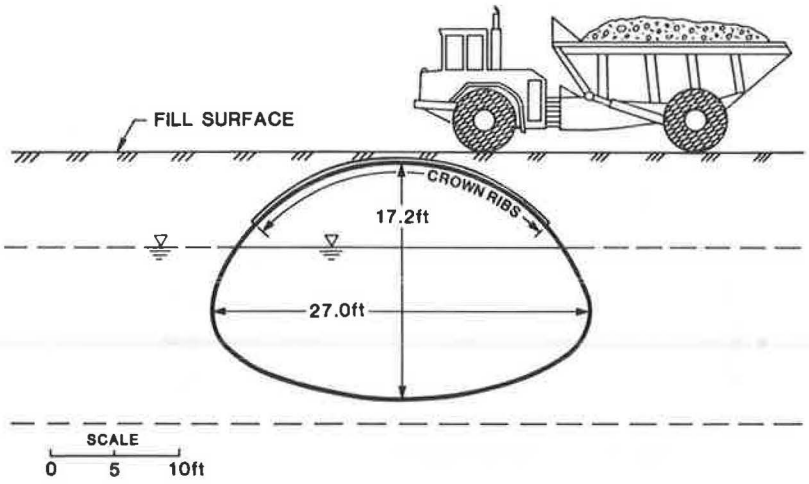

(a) Schematic Cross-Section Showing Backfill Configuration and Critical Live Vehicle Loading at Failure Conditions

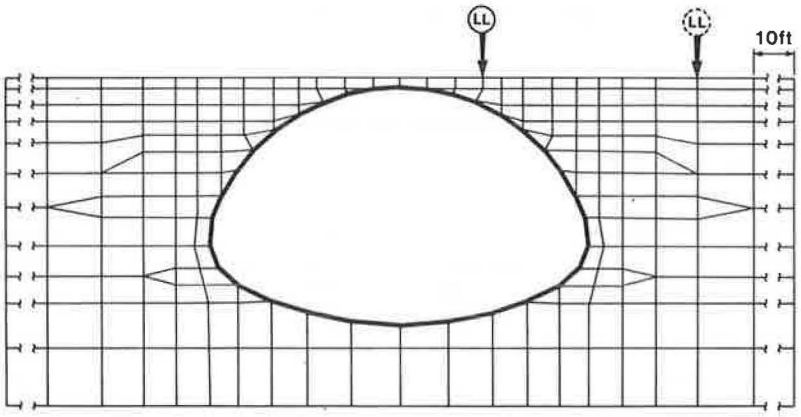

(b) Finite Element Mesh Representing Conditions at Failure

FIGURE 4 Twenty-seven-ft span pipe-arch culvert structure near Cooper City, Florida (a) Schematic cross-section showing backfill configuration and critical live vehicle loading at failure conditions, (b) Finite element mesh representing conditions at failure.

structure has a span of 27 ft and a rise of 17 ft 2 in. The culvert consists of 0.125-in.-thick 9 × 2 1/2-in. corrugated aluminum plate with Type II aluminum stiffening ribs spaced at 54 in. on center across the crown. Backfill and foundation soils are essentially the same as those described previously for the 28-ft span pipe arch culvert, and the structure had a 10-in.-thick concrete relieving slab immediately above the crown of the structure, overlain by an additional 8 to 10 in. of compacted crushed shell and stone intended as a road base.

The relieving slab covered the entire central portion of the culvert, which was designed to carry HS-20 live traffic loading. Unfortunately, after completion of slab construction, backfill placement, and even road paving before installation of road curbs, a fully-loaded 16-yd^3 dump truck traveled off the edge of the paved zone and collapsed the crown of the end of the culvert outside the zone protected by the concrete relieving slab. A schematic illustration of conditions at the time of this failure is shown in Figure 4 (*a*). The large truck halted (parked) with its front wheels approximately 6 ft from the center line of the culvert, and the collapse proceeded fairly slowly with the front axle of the truck descending slowly into the canal and the driver sustaining no injury.

This failure was modeled with the program SSCOMP using the same procedures as described previously. Figure 4(*b*) shows the finite element mesh used for these analyses. Backfill and foundation soils were similar to those described previously for the 28-ft span pipe arch culvert, and the soil model parameters listed in Table 1 were again used to model the foundation and backfill soils. Structural properties used to model the culvert itself differ slightly from those of the previous study; the structural properties modeled in this analysis are listed in Table 4.

TABLE 4 STRUCTURAL PROPERTIES USED TO MODEL 27-FT-SPAN COOPER CITY PIPE-ARCH CULVERT STRUCTURE

Structural Component	Modulus: E (kip/ft^2)	Area (ft^2/ft)	I ($\times 10^{-4}$) (ft^4/ft)	Plastic Moment Capacity: M_p (kip-ft/ft)
Crown with ribs	1,468,800	0.015	1.20	4.62
Invert and haunches	1,468,800	0.012	0.60	2.65

The equivalent line load used to provide a representative plane strain modeling of the actual discrete vehicle loading was again based on the modified Duncan empirical load estimation procedure. The front axle of the 16-yd³ dump truck carried a load of approximately 42 kips on two wheels. After allowing for observed rutting or tire indentation of approximately 8 in. in the unpaved backfill surface (the truck traveled off the paved surface underlain by the relieving slab), the remaining depth of soil cover between the base of the wheels and the top of the culvert plate was approximately 12 in., and the corresponding live load factor from Table 3 is $K4 = 4.3$ ft. This led to modeling of the front wheel loads with an equivalent line load of LL = 42 kips/4.3 ft = 9.8 kips/ft. The rear wheels of the truck were far enough from the structure so that they contributed negligibly to the culvert stresses. This was verified by performing analyses with and without modeling the rear axle as a line load of 10 kips/ft. Inclusion or omission of the rear axle line load changed the calculated bending moments in the culvert by less than 5 percent.

Calculated bending moments in the culvert before and after application of the 9.8-kip/ft. line load modeling the front axle of the truck is shown in Figure 5. The dashed line represents moments resulting from backfill loads only, and corresponds to an FS with respect to flexural failure of more than 3.0 throughout the crown region. The solid line represents moments with the live vehicle loading applied. The two points circled on this figure indicate bending moments of 4.64 kip-ft/ft and 8.31 kip-ft/ft, both of which equal or exceed the flexural plastic moment capacity of the culvert crown region, which is approximately 4.62 kip-ft/ft. This analysis, therefore, also appears to provide good agreement with observed field behavior, which in this case involved failure of the crown region in flexure.

RANCHO FLEXIBLE BOX CULVERT STRUCTURE

The third case study considered a 15-ft span corrugated aluminum box culvert structure near Rancho, California, that was crushed by a 95-kip scraper that passed over the crown of the structure, greatly exceeding the allowable design live loading, in March 1985. The structure has since been replaced and has performed well under design loading conditions.

A schematic cross-section of the box culvert and live load conditions at the time of failure is shown in Figure 6. The

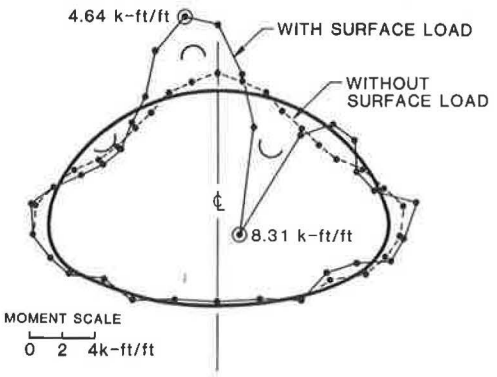

FIGURE 5 Calculated bending moments with and without live load application: 27-ft span pipe-arch culvert.

structure was a corrugated aluminum box culvert with a span of 14 ft 8 in. and a rise of 4 ft 1 in., installed to provide a roadway bridge over a stream. The culvert consisted of a 0.175-in.-thick 9 × 2 1/2-in. corrugated aluminum plate with Type IV aluminum bulb angle stiffening ribs at 27-in. spacing reinforcing the crown and upper haunch regions, and Type II aluminum bulb angle stiffening ribs at 27-in. spacing reinforcing the lower haunch regions. The culvert was cast into a full reinforced concrete invert slab. The structure was designed to support HS-20 live traffic loads at the final backfill configuration, which would consist of 24 in. of soil cover above the crown of the culvert overlain by a paved road surface.

In March 1985 the structure failed during inadvertent crossing by a fully loaded scraper with a total weight of approximately 95 kips. This crossing was the result of operator error, as such large vehicle loads were proscribed by both design and operating regulations.

This failure was modeled with the program SSCOMP using the same procedures as those described previously. The finite element mesh used for these analyses is shown in Figure 7. As the rear wheels of the scraper contributed negligibly to the failure, the problem was symmetric about the box culvert center line and only a half mesh was used. Nodal points out that the right-hand boundaries of this mesh were free to translate vertically but were fixed against both lateral translation and rotation. Backfill and foundation soils were a silty clay of low plasticity (CL) compacted to a minimum of 90 percent relative compaction (modified AASHTO, ASTM D1557), and were modeled with the following hyperbolic soil model parameters: $\lambda m = 125/ft^3$, $K = 150$, $n = 0.45$, Rf = 0.7, Kb = 110, m = 0.25, c = 400 ft² and $\phi = 30$ degrees. The structural properties used to model the box culvert and invert slab are listed in Table 5.

Examination after the failure showed that the box culvert structure failed when the front axle of the scraper was essentially directly over the center line of the box culvert. The surface of the fill had not yet been paved and the scraper wheels rutted or indented into the fill surface so that the effective backfill cover depth between the bases of the front wheels and the crown of the structure was approximately 18 or 19 in. The front axle load was approximately 60 percent of the total vehicle load, or about 57 kips, which greatly exceeded the 32 kip HS-20 single axle design load intended for a paved fill surface. This front axle load was again modeled as a representative equivalent line load based on the modified Duncan empirical load estimation procedure, with K4 − 4.85 ft. The 57-kip front axle load on two wheels with 19 in. of soil cover was thus modeled as an equivalent line load of 57 kips/4.85 ft = 11.8 kips/ft. One-half of this line load (5.9 kips/ft) was applied to the surface of the backfill above the culvert center line (at the extreme right edge of the finite element mesh shown in Figure 7).

The calculated bending moments in the box culvert before and after application of the 5.9 kip/ft line load modeling the front wheels of the scraper are shown in Figure 8. The dashed line represents moments caused by backfill loads only and these moments are small relative to the flexural capacities of the culvert crown and haunch regions. The solid line represents moments with the live vehicle loading applied. The maximum calculated bending moments of 14.0 kip-ft/ft and 12.6 kip-ft/ft at the center line and tops of the two haunches, respectively, both exceed the culvert plastic moment capac-

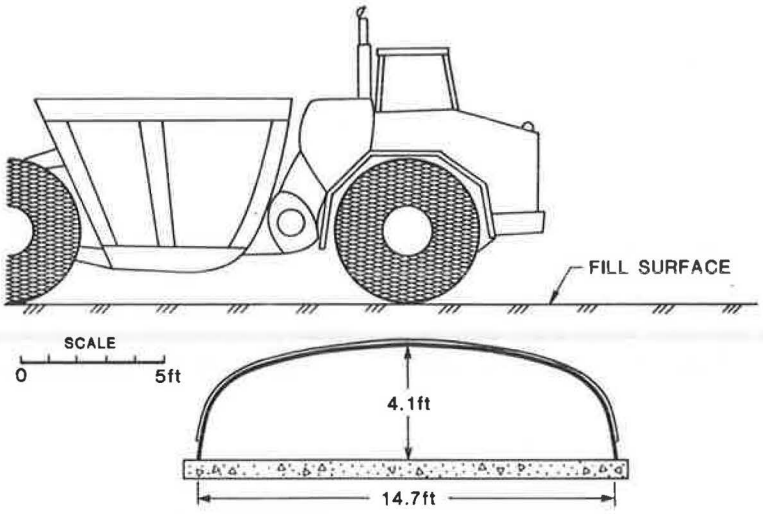

FIGURE 6 Schematic cross-section of the Rancho box culvert showing critical vehicle loading at the time of failure.

ities of 10.39 and 7.94 kip-ft/ft, respectively (as shown in Table 5). The locations of these calculated maximum moments closely correspond to the observed locations of flexural failure, as manifested by clearly discernible creasing and tearing of the corrugated aluminum structural plate. These analyses, therefore, appear once again to provide excellent agreement with observed field behavior.

SUMMARY AND CONCLUSIONS

Three full-scale field case studies were considered involving failure of flexible long-span culvert structures caused by exceptional live loads. Each case was analyzed using nonlinear FEM. An empirical procedure was proposed for developing equivalent line loads used to provide a representative plane strain modeling of actual discrete vehicle wheel loads. This empirical procedure represents a slight modification of an earlier procedure proposed by Duncan and Drawsky (*4*).

For all three field cases considered, the nonlinear finite element analyses performed provided excellent agreement with observed field behavior, correctly predicting not only failure conditions but also observed failure modes. This provides good support for the accuracy and reliability of the FEM and equivalent line load modeling procedures employed in these studies. This is particularly so because the case studies con-

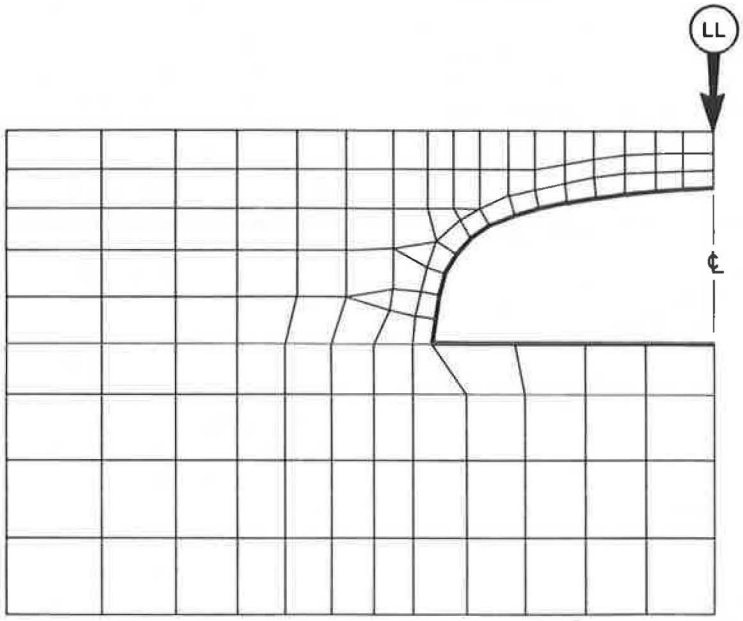

FIGURE 7 Finite element mesh representing the Rancho box culvert structure at the time of failure.

TABLE 5 STRUCTURAL PROPERTIES USED TO MODEL 15-FT-SPAN BOX CULVERT STRUCTURE AT RANCHO CALIFORNIA

Structural Component	Modulus: E (kip/ft²)	Area (ft²/ft)	I ($\times 10^{-4}$) (ft⁴/ft)	Plastic Moment Capacity: M_p (kip/ft/ft)
Crown with Type IV ribs	1,468,800	0.026	3.70	10.39
Invert and haunches with Type II ribs	1,468,800	0.022	2.72	7.94
Concrete invert slab	520,000	0.67	250	Large

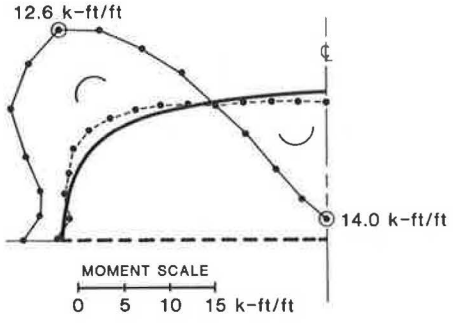

FIGURE 8 Calculated bending moments with and without live load application: 15-ft span Rancho box culvert.

sidered involve situations wherein field evidence suggests that the exceptional live vehicle loadings applied only barely exceeded the structural capacities of the culvert systems (structural capacities were exceeded by less than 10 percent for three of the six flexural failures predicted by the analyses performed) so that back analysis of these cases provides a good basis for evaluation of the accuracy and reliability of these analytical methods.

ACKNOWLEDGMENTS

Financial support for these studies was provided by Kaiser Aluminum and Chemical Corporation and by the National Science Foundation. The authors wish to express their gratitude to Kaiser Aluminum and Chemical Corporation for providing access to the three case studies considered in these studies.

REFERENCES

1. Raymond B. Seed and J. M. Duncan. *SSCOMP: A Finite Element Analysis Program for Evaluation of Soil-Structure Interaction and Compaction Effects.* Geotechnical Engineering Research Report UCB/GT/84-02, University of California, Berkeley, Feb. 1984.
2. J. M. Duncan, P. Byrne, K. S. Wong, and P. Mabry. *Strength, Stress-Strain, and Bulk Modulus Parameters for Finite Element Analyses of Stresses and Movements in Soil Masses.* Geotechnical Engineering Research Report UCB/GT/80-01, University of California, Berkeley, Jan. 1980.
3. Raymond B. Seed and J. M. Duncan. *Soil-Structure Interaction Effects of Compaction-Induced Stresses and Deflections.* Geotechnical Engineering Research Report UCB/GT/83-06, University of California, Berkeley, Dec. 1983.
4. J. M. Duncan and R. H. Drawsky. *Design Procedures for Flexible Metal Culvert Structures.* Geotechnical Engineering Research Report UCB/GT/83-02, University of California, Berkeley, May 1983.
5. J. Boussinesq. *Application des Potentials a L'Etude de l'Equilibre et du Mouvement des Solides Elastiques.* Gauthier-Villars, Paris, France, 1885.

Publication of this paper sponsored by Committee on Subsurface Soil-Structure Interaction.

Allowable Fill Heights for Corrugated Polyethylene Pipe

MICHAEL G. KATONA

Provided in this study are fill height tables and graphs that give the maximum allowable burial depth of regularly produced sizes of corrugated polyethylene pipe with diameters ranging up to 30 in. The employed design criteria satisfy the proposed American Association of State Highway and Transportation Officials specifications for service load design of plastic pipe including thrust stress, vertical deflection, flexural strain, and buckling. Both short-term and long-term polyethylene properties are used for the design evaluation, as well as the influence of soil type and compaction. Design solutions are determined with the aid of the CANDE computer program and compare favorably with laboratory test data. As a final result, knowing values for the inside and outside diameter along with the corrugated sectional area, an engineer may determine the maximum allowable burial depth for a 50-year design life by directly reading from the tables and graphs that are presented as a function of soil type and compaction. In addition, design guidelines are provided to interpolate the increase in allowable burial depths for design periods less than fifty years.

Corrugated pipe composed of high density polyethylene has become an economically attractive alternative to corrugated metal, clay, and reinforced concrete pipe in small-diameter culvert applications. Prior to this work, however, a rational set of tables and guidelines to determine the maximum allowable burial depth of corrugated polyethylene pipes has not been published in the open literature. Such fundamental information is required for a variety of applications, such as culverts under deep highway embankments.

Herein lies the objective of this paper. Using proven principles and techniques of soil-structure interaction analyses, tables are developed that give the maximum allowable fill height for corrugated polyethylene pipe based on structural considerations that take into account pipe size, corrugation geometry, backfill soil quality, and design life.

Pipe sizes (i.e., the inside diameters) considered in this study are 4, 6, 8, 10, 12, 15, 18, 24, and 30 in. For each pipe size, the corrugated sectional area (i.e., area resisting hoop compression per unit length of pipe) is treated as the major design variable. Coupled with each pair of values for pipe size and sectional area are polyethylene property variations for short- and long-term behavior. Also considered are soil property variations, ranging from fair to good quality dependent on soil type and level of compaction.

All combinations of these variables constitute the input data to the soil-structure analysis program, CANDE (*1*). Output is the allowable fill height as a function of input in conformance with the American Association of State Highway and Transportation Officials (AASHTO) design criteria and specifications (*2*). Details of the design input variables, design methodology, and final results are presented in sequential order.

The following limitations and restrictions should be kept in mind. Results are only applicable to high-fill installations, that is, live loads are negligible. The soil envelope surrounding the pipe is assumed homogeneous and properly compacted; this excludes the use of hard beddings or stiff inclusions, or both, as well as loose or soft backfill materials within two diameters of the pipe circumference. In spite of these restrictions, the overall design approach is very conservative so that the allowable fill heights may be used with a great deal of confidence.

CORRUGATED PLASTIC PIPE PROPERTIES

For structural analysis, the robustness of a corrugated pipe can be assessed by the hoop stiffness, which is proportional to the corrugated section area, and by the flexural (ovaling) stiffness, which is proportional to the corrugation moment of inertia. As will be shown later, the corrugated section area is the key section property that controls the allowable burial depth because thrust stress (hoop stress) is almost always the controlling design criterion. Accordingly, the moment of inertia does not influence the allowable burial depth as long as its value is greater than a certain minimum value that precludes deflection, flexural strain, or buckling from controlling the design.

Unlike the corrugated metal pipe industry, the manufacturers of corrugated plastic pipe do not employ a standardized set of corrugated shapes for each pipe diameter. Rather, a typical plastic pipe manufacturer makes only one corrugation size per pipe size. However, the corrugated shape made by one manufacturer and that of another may differ markedly in material thickness, shape, and height of the corrugation. The only geometric pipe property that is reasonably well standardized is the inside diameter, also called the pipe size.

A special study on the corrugated section properties was obtained from five of the largest plastic pipe manufacturers and is described as follows.

A STUDY OF CORRUGATED SECTION PROPERTIES

Manufacturers' Data

Shown in Figure 1 is a typical corrugated cross-section and listed in Table 1 are corrugated section properties reported

Ballistic Missile Division, P.O. Box 1310, San Bernardino, Calif. 92402.

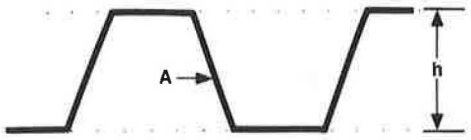

(a) Typical manufactured plastic corrugation.

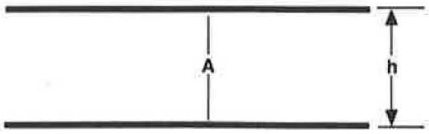

(b) Idealized maximum moment of inertia.

(c) Idealized minimum moment of inertia

FIGURE 1 Corrugated sections, with A and h constant.

by five of the largest plastic pipe manufacturers from a letter survey. The variation in section properties within each pipe size is readily apparent. This expected scatter of values, however, is amplified by computational errors in computing or reporting the section properties. Thus, a reliable method of determining corrugated section properties needs to be developed before a workable design methodology can be established. These issues are addressed for the corrugated section area, moment of inertia, and corrugation height in the following.

Section Area

A simple, yet reliable, method of determining the section area was suggested by William Altermatt of Hancor, Inc. The method entails weighing a pipe of length L, and measuring the inside and outside diameters. Knowing the density of polyethylene, the section area is then given by

$$A = 2W/[L\, d\, \pi\, (ID + OD)] \tag{1}$$

where

A = cross-sectional area (in.^{2}/in.),
W = weight of pipe (lb),
d = polyethylene density (lb/in.^{3}), high density polyethylene = 0.0344 lb/in.^{3},
ID, OD = inside and outside diameters (in.), and
π = 3.14.

Equation 1 is derived by equating the measured weight W to the product of the pipe's solid volume times the density d. The solid volume is given exactly by the product $2\pi ALR$, where R is the pipe's radius to the geometric centroid of the corrugated section. In Equation 1, it is assumed that the corrugation is symmetric so that R = (ID + OD)/4 (i.e., R is at mid-height of corrugation). For nonsymmetric corrugations, Equation 1 introduces a small error, but certainly less than 5 percent.

Following a second letter survey, the five manufacturers recomputed the section areas in accordance with Equation 1, and the results are shown in the last column of Table 1. It may be observed that these values show more uniformity than the original set, and it is believed that the variations that do exist in the revised properties reflect real differences between pipe products.

Moment of Inertia

As already stated, the moment of inertia does not influence the allowable burial depth because thrust stress usually controls the design. Thus, for design purposes, a relationship is sought that serves as a lower bound for the "actual" moment of inertia used in manufactured products. If it is found that the lower bound is adequate (i.e., thrust is still the weak link), then it can be assumed that the actual moment of inertia is adequate.

To establish a lower bound, consider the following expression for the moment of inertia, I:

$$I = Ah^2/z \tag{2}$$

where

A = corrugation sectional area,
h = height of corrugation = (ID − OD)/2, and
z = a constant, dependent on corrugation form.

Given that A is known (e.g., by Equation 1), and because h is easily measured, then the value of I in Equation 2 depends on the shape parameter z, that is, how the material is distributed about the centroid. Now the largest possible value for I would be achieved by splitting the net area into two parts separated by the corrugation height h, as shown in Figure 1(b). Although this is not physically possible because it does not leave any web material to connect the two parts, it is an upper bound for I from which the parameter z is easily deduced: $z = 4$. If, on the other hand, all the material area is distributed to web-like connectors, as shown in Figure 1(c), then a theoretical lower bound on I is found from which the parameter z is again easily determined: $z = 12$.

Using these theoretical upper and lower bounds, the consistency of manufacturers' data in Table 1 can be checked and a practical lower bound established. From Equation 2 $z = Ah\,h/I$ can be computed, where I, A, and h are taken directly from Table 1 [A is the revised area, and h = (OD − ID)/2]. These values of z are shown in Figure 2 as a range of five values for each pipe size. Note that some of the plotted z values are less than 4, implying that the associated values for I are clearly too high, exceeding the theoretical upper bound. Note that the z values are greater than 12, implying none of the reported values for I are clearly too low. As shown in Figure 2(c), the line $z = 10$ provides a reasonable lower bound estimate for design. Said another way, all reported values of I are greater than the value of I given by Equation 2 with $z = 10$.

TABLE 1 MANUFACTURED SECTION PROPERTIES

NOMINAL DIAMETER in	MANU-FACTURER*	INSIDE DIA. in	OUTSIDE DIA. in	AREA (ORIGINAL) in^2/in	MOMENT INERTIA in^4/in	AREA (REVISED) in^2/in
4	A	4.02	4.72	0.0533	0.001103	0.056
	O	3.94	4.86	0.186	0.00211	0.060
	P	4.10	4.70	0.0564	0.000834	0.053
	U	4.06	4.65	0.0644	0.000966	--
	H	--	--	--	--	0.053
6	A	6.00	6.92	0.0717	0.00343	0.086
	O	5.91	6.89	0.2234	0.00795	0.081
	P	5.94	6.87	0.1150	0.00389	0.075
	U	6.06	6.75	0.0873	0.00201	--
	H	--	--	--	--	0.060
8	A	8.12	9.50	0.0917	0.010	0.102
	O	7.87	9.25	0.234	0.0151	0.102
	P	7.79	9.47	0.112	0.00791	0.092
	U	8.16	9.63	0.111	0.00709	--
	H	--	--	--	--	0.081
10	A	10.11	11.90	0.125	0.019	0.128
	O	9.84	11.81	0.222	0.0364	0.144
	P	9.98	11.71	0.145	0.0146	0.120
	U	10.20	11.83	0.0886	0.0171	--
	H	--	--	--	--	0.114
12	A	12.10	14.80	0.125	0.034	0.166
	O	11.81	13.98	0.235	0.046	0.161
	P	11.77	14.16	0.292	0.0505	0.173
	U	12.18	14.42	0.117	0.0283	--
	H	11.85	14.03	0.168	0.0260	0.156
15	A	15.05	18.80	0.178	0.070	0.193
	O	15.75	18.50	0.250	0.0612	0.212
	P	14.35	18.70	0.227	0.0917	0.196
	U	15.00	18.44	0.396	0.153	--
	H	14.81	17.74	0.224	0.059	0.184
18	A	17.86	21.41	0.230	0.090	0.231
	O	17.72	20.67	0.276	0.0867	0.238
	P	--	--	--	--	0.224
	U	18.10	21.28	0.296	0.111	--
	H	18.20	21.51	0.214	0.077	0.227
24	A	23.86	28.16	0.353	0.200	0.336
	O	23.62	27.95	0.297	0.1696	0.332
	P	--	--	--	--	0.289
	U	24.375	27.875	0.322	0.159	--
	H	24.20	28.40	0.277	0.155	0.299
30	A	--	--	--	--	
	O	--	--	--	--	--
	P	--	--	--	--	--
	U	30.00	34.55	0.356	0.244	--
	H	--	--	--	--	--

*MANUFACTURERS

A = ADS
O = Big O
U = United Extrusions
P = Plastic Service, Inc.
H = Hancor

Corrugation Depth

Although the corrugation depth is easily measured, a design relationship is sought that will give a lower bound estimate for h as a fraction of pipe size. Shown in Figure 3 are the data points, ID/h versus ID, taken from Table 1. Here it is observed that ID/h = 14 provides the desired relationship, that is, in all cases the corrugation height is greater than 1/14 of the diameter.

To summarize, this study provides a simple method to accurately determine the section area A using Equation 1. Knowing A, a lower bound estimate for the moment of inertia is given by Equation 2 in which the corrugation height can be taken as 1/14 of the inside diameter.

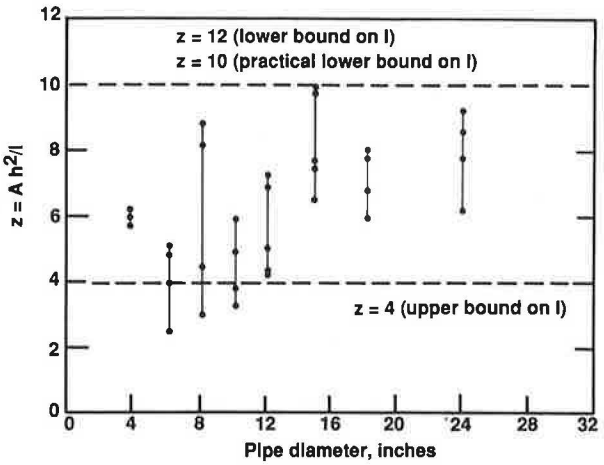

FIGURE 2 Consistency check on moments of inertia.

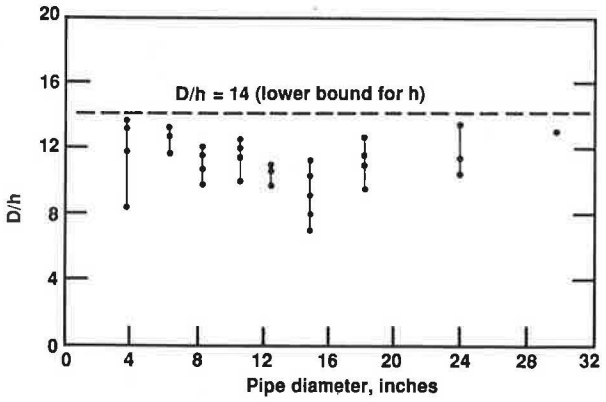

FIGURE 3 Reported diameter-to-corrugation height ratios.

Pipe Geometry

Based on this study, the "matrix" of corrugated section areas selected for the design study is listed in Table 2. That is, for each pipe diameter, three corrugated section areas are chosen and designated as low, medium, and high values so that the high and low values bracket the actual values reported by the manufacturers. For the sake of uniformity, the range between high and low values of sectional areas is kept constant at 0.1 in.²/in.

Associated with each pipe size and sectional area in Table 2, the design procedure conservatively assumes that the corresponding moment of inertia is given by Equation 2 and the corrugation height is given by Equation 1.

Pipe Material

Polyethylene exhibits significant creep behavior under constant loading. Thus, the effective long-term modulus is considerably lower than the short-term modulus. Summarized in the following table is the AASHTO M294 specification.

Time Period (yrs)	*Young's Modulus (lb/in.²)*	*Tensile Strength (lb/in.²)*
Short term (0.05)	110,000	3,000
Long term (50.0)	22,000	900

It can be seen from this table that the recommended modulus for the long term (50 years) is five times less than it is for the short term. Stiffness reductions of this order are typical for polyethylene, as shown, for example, in linear log (modulus) versus log (time) plots (*3*).

Strength behavior is not as well studied or understood as stiffness. The AASHTO specifications, as shown in this table, suggest that the long-term strength is reduced by a factor of 3.3 from the short-term strength, a seemingly rather large reduction. In any event, the properties in the table are adopted from this study with the firm belief that they are conservative values in keeping with the stated design philosophy.

DESIGN METHODOLOGY

CANDE Program

CANDE (Culvert Analysis and Design) is a well-known and well-accepted finite element computer program developed especially for the structural design and analysis of buried conduits (*1*, *4–6*). Both the pipe and the surrounding soil envelope are incorporated into an incremental, static plane strain formulation. The pipe is modeled with a connected sequence of beam-column elements, and the soil is modeled with continuum elements. For this study, CANDE was modified to automatically determine the allowable fill height, described subsequently. The fundamental analysis assumptions are small deformation theory, linear elastic polyethylene properties (short and long term), bonded pipe-soil interface, Level 2 solution method, and the Duncan soil model.

Design Criteria

Listed in the following table are the four design criteria for polyethylene pipe, of which the measures of pipe distress are

TABLE 2 RANGE OF SECTION AREAS ANALYZED*

Pipe ID	Corrugation Area: in²/in		
in.	low	medium	high
4	0.04	0.09	0.14
6	0.05	0.10	0.15
8	0.06	0.11	0.16
10	0.08	0.13	0.18
12	0.10	0.15	0.20
15	0.15	0.20	0.25
18	0.20	0.25	0.30
24	0.25	0.30	0.35
30	0.30	0.35	0.40

*For all analyses: h = ID/14 and I = Ah²/10.

thrust stress, relative deflection, flexural strain, and buckling pressure. These criteria satisfy the AASHTO requirements for service load design (*2*). In this study, the criteria are applied to both long- and short-term design life. These criteria are accepted here at face value, even though the thrust stress criterion is thought to be very conservative.

Distress Measure	*Allowable Limit*
Thrust stress	½ yield stress
Flexural strain	5.0 percent
Relative deflection (vertical)	7.5 percent
Buckling pressure	½ critical pressure [Chelapati-Allgood buckling theory (*1*)]

Soil Model

All design cases are analyzed for two soil conditions generically called "fair" and "good" quality soil. Specifically these two cases were represented by the Duncan soil models for silty clayey sand at 85 percent compaction (fair = SC 85) and silty clayey sand at 100 percent compaction (good = SC 100). The Duncan model parameters for these two soil conditions are listed in Table 3. More general interpretations for these two bracketing cases are given elsewhere in this paper, allowing the solutions to be interpolated over a range of soil types and conditions.

Design Procedure

The design procedure is best described by summarizing the CANDE input and output. Table 2 contains 27 different input geometries composed of 9 pipe sizes with 3 sectional areas per pipe size. Each of these input geometries is analyzed four times, that is, all combinations of short- and long-term polyethylene properties listed in the in-text table in the Pipe Material section of this paper together with the two soil models representing fair and good soil quality. Overall, 108 design solutions were obtained with CANDE. Each design solution is obtained by sequentially placing layer after layer of soil above the pipe in 2- to 3-ft increments until one of the four design criteria is violated. At that point, the program determines what proportion of the last increment exactly satisfies the controlling design criterion, thereby determining the precise allowable fill height. Output consists of the allowable fill height, the controlling design criterion along with the status of the other criteria, and the complete set of structural responses at the allowable burial depth.

RESULTS

Comparative Studies

As a prelude to presenting the complete set of design solutions, it is instructive to compare how the four design criteria independently control the allowable fill height and, at the same time, compare predicted performance with experimental laboratory data from Utah State University (*7*). Computed allowable fill heights for an 18-in. corrugated plastic pipe with a sectional area of 0.22 in.^{2}/in. used in the Utah State University study are shown in Figure 4. For each of the four design criteria, four different fill heights are shown representing the four combinations of two soil conditions and two polyethylene conditions. It is evident that the thrust stress criterion controls in all cases, however, less so for fair soil than for good soil. Superimposed on the figure is a data point for the deflection criterion from a simulated deep burial test in the Utah State University soil cell in which the soil was reported as a silty clayey sand compacted to 85 percent AASHTO T-99 (fair soil). A deflection reading of 7.5 percent was recorded at an over pressure of 4,700 lb/ft^2, or 40 ft of equivalent fill height, which agrees remarkably well with the calculated fill height of 43 ft for the 7.5 percent deflection criterion for the case of fair soil and short-term loading. The Utah State University test did not include strain gauges so the thrust stress or flexural strain criterion could not be checked, however, Utah State University investigators observed the initiation of corrugation dimpling at 7,500/ft^2 (63 ft of fill).

Design Tables

The allowable fill heights for all 108 cases are listed in Table 4. The thrust stress criterion controlled in all cases except for four cases (marked with asterisks), in which the deflection criterion controlled marginally. On average for all cases, the deflection criterion would allow 25 percent more fill height, the flexural criterion would allow 30 percent more fill height, and the buckling criterion would allow 55 percent more fill height than the controlling thrust criterion. There is, however, substantial variation of individual cases from these average trends.

A graphic representation of Table 4 is shown in Figures 5, 6, and 7. Here, the dramatic influence of soil quality on the allowable fill height is readily apparent, as is the effect of short-term versus long-term pipe properties. In addition to showing how deep given pipe geometry can be buried as a function of soil quality and design life, these figures also answer

TABLE 3 STANDARD HYPERBOLIC PARAMETERS (*5*)

Soil Type	ϕ (deg)	$d\phi$ (deg)	C (psf)	K -	n -	Rf -	Kb -	m -
(SC-85)	33.0	0.0	200.	100.	0.6	0.7	50.0	0.5
(SC-100)	33.0	0.0	500.	400.	0.6	0.7	200.0	0.5

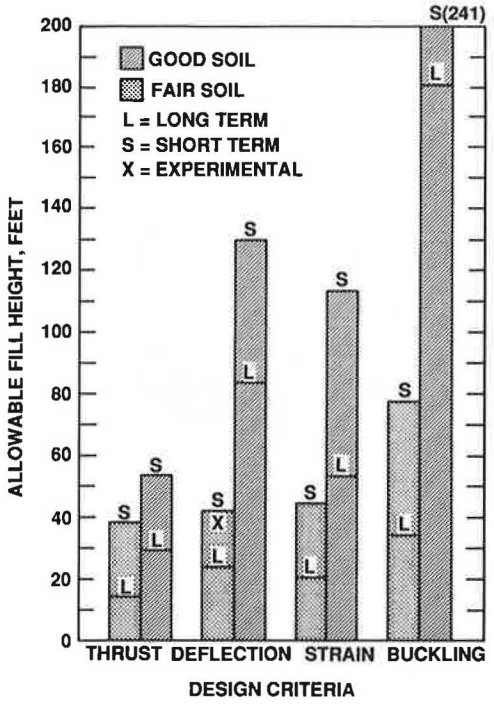

FIGURE 4 Allowable fill height versus design criteria.

the inverse question: what sectional area is required to withstand a given burial depth?

DESIGN GUIDELINES

The use of Table 4 and the associated Figures 5, 6, and 7, is straightforward as long as the design problem matches the prescribed conditions, that is, soil density is 120 lb/ft^3, soil quality is either fair or good, and design life is long term or short term only. For more generality, the following interpolation schemes are provided to permit design solutions for variations in soil density, soil quality, and design life.

Soil Density

The allowable fill height given in Table 4 or, equivalently, in Figures 5, 6, and 7, is based on a reference soil density, S = 120 lb/ft^3. Letting S^* denote the actual soil density, then the corresponding fill height H^* may be computed as,

$$H^* = (S/S^*)H \tag{3}$$

TABLE 4 DESIGN TABLE FOR ALLOWABLE FILL HEIGHT

PIPE PROPERTIES		ALLOWABLE FILL HEIGHTS			
		Good Quality Soil		Fair Quality Soil	
ID	Corrugation Area	S	L	S	L
in	in^2/in	(ft)	(ft)	(ft)	(ft)
4	.04	45.0	25.2	31.5	12.0
	.09	87.3	41.4	63.4*	23.7
	.14	125.2	56.6	76.9*	35.2
6	.05	39.0	23.0	26.3	10.3
	.10	68.6	34.3	51.3	18.2
	.15	95.5	44.9	65.7*	26.0
8	.06	35.6	21.9	23.6	9.6
	.11	58.1	30.6	42.3	15.2
	.16	79.1	38.6	58.8*	21.3
10	.08	37.3	22.8	25.0	10.1
	.13	55.3	29.7	40.0	14.8
	.18	72.4	36.2	54.8	19.5
12	.10	38.4	23.4	26.0	10.4
	.15	53.4	29.2	38.4	14.4
	.20	67.8	34.6	50.7	18.3
15	.15	44.0	25.8	30.7	12.0
	.20	55.9	30.3	40.6	15.1
	.25	67.5	34.6	50.5	18.2
18	.20	48.1	27.6	34.0	12.8
	.25	57.9	31.4	42.3	15.8
	.30	67.5	34.9	50.5	18.3
24	.25	47.9	28.4	33.4	13.1
	.30	55.9	31.5	40.0	15.2
	.35	63.7	34.4	46.6	17.2
30	.30	43.7	26.7	30.2	12.2
	.35	49.7	29.0	35.2	13.8
	.40	55.6	31.3	40.2	15.3

S = Short-term design life (0.05 years)
L = Long-term design life (50 years)

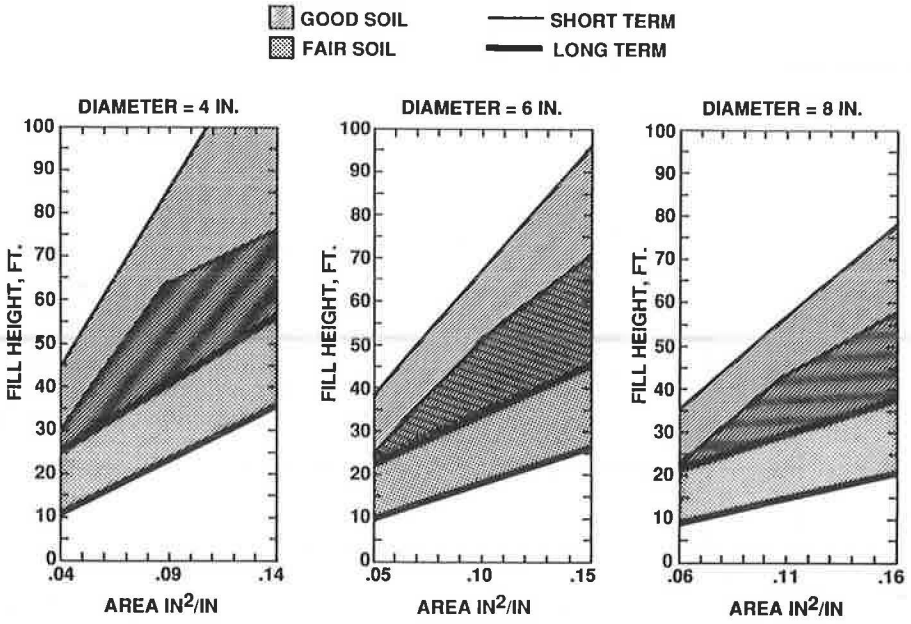

FIGURE 5 Allowable fill height for 4-, 6-, and 8-in. pipes.

Soil Quality

To interpolate between fair and good soil quality, Table 5 may be used with the following guidelines. Let *Hf* and *Hg* be the allowable fill heights for fair and good soil quality as read from the design tables or figures. Then for a selected intermediate soil quality listed in Table 5, the corresponding intermediate fill height, *Hi*, may be computed as

$$Hi = Hf + r(Hg - Hf) \quad (4)$$

where r varies between 0 and 1.0 and is given in Table 5 as a function of percent compaction for three classes of soil. These results were taken from a previous study (*5*).

Design Life

For design lives of 50 years or more, the long-term allowable fill height is appropriate. If the design life is to be significantly less than 50 years, then the allowable fill height lies between the long- and short-term solutions. This can be estimated based on a linear log-log relationship in which the short-term

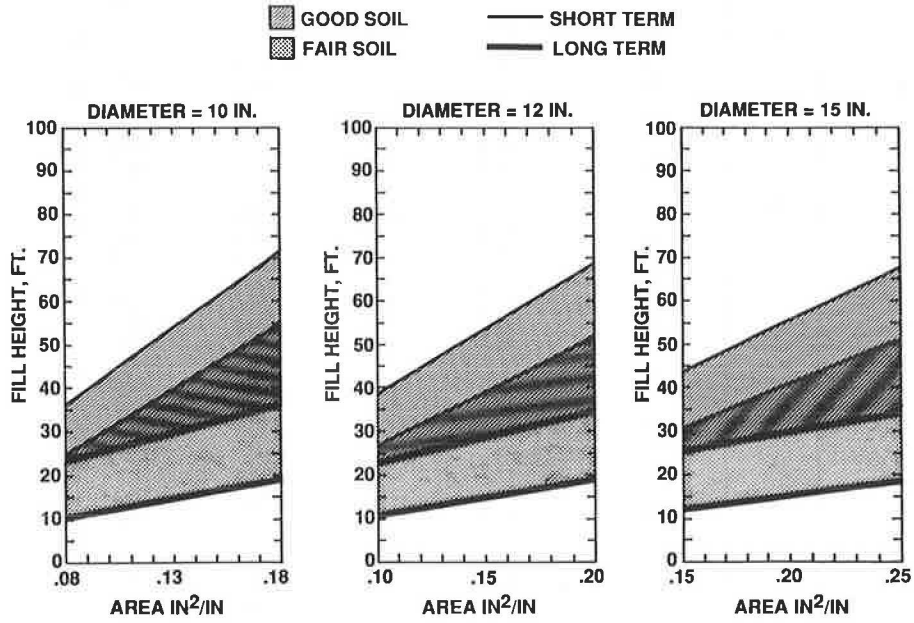

FIGURE 6 Allowable fill height for 10-, 12-, and 15-in. pipes.

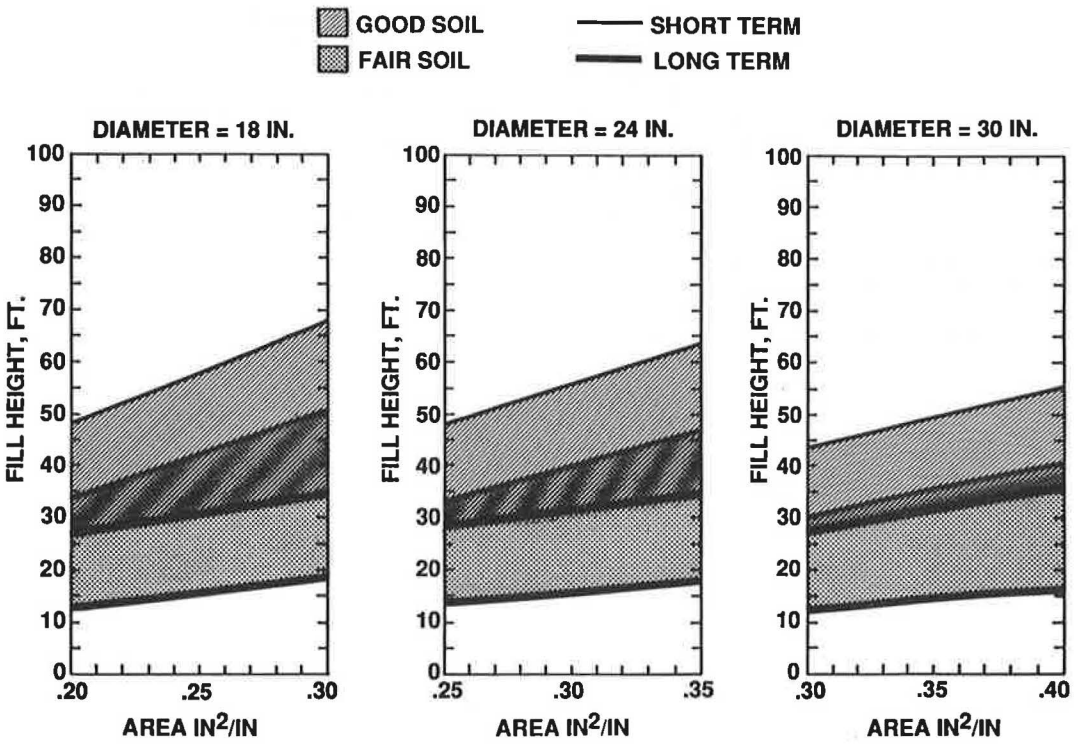

FIGURE 7 Allowable fill height for 18-, 24-, and 30-in. pipes.

time period is taken as 0.05 years and the long-term as 50 years. Letting *Hs* and *HI* represent the allowable fill heights for short- and long-term design periods, and denoting the actual design-life time as *t*, then the corresponding fill height, *Ht*, is given by

$$Ht = HI\,(50/t)^{m} \tag{5}$$

where the exponent $m = \log(Hs/HI)/3$; here the divisor 3 comes from evaluating log(50/.05).

Example Design Problems

A 24-in. plastic pipe with a sectional area of 0.3 in.²/in. is to be in service for at least 50 years in a well-graded silty sand weighing 130 lb/ft³ at 85 percent relative compaction. Determine the maximum allowable burial depth.

Referring to Table 5 for a SM-85 percent soil condition, it is determined that $r = 0.5$. Using this value in Equation 4 along with $Hf = 15.2$ ft and $Hg = 31.5$ ft from the long-term fill heights in Table 4, the temporary result is that $HI = 23.4$ ft. Readjusting this value for a density of 130 lb/ft³, the final answer is $Hi^{*} = 21.6$ ft.

Now suppose the problem is to be reworked for a 2-year design life, all else remains unchanged. The answer is given by Equation 5, in which $HI = 21.6$ ft from above, and *Hs* is determined in the same manner using short-term fill height values to get $Hs = 44.3$ ft. Thus, the exponent $m = 0.104$, and the final allowable fill height for a 2-year service life is $Ht = 30.2$ ft.

TABLE 5 CORRESPONDENCE OF INTERPOLATION RATIO TO PERCENT COMPACTION

Interpolation Ratio r	Granular SM %	Mixed SC %	Cohesive CL %
(Fair) 0.0	80	85	90
0.25	82	87	95
0.50	85	90	100
0.75	90	95	NA
1.00 (Good)	95	100	NA

SM = Silty Sand, Well Graded
SC = Silty Clayey Sand
CL = Clay (No Organic)

CONCLUSION

The design results are applicable to all corrugated plastic pipe whose material properties conform to AASHTO specifications (2), whose sectional areas are within limits of Table 2, and whose corrugation height is at least 1/14 of the diameter. Within the stated restrictions, the allowable fill heights may be used with conservative confidence.

ACKNOWLEDGMENTS

Thanks are extended to the Corrugated Plastic Tubing Association for their support of this study and to William Altermatt of Hancor, Inc., and James Goddard of Advanced Drainage Systems for their technical guidance.

REFERENCES

1. M. G. Katona. *CANDE: A Modern Approach for the Structural Design and Analysis of Buried Culverts.* Report FHWA-RD-77-5, Federal Highway Administration, Washington, D.C., Oct. 1976.
2. *Soil-Plastic Pipe Interaction Systems.* Section 18, American Association of State Highway and Transportation Officials Flexible Culvert Committee, San Francisco, Calif., Feb. 26, 1986.
3. Lars-Eric Janson. Investigation of the Long-Term Creep Modulus for Buried Polyethylene Pipes Subjected to Constant Deflection. Advances in Underground Pipeline Engineering. In *Proc., International Conference, Pipeline Division, ASCE*, Madison, Wis., Aug. 1985.
4. M. G. Katona. CANDE: A Versatile Soil-Structure Design and Analysis Computer Program. *Journal of Advances in Engineering Software*, Vol. 1, No. 1, 1978. pp. 3–9.
5. M. G. Katona. *CANDE-1980: Box Culverts and Soil Models.* Report FHWA-RD-172, Federal Highway Administration, U.S. Department of Transportation, May 1981.
6. M. G. Katona and A. Y. Akl. Design of Buried Culverts with Stress-Relieving Joints. In *Transportation Research Record 1129*, TRB, National Research Council, Washington, D.C., 1987, pp. 39–54.
7. R. K. Watkins, J. M. Dwiggins, and W. E. Altermatt. Structural Design of Buried Corrugated Polyethylene Pipes. In *Transportation Research Record 1129*, TRB, National Research Council, 1987, pp. 12–20.

Publication of this paper sponsored by Committee on Subsurface Soil-Structure Interaction.

Field Performance of Corrugated Metal Box Culverts

JOHN O. HURD AND SHAD SARGAND

Thirty-nine corrugated aluminum and 10 corrugated steel rib stiffened box culverts were evaluated. In situ chord and chord-ordinate dimensions were measured and compared to design dimensions. In addition, durability information was obtained. Eight of the box culverts had not been manufactured in conformance with the design shape. The most common deviation was a larger crown width and shorter leg length. There was a significant difference between the constructed crown shapes of steel and aluminum box culverts. The steel box culverts were in general crowned, whereas the aluminum box culverts had mid-chord-ordinate dimensions less than the design dimension. The amount of crowning in the steel box culverts decreased with increased crown widths. A potential crown corrosion problem exists on metal box culverts caused by seepage of groundwater containing road salt through bolted seams. The problem is of greater concern on steel boxes because the plate as well as the bolts have corroded. Finite element analyses of the structure capacity of erected shapes different from the design shape of the structures were performed. Slight variation in the culvert geometry has a noticeable but not severe effect on deflections and moments.

Large prefabricated culvert structures have within the past decade become economic alternatives to conventional bridges and cast-in-place box culverts for the replacement of deteriorating small bridges. These prefabricated structures include reinforced concrete arches, three-sided concrete box structures, four-sided concrete box culverts, and corrugated metal long-span structures and box culverts. This particular study addresses the field performance of corrugated metal box culverts.

At the time of this study the Ohio Department of Transportation (ODOT) had installed 49 circumferential rib stiffened corrugated metal box culverts. Twenty-eight structures were installed by ODOT maintenance forces and 21 were installed by contract. Thirty-nine of the structures were bulb angle stiffened 9 × 2½-in. corrugated aluminum plate structures. Four were angle stiffened 6 × 2-in. corrugated steel plate structures, and six were 6 × 3-in. corrugated plate stiffened 6 × 2-in. corrugated steel plate structures. Schematic diagrams of the circumferential structural cross sections of each structure type are shown in Figures 1 and 2.

The structural design of these culverts is based on composite action of the rib or plate section and a standard design shape (*1–3*). The design shape of the various sizes are composed of a standard crown radius with incremental crown angles, standard haunch radius and angle, and incremental leg lengths, as shown in Figure 3. Table 1 provides the design angles, radii, and leg lengths for the sizes of structure studied. Plate thickness and rib spacing are designed to provide an adequate section for a given loading condition. Thirty-two of the culverts had full metal plate inverts, 14 had concrete footers, and 3 had metal plate footer pads. No distinction is made among the footers in the design of the structure.

The as-erected and as-built shapes of small and large flexible culverts sometimes vary significantly from the theoretical design shape (*4–6*). Large changes can significantly affect the load-carrying capacity (*6, 7*). Most current research has been done on carefully monitored structures where erection and backfill procedures have been carefully controlled (*8, 9*). This study was undertaken to determine how in situ structure shapes for "real world" installations compared with design shapes and what effect any deviation might have on structural performance. Because of the nature of this study, precise information on installation procedures was not available.

In addition to the structural aspects, the culverts were evaluated with respect to culvert durability. Because of recent observations of crown corrosion in pipe arches and other structural plate structures (*6, 10*) caused by groundwater seepage containing road salt, the crowns of the structures were observed to detect any sign of bolt or seam corrosion. The inverts were also observed to detect corrosion-caused stream flow.

DATA COLLECTION

Culvert structural details including size, plate thickness, rib configurations and footer type were obtained from construction plans for contract installations and from district bridge engineers for maintenance installations. The information was field verified at each site and compared with the recommended designs in manufacturers' brochures. The height of cover, which ranged from 1.25 to 5.7 ft above the crown of the structure, was obtained in the same manner and field verified.

All structures were backfilled with granular material meeting the gradation requirements shown in Table 2. ODOT requires the premium backfill envelope to extend horizontally at least 30 in. on each side of the structure and vertically to the roadway subbase. The material is to be placed in 8-in. maximum depth loose lifts and compacted to 95 percent standard proctor density. Normally, contract installations are reasonably well monitored by ODOT inspectors, but not as precisely controlled as research sites. Installations by ODOT

J. O. Hurd, Ohio Department of Transportation, 25 S. Front Street, Columbus, Ohio 43215. S. Sargand, Department of Civil Engineering, Ohio University, Athens, Ohio 45701.

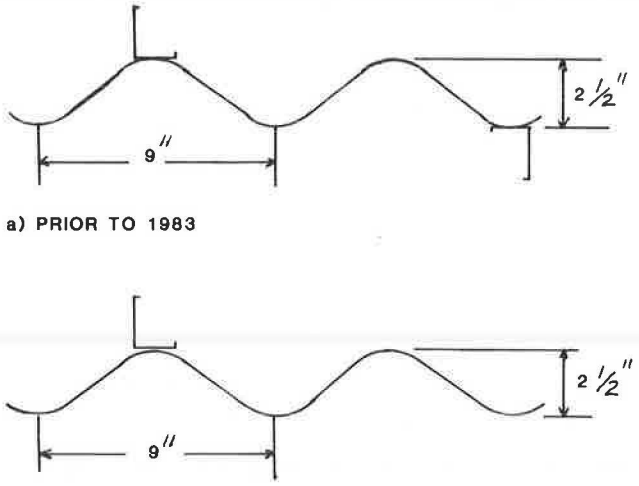

FIGURE 1 Structural cross section of aluminum box culvert.

maintenance forces are normally not controlled to the extent of contract installations.

Chord and chord-ordinate dimensions, as shown in Figure 4, were taken in the field at a representative location under the pavement to obtain the in situ shape of the structure (*11*). These were compared with chord and chord-ordinate dimensions calculated from design angles and radii. The design chord dimensions for those structures in Table 1 are given in Tables 3 and 4. In several cases the rise and span were not available because the invert footings had been placed below the streambed level. However, the span at the bottom of the haunch, *A* ft, and crown-haunch rise, *B* ft, proved to adequately describe

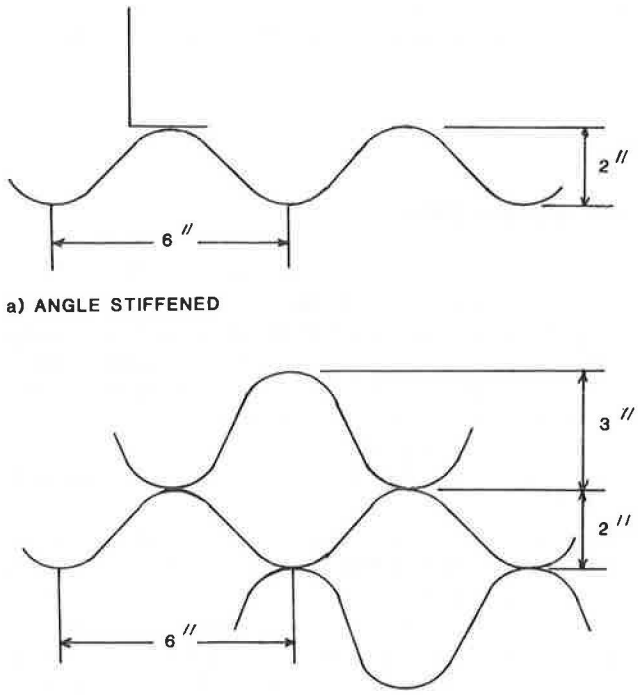

FIGURE 2 Structural cross sections of steel box culvert.

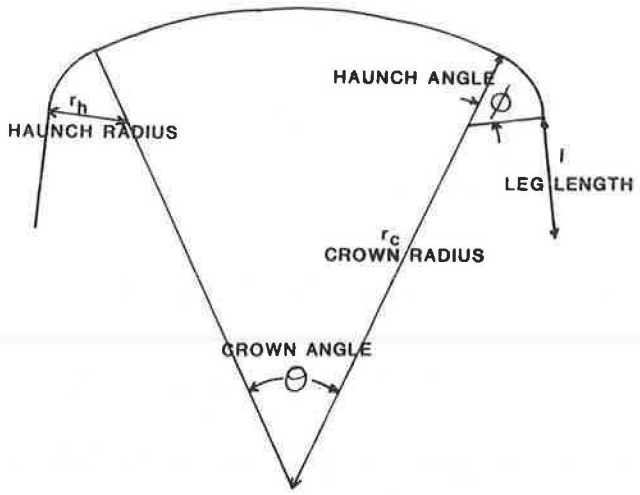

FIGURE 3 Schematic of metal box culvert shape.

the structure shape for comparison purposes. It should be noted that these measurements are not precise because radius breaks do not occur at bolted seams but are formed into a section of plate that is made up of the entire haunch, part of the crown, and part or all of the leg. The accuracy is reasonable enough to provide a comparison with the design shape of the structure. Design and measured crown and haunch dimensions are shown in Table 5.

The single-asterisked dimensions appeared to have measurement or recording errors. The double-asterisked measurements are on culverts that were clearly not manufactured to the design shape. In the case of the four aluminum culverts and two steel culverts, the haunches had been rotated downward producing a much larger crown and shorter leg. All four aluminum structures were manufactured in the same year. For these six structures, adjusted design crown chord-ordinates were used in calculating the amount of deflection. Three of the steel structures had smaller haunches than the design shape. All other differences can be attributed to fabrication, erection, and load-induced deflections and minor measurement errors. Because of the very small mid-chord-ordinates on smaller sizes, the greater range of the scatter on small structures was more the result of measurement accuracy than that for the larger structures where the measurement-induced differences would be minimal. From observation of the initial data, flattening of the mid-chord-ordinate appeared to be the most common shape change. Those culverts with missing measurement dimensions were not measurable because of high water.

In addition to measuring structure dimensions, any loose bolts, poor-fitting seams, poor rib or plate contact, severe crimps in the plate, poor support of the invert, or other structural imperfections were noted. A summary of the imperfections worth noting is given Table 6. These imperfections did not appear to have any effect on the shape of the structures except for the serious foundation settlement of the 18 ft 8-in. × 6 ft 8-in. aluminum box culvert. Some of the 22 percent mid-chord-ordinate deflection in this structure may have been caused by the severe foundation settlement.

Although the imperfections in general did not appear to affect the structure shape, it should be noted that any poor fit between plates and ribs or plates and plates would reduce

TABLE 1 STRUCTURE DIMENSIONS FOR ODOT METAL BOX CULVERTS

Size and Type	r_h"	g°	r_c"	0"	1
8'-9"x2'-6"Alum	30.25	70	297.5	9.23	0.5n
9'-2"x3'-3"Alum	30.25	70	297.5	9.23	1.5n
9'-7"x4'-1"Alum	30.25	70	297.5	9.23	2.5n
10'-0"x4'-10"Alum	30.25	70	297.5	9.23	3.5n
10'-6"x5'-7"Alum	30.25	70	297.5	9.23	4.5n
10'-2"x2'-8"Alum	30.25	70	297.5	12.92	0.5n
10'-7"x3'-5"Alum	30.25	70	297.5	12.92	1.5n
10'-11"x4 -3"Alum	30.25	70	297.5	12.92	2.5n
11'-4"x5'-0"Alum	30.25	70	297.5	12.92	3.5n
11'-9"x5'-9"Alum	30.25	70	297.5	12.92	4.5n
12'-1"x6 -7"Alum	30.25	70	297.5	12.92	5.5n
12'-11"x6'-0"Alum	30.25	70	297.5	16.61	4.5n
13'-3"x6'-9"Alum	30.25	70	297.5	16.61	5.5n
13'-7"x4'-7"Alum	30.25	70	297.5	20.3	2.5n
13'-10"x5'-5"Alum	30.25	70	297.5	20.3	3.5n
14'-10"x4'-10"Alum	30.25	70	297.5	24.0	2.5n
15'-1"x5'-8"Alum	30.25	70	297.5	24.0	3.5n
15'-4"x6'-5"Alum	30.25	70	297.5	24.0	4.5n
15'-6"x7 -3"Alum	30.25	70	297.5	24.0	5.5n
16'-6"x6'-8"Alum	30.25	70	297.5	27.7	4.5n
16'-10"x8'-3"Alum	30.25	70	297.5	27.7	6.5n
17' 6"x6'-2""Alum	30.25	70	297.5	31.4	3.5n
18'8"x6'-5"Alum	30.25	70	297.5	35.1	3.5n
18'-7"x5'-4"Alum	37.38	57	258.75	36.0	2.5n
22'-1"x0'-3"Alum	37.38	57	258.75	44.5	6.5n
23'-4"x7'-8"Alum	37.38	57	258.75	53.0	3.5n
13 -3"x6'-0"Steel	30.25	70	297.5	16.61	5.5n
10 -1"x3'-4"Steel	38.25	70	297.5	9.24	1.0n
9'-9"x2'-7"Steel	38.25	70	297.5	9.24	0.0n
16 -9"6'-9"Steel	38.25	70	297.5	25.9	4.0n
14'-5"x6'-2"Steel	38.25	70	297.5	18.40	4.0n
20'-10"x7'-1"Steel	38.25	70	297.5	38.8	30.n
18 -4"x6'-4"Steel	36.0	69	293.0	16.22	3.0n
10'-7"x4'-2"Steel	36.0	69	293.0	10.03	2.0n
18'10 x5'-8"Steel	36.0	69	293.0	34.0	2.0n

Note: n=9.6"

TABLE 2 GRADATION REQUIREMENTS OF ODOT METAL BOX CULVERT BACKFILL

	Total Percent Passing	
Sieve	Grading *A*	Grading *B*
2½ in.	100	100
1 in.	70–100	70–100
No. 4	25–100	25–100
No. 40	5–50	10–50
No. 200	0–10	5–15

the amount of composite action until deflections become large enough to provide plate-to-rib and plate-to-plate load transfer via bolt contact.

The condition of the roadway over the culverts was observed. Most cracks and settlement observed was not over the culvert but outside the structure. This would indicate little permanent structure deflection as a result of live loads after construction.

Because of the short time (7 year maximum) that the culverts had been installed, only two structures showed any signs of invert wear or corrosion. One 6-year-old aluminum culvert downstream from a cheese factory had a very slight pitting at the edge of the invert plate. The steel angle used to seat a 3-year-old aluminum box on a concrete footing was very rusty. However, neither the steel bolts nor the aluminum plates showed any signs of corrosion.

The presence of any deposits caused by the seepage of groundwater containing road salts through the bolted seams was noted as well as any bolt or plate corrosion. Because ODOT uses sodium chloride for snow and ice removal, a taste test was used to detect the presence of this salt in deposits. The number of each type (aluminum or steel) of culvert with

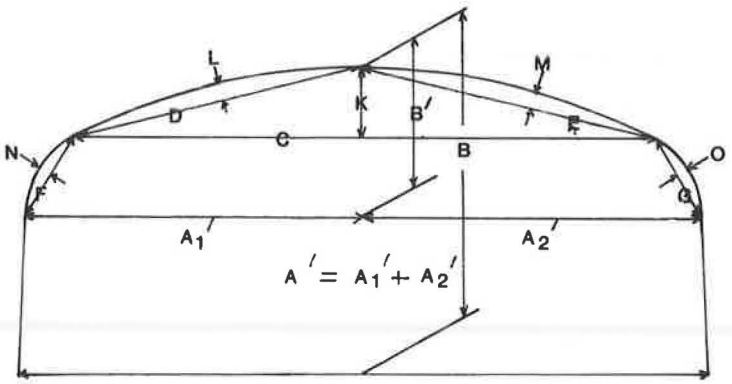

FIGURE 4 Chord and chord-ordinate dimensions for metal box culverts.

different degrees of seepage-induced corrosion are listed in Table 7. The amount of deposits and corrosion were always greatest beneath the edge of pavement, further verifying road salt presence. It is obvious from observing the table that a potential crown corrosion problem exists on the shallow structures. This is of particular concern on the steel structures where the plate in the vicinity of seams as well as the bolts shows signs of deterioration.

STATISTICAL ANALYSIS OF DATA

In situ measured-to-design chord-ordinate ratios were compared with various structure dimensions, plate thickness, rib configurations, metal type, age, height of cover, type of footing, and type of installation for all measured structures. The only significant relation was that between mid-chord-ordinate ratio and metal type. Steel box culverts had significantly larger in situ to design mid-chord-ordinate ratios than the aluminum box culverts. However, this only accounted for 32 percent of the scatter in the data. Observation of Table 5 shows that 7 out of the 8 steel box culverts measured had in situ mid-chord-ordinates larger than the design mid-chord-ordinates. On the other hand, 29 of the 37 aluminum box culverts measured had in situ mid-chord-ordinates less than the design mid-chord-ordinate.

There was no significant relationship between chord-ordinate ratio and type of installation for the entire range of box sizes. However, it was noted that for boxes with top chord lengths greater than 11 ft, the mid-chord-ordinate ratios for contract installations were always greater than for ODOT maintenance installations. This indicates that the larger structures were more susceptible to less controlled backfill procedures than smaller ones.

Because of the difference in performance between the aluminum and steel structures, the data set was divided into steel and aluminum box culverts. There was a small significant correlation between mid-chord-ordinate ratio and footing type for the aluminum boxes. Boxes with concrete footings had less deflection than those with full metal inverts or footer plates. The average mid-chord-ordinate ratio for boxes with concrete footings was 0.96, whereas that for boxes with full inverts was 0.87. There was a strong correlation between mid-chord-ordinate ratio and crown width for steel boxes. The amount of crowning was less for larger structures.

Mid-chord-ordinate ratios for steel and aluminum box culverts are shown plotted against top chord length in Figure 5. As the statistical analyses showed, no pattern can be observed for the aluminum box culverts. However, the amount of crowning on steel box culverts is clearly reduced with increased crown width. This reduction is represented by the regression line plotted in Figure 5.

Except for the slight difference because of footing type for aluminum box culverts, the scatter about the average mid-chord-ordinate value for aluminum boxes and that about the regression line for steel boxes is caused by manufacturing- and erection-induced deflections and difference in backfill procedures. The difference between the average mid-chord-ordinate ratio of 0.89 for aluminum box culverts and 1.0, the

TABLE 3 DESIGN HAUNCH CHORD AND CHORD-ORDINATE DIMENSIONS FOR METAL BOX CULVERTS

r_n in.	0°	F in. = G ft	N ft = 0 ft
30.25	70	2.89	0.46
37.38	57	2.97	0.38
38.25	70	3.66	0.58
36.00	69.37	3.41	0.53

TABLE 4 DESIGN CROWN CHORD AND CHORD-ORDINATE DIMENSIONS FOR METAL BOX CULVERTS

r_c in.	0°	C ft	K ft	D ft = E ft	L ft = M ft
297.50	9.23	3.99	0.08	2.00	0.020
297.50	12.92	5.58	0.16	2.79	0.040
297.50	16.61	7.16	0.26	3.59	0.065
297.50	20.3	8.74	0.39	4.39	0.097
297.50	24.0	10.3	0.54	5.18	0.136
297.50	27.7	11.9	0.72	5.98	0.18
297.50	31.4	13.4	0.92	6.77	0.23
297.50	35.1	15.0	1.15	7.56	0.29
258.75	36.0	13.3	1.06	6.75	0.27
258.75	44.5	16.3	1.61	8.32	0.41
258.75	53.0	19.2	2.26	9.88	0.57
297.50	18.4	7.93	0.32	3.98	0.08
297.50	25.9	11.1	0.63	5.58	0.16
297.50	38.8	16.5	1.41	8.35	0.35
293	9.36	3.98	0.08	2.00	0.020
293	31.80	13.4	0.93	6.75	0.23
293	33.80	14.2	1.05	7.18	0.27

TABLE 5 DESIGN AND MEASURED IN SITU CHORD AND CHORD-ORDINATE DIMENSIONS FOR METAL BOX CULVERTS

	C		K		F		N		G		O	
Type	Des.	Meas.	Des.	Meas	Des	Meas.	Des.	Meas.	Des.	Meas.	Des.	Meas.
A	4.0	4.0	0.08	0.07	2.9	2.9	0.46	0.45	2.9	2.85	0.46	0.45
A	4.0	3.9	0.08	0.06	2.9	2.8	0.46	0.40	2.9	2.8	0.46	0.43
A	4.0	3.8	0.08	0.06	2.9	2.9	0.46	0.45	2.9	3.15*	0.46	0.57*
A	4.0	4.1	0.08	0.06	2.9	2.8	0.46	0.44	2.9	2.95	0.46	0.44
A	4.0	3.9	0.08	0.095	2.9	2.9	0.46	0.48	2.9	3.0	0.46	0.49
A	4.0	4.2	0.08	0.06	2.9	2.9	0.46	0.44	2.9	2.8	0.46	0.44
A	4.0	4.0	0.08	0.05	2.9	2.8	0.46	0.45	2.9	2.8	0.46	0.43
A	4.0	4.0	0.08	0.06	2.9	2.9	0.46	0.44	2.9	2.8	0.46	0.42
A	4.0	4.0	0.08	0.09	2.9	2.85	0.46	0.45	2.9	2.9	0.46	0.45
A	4.0	4.55**	0.08	0.09	2.9	2.85	0.46	0.41	2.9	2.85	0.46	0.41
A	4.0	3.85	0.08	0.08	2.9	2.9	0.46	0.45	2.9	3.0	0.46	0.44
A	4.0	4.55**	0.08	0.08	2.9	3.0	0.46	0.46	2.9	3.0	0.46	0.46
A	4.0	3.95	0.08	0.08	2.9	2.9	0.46	0.45	2.9	2.8	0.46	0.45
A	4.0	4.0	0.08	0.07	2.9	2.9	0.46	0.45	2.9	2.85	0.46	0.45
A	5.6	5.5	0.16	0.14	2.9	2.8	0.46	0.41	2.9	2.9	0.46	0.44
A	5.6	5.45	0.16	0.15	2.9	2.8	0.46	0.41	2.9	2.85	0.46	0.47
A	5.6	5.45	0.16	0.15	2.9	2.8	0.46	0.46	2.9	2.8	0.46	0.42
A	5.6		0.16		2.9		0.46		2.9		0.46	
A	5.6	5.6	0.16	0.14	2.9	2.8	0.46	0.44	2.9	2.8	0.46	0.45
A	5.6	5.45	0.16	0.15	2.9	2.8	0.46	0.43	2.9	2.9	0.46	0.44
A	5.6	5.8**	0.16	0.14	2.9	2.85	0.46	0.45	2.9	2.85	0.46	0.41
A	5.6	5.47	0.16	0.12	2.9	2.85	0.46	0.42	2.9	2.93	0.46	0.46
A	5.6	5.7	0.16	0.12	2.9	2.9	0.46	0.46	2.9	2.8	0.46	0.44
A	7.2	7.6**	0.26	0.22	2.9	2.95	0.46	0.46	2.9	3.0	0.46	0.46
A	7.2	7.5	0.26	0.24	2.9	2.84	0.46	0.45	2.9	2.85	0.46	0.44
A	8.74	8.6	0.39	0.33	2.9	2.9	0.46	0.45	2.9	3.0	0.46	0.48
A	8.74	8.75	0.39	0.34	2.9	2.9	0.46	0.45	2.9	2.95	0.46	0.48
A	10.3	10.2	0.54	0.50	2.9	2.8	0.46	0.45	2.9	2.9	0.46	0.45
A	10.3	10.4	0.54	0.55	2.9	2.9	0.46	0.45	2.9	2.8	0.46	0.42
A	10.3	10.3	0.54	0.45	2.9	2.9	0.46	0.45	2.9	2.9	0.46	0.46
A	10.3	10.3	0.54	0.59	2.9	2.8	0.46	0.44	2.9	2.9	0.46	0.43
A	10.3	10.3	0.54	0.48	2.8	2.35	0.46	0.43	2.9	2.9	0.46	0.45
A	11.9	12.1	0.72	0.65	2.9	2.75	0.46	0.42	2.9	2.35	0.46	0.46
A	11.9	11.95	0.72	0.63	2.9	2.8	0.46	0.42	2.9	2.9	0.46	0.45
A	13.4	13.5	0.92	0.86	2.9	2.85	0.46	0.46	2.9	2.85	0.46	0.46
A	15.0	15.2	1.15	0.90	2.0	2.8	0.46	0.42	2.9	2.85	0.46	0.48
A	13.3		1.06		2.97		0.38		2.97		0.38	
A	16.3	16.6	1.61	1.35	2.97	2.85	0.38	0.35	2.97	2.85	0.38	0.35
A	19.2	19.2	2.35	2.33	2.97	3.0	0.38	0.39	2.97	3.20	0.38	0.41
S	7.2	7.3	0.26	0.31	2.9	2.8	0.46	0.44	2.9	2.8	0.46	0.44
S	4.0		0.08		3.66		0.58		3.66		0.58	
S	4.0	4.6**	0.08	0.14	3.66	3.5	0.58	0.58	3.66	3.6	0.58	0.62
S	4.0	3.9	0.08	0.10	3.41	3.3	0.53	0.48	3.41	3.4	0.53	0.54
S	9.93	8.3**	0.32	0.39	3.66	3.25**	0.58	0.41**	3.66	7.3**	0.58	0.41**
S	11.1	11.4	0.63	0.65	3.66	3.2**	0.58	0.44**	3.66	3.3**	0.58	0.48**
S	13.4	13.3	0.93	0.87	3.41	3.6	0.53	0.67	3.41	3.6	0.53	0.64
S	14.2	14.2	1.05	1.10	3.41	2.8**	0.53	0.38**	3.41	2.8**	0.53	0.38**
S	14.2		1.05		3.41		0.53		3.41		0.53	
S	16.47	16.4	1.41	1.47	3.66	3.63	0.58	0.62	3.66	3.64	0.58	0.59

*Appeared to have measurement or recording errors.
**On culverts not manufactured to design shape.

TABLE 6 SUMMARY OF STRUCTURAL IMPERFECTIONS

Type of Imperfection	Culvert Size and Type
Reinforcing rib wavy or twisted.	18 ft 4 in. × 6 ft 4 in. steel
Seams not drawn together flush.	14 ft 5 in. × 6 ft 2 in. steel
	10 ft 7 in. × 4 ft 2 in. steel
	18 ft 7 in. × 5 ft 4 in. aluminum
	16 ft 10 in. × 8 ft 3 in. aluminum
	10 ft 4 in. × 4 ft 10 in. aluminum
Bolts drawn through corrugated plate or rib.	10 ft 1 in. × 3 ft 4 in. steel
	23 ft 4 in. × 7 ft 8 in. aluminum
	16 ft 10 in. × 8 ft 3 in. aluminum
	9 ft 7 in. × 4 ft 1 in. aluminum
Differential settlement of full invert.	18 ft 8 in. × 6 ft 5 in. aluminum
	11 ft 4 in. × 5 ft 0 in. aluminum
	9 ft 2 in. × 3 ft 3 in. aluminum
No support in middle of full invert.	16 ft 6 in. × 6 ft 8 in. aluminum
	10 ft 2 in. × 2 ft 8 in. aluminum
	10 ft 6 in. × 5 ft 7 in. aluminum
	9 ft 7 in. × 4 ft 1 in. aluminum
	9 ft 2 in. × 3 ft 3 in. aluminum
Plate crimped at radius break.	9 ft 7 in. × 4 ft 1 in. aluminum

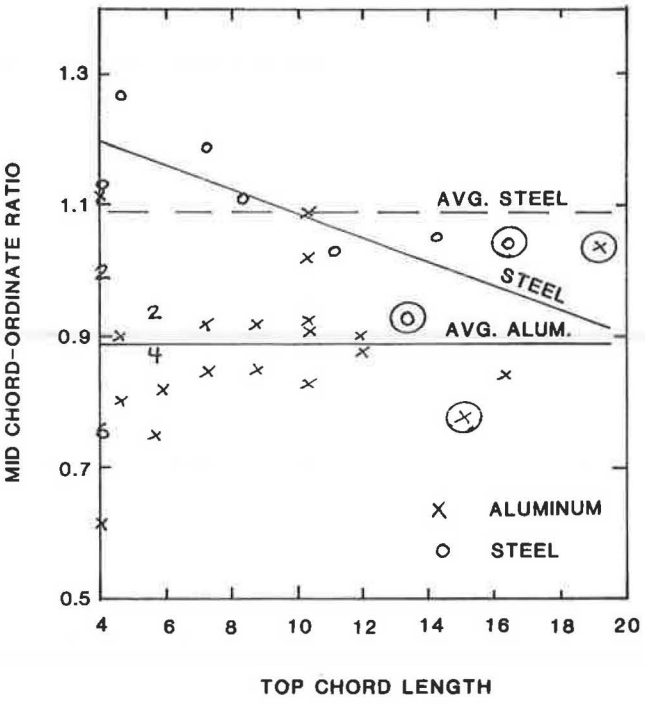

FIGURE 5 Measured-design mid-chord-ordinate ratios.

equivalent of design shape or zero percent deflection, is representative of a consistent reaction for backfill-induced deflection. The difference between the mid-chord-ordinate regression line for steel boxes and 1.0 is representative of decreased crowning from backfill as structure size increases.

Other structural observations and road conditions were compared with the same group of variables as the chord-ordinate ratios. No significant relationships existed.

The presence of salt deposits and seepage-induced corrosion was also compared with the same independent variables. As would be expected from observation of Table 6, there was a significant difference between the performance of the steel and aluminum box culverts. The steel box culverts had a more serious corrosion problem. The corrosion was significantly worse as culvert age increased. Surprisingly, increased cover over the culvert did not have any significant effect in reducing corrosion problems.

TABLE 7 SUMMARY OF GROUNDWATER SEEPAGE AND CROWN CORROSION ON METAL BOX CULVERTS

Condition	Culverts			
	Aluminum		Steel	
	No.	Percent	No.	Percent
No salt seepage	11	28	1	10
Slight salt seepage	14	36	2	20
Significant salt seepage	2	5	1	10
Slight bolt corrosion	10	26	4	40
Significant bolt corrosion	2	5	0	0
Bolt and plate corrosion	0	0	2	20

FINITE ELEMENT ANALYSIS OF STRUCTURE SHAPE

Because field data indicated that the actual erected culvert shapes were different from the design shapes, finite element analysis of the structural performance of in situ shapes and design shapes of the circled structures in Figure 5 and a 15-ft 9-in. × 5-ft 0-in. steel structure was performed using CANDE (*12*) with assumed constant soils and backfill properties.

A granular pipe backfill material was selected from the CANDE library that was representative of ODOT standard backfill. Backfill dimensions were assumed to be the minimum required. An HS-20 live load was imposed on the installed structure with dimensions shown in Figure 6 and Table 8.

The variation in culvert geometry has a noticeable but not severe effect on deflection and moment for constant loads and backfill properties. The variation in moment and deflec-

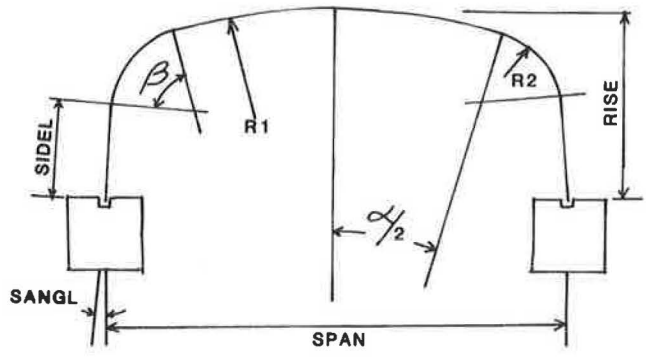

FIGURE 6 Design dimensions used in generating pipe nodes and elements.

TABLE 8 PERCENT CHANGE IN CANDE SOLUTION RESULTING FROM CHANGE IN GEOMETRY

Type	Percent Change		
	Crown Moment	Crown Deflection	Haunch Moment
23 ft 4 in. × 7 ft 8 in. aluminum[a]	−10.48	−6.50	−6.46
18 ft 8 in. × 6 ft 5 in. aluminum[a]	26.29	26.61	15.25
18 ft 4 in. × 6 ft 4 in. steel[a]	5.09	7.69	1.04
20 ft 10 in. × 7 ft 1 in. steel[a]	−3.74	−3.13	−0.26
15 ft 9 in. × 5 ft 0 in. steel[b]	17.9	7.8	12.24
[b]	−9.7	−4.6	−9.00

[a] Measured versus design.
[b] Assumed ±20 percent deflected versus design.

tion as predicted by CANDE for the design versus in situ shapes of the structures analyzed is shown in Table 8.

CONCLUSIONS

The following conclusions were reached:

1. Not all metal box culverts had manufactured shapes matching the design shapes provided by manufacturers in brochures or design drawings.
2. A potential crown corrosion problem exists on metal box culverts caused by seepage of groundwater containing road salt through the bolted seams. This is of greater concern on steel boxes where the plate along the seam as well as the bolts corrode. Increased cover height from 1.25 to 5.7 ft did not reduce the severity of seepage or corrosion, or both.
3. There was a significant difference between the constructed crown shapes of steel and aluminum box culverts. Steel box culverts were in general crowned, having in situ mid-chord-ordinates larger than the design dimension, whereas aluminum box culverts in general had in situ mid-chord-ordinates smaller than the design dimension.
4. The amount of crowning on the steel box culverts was significantly reduced as crown width increased.
5. There was significantly less deflection (approximately 10 percent) of the mid-chord-ordinates in aluminum box culverts with concrete footings than in aluminum box culverts with full metal inverts or metal footing pads.
6. There is a large scatter about the average mid-chord-ordinate ratio line for aluminum box culverts and about the mid-chord-ordinate ratio regression line for steel box culverts. The scatter is probably caused by a combination of manufacturing, erection, and variable backfill-induced deflections.
7. Changes in structure shape produce noticeable but not severe differences in deflection and bending moments caused by backfill and live loadings.

RECOMMENDATIONS

1. Better-quality control should be instituted to assure that manufactured shapes are the same as design shapes.
2. The outside of corrugated steel box culverts should be coated to prevent seepage of groundwater through the bolted seams.
3. Consideration should be given to coating the outside of aluminum box culverts to prevent seepage of groundwater through bolted seams.
4. Consideration should be given to the variation in the as-erected shape in the design of corrugated metal box culverts.

ACKNOWLEDGMENTS

This research was sponsored by the Ohio Department of Transportation and the Ohio University. The findings and opinions expressed therein are those of the authors and do not constitute a standard or specification.

REFERENCES

1. C. D. Gorman. *A Comparison of Field Results with the Theoretical Analysis of Lane Metal Product's Low-Profile Culvert.* Report 79-67-1, Technical Service Division, Engineering Department, Bethlehem Steel Corporation, Pa., April 1981.
2. E. T. Selig, F. F. Abel, and F. H. Kalhaway. Long-Span Buried Structures, Design and Construction. *Journal of the Geotechnical Engineering Division, ASCE*, Vol. 104, GT-7, July 1978.
3. J. M. Duncan. *Field Instrumentation Study of an Aluminum Box Culvert Structure.* Report UCB/GR.92-09. Department of Civil Engineering, University of California, Berkeley, March 1982.
4. J. O. Hurd. Field Performance of Corrugated Polyethylene Pipe Culverts in Ohio. In *Transportation Research Record 1087*, TRB, National Research Council, Washington, D.C., 1986, pp. 1–6.
5. R. B. Seed and C-Y. Ou. Measurements and Analysis of Compaction Effects on a Long-Span Culvert. In *Transportation Research Record 1087*, TRB, National Research Council, Washington, D.C., 1986, pp. 37–45.
6. D. C. Cowherd and C. H. Degler. *Evaluation of Long-Span Metal Structures.* FHWA/OH/-86/011. Bowser-Morner Associates, Inc., Dayton, Ohio, 1986.
7. G. I. Crabb and D. R. Carder. *Loading Tests on Buried Flexible Pipes To Validate a New Design Model.* TRRL Research Report 28, Transport and Road Research Laboratory, Crowthorne, Berkshire, England, 1985.
8. S. M. Sargand, G. A. Hazen, and T. T. Boon. *Composite Action in Rib Plate Structure of a Box Culvert.* Ohio University, Athens, Ohio, 1987.
9. J. M. Duncan, R. B. Seed, and R. H. Drawsky. Design of Corrugated Metal Box Culverts. In *Transportation Research Record 1008*, TRB, National Research Council, Washington, D.C., 1985, pp. 33–41.
10. G. H. Degler. *An Analysis of Visual Field Inspection Data of 900 Pipe-Arch Structures.* Bowser-Morner, Inc., Dayton, Ohio, 1987.
11. D. C. Cowherd and G. H. Degler. *Evaluation Procedures for Long-Span Corrugated Metal Structures (in situ).* FHWA/OH-86/013. Bowser-Morner, Inc., Dayton, Ohio 1986.
12. M. G. Katona, P. D. Vittes, C H. Lee, and H. T. Ho. *CANDE-1980: Box Culverts and Soil Models.* Report FHWA-RD-80-172, Federal Highway Administration, Washington, D.C., May 1981.

Publication of this paper sponsored by Committee on Subsurface Soil-Structure Interaction.

An Analysis of Visual Field Inspection Data of 900 Pipe-Arch Structures

GERALD H. DEGLER, DAVID C. COWHERD, AND JOHN O. HURD

Approximately 50 percent of the structural plate corrugated metal pipe structures under the jurisidiction of the Ohio Department of Transportation are of the pipe-arch configuration. Because these structures have experienced numerous problems, the Ohio Department of Transportation established a research project to identify and determine the causes of these problems. The initial phase of this project involved a field inspection of 890 pipe-arch structures. The inspection was conducted by each of the 12 Ohio Department of Transportation district offices. The inspection consisted of a visual examination plus limited dimensional measurements. Specific areas that received a rating included (a) the amount of structure distortion, (b) the occurrence and severity of multiplate and bolt erosion and seepage, (c) the occurrence and extent of cracking of the multiplates, (d) the condition of the pavement over the structure, and (e) the condition of the channel bottom. A statistical analysis of the field data was performed to determine the dominant modes of structure failure and interrelationships between the structural failures and such variables as age, depth of cover, gauge of the multiplate, and geographic location. Attempts were also made to determine whether one failure mode influenced another (e.g., distortion of the structure causing cracking, or vice versa). Results of the statistical analysis show that the dominant modes of failure or deterioration are (a) fairly heavy corrosion of the multiplates and fasteners (27 percent), (b) significant distortion or flatness of the structure's crown (12 percent), and (c) cracking of the multiplate at the corner radius bolt line (3 percent). Interrelationships were demonstrated with correlation coefficients of 0.9 or greater for (a) age versus durability, (b) durability versus geographic location, and (c) shape problems contributing to cracking problems, and so on.

The Ohio Department of Transportation (ODOT) requires that all bridges with spans of 10 ft or more be inspected annually in accordance with the Federal Bridge Inspection Program. Because corrugated metal pipes (CMP) are commonly used as drainage structures under Ohio roads, these structures must be inspected annually under this program if their spans are in excess of 10 ft.

CMP come in a variety of shapes including circular, elliptical, pear, and arched. The most popular and widely used structural plat CMP shape is the pipe arch (see Figure 1). It should be noted that these structures are flexible and that the soil backfill surrounding the structure is an integral part of this structure. If the backfill is soft and compressible, the sides of the pipes move out and the top of the pipe becomes flat. When the top radius of the pipe reaches a critical value, the pipe collapses.

In order to establish a general overview of the condition of CMP in Ohio, ODOT requested each of their district offices to conduct field inspections of all pipe-arch corrugated metal structures. The pipe-arch shape was selected because this type of structure has been demonstrated to have more structural problems than any other CMP configuration. It also represents approximately 50 percent of Ohio's CMP population.

During February and March 1987, the 12 districts of ODOT conducted visual and limited dimensional inspections of 962 corrugated metal pipe-arch structures. A copy of the field inspection report used during this evaluation is shown on Table 1. These inspections required measurement of the rise and span at two different locations (preferably at locations where obvious structure deformation had occurred), noting the pavement type and condition immediately above the structure (whether settling had occurred), the type of channel bottom and its condition, and quantifying on a scale from 0 to 9 such factors as structure shape, corrosion of the metal pipe, corrosion of the seams and bolts within the structure, and the presence of cracking along the bolt joints. A rating of 9 was given when the factor under consideration was in perfect condition. On review of this field data, it was observed that, of the 962 structures investigated, 890 structures were fully evaluated, partial data were available on 31 structures, and no data were available for 41 structures. The reasons that data were unavailable for the 41 structures included

1. Inability to locate the structure;
2. The structure was too full of water, or silt, or both, to permit inspection; and
3. The structure was removed some time in the past.

The remaining 890 field inspection reports were then subjected to a statistical analysis in an attempt to identify potential interrelationships between structure failures and such factors as structure age, size, depth of cover, gauge, and so on. The purpose of this paper is, therefore, to present the results of the analysis of the 890 pipe-arch structures located within the state of Ohio. A distribution of the pipe-arch structures by district is presented in Figure 2.

DESCRIPTION OF PIPE-ARCH STRUCTURES

The multiplate pipe-arch structures are made of steel sections with corrugations 6 in. wide by 2 in. deep running at right

G. H. Degler and D. C. Cowherd, Bowser-Morner Associates, Inc., 420 Davis Avenue, P.O. Box 51, Dayton, Ohio 45401. J. O. Hurd, Ohio Department of Transportation, 25 South Front Street, P.O. Box 899, Columbus, Ohio 43216.

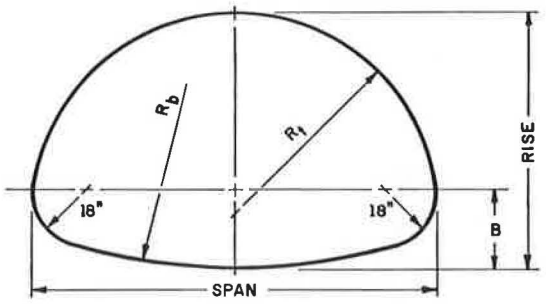

FIGURE 1 Structural plate steel pipe arch.

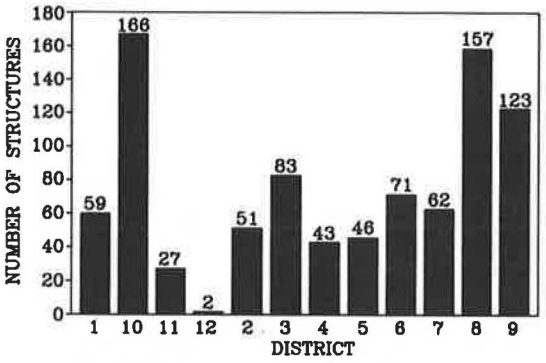

FIGURE 2 Number of pipe-arch structures by district.

angles to the length of the section. Sections vary in thickness from approximately 0.280 in. for No. 1 gauge to 0.109 in. for No. 12 gauge. A typical cross section of the pipe-arch structure would be eight separate sections in 10- to 12-ft lengths bolted together with ¾-in. diam bolts. All of the structures installed in Ohio have an 18-in. corner radius with 6 by 2-in. corrugations. Typically, the crown of the structure is constructed of a lighter gauge material than the bottom or invert. A commonly used configuration is a 10-gauge thickness for the crown and an 8-gauge thickness for the bottom. A tabulation of the number of structures as a function of the top gauge thickness is presented in a frequency histogram in Figure 3. A review of this data reveals that the majority of the structures have a crown gauge thickness of between 7 and 10. The structures ranged in size from a span and rise of 6 ft 1 in. by 4 ft 7 in. to 16 ft 7 in. by 10 ft 1 in.

The structures were installed from 1933 through 1986. The frequency of distribution of the various gauge installations is presented in Figure 4. As can be seen from reviewing this information, the majority of the pipe-arch structures in Ohio

TABLE 1 BRIDGE INSPECTION REPORT

District _____

A. BACKGROUND INFORMATION
1. Structure no. _____
2. Structure file no. _____ 3. Structure location _____
4. Year installed _____ 5. Corrugation _____
6. Depth of cover (ft) _____ 7. Metal gauge: Top ___ Bottom: ___
8. Design rise × span (ft) ____ 9. Plate configuration _____
10. Original foundation/backfill information available: Yes ___ No ___

B. MEASUREMENT
1a. Measured rise × span (ft) ___ Location _____
1b. Measured rise × span (ft) ___ Location _____
2. Pavement type and condition _____
3. Channel bottom type and condition _____

4. Structure Shape	Rating	Condition
a. Symmetrical throughout	9	
b. Slight nonsymmetrical sections, minor sag	7–8	
c. Significant distortion and flatness (one section)	6	
d. Significant distortion and flatness (throughout)	4–5	
e. Extreme distortion (one section)	3	
f. Extreme distortion (throughout)	2–1	
g. Partial collapse; reverse curvature	0	
h. Other observations _____		

5. Metal Plate	
a. No defects or corrosion	9
b. Minor defects and superficial corrosion	7–8
c. Fairly heavy corrosion, light pitting	6
d. Fairly heavy corrosion, moderate pitting	4–5
e. Severe local corrosion and pitting	3
f. Severe corrosion (throughout)	2–1
g. Widespread corrosion and pitting	0
h. Other observations _____	

6. Metal Seams/Bolts	
a. No defects or corrosion	9
b. Slight water seepage and superficial corrosion	7–8
c. Water seepage with fairly heavy local corrosion	5–6
d. Water seepage with fairly heavy local corrosion throughout	3–4
e. Water seepage with severe local corrosion	0–2

7. Seams—Cracking	
a. Properly assembled	9
b. Minor metal cracking and/or seam openings	7–8
c. Major cracking (one location) and infiltration	6
d. Major seam cracking throughout and infiltration	4–5
e. Severe cracking (>3 in.) throughout	3
f. Severe cracks continuous from bolt hole to bolt hole with significant infiltration	2–1
g. Major cracks continuing from bolt hole to bolt hole with backfill pushing into structure	0
h. Other observations (percent of length experiencing cracks) _____	

C. INSPECTOR
1. Name _____ Date _____

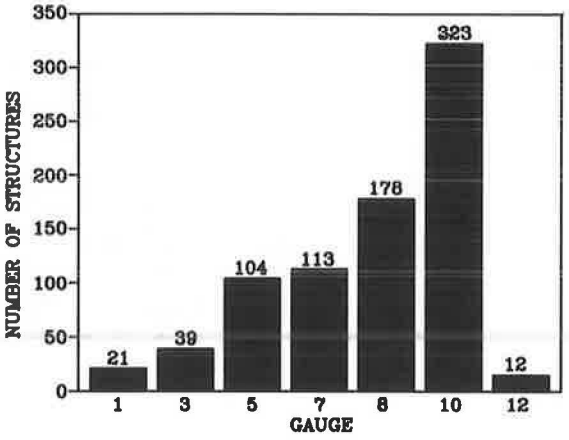

FIGURE 3 Distribution of number of structures by top gauge thickness.

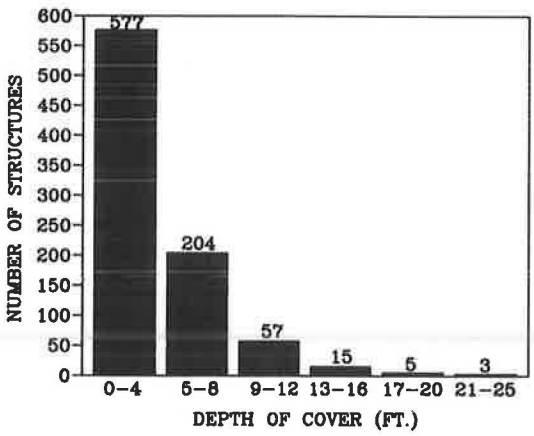

FIGURE 5 Number of structures installed at various cover depths.

were installed during the years 1951 through 1965. The average age of the structures is 25 yr. A total of 365 structures or 41 percent of the total structures installed are 30-yr old and older. This information becomes significant when observing the durability of the structures as a function of age (presented later in this paper).

The depth of cover over the pipe-arch structures ranged between 1 and 25 ft. The distribution of the number of structures at the various depths of cover is illustrated in Figure 5. A review of these data shows that 46 percent of all the structures have a cover of 4 ft or less and 70 percent of the structures have a cover of 6 ft or less. The significance of these data relates to the effect of live and dead load on the structure as a function of the depth of cover (see Table 2).

Because durability of the pipe-arch structures could be a function of the geographic location within the state, the number of structures located at each ODOT district was tabulated. This tabulation will provide a basis for attempting to show a correlation between structure durability and those areas of the state with high abrasive stream loads or acid mine drainage, or both.

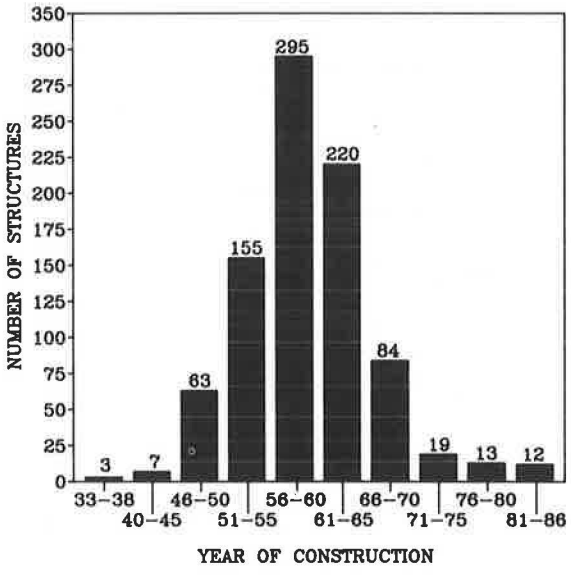

FIGURE 4 Number of structures installed by year of installation.

ANALYSIS OF FIELD DATA

Areas of Analysis

All of the field data shown on the bridge inspection report were entered into a computer program to permit a statistical evaluation of all parameters for determining any potential interrelationships. More specifically, this evaluation sought to determine the answers to the following questions:

1. Does the durability of the structure (susceptibility to corrosion and abrasion) have any relationship to its age?
2. Does the durability of the structure have any relationship to its geographic location (i.e., pH and abrasion effects)?
3. Does the durability of the structure have any relationship to such problems as distortion or cracking of the structure, or both?
4. Does the gauge of the multiplate sections have any relationship to the structure's distortion or cracking problems, or both?
5. Does the depth of cover over the structure have any relationship to the structure's distortion or cracking problems, or both?

TABLE 2 RELATIONSHIP OF DEPTH OF COVER TO STRUCTURE LOADING

Depth of Cover (ft)	[a]Live Load (lb/ft²)	[b]Dead Load (lb/ft²)	[c]Design Load (lb/ft²)
1	1,800	120	1,651
2	800	240	894
3	600	360	826
4	400	480	757
5	250	600	731
6	200	720	791
7	175	840	873
8	100	960	912

[a] Highway H20 loading.
[b] Weight of soil = 120 lb/ft³.
[c] Assumes an 85 percent compaction of the backfill.

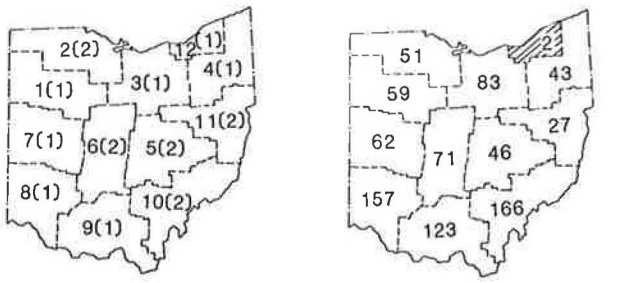

FIGURE 6 Number of inspectors and pipe structures by district.

6. Does distortion of the structure's shape have any relationship to the occurrence of the cracking problem?
7. What are the dominant modes of failures and the causes of these failures?
8. What is the frequency of distribution of the number of structures and their rating (by total and by category)?
9. What is the geographic location of those structures receiving perfect or poor scores, or both (by total and by category)?
10. Is there any noticeable difference in the subjective ratings established by the inspectors in each of the 12 ODOT districts?

Subjectiveness of the Field Inspector's Evaluation

Presented in Figure 6*A* are the number of inspectors in each ODOT district and in Figure 6*B* the number of pipe arches inspected in each district. Because there were 18 different inspectors involved in the evaluation of the pipe-arch structures, it was necessary to conduct a comparison of the rating scores between each of the inspectors to determine whether any of the inspectors' scores needed to be normalized to account for differences in establishing the rating of 0 to 9 for each of the four categories evaluated. Because a maximum of 9 could be given for each of the four categories, a perfect score would be 36. A listing of the individual inspectors, the number of structures, and the average score given by that inspector is presented in Table 3. The weighted average for scores given by all of the inspectors was 30.3. The standard deviation was 2.54. A close review of the scoring by the various inspectors shows that the majority of the readings were comparable, with the exception of inspectors *M*, *O*, and *P*, all of District 10. Because this district is known for its high abrasive stream loads with low pH values, the low scores could possibily be attributed to structure durability problems. However, because inspector *N* in District 10 posted high scores, any attempt to offer a conclusive explanation of the District 10 score variations would be inappropriate without cross checking inspectors. Because all other district scores compared favorably, it was decided to proceed with the statistical evaluations using the field data exactly as presented in the field inspector reports.

TABLE 3 AVERAGE STRUCTURE SCORE BY EACH INSPECTOR

Inspector	District No.	No. Inspected	Score
A	1	59	29.5
B	2	50	30.2
C	3	83	31.5
D	4	42	32.5
E	5	28	31.9
F	5	16	30.8
G	6	10	30.3
H	6	61	29.9
I	7	58	30.1
J	7	3	34.7
K	8	154	30.0
L	9	119	29.9
M	10	64	26.1
N	10	92	32.2
O	10	3	23.3
P	10	7	25.6
Q	11	25	30.8
R[a]	12	2	30.0
Unknown		13	31.0
Total		890	30.3
Weighted average = 30.3			

[a] Included with District 3 during the evaluation.

Statistical Evaluation

Method of Approach

A statistical evaluation was conducted to determine whether an interrelationship existed between such problem areas as (a) distortion or sag of the structure, (b) cracking of the multiplates, (c) corrosion of the multiplates, and (d) corrosion of the seams and bolts and such independent variables as age, depth of cover, gauge of the multiplate, and geographic location. This analysis also attempted to determine the influence that one problem category might have on another (e.g., distortion of the crown on cracking of the multiplate structure). The evaluation also addressed the frequency of occurrence of various modes of failure or deterioration. For purposes of simplifying the presentation of the data, the following abbreviated definitions have been established:

Problem Categories

1. Shape: Refers to a rating of 0 to 9 based on the amount of distortion or sag in the structure.
2. Seams: Refers to a rating of 0 to 9 based on the amount of cracking of the multiplate within the structure.
3. Plate: Refers to a rating of 0 to 9 based on the severity of corrosion occurring on the multiplate.
4. Metal: Refers to a rating of 0 to 9 based on the amount of corrosion and seepage occurring on the bolt and seam joints.

Independent Variables

1. Age: Years since installed.
2. Cover: The amount of cover (in ft) over the structure.

3. Top gauge: The thickness of the multiplate structure (crown).
4. Geographic location: Categorized by ODOT district.

The ratings for the four problem categories were averaged according to year and ODOT district. These average values were then grouped in 5-yr increments beginning in 1940 and average values were established for each subsequent 5-yr grouping. This resulted in 9 data points (the years 1933 to 1939 were eliminated because only 2 data points were accumulated during this time period). These data were then processed using the least-square method of regression for the following relationships:

1. Age as a function of shape, plate, metal, seams, plate and metal (durability) and total score.
2. Depth of cover as a function of shape, plate, metal, seams, and total score.
3. Gauge of pipe-arch crown as a function of shape, plate, metal, seams, and total score.

Attempts were made to fit the data to three different types of regression curves: for example, linear, exponential, and power. Coefficients of determination (r^2) were established for each of these regression curves.

Results of Analysis

1. Age versus shape, plate, metal, seams, durability, and total score.

The results of attempting to fit the various types of regression curves to the data are shown in Table 4. The quality of fit was found to be greater than 0.9. As might be expected, the age of the structure showed good correlation with those variables that directly relate to structure durability factors (e.g., corrosion or seepage, or both); of plate and metal seams and bolts, the combination of these two scores, and the total score for each of the four variables evaluated. Distortion of the structure and the occurrence of cracking along the seams had

TABLE 4 RESULTS OF REGRESSION CURVE ANALYSIS

VARIABLE x	VARIABLE y	TYPE OF REGRESSION	EQUATION	COEFFICIENT OF DETERMINATION
Age	Shape	linear	-	0.75
		exponential	-	0.74
		power	-	0.56
Age	Plate	linear	-	0.89
		exponential	$y=9.0-0.45\ e^{0.05x}$	0.91
		power	-	0.89
Age	Metal	linear	-	0.87
		exponential	-	0.89
		power	$y=9.0-0.06x^{1.04}$	0.95
Age	Seams	linear	-	0.69
		exponential	-	0.44
		power	-	0.71
Age	Plate & Metal (Durability)	linear	$y=18.0-0.19x$	0.89
		exponential	$y=18.0-0.75e^{0.06x}$	0.93
		power	$y=18.0-0.20x^{0.92}$	0.94
Age	Total Score	linear	$y=35.3-0.21x$	0.94
		exponential	$y=36.0-1.85e^{0.04x}$	0.95
		power	$y=36.0-0.74x^{0.65}$	0.91
Cover	Shape	linear	-	0.29
Cover	Plate	linear	-	0.19
Cover	Metal	linear	-	0.05
Cover	Seams	linear	-	0.34
Cover	Total Score	linear	-	0.77
Top Gage	Shape	linear	-	0.13
Top Gage	Plate	linear	-	0.06
Top Gage	Metal	linear	-	0.74
		exponential	-	0.75
		power	-	0.56
Top Gage	Seams	linear	$y=8.25+0.25x$	0.93
Top Gage	Total Score	linear	-	0.67

no correlation with the age of the structure. The relationship between age and plate, as well as between age and total score, were best described by an exponential curve fitting. A linear relationship for total score and age gives about the same good result as an exponential curve. A power curve provides the best method for describing the relationship between age and the occurrence of corrosion and seepage along the seams and fasteners.

Because the ratings for plate and metal represent the durability of the pipe-arch structure, these two categories were combined in an attempt to improve on the coefficient of determination. However, this combination produced a coefficient that was slightly lower than the age versus metal power relation (0.95 to 0.94).

Illustrated in Figures 7, 8, and 9 are the relationships of age to metal, plate, and total composite score. It should be noted that although an exponential curve fit was used to describe the relationships in Figures 8 and 9, a linear curve could also have been used because the coefficient of determination for a linear relationship was only slightly lower. It is interesting to note that the decrease in the total composite score with age (see Figure 9) indicates that a newly installed structure has, on the average, a score of 34 (a decrease of 2). This could possibly be explained by the experience of some structures with shape problems during installation.

The overall deterioration (total composite score of the 890 structures) as a function of time is shown in Figure 10. This curve generally describes a linear deterioration of the structure with approximately a 30 percent reduction in the total composite score over a 50-yr period.

2. Depth of cover versus shape, plate, metal, seams and total score.

Because much of the corrosion of corrugated metal structures can be attributed to salt water seepage into the structure that has originated from the road surface, it was hypothesized that those structures with very little depth of cover would show more extensive corrosion and seepage problems than those structures with a considerable amount of coverage. Further, because the corrugated metal pipe structures are more susceptible to live loads with shallow cover and dead loads with excessive amounts of cover, it was thought that there might be a relationship of depth of cover to shape or distortion problems. However, as can be seen from Table 4, no correlation was established with any of the test variables.

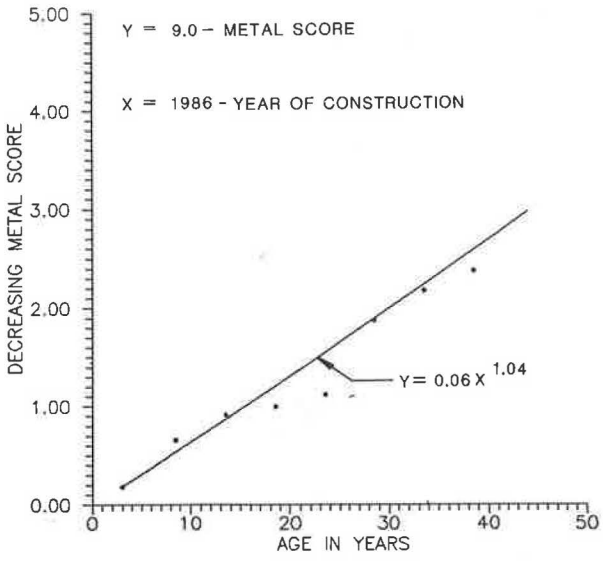

FIGURE 7 Decrease in metal score with age of structure.

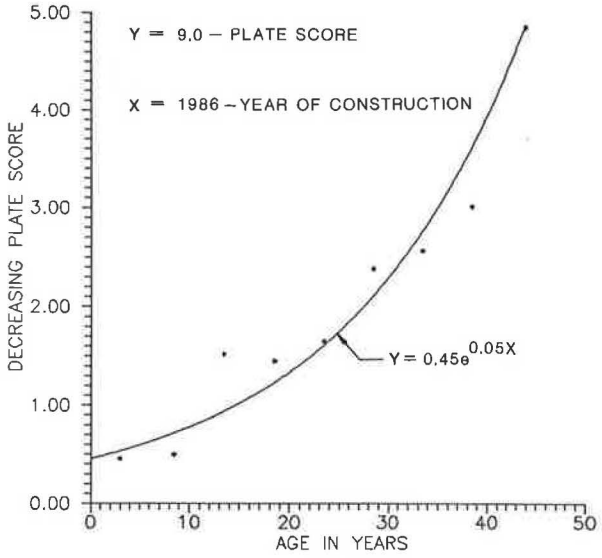

FIGURE 8 Decrease in plate score with age of structure.

3. Top gauge versus shape, plate, metal, seams and total score.

Typically, the multiplate pipe-arch structures are constructed with a 10-gauge material for the crown and an 8-gauge material for the bottom invert. The bottom invert is typically 1 to 2 gauge numbers heavier than the crown. Because data on the bottom gauge numbers were missing for many of the

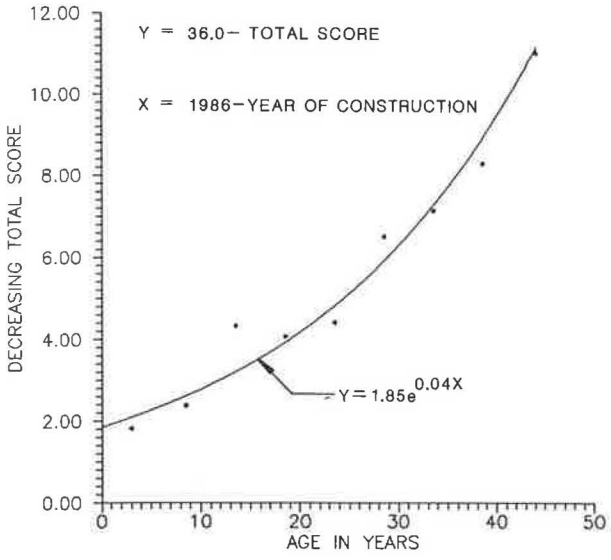

FIGURE 9 Decrease in total composite score with structure age.

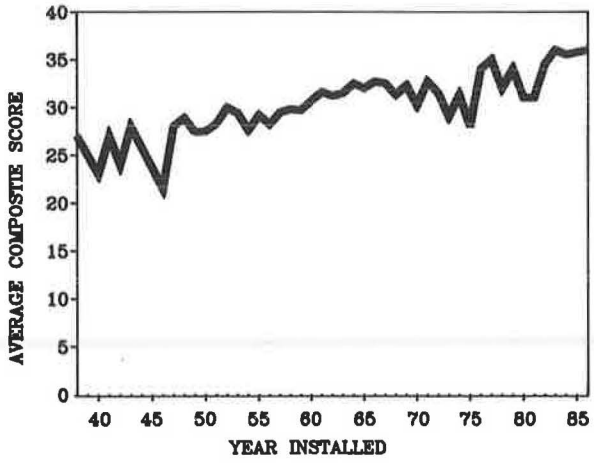

FIGURE 10 Average composite score of structures based on year of installation.

structures, it was decided to perform this analysis using the top gauge numbers. It was hypothesized that some relationship could exist between gauge thickness and structure durability or seam cracking, or both. Because movement or distortion of the structure is totally dependent on the type of backfill and its compaction, no relationship was anticipated between the gauge number and shape score. Results of the regression curve fitting for each of the test variables indicated that the only relationship that existed was between the top gauge and seams or cracking, or both. However, further analysis of this relationship revealed that the significance of this correlation is questionable because the seam rating score decreases only 0.25 when the top gauge increases by 10.

4. Geographic effects.

Because the eastern and southeastern sections of Ohio typically have streams with low pH values (5.1 to 7.1) and high

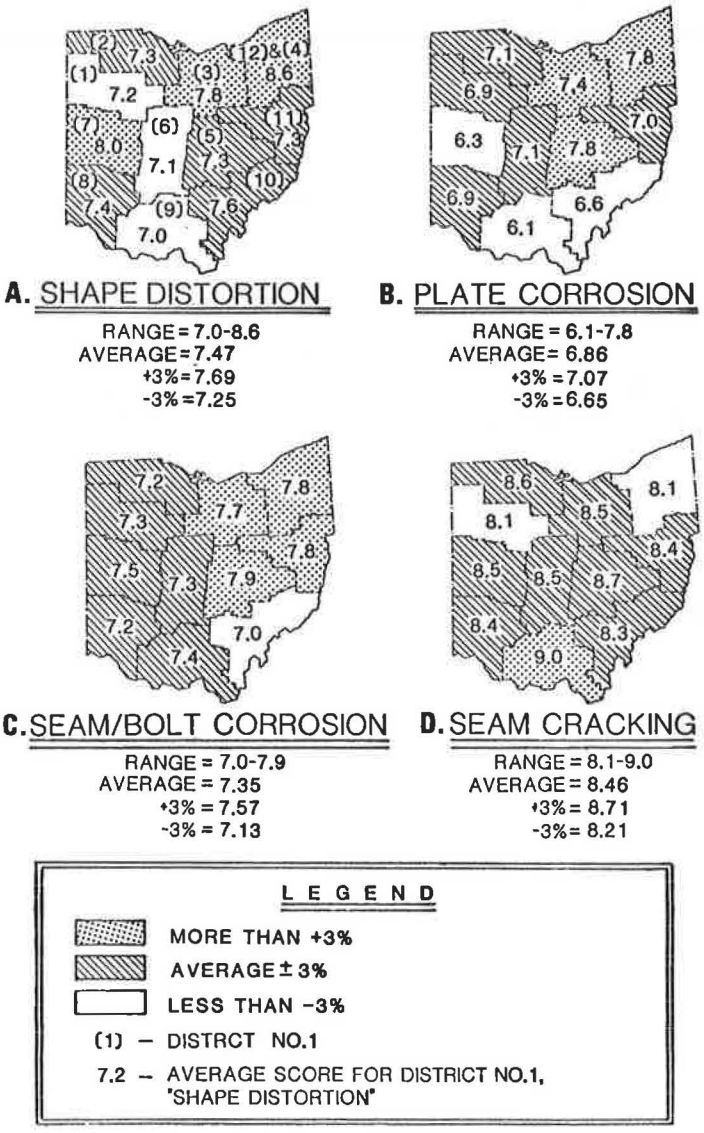

FIGURE 11 Geographic influence of pipe-arch problem area.

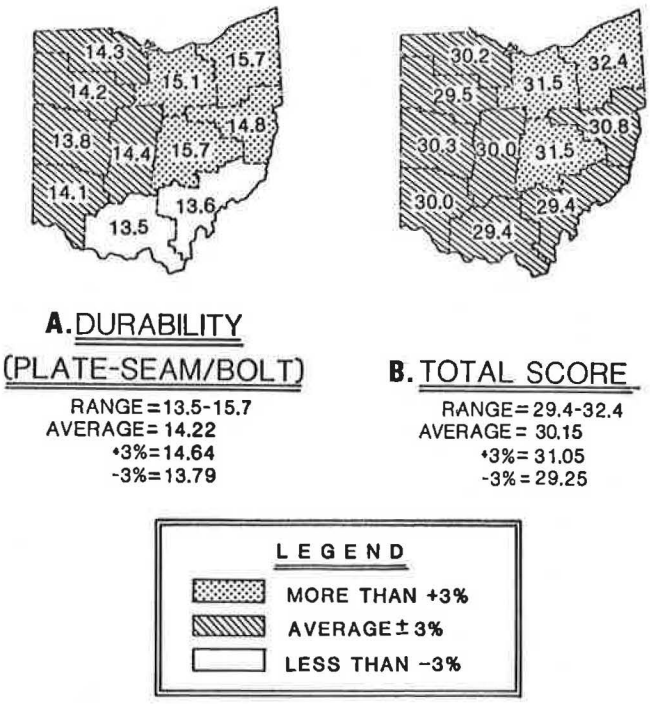

FIGURE 12 Geographic effects on structure durability and total composite score.

abrasive bed loads, an attempt was made to establish a correlation of shape, seam, plate, and metal (seam or bolt) corrosion with the geographic areas of the state. Presented in Figures 11*A*, 11*B*, 11*C*, and 11*D* are the average scores (by district) for each of the four categories evaluated. These scores represent an average of the scores for all structures within a district. Note that the dotted areas of the state represent districts where the scores were greater than 3 percent of the state average. Conversely, areas with no shading represent districts where the scores were less than 3 percent of the state average. Areas with shading represent districts that had scores within ±3 percent of the state average. A score of 9 represents no deterioration.

An evaluation of this data indicates that pipe arches in the northeastern area of the state are in better shape than those in the south or southeast. The low plate corrosion scores in southeastern Ohio were expected in view of the low pH values of the streams in this area. A low seam or bolt corrosion score also occurred in District 10. Because both the plate and metal seam or bolt scores provide a measure of the effects of corrosion and seepage on the structure, these two scores were combined (see Figure 12*A*). As expected, the southeastern portion of the state had the lowest durability scores whereas the northeastern area had the highest scores.

TABLE 5 COEFFICIENT OF DETERMINATION FOR DURABILITY VERSUS AGE REGRESSION CURVES

Regression Curve	9 and 10	1, 2, 6, 7, 8	3, 4, 5, 11, 12
Linear	0.85	0.90[a]	0.89
Exponential	0.78	0.85	0.86
Power	0.52	0.65	0.65

[a] Durability score = 18.54 − 0.19 age (see Figure 7).

Seam cracking does not appear to be a problem in the south whereas the northeastern and northwestern portion of the state have a significant occurrence of seam cracking. The offsetting effects of the corrosion problems in southeastern Ohio and the seam cracking problem in the northern portion of the state resulted in a more uniform total score for the state, as evidenced by a majority of the scores falling within the range of ±3 percent of the average score (see Figure 12*B*). This canceling effect suggests that better regressions may be obtained between various parameters if data were separately processed in groups of two or three districts. This grouping and regression analysis was done for durability (plate and metal) versus age, with the results shown in Table 5 and in Figure 13.

Comparing the coefficients of determination shown in Table 5 with the data in Table 4 fails to demonstrate any improvement by this grouping of data. It can, therefore, be concluded that it is more appropriate to conduct the analyses on a statewide basis than by separate groupings of districts. Nevertheless, separate regressions for small groups of districts show different regression curves. For example, in Figure 13 it can be seen that the decrease in the durability scores is slower in Districts 3, 4, 5, 11, and 12 than in all the other districts.

It is also shown in Figure 13 that a two-slope line (similar to an exponential curve) would better describe the durability relationship to age than does a straight line. The slope of the curves corresponding to the decrease of durability with time experiences a significant increase after the age of about 35 yr.

5. Frequency of occurrence evaluation.

Various computer sorts of the field inspection data for the 890 structures were performed in an attempt to reveal major

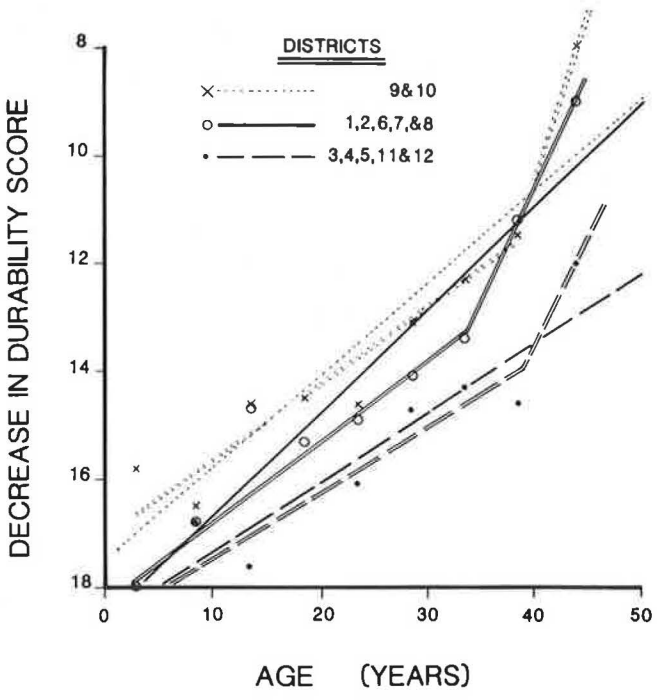

FIGURE 13 Decrease in durability score with increasing age of structure.

TABLE 6 STRUCTURE SCORE VERSUS FREQUENCY OF OCCURRENCE

Score	Metal		Seams	Shape
	Seams/Bolts	Plate		
0	8	1	0	2
1	2	4	0	1
2	4	11	0	6
3	7	48	2	7
4	6	41	2	17
5	74	49	5	21
6	47	82	11	50
7	276	314	144	343
8	256	181	101	217
9	191	140	596	208
No data	19	19	29	18
Total	890	890	890	890

problem areas and the causes of problems. Presented in Table 6 are a frequency of occurrence for the structure score for metal durability (seams or bolts and plate), seams (cracking), and shape. The number of structures receiving the score rating from 0 to 9 are shown in this table. A review of these data reveals that 20 structures (2.2 percent) experienced major cracking (score of 6 or less) at either one location or throughout the structure. A total of 104 structures (11.7 percent) experienced significant flatness or distortion (score of 6 or less) at least one section within the structure. An additional 343 structures (27.3 percent) experienced slight nonsymmetrical distortion or minor sagging (score of 7) at one or more locations throughout the structure.

With regard to durability, a total of 64 (7.2 percent) of structures experienced severe corrosion and pitting (score of 3 or less), either locally or throughout the structure. An additional 172 (19.3 percent) of structures experienced fairly heavy corrosion with either light or moderate pitting (score of 4 to 6) throughout the structure. A total of 148 (16.2 percent) structures experienced significant water seepage with fairly heavy corrosion (score of 6 or less) occurring at the seam or bolt joints.

Because information on whether significant distortion or sagging of the structure influenced the occurrence of seam cracking was required, a frequency of occurrence of seam versus shape scores was prepared (see Table 7). As a review of this table indicates, the number of structures with a low score (6 or less) is very small. Therefore, a grouping of the structures (shown in Table 8) was prepared and used for the linear regression analysis. The results of this analysis indicated a linear regression curve fit of the data with an excellent coefficient of determination ($r^2 = 0.99$). This relationship may be expressed as seam score = 7.06 + 0.19 × shape score. This relationship should only hold for shape scores of 5 or greater because there are insufficient data points below this rating to establish any degree of confidence for the equation holding true.

An evaluation of shape scores as a function of span or rise dimensions failed to show any correlation. This evaluation was based on a total population of 715 pipe-arch structures.

Presented in Table 9 is a listing by district of the number of structures that received a perfect rating (a score of 36). A total of 48 structures received a perfect score. This represents 5.4 percent of the total number of structures in the field. The structures were built during the period 1947 to 1986, with the average age being 24 yr. An interesting observation from this table is the unusually high percentage (24 percent) of the 83 structures installed in north central Ohio receiving a perfect score. The average age of these structures is 37 yr. This area of the state has a very low stream abrasion, with stream pH values ranging from 7.9 to 8.3.

A listing of the number of structures receiving the lowest scores is presented in Table 10. This listing represents a range of scores between 7 and 24. A review of these data shows that District 10 has the highest percentage of structures with low scores. This was expected because the stream loads in this area are highly abrasive and the pH values range from 5.1 to 6.5. An unusual observation from this table is the relatively high number of structures receiving a low score in District 3. This is the same district that had the highest percentage of structures receiving a perfect score. The frequency of occurrence of these low scores is presented in Table 11.

Presented in Figure 14 is a histogram of the frequency of occurrence of the scores ranging from 14 to 36. The total composite score ranged from 7 to 36. The average of the total composite score was 30.15, with a standard deviation of 4.0 and a variance of 15.6. Presented in the following table are the average score, standard deviation, and variance for each of the four problem area categories evaluated: shape, plate, metal, and seams.

Problem Area	*Score*	*Standard Deviation*	*Variance*
Shape	7.5	1.3	1.8
Seam Cracking	8.5	0.9	0.8
Plate Corrosive	6.9	1.7	3.0
Metal (seam or bolt corrosion)	7.4	1.5	2.3

TABLE 7 FREQUENCY OF OCCURRENCE OF SEAM VERSUS SHAPE SCORES

Seam Score	Shape Score											Total
	0	1	2	3	4	5	6	7	8	9	No Data	
3	1	0	0	0	0	0	1	0	0	0	0	2
4	0	0	0	1	1	0	0	0	0	0	0	2
5	0	0	0	0	0	1	2	0	1	0	1	5
6	0	0	0	0	0	1	1	7	1	1	0	11
7	1	0	3	3	4	7	8	88	17	13	0	144
8	0	0	0	0	1	4	5	30	39	21	1	101
9	0	1	3	2	10	8	32	210	159	167	4	596
No data	0	0	0	1	1	0	1	8	0	6	12	29
Total	2	1	6	7	17	21	50	343	217	208	18	890

TABLE 8 CORRELATION OF SHAPE VERSUS SEAM SCORES

Shape Scores		No. of Structure		Average Seam Scores
0		2		
1	1.5	1	16	7.33
2		6		
3		7		
4	4.5	17	38	7.94
5		21		
6		50		8.22
7		343		8.32
8		217		8.63
9		208		8.75

TABLE 9 NUMBER OF STRUCTURES WITH PERFECT SCORES

Number of Structures			
District	Perfect Scores	No. Installed	Percentage
1	0	59	0
2	0	51	0
3	19	83	24.0
4	4	43	9.3
5	1	46	2.2
6	3	71	4.2
7	3	62	4.8
8	12	157	7.6
9	4	123	3.3
10	2	166	1.2
11	1	27	3.7
12	0	2	0
Total	49	890	5.4

CONCLUSIONS

Before the initiation of the analysis of the field inspection data, a number of questions were presented to establish if there was an interrelationship between certain design parameters for pipe arches and the problem areas of shape; distortion or sagging, or both; seam cracking; and durability. Results of the analysis permit the following conclusions:

1. Durability: The durability rating of the structure (susceptibility to corrosion and seepage) has been established as a linear relationship with age until the structure is approximately 35-yr old, at which time the rate of the structure deterioration increases.

2. Durability versus geographic location: The field data clearly indicated that the pipe arches located in southeastern Ohio (which have high abrasive stream loads with a low pH value) result in a higher rate of structure deterioration (decreasing durability scores) than other geographic areas of the state.

3. Durability versus distortion or cracking: There was no apparent relationship indicated between the structure's shape and seam cracking problems and the amount of corrosion or abrasion, or both.

4. Gauge versus distortion or cracking problems: There is no apparent relationship indicated between the gauge of the multiplate sections and the problems of shape distortion, durability, or seam cracking.

5. Depth versus distortion or cracking: There is no correlation indicated between the depth of cover and the shape distortion, durability, or cracking problems.

TABLE 10 NUMBER OF STRUCTURES WITH LOW SCORES (RANGE FROM 7 TO 24)

Number of Structures			
District	Low Scores	No. Installed	Percentages
1	6	59	10.2
2	1	51	2.0
3	10	83	12.1
4	0	43	0
5	3	46	6.5
6	2	71	2.8
7	5	62	8.1
8	11	157	7.0
9	9	123	7.3
10	23	166	13.8
11	2	27	7.4
12	0	2	0
Total	72	890	

TABLE 11 FREQUENCY OF OCCURRENCE OF LOW SCORES

Scores	No. of Occurrences
7	1
14	1
15	3
16	1
17	2
18	2
19	1
20	5
21	10
22	10
23	16
24	20
Total	72

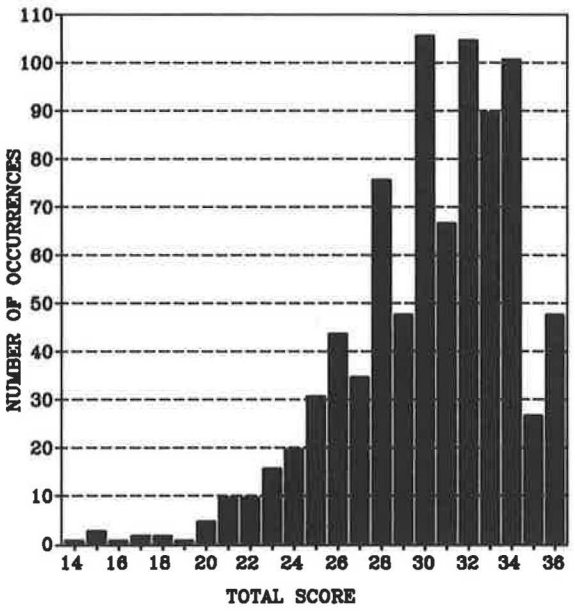

FIGURE 14 Frequency of occurrence of each score (total composite).

6. Shape versus cracking problems: A linear relationship was indicated for these two problem areas for the higher score values (i.e., seam scores of 7 and greater and shape scores greater than 5). Insufficient data were available to establish a relationship at the lower scores.

7. Dominant modes of failure: The most dominant problem area of the pipe-arch structure is the occurrence of corrosion and pitting of the multiplate structure, and seepage and corrosion of the bolted joints. A total of 27 percent of the structures experienced fairly heavy corrosion. Sagging or deflection of these structures was also a problem area with 11.7 percent of the structure showing significant distortion or flatness, or both, in one or more sections throughout the structure.

8. Cracking: Cracking was observed to be only a minor problem, with only 2 to 3 percent of the structures indicating 1- to 1½-in. cracks occurring on either side of the bolt hole along the corner spring-line seam joint.

9. Fidelity of data: Although there were 18 different inspectors involved in the field evaluation of the 890 pipe arch structures, the method of rating generally produced reliable, valid data. When these structures are again inspected by different inspectors, the validity of the field inspection reporting approach will be further verified.

See also "Evaluation of Corrugated Metal Pipe-Arches," Volumes 1 and 2. (*1*, *2*).

REFERENCES

1. G. H. Degler, V. G. Perlea, and D. C. Cowherd. *Evaluation of Corrugated Metal Pipe-Arches*, Vol.1. FHWA-89-003, U.S. Department of Transportation (prepared by Bowser-Morner Associates, Inc.), Dec. 1988.
2. V. G. Perlea and D. C. Cowherd. *Evaluation of Corrugated Metal Pipe-Arches*, Vol. 2. FHWA-8-89-0, U.S. Department of Transportation, (prepared by Bowser-Morner Associates Inc.), Dec. 1988.

Publication of this paper sponsored by Committee on Subsurface Soil-Structure Interaction.

Elastic Buckling Strength of Buried Flexible Culverts

IAN D. MOORE, ERNEST T. SELIG, AND ATEF HAGGAG

Buckling of buried flexible culverts is defined as the loss of resistance to flexural deformations. Alternative theories are described. Then the procedures used by the most common current design codes are summarized and their limitations explained. The continuum theory is proposed as the best available approach to evaluate the buckling strength of buried flexible culverts because it most realistically models the soil properties and geometry. The suggested means of applying the continuum theory is presented. Example calculations show how the continuum theory results compare with those of existing codes. A major conclusion is that the substantial reduction in stability as structure size increases, as indicated by most approaches, is not correct according to the continuum theory. Commonly used theories are shown to be very conservative in most cases compared with the continuum theory. However, in some cases, for example shallow burial, the reverse may be true.

A characteristic feature of corrugated metal culverts is their bending flexibility. Early in the history of long-span metal culverts, workers recognized that these flexible structures could potentially fail by buckling (*1*). In fact, various buckling collapses have been observed in the field. Unfortunately most of these are not documented in the literature, and there is also ongoing debate as to which cases involving distorted structures constitute buckling. A structure buckles elastically or inelastically when compressive membrane forces act to reduce the flexural stiffness so that there is no resistance to lateral movement.

Currently, codes of practice and design handbooks use a variety of procedures for estimating buckling strengths of flexible structures [e.g., the American Association of State Highway and Transportation Officials (AASHTO) (*2*), the American Iron and Steel Institute (AISI) (*3*), the American Water Works Association (AWWA) (*4*), and the Ontario Ministry of Transportation and Communications (OMTC) (*5*)], although in some cases there is no requirement for the largest of these, known as long span structures, to be designed for buckling (*2*, *3*). The design procedures are generally based on the Winkler (i.e., elastic spring) soil model, and are largely empirical in nature.

This paper begins with a brief review of the theoretical buckling analyses and code procedures, and comparisons are made with available test data. An approach to the problem based on the elastic continuum model is then described that permits rational predictions of culvert buckling strength. Finally, a number of example problems are considered, to demonstrate how the elastic continuum theory differs from existing design rules.

I. D. Moore, Department of Civil Engineering and Surveying, University of Newcastle, New South Wales 2308, Australia. E. T. Selig and A. Haggag, Department of Civil Engineering, University of Massachusetts, Amherst, Mass. 01003.

DEFINITION OF BUCKLING

Buckling is directly associated with the effect of changes in geometry on structural stiffness (i.e., geometrical nonlinearity). The simplest type of buckling analysis deals with the structure in its initial position. This is illustrated in Figure 1 for the Euler buckling problems (i.e., a straight column). If large in-plane forces (hoop thrusts N) are present and the structure deforms slightly (displacement W), then moments (M) are generated as a result of the in-plane forces acting at some eccentricity. The hoop thrusts therefore induce further bending and so decrease the effective flexural stiffness. Linear buckling theories involve the calculation of the hoop thrusts, which lead to zero flexural stiffness in the initial position.

For a soil-supported structure, the combined flexure stiffness of the complete soil-structure system must be considered, and in general soil support increases the buckling strength of the metal culvert significantly (Figure 2). Although not generally appreciated, the soil provides resistance to incremental deformations inward as well as outward.

A structure may or may not become unstable at critical load levels predicted by the linear buckling analysis. Deformations at lower load levels lead to changes in geometry. The loss of flexural stiffness then may never occur, or alternatively it may develop at load levels less than those predicted by linear analysis. A nonlinear analysis involving the study of incremental equilibrium in the deformed state is necessary to determine whether the critical load calculated using linear theory is a useful measure of buckling strength.

In this paper, buckling will be used to refer to the theoretical loss of resistance to flexural deformations. In practice this may be manifest by the development of wavelike deformations or flattening on the circumference, perhaps followed by catastrophic collapse (flattening, however, does not necessarily mean buckling). Elastic buckling means that buckling is initiated before the metal structure yields, whereas inelastic buckling means that the buckling response occurs after yield. Yield may occur after elastic buckling is initiated, but the response will nevertheless be called elastic buckling.

Only elastic buckling is addressed in this paper. More theoretical work is needed to determine how structural yield can influence buckling strength.

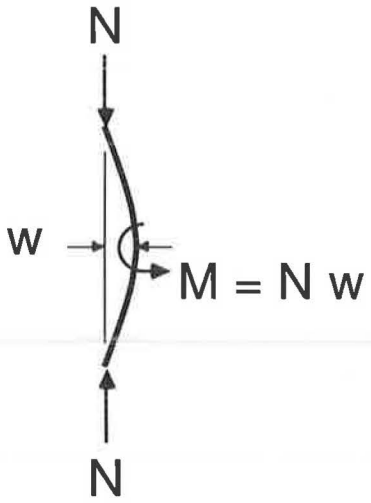

FIGURE 1 Euler buckling.

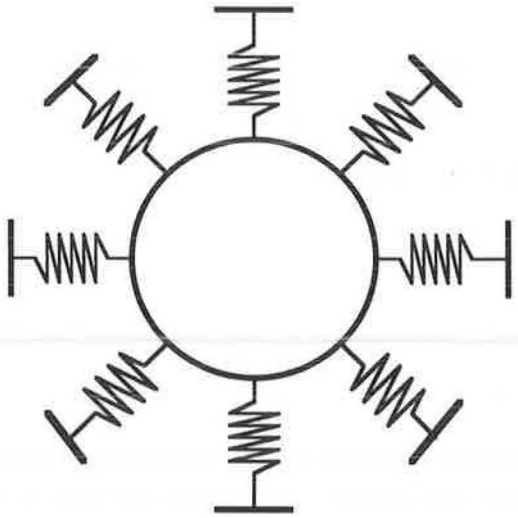

FIGURE 3 Winkler model.

DISCUSSION OF BUCKLING THEORIES

Both linear and nonlinear buckling theories have been developed for buried flexible cylinders.

Linear Theories

Linear theories have generally focused on the linear elastic buckling strength as a number of buckles form around the circumference of a uniformly stressed circular structure. The ground support restrains structural movement and therefore increases stability.

The ground support at the interface can be modeled using a series of elastic springs, as in the Winkler theory (Figure 3), where the spring stiffness is called the coefficient of soil reaction (*1*, *6*, *7*). Unfortunately, ground resistance to structural movements is a complex function of structural geometry, burial depths, and soil properties. The difficulty in using the Winkler model lies in estimating the spring stiffness. Three approaches are possible for doing this:

1. Experimental measurements of buckling strength can be used to back calculate spring stiffness. An extensive testing program to cover the full range of culvert types, soil conditions, and burial depths is needed for this empirical approach to be reliable.
2. Spring stiffness can be expressed as a simple function of some measurable soil properties such as soil modulus (*1*, *7*). This approach can only be an uncertain approximation because the influences of structure size and shape, burial depth, the geometry of the backfill zone, and the embankment soil condition are not defined.
3. A rigorous theoretical analysis can be used in which the material properties and geometry of the soil system are modeled [e.g., Duns and Butterfield (*8*)]. One such approach is introduced in this paper.

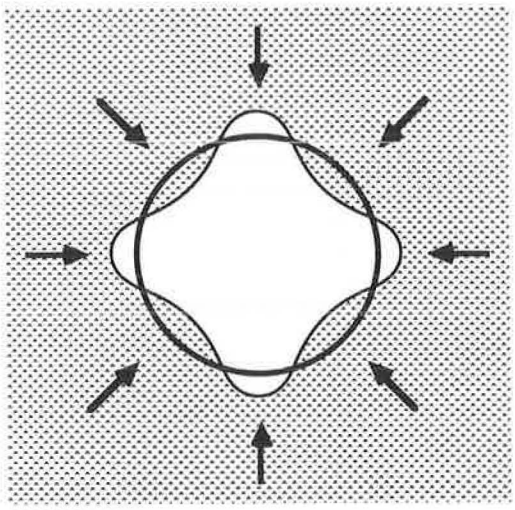

FIGURE 2 Flexible pipe buckling.

The elastic continuum model is a useful tool for assessing the extent of ground restraint at the soil-structure interface [e.g., Forrestal and Herrmann (*9*)]. Because this model represents the whole soil region, it has the potential to reveal how soil quality and quantity, hoop thrust distribution, and other factors influence buckling strength (Figure 4). Rational designs for burial depth (*10*) and the zone of select backfill (*11*) are therefore possible.

Nonlinear Theories

It is certainly important to consider the possibility that buried structures may be imperfection sensitive (i.e., deformations before buckling may reduce buckling strength below that predicted from linear theory). A number of workers have developed nonlinear buckling theories for buried structures (*12*–*14*), and it has been established that structures are not imperfection sensitive when earth loads induce the ring thrusts. However, there may be substantial decreases in buckling

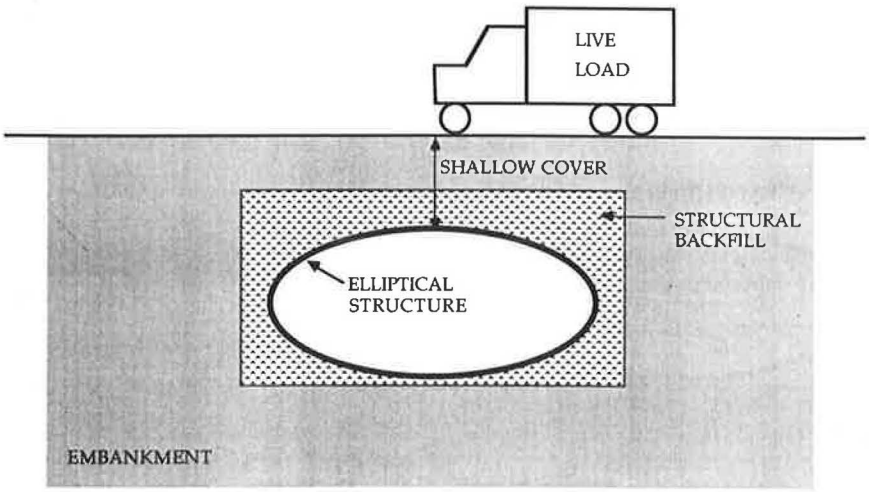

FIGURE 4 Factors considered in the continuum model.

strength when external fluid or internal vacuum loadings predominate.

Current Design Procedures

The design procedures outlined by AASHTO (*2*), AISI (*3*), AWWA (*4*), and OMTC (*5*) all feature calculations of elastic buckling strength based on the Winkler soil model. The first two are only loosely based on the Winkler theory, because they employ a single soil stiffness value that was selected on the basis of one set of experiments (*15*). The other two models feature variable spring stiffness, with empirical corrections for the effect of finite burial depth. AWWA has spring stiffness given as a linear function of constrained soil modulus, whereas the Ontario code provides a list of spring stiffness values for various soil types and densities.

COMPARISON WITH TEST DATA

Field test results indicate that hoop thrust in flexible metal culverts is nonuniformly distributed [e.g. Selig, Lockhart, and Lautensleger (*16*), Selig and Musser (*17*), and Beal (*18*)]. Theoretical analysis indicates that maximum hoop thrust controls the elastic stability (*19*). Therefore the test data used in this paper are limited to those cases in which the static structural response could be analyzed to evaluate soil modulus E_s, and where maximum hoop thrust around the structure at buckling could be estimated. The data, plotted in Figure 5, are from Allgood and Ciani (*20*), Howard (*21*), Gumbel (*22*), and Crabb and Carder (*23*). Also shown in Figure 5 are lines corresponding to (a) elastic continuum theory for a smooth, uniformly stressed, deeply buried cylinder in homogeneous ground (*24*), (b) Winkler theory in which spring stiffness k_s is given in terms of soil, Young's modulus E_s and Poisson's ratio υ_s by

$$k_s = E_s/(1 + \upsilon_s)$$

(c) AASHTO (*2*), and (d) AISI (*3*). Critical hoop thrust N_c is normalized using structure flexural rigidity EI and tube radius R. Results are expressed as a function of stiffness ratio

$$8E_s^*R^3/EI$$

where

$$E_s^* = E_s/(1 - \upsilon_s^2).$$

In these calculations the soil Poisson's ratio is assumed to be 0.3, but Young's modulus E_s is back calculated from static deformation response.

Clearly the approaches outlined in AASHTO (*2*) and AISI (*3*) are simplistic and can yield both excessively conservative and excessively unconservative solutions. The fact that these solutions do not account for shallow burial and other factors exacerbates the problems.

The Winkler solution, using the relationship between spring stiffness and soil modulus, is better but also does not follow the experimental trends satisfactorily, particularly for very flexible structures. The best fit line for the test data is almost parallel to the continuum theory line, which is effectively an upper bound to the experimental results. The difference between theory and experiment probably results from the nonlinear nature of soil behavior. Secant modulus, as calculated from static soil-structure response, may be consistently different from the soil modulus that controls buckling.

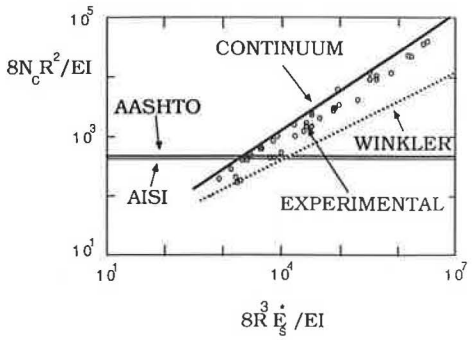

FIGURE 5 Comparison of buckling theories with experimental results.

The remainder of the paper deals with the use of elastic continuum theory predictions of buckling strength after calibration to give lower bound rather than upper bound buckling strength predictions.

APPLICATION OF CONTINUUM THEORY

The critical hoop thrust N_c, which elastically destabilizes the metal culvert, is conveniently expressed as

$$N_c = \phi N_{ch} R_h R_s \quad (1)$$

where ϕ is a calibration factor to account for experimental variation and soil nonlinearity; N_{ch} is the buckling strength of a uniformly stressed, deeply buried circular culvert in homogeneous ground; R_h represents the correction factors for shallow burial and the geometry of the backfill zone; and R_s is a correction factor for culvert shape.

Calibration Factor

Statistical analysis of test data presently available suggests that a value of 0.55 gives a reasonable lower bound for granular soil (*24*). The calibration factor for clay material should probably be less.

Deeply Buried Culvert

The critical thrust N_{ch} for a smooth, circular, deeply buried culvert of radius R and flexural stiffness EI is given by

$$N_{ch} = \frac{(n^2 - 1)EI}{R^2} + \frac{E_s^* R}{2n + (1 - 2\upsilon_s)/(1 - \upsilon_s)}, \quad (2)$$

which is minimized with respect to harmonic number n, an integer greater than or equal to 2 (*25*). For typical flexible metal culverts, that is, $EI/E_s^* R^3 \leq 10^{-2}$, Equation 2, reduces to

$$N_{ch} \approx 1.2(EI)^{1/3}(E_s^*)^{2/3}. \quad (3)$$

For these same deeply buried flexible structures, buckling wavelength is given approximately by [Moore (*10*)]:

$$\lambda = 2\pi(4EI/E_s^*)^{1/3}, \quad (4)$$

which increases as soil stiffness E_s^* is reduced.

Backfill Geometry

Backfill geometry effects can be examined using various solutions for the linear buckling problem. To date, two idealized configurations have been considered, as shown in Figure 6:

1. A circular culvert buried close to the ground surface in homogeneous soil. This solution was obtained using the finite element method (*10*). Correction factors R_{hs} are shown in Figure 7 relative to the stiffness ratio $4EI/E_s^* R^3$ for various ratios of crown cover depth h to culvert radius R. The soil-culvert interface is smooth (frictionless).
2. A deeply buried circular culvert in a circular zone of backfill. A closed-form analytical solution (*11*) was obtained for this case for various ratios of backfill zone width w to culvert radius R. Shown in Figure 8 are R_{hd} values for $w/R = 0.1$ and a range of modulus ratios E_o^*/E_s^*, where $E_o^* = E_o/(1 - \upsilon_o^2)$ characterizes the stiffness of the material surrounding the select backfill.

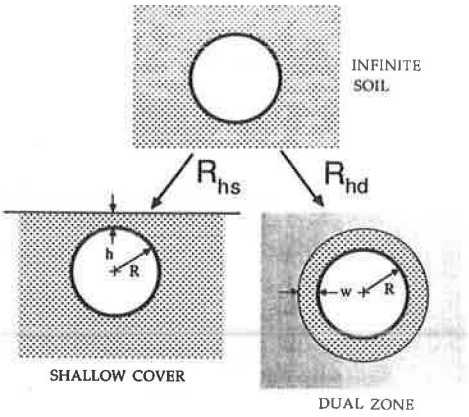

FIGURE 6 Backfill geometry correction factors.

To obtain Figures 7 and 8, the soil Poisson's ratio was taken as 0.48. However, the effect of changing Poisson's ratio on the value of correction factors is small.

The wavelength of the buckling deformation can lengthen significantly as the parameter w, representing backfill quantity, or h, representing burial depth, is reduced.

Noncircular Culverts

The linear finite element buckling analysis can also be used to examine the buckling strength of noncircular structures (Figure 9). Elliptical culverts have been examined (*26*). The results show that the buckling strength of a deeply buried ellipse is approximately equal to that of a circular tube of

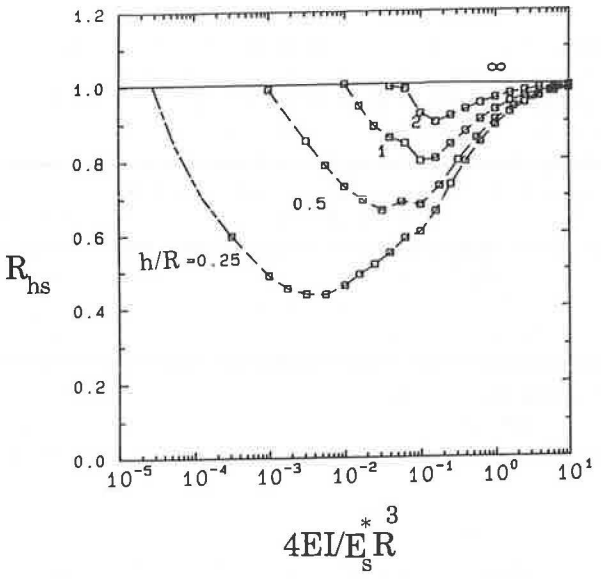

FIGURE 7 Correction factor for shallow cover.

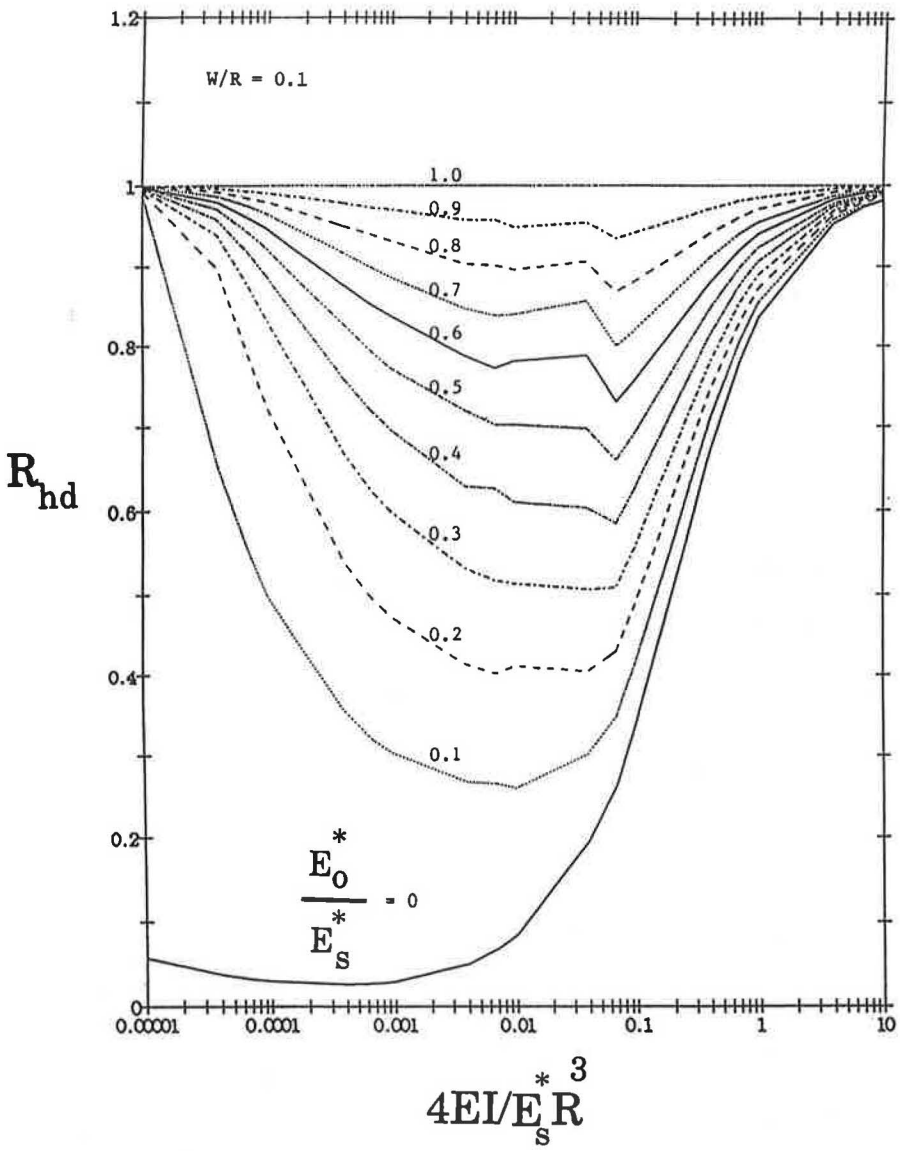

FIGURE 8 Correction factor for dual zone of soil.

equal circumference (i.e., $R_{se} = 1$). Thus the stability of shallow buried ellipses can be evaluated from Figure 7, where R in the stiffness ratio $4EI/E_s^*R^3$ is equated to the ellipse circumference divided by 2π. The burial depth ratio h/R in Figure 7 is equated to burial depth over the half span for the ellipse.

Nonlinear buckling analysis of shallow buried elliptical structures may be needed to confirm the validity of these findings obtained using linear buckling theory.

Factor of Safety

The safety factor F is defined as

$$F = \frac{N_c}{N_m}, \tag{5}$$

for critical thrust N_c from Equation 1 and maximum thrust N_m. Maximum thrust is best calculated using static finite element analysis.

Soil Modulus

Naturally, an important step in using the continuum theory lies in estimating E_s^*, because buckling strength primarily arises from the soil restraint, as shown by Equation 3. The comparison between measured and predicted buckling thrust shown in Figure 5 was based on secant soil modulus backfigured from experimental data, and the theory has been calibrated on that basis. Reasonable lower bound values for secant soil modulus are therefore needed for design.

EXAMPLE CALCULATIONS

A series of example problems will be given to demonstrate the implications of the continuum theory solution. Shown in Figures 10 to 13 for various cases are the ratios of buckling thrust to the thrust that induces wall crushing by material yielding. Four different methods are used to estimate this ratio, namely the continuum model and the procedures out-

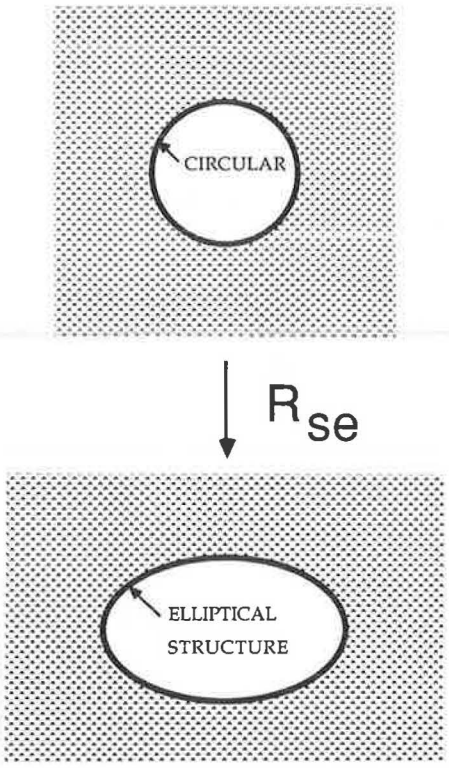

FIGURE 9 Correction factor for structural shape.

lined by OMTC (*5*), AASHTO (*2*) and AISI (*3*). Table 1 contains parameter values used in these calculations.

First, the effect of backfill quality and the size of the backfill zone are examined (Figure 10). The buckling strength of deeply buried 25-ft-diameter circular culverts is considered in turn for low-stiffness backfill, a thin ring of good-quality soil, a more extensive soil envelope, and finally good-quality soil alone. The continuum theory suggests that for low-stiffness soil, buckling precedes wall crushing. As the quantity of good-quality soil increases, buckling strength steadily improves until material strength controls stability. The continuum theory can be used to make a rational assessment of these various types of ground support.

The Ontario code permits an assessment of soil stiffness and its influence on buckling strength but is not able to rationally predict the effect of backfill quantity. Neither AASHTO nor AISI suggest how backfill quality influences buckling strength. For this problem, they appear unconservative for low-stiffness soil but overconservative for stiff ground.

CASE	CONTINUUM	OMTC	AASHTO	AISI
A	0.7	0.3	1.2	1.1
B	0.9	1.0	1.2	1.1
C	1.9	1.0	1.2	1.1
D	2.7	1.0	1.2	1.1

FIGURE 10 Effect of backfill conditions on ratio of buckling to thrust yield stress.

CASE	CONTINUUM	OMTC	AASHTO	AISI
D	2.7	1.0	1.2	1.1
E	2.7	0.9	0.7	1.1
F	2.7	0.85	0.5	0.4
G	2.7	0.8	0.2	0.4

FIGURE 11 Effect of size and shape of culvert on ratio of buckling to thrust yield stress.

A significant difference between Winkler soil models and the continuum theory lies in the perceived effect of structural size and shape on elastic buckling. Compared in Figure 11 are predictions of the buckling-to-yield ratio for two deeply buried circular culverts (spans 25 and 40 ft) and two deeply buried elliptical structures (span 25 ft, height 15 ft; and span 40 ft, height 29 ft).

The continuum model suggests that buckling thrust N_c is independent of culvert size and shape. In each case the buckling thrust is 2.7 times the thrust that induces wall crushing.

AASHTO and AISI indicate that there is a substantial reduction in stability as span increases for the same shape. The radius of curvature at the crown of the elliptical culverts is larger than the radius of circles of equal span. Thus OMTC and AASHTO both suggest that buckling is more likely for elliptical culverts than for circular culverts of equal span. Size and shape effects in OMTC are small. It is well known that the AASHTO and AISI buckling equations contradict field experience in that long-span culverts currently in service are performing satisfactorily, whereas these methods indicate that the culverts are overloaded. This partially explains the fact that long-span structures are currently exempted by AASHTO and AISI from satisfying the buckling criteria. There is no reason to believe that long spans are less susceptible to buckling failure than the smaller span structures. Thus the assessment of long-span structures for the possibility of buckling failure is desirable for reasons of safety and economy. The proposed continuum method should make this possible.

CASE	CONTINUUM	OMTC	AASHTO	AISI
D	2.7	1.0	1.2	1.1
H	0.5	0.2	1.2	1.1

FIGURE 12 Effect of cover depth on ratio of buckling to thrust yield stress.

CASE	CONTINUUM	OMTC	AASHTO	AISI
E 	2.7	0.9	0.7	1.1
I 	3.5	1.1	0.7	1.1

FIGURE 13 Effect of culvert wall thickness on ratio of buckling to thrust yield stress.

Ground support contributes significantly to the buckling strength of metal culverts. As cover over the culvert crown is reduced, ground restraint decreases over the structure and load capacity is reduced. Predictions of buckling thrust relative to yield thrust for a deeply buried circular culvert and a shallow buried structure are compared in Figure 12. Soil and culvert properties remain unchanged. Once again four predictions are shown for each culvert case.

Neither AASHTO (*2*) nor AISI (*3*) include an assessment of the influence of shallow burial on buckling strength. Both the OMTC (*5*) design approach and the continuum theory indicate that significant reductions in buckling strength occur as cover is decreased. The former makes use of a number of empirical corrections for shallow burial. The latter is a theoretical procedure for estimating burial depth effects given directly by the continuum model. The failure mode has converted from ring crushing to elastic buckling with the decrease in crown cover. The empirical buckling equations given by AASHTO and AISI may be quite unconservative for this problem. Rational predictions of minimum cover can be made based on the continuum buckling theory. These complement empirical guidelines for minimum cover such as presently in use by OMTC and those based on analyses of stability using soil failure and limiting bending moment.

To complete the examples, the buckling strengths of deeply buried elliptical culverts for different sets of wall moment of inertia I and wall area A (resulting from a change in plate thickness) have been compared in Figure 13. Both empirical solutions suggest that the ratio of critical thrust to crushing force is unchanged. The other models indicate that wall crushing becomes even more dominant as plate thickness is reduced. It appears that elastic buckling is relatively more significant for the thicker steel plates used commonly on long-span structures.

In general, then, the empirical models currently incorporated in AASHTO (*2*) and AISI (*3*) include corrections for culvert span that are questionable, and cannot account for the effects of ground modulus or burial depth on buckling strength. For the structures considered, continuum theory predicts considerably higher buckling strengths for good-quality backfill. It does suggest, however, that buckling strength may control shallow cover situations in which stability is reduced significantly. The Ontario code (*5*) is, in general, the most conservative of the four theories.

SUMMARY AND CONCLUSIONS

The elastic buckling of flexible metal culverts has been considered. An examination of experimental results indicated that linear buckling theory based on the elastic continuum ground model provides a better estimate of buckling strength than other methods [Winkler models, AASHTO (*2*) and AISI (*3*)]. The continuum model is based on well-defined soil parameters and can consider the effect of shallow cover, the quality and quantity of backfill used to support the corrugated metal structure, and the culvert shape.

A procedure has been described for predicting metal culvert elastic buckling strength. With this procedure, the stability of both circular and elliptical structures can be evaluated for deep and shallow burial in homogeneous ground. The stability of deeply buried circular structures surrounded by a finite envelope of backfill can also be assessed. Rational design of structure backfill and minimum cover height is now possible. Linear buckling solutions of this type are suitable when hoop thrust is generated from earth loads rather than from fluid pressure or internal vacuum.

A number of example problems were considered in order to examine the implications of the new procedure. Estimates

TABLE 1 GEOMETRY AND MATERIAL PROPERTIES FOR EXAMPLE CALCULATIONS

Problem	Span (ft)	Rise (ft)	E_s,E' (lb/in.^{2})	I (in.^{4}/in.)	A (in.^{2}/in.)	R_h	R_t (ft-in.)
A	25	25	500	0.166	0.343	1	12-6
B	25	25	4,000	0.166	0.343	0.33 (w/R = 0.1)	12-6
C	25	25	4,000	0.166	0.343	0.70 (w/R = 0.3)	12-6
D	25	25	4,000	0.166	0.343	1	12-6
E	25	15	4,000	0.166	0.343	1	16-8
F	40	40	4,000	0.166	0.343	1	20
G	40	29	4,000	0.166	0.343	1	28-4
H	25	25	4,000	0.166	0.343	0.2 (h/R = 0.12)	12-6
I	25	15	4,000	0.108	0.228	1	16-8

NOTE: For steel $E = 30 \times 10^6$ lb/in.^{2} and yield stress $= 33 \times 10^3$ lb/in.^{2}. For soil $\upsilon_s = 0.33$.

of buckling strength were compared with calculations based on three other design procedures [OMTC (*5*), AISI (*3*), and AASHTO (*2*)].

The empirical elastic buckling equations specified in AASHTO and AISI suggest that buckling strength is independent of soil stiffness and burial depth. They also indicate that substantial reductions in stability occur as structural size is increased. These trends are believed to be incorrect.

The Ontario code used a linear buckling solution based on the Winkler model, in which modulus of subgrade reaction is treated as a material constant and empirical corrections are included for considering burial close to the ground surface. It is believed to be very conservative.

The continuum theory solution indicated that for typical deeply buried culverts, buckling strength is a function of the flexural stiffness of the structure and ground modulus rather than is span or perhaps even shape. However, the continuum theory also demonstrates that shallow burial or poor backfill can reduce stability dramatically. The assessment of buckling strength for long-span culverts is currently not required by AASHTO or AISI, probably because of the excessively conservative nature of the empirical buckling equations when used for those structures. However, it is important to assess the buckling strength of all flexible metal culverts, and continuum solutions are believed to yield rational and reliable estimates of stability that enable all structures to be considered.

Further developments of the continuum solutions are envisaged, using a linear finite element buckling solution. Studies of various field installations should provide valuable data for comparisons with the model.

REFERENCES

1. G. G. Meyerhof and L. D. Baikie. Strength of Steel Culvert Sheets Bearing Against Compacted Sand Backfill. In *Highway Research Record 30*, HRB, National Research Council, Washington, D.C., 1963, pp. 1–14.
2. *Bridge Design Code*. American Association of State Highway and Transportation Officials, Washington, D.C., 1983.
3. *Handbook of Steel Drainage and Highway Construction Products*, 3rd ed., American Iron and Steel Institute, Washington, D.C., 1983.
4. *Revised Recommendations for Elastic Buckling Design Requirements for Buried Flexible Pipes*. American Water Works Association, Denver, Colo., Jan. 1982.
5. *The Ontario Bridge Code*. Ontario Ministry of Transportation and Communications, Downsview, Ontario, Canada, 1983.
6. G. W. H. Stevens. The Stability of a Compressed Elastic Ring and of a Flexible Heavy Structure Spread by a System of Elastic Rings. *Quarterly Journal of Mechanics and Applied Mathematics*, Vol. V, Pt. 2, 1952, pp. 221–236.
7. U. Luscher. Buckling of Soil-Surrounded Tubes. *Journal of the Soil Mechanics Foundation Division*, ASCE, Vol. 92, No. SM6, Nov. 1966, pp. 211–228 (discussed in Vol. 93, No. SM2, 1967, p. 163; No. SM3, pp. 179–183; No. SM5, pp. 337–340; Author's Closure, Vol. 94, No. SM4, 1968, pp. 1037–1038).
8. C. S. Duns and R. Butterfield. Flexible Buried Cylinders, Part III: Buckling Behavior. *International Journal of Rock Mechanics and Mining Sciences and Geomechanics Abstracts*, Vol. 8, No. 6, Nov. 1971, pp. 613–627.
9. M. J. Forrestal and G. Herrmann. Buckling of a Long Cylindrical Shell Surrounded by an Elastic Medium. *International Journal of Solids and Structures*, Vol. 1, 1965, pp. 297–310.
10. I. D. Moore. The Elastic Stability of Shallow Buried Tubes. *Geotechnique*, Vol. 37, No. 2, 1987, pp. 151–161.
11. I. D. Moore, A. Haggag, and E. T. Selig. *Buckling of Cylinders Supported by Nonhomogeneous Elastic Ground*. Internal Report No. TRB 88-346I, Geotechnical Engineering Department, University of Massachusetts, Amherst, Maine, Feb. 1988.
12. J. A. Cheney. Pressure Buckling of Ring Encased in a Cavity. *Journal of Engineering Mechanics Division*, ASCE, Vol. 97, No. EM2, April 1971, pp. 333–342.
13. B. Falter. Grenzlasten von einseitig elastisch gebetteten kreiszylindrischen Konstructionen. (Critical Loads for Circular Cylindrical Structures with One-Sided Elastic Support.) *Bauingenieur* 55(10), 1980, pp. 381–390.
14. I. D. Moore. *The Stability of Buried Tubes*. Ph.D. dissertation, School of Civil and Mining Engineering, University of Sydney, Australia, 1985.
15. R. K. Watkins and A. P. Moser. *The Structural Performance of Buried Corrugated Steel Pipes*. Engineering Experiment Station, Utah State University, Logan, Utah, Sept. 1969.
16. E. T. Selig, C. W. Lockhart, and R. W. Lautenslegar. Measured Performance of Newtown Creek Culvert. *Journal of the Geotechnical Engineering Division*, ASCE, Vol. 105, No. GT7, Sept. 1979, pp. 1067–1087.
17. E. T. Selig and S. C. Musser. Performance Evaluation of a Rib-Reinforced Culvert. In *Transportation Research Record 1008*, TRB, National Research Council, 1985, pp. 117–122.
18. D. B. Beal. Field Tests of Long-Span Aluminum Culvert. *Journal of the Geotechnical Engineering Division*, ASCE, Vol. 108, No. GT6, June 1982, pp. 873–890.
19. I. D. Moore and J. R. Booker. The Behavior of Buried Flexible Cylinders Under the Influence of Nonuniform Hoop Compression. *International Journal of Solids and Structures*, Vol. 21, No. 9, 1985, pp. 943–956.
20. J. R. Allgood and J. B. Ciani. The Influence of Soil Modulus on the Behavior of Cylinders in Sand. In *Highway Research Record 249*, HRB, National Research Council, Washington, D.C., 1968, pp. 1–13.
21. A. K. Howard. Laboratory Load Tests on Buried Flexible Pipe. *Journal of the American Water Works Association*, Vol. 64, No. 10, Oct. 1972, pp. 655–662.
22. J. E. Gumbel. *Analysis and Design of Buried Flexible Pipes*. Ph.D. dissertation, Department of Civil Engineering, University of Surrey, Guildford, England, 1983.
23. G. I. Crabb and D. R. Carder. *Loading Tests on Buried Flexible Pipes To Validate a New Design Model*. Research Report 28, Transport and Road Research Laboratory, Crowthorne, Berkshire, England, 1985.
24. I. D. Moore. *Elastic Buckling of Buried Flexible Tubes—A Review of Theory and Experiment*. Department of Civil Engineering and Surveying, Research Report 025.09.87, University of Newcastle, New South Wales, Australia, 1987.
25. I. D. Moore and J. R. Booker. Simplified Theory for the Behavior of Buried Flexible Cylinders Under the Influence of Uniform Hoop Compression. *International Journal of Solids and Structures*, Vol. 21, No. 9, 1985, pp. 929–941.
26. I. D. Moore. Buckling of Buried Flexible Tubes of Noncircular Shape. In *Proc., International Conference on Numerical Methods in Geomechanics*, Innsbruck, Austria, April 1988.

Publication of this paper sponsored by Committee on Subsurface Soil-Structure Interaction.

Current Practice of Reinforced Concrete Box Culvert Design

MAHER K. TADROS, CONSTANCE BELINA, AND DALLAS W. MEYER

Although the state of Nebraska alone spends about $2.50 million annually on construction of reinforced concrete box culverts, relatively little research has been devoted to them in recent years. The research described in this paper was, in part, directed at establishing the state of the art of the design of these culverts. Specifically, a summary is given in this paper of the results of recent field measurements. It has been found that the field measurements of soil pressures indicated higher pressures than those given by the American Association of State Highway and Transportation Officials specifications. The responses of state bridge engineers, or those with similar responsibilities, to a questionnaire on their design practices are reported herein. Several inconsistencies in the American Association of State Highway and Transportation Officials specifications were reported. Despite these inconsistencies and the apparent underestimation of soil loading, very little structural distress was observed. Lack of distress may be attributed to several causes. For example, some of the states use higher soil pressures than American Association of State Highway and Transportation Officials' specified values. Also, the conservative criteria associated with the working stress design increase the margin of safety against failure and reduce the effect of underestimating the soil loads.

Use of cast-in-place reinforced concrete box culverts (RCBCs) as underground conduits is common throughout the United States. In the state of Nebraska the Department of Roads currently spends about $2.6 million on RCBC construction annually. Typical design of the RCBC within the United States is based on the American Association of State Highway and Transportation Officials (AASHTO) Standard Specifications for Highway Bridges (*1*). Soil loads are usually based on the AASHTO Group *X* loading for culverts.

Relevant full-scale testing by previous investigators is summarized herein. This testing has indicated a substantial discrepancy between the AASHTO design loads and in situ measured values. Because of these discrepancies, a survey was taken of the various state highway departments to determine their design practices. The topics addressed in the survey included the design method, load factors, soil loadings, and any structural distress encountered.

A discussion of the results of the survey is presented herein. The various practices are compared with the AASHTO specifications. It is shown that some of the states have recognized recent experimental and analytical evidence that the AASHTO specifications generally underestimate soil pressures on RCBCs.

The survey also indicates that a number of the states have adopted the load factor design approach as opposed to the older, and generally more conservative, service load design method. It is interesting to note that very few cases of structural distress were reported in the survey. Reasons for this apparently good performance, despite the use of relatively small loads in design, are discussed herein.

The subject of this paper is primarily the current design practices of cast-in-place RCBC. Recent analytical work (*2*) has indicated the need for critical review of the AASHTO specified soil pressures on RCBCs. The work was done with the aid of the computer program CANDE (*3*, *4*). Discussion of that work is beyond the scope of this paper.

Excellent work on precast concrete box culverts has recently been conducted by Heger et al. (*5–7*), Boring et al. (*8*), and LaTona et al. (*9*). This work confirms that soil pressures specified in Sections 3 and 6 of the AASHTO bridge specifications are lower than those obtained from field measurements and from rigorous soil-structure interaction analysis. LaTona et al. (*9*) discuss the computer program that led to ASTM C789 and C850 standard specifications for precast reinforced concrete box sections (*10*, *11*).

SURVEY OF STATE HIGHWAY DEPARTMENTS

In July 1984, bridge engineers, or those with similar responsibilities in all 50 state highway departments, received a letter that requested data on the concrete box culvert design practices used in their respective states. A copy of this letter is given in Figure 1. Thirty responses were received by letter or by telephone. Some responses were very brief; others, however, discussed their design practice in some detail. Remarks from several states included copies of design manuals for box culvert design. A synthesis of the information received is shown in Table 1. The following is a summary of the responses to the five questions asked in the letter.

Design Method

At the time they responded to the survey, 10 states used the load factor design (LFD) method. Twenty states used the service load design (SLD) method; however, 7 of the 20 use LFD for certain cases, as explained in the table.

Load Factors

In general, states that used either design method applied load factors in accordance with the *1983 AASHTO Standard Spec-*

M. K. Tadros and D. W. Meyer, University of Nebraska-Lincoln, 60th and Dodge Streets, Omaha, Nebr. 68182-0178. C. Belina, 812 Leawood Drive, Omaha, Nebr. 68154.

University of Nebraska Lincoln

Address All Replies To:
Department of Civil Engineering
60th & Dodge Streets
Omaha, Nebraska 68182-0178

We are presently conducting research on the design of reinforced concrete box culverts for the Nebraska Department of Roads and the Federal Highway Administration. Finite element modeling of the culverts and the surrounding soil has indicated to us that the soil loads specified by the current AASHTO Bridge Specs are probably too low. Our analysis indicates a vertical soil pressure in excess of the AASHTO value of (0.7) X (120 pcf) X (fill height). Our analysis also indicates that the lateral pressure of (30 pcf) X (soil depth) specified by AASHTO is probably too low.

The comparisons we have made so far are analytical, using the computer program "CANDE." As you probably know, this comprehensive program was primarily developed by Notre Dame University for the FHWA.

The only recent experimental results available to us on box culverts at this time are those reported by Kentucky during the 70's. Settlements and soil pressures were measured on a 4ft X 4ft single cell box with a 77ft. fill. Their results indicate higher soil pressures than AASHTO specified values.

We are wondering whether your state has conducted studies of loads on box culverts, in particular, or of design of these culverts, in general. Results of experimental work would be most helpful. We would also like to know the procedures and design philosophy followed in your state. For example, (1) Do you use the strength or the working stress design method? (2) What load factors are assigned to soil and live loads, if any? (3) Do you design for soil loads that differ from the AASHTO Specs? On what basis? (4) Do you specify Grade 40 or Grade 60 steel? (5) Have your box culverts experienced any consistent form of distress or excessive deformation?

Your time and effort in responding to this request will be most appreciated. If you would like to discuss this matter further, or transmit your response by telephone, please call me collect at (402) 554-3286.

Sincerely,

Maher K. Tadros

FIGURE 1 Questionnaire sent to state departments of transportation.

ifications for Highway Bridges and subsequent interims. In the AASHTO specifications, RCBC are categorized into the AASHTO Group X loadings. The equation for Group X loading is

$$\text{AASHTO Group } X = \gamma[\beta_D D + \beta_L (L + I) + \beta_E E]$$

For SLD, $\gamma = 1.0$, $\beta_D = 1.0$, $\beta_L = 1.0$, $\beta_E = 0.7$ for vertical and 1.0 for lateral loads on RCBC. If the reinforced concrete box culvert is designed as a rigid frame, $\beta_E = 0.5$ or 1.0 for lateral loads, depending on which one controls.

For LFD, $\gamma = 1.3$, $\beta_D = 1.0$, $\beta_L = 1.67$, and $\beta_E = 1.0$ for vertical loads. Again, $\beta_E = 0.5$ or 1.3 for lateral loads, depending on which one controls. Several states, however, used a modified version of the AASHTO Group X loads, as shown in Table 1.

Comments from three states, South Dakota, Washington, and Virginia, indicated that they prohibit the reduction of vertical soil pressure to 70 percent of the actual load, as allowed by AASHTO for SLD. The chief structural engineer from South Dakota commented that his department felt that the β_E coefficients specified by AASHTO for LFD were too low because soil pressures on reinforced concrete box culverts are less predictable than are dead loads. The Virginia chief engineer's comments reflected the feeling that soil bridging may not exist over new reinforced concrete boxes. Washington reported experience with negative arching, that is, loads on the culvert that are greater than the weight of the soil prism above the box.

Several states indicated that the 0.7 reduction factor applied to vertical soil pressure in the AASHTO service load method was never intended to account for the effect of soil arching. Rather, the purpose of the 0.7 factor was to effect an increase

TABLE 1 SURVEY OF HIGHWAY DEPARTMENT RESPONSES

State	Design Method Used[a]	Load Factors	Design Vertical Soil Loading, lb/ft³	Design Horizontal Soil Loading,[b] lb/ft³	Reinforcement Grade Specified
Arizona	SLD	AASHTO Group *X*	120	30	See[c]
California	LFD	$(\gamma\beta_D/\phi) = (\gamma\beta_E/\phi) = 1.5$ $(\gamma\beta_L/\phi) = 2.5$	140	42 or 140	60
Connecticut	SLD[d]	AASHTO Group *X*	120	30	60
Idaho	SLD	–	–	45 or field test	40
Illinois	LFD	$\gamma = 1.5$ for $D + E$ $\gamma = 1.3$ for $L + I$ $\beta_E = 1.3$ for lateral E and 0.5 for checking + M in slabs	120	40 for fill height 50 for barrel height	60
Iowa	LFD	AASHTO Group *X*	140	36	40
Kentucky	LFD	AASHTO Group *X*	120	34–45	60
Maine	LFD	$\beta_E = 1.3$		36	60
Michigan[e]	LFD	$\gamma = 1.3$ for D + vertical E $\gamma = 1.69$ for horizontal E	120	15 or 30	60
Minnesota	LFD	–	–	75%, 33%, 16.5% of vertical pressure	60
Mississippi	SLD	AASHTO Group *X*	120	30	40
Missouri	SLD[f]	AASHTO Group *X*	120	30	60
Montana[g]	–	–	–	–	–
Nebraska	SLD	AASHTO Group *X*	120	15 or 30	40
New Hampshire	SLD	AASHTO Group *X*	120	Varies with fill height *H*: 15 or 45 for $H < 30$ ft 15 or 60 for 30 ft < H < 60 ft 30 or 90 for 60 ft < H < 90 ft	60
New Jersey	SLD	AASHTO Group *X*	120	35	60[h]
New York	SLD	AASHTO Group *X*	120	30	60
North Carolina	LFD	AASHTO Group *I*	120	30	60
North Dakota	LFD	–	120	40	60
Oklahoma	SLD[i]	AASHTO Group *X*	120	36	40
Oregon	SLD	–	–	–	60
Rhode Island	SLD[d]	–	–	35	60
South Carolina	SLD	AASHTO Group *X*	120	30	40[j]
South Dakota	SLD[d]	$\beta_E = 1.0$ for vertical soil pressure	120	20 or 40	60
Tennessee	SLD[k]	AASHTO Group *X*	120	30	60
Texas	SLD[l]	–	120	20 or 40	See[l]
Virginia	SLD[d]	$\beta_E = 1.0$ for vertical soil pressure	–	–	40[j]
Washington	SLD	$\beta_E = 1.0$ for vertical soil pressure	130	15 or 60	40[j]
West Virginia	SLD	AASHTO Group *X*	120	30	40
Wyoming	LFD	AASHTO Group *X*	120	36	60

[a] LFD = Load Factor Design, SLD = Service Load Design.
[b] Equivalent Fluid Pressure.
[c] Arizona specifies grade 40 for bar sizes #6 and smaller and grade 60 for bars larger than #6.
[d] Precast concrete culverts are designed by LFD.
[e] SLD is used for 3-cell boxes.
[f] Triple boxes and special conditions are designed by LFD. Eventually all design will be by LFD.
[g] No recent experience with RCBCs.
[h] Contractor may submit an alternate design using grade 40 reinforcing.
[i] LFD is used to check strength in special cases.
[j] Grade 60 reinforcing may be substituted for grade 40.
[k] Tennessee has discussed changing to LFD.
[l] LFD has been used for special cases with grade 60 steel only when needed.

in the allowable stress under dead load, as compared with that allowed under live load. The same explanation for the reduction factor has been reported in the literature [see, for example, work by Davis and Bacher (*12*)].

Soil Loading

At the time of the survey, AASHTO specifications recommended the use of a vertical soil pressure of 120 lb/ft³ and a horizontal soil pressure of 30 lb/ft³ equivalent fluid pressure for the design of reinforced concrete box culverts. Eleven states, out of those who supplied information on soil pressures used in design, indicated use of the AASHTO loads without modification. Three states used values other than 120 lb/ft³ for vertical soil loads. Eighteen states reported the use of horizontal soil pressures different from AASHTO values.

Several states specified minimum and maximum values of horizontal soil pressure, apparently to conform to AASHTO Section 3.20.2., which requires that only one-half of the bending moment caused by lateral soil pressure may be used to reduce positive moment in the slabs. California required

equivalent fluid densities of 42 and 140 lb/ft³ to be used in design. The former loading is based on a drained embankment condition, whereas the latter represents a saturated soil condition.

Structural Materials

In the LFD method, the computed ultimate structural strength is highly dependent on the strength of the reinforcing steel. This question was addressed in the questionnaire with most states reporting the use of grade 60 reinforcing bars. Some states specified grade 40 but allowed the use of grade 60 reinforcing.

Structural Distress

In general, the states responding to the questionnaire have had good experience with reinforced concrete box culverts, with few instances of structural distress reported. Three states reported some cracking, which was attributed to differential settlement. One state experienced cracking in the positive moment areas of the top slab under higher fill heights. Another state reported cracking in the positive moment zone of the bottom slab of a culvert, under which it was suspected that swelling of the bedding material had occurred.

It should be pointed out that the negative moments at the corners of RCBCs are generally higher than the positive moments at the center of the spans. Thus, cracking is on the side adjacent to the soil where it cannot be easily observed. This cracking is perhaps more serious in terms of corrosion of the reinforcing steel.

Studies done at the University of Nebraska (*2*) show that the service load design method, when applied to RCBCs, produces designs with excessive factors of safety against failure. The underestimation of soil loads appears to be offset by this excessive factor of safety.

FIELD TEST DATA

Four groups of researchers have conducted projects, which have included observations of soil pressures on reinforced concrete culverts. The Kentucky Department of Transportation has compiled data from one pipe culvert location and seven box culvert installations, four with the imperfect trench and three without (*13–16*). The imperfect trench method of

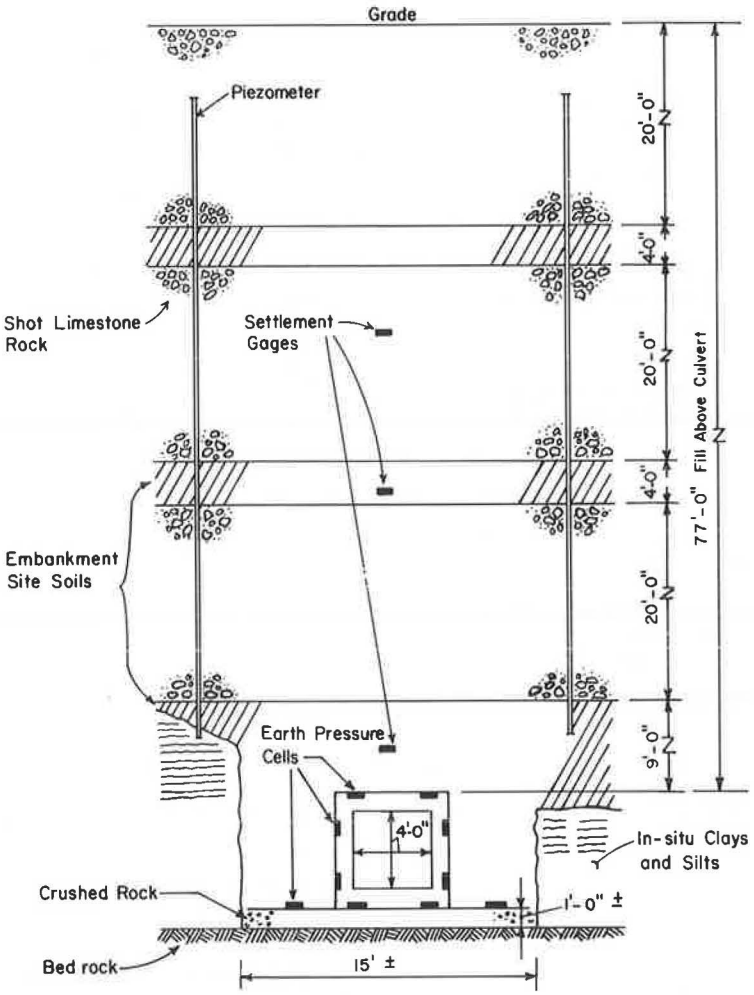

FIGURE 2 Field instrumentation, 4- by 4-ft box culvert (77-ft fill), Station 123+95, Clark County, Kentucky.

culvert construction involves the excavation of a trench in the embankment above the culvert. The trench is filled to some height with loose material, such as soil or baled straw, and is then covered with normally compacted embankment material. Only projects constructed without the imperfect trench condition are discussed. The three box culverts constructed without the imperfect trench had dimensions that varied from 4 ft by 4 ft to 6 ft by 6 ft. Fill heights varied from 37.5 ft on a 5 ft by 4 ft culvert to 77 ft on the 4 ft by 4 ft culvert.

Figure 2 is shown to illustrate the testing configuration for the 4-ft by 4-ft culvert with 77 ft of fill. Figures 3, 4, and 5 illustrate the test results compared with the AASHTO Group *X* loadings for the 4 by 4-, 5 by 4-, and 6 by 6-ft boxes, with normal pressure, lb/in^2.

A recent study funded by the Texas Highway Department and the Federal Highway Administration (*17*) involved instrumentation of one reinforced concrete box culvert. Soil pressure readings were taken at fill heights varying from 8 in. to 8 ft. This research focused on evaluation of the soil-culvert system under both backfill and live loads.

A research team from Northwestern University has instrumented two 60-in.-diameter reinforced concrete pipe culverts, one in the embankment condition and one in a trench condition (*18–20*). In the embankment case, the culvert was founded on natural ground and approximately 25 ft of embankment material was placed around it on both sides and on top. For the other case, a deep and narrow trench was dug in natural soil; the culvert was placed in the trench and covered with fill material to approximately 30 ft.

The California Department of Transportation has conducted a research project that included measurements of soil pressures under imperfect trench conditions. Three of the structures tested were reinforced concrete arches including a 10-ft arch with 200 ft of fill, an 8-ft arch with 240 ft of fill, and a 22-ft arch with 190 ft of fill. Two 84-in. diameter reinforced concrete pipes were instrumented at two locations, with fill heights of 136 ft and 183 ft. A 96-in. prestressed concrete pipe with 200 ft of fill was also tested. (*21–29*).

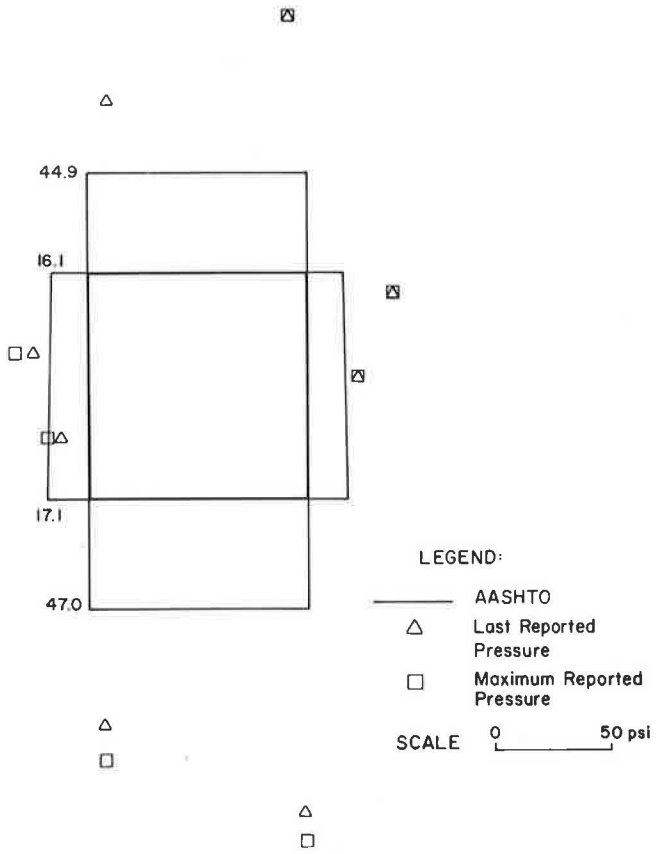

FIGURE 3 Comparison of test and AASHTO results: 4- by 4-ft box culvert (77-ft fill), yielding foundation, Station 123+95, Clark County, Kentucky.

SUMMARY OF FIELD TESTS

Several observations can be made about the research projects mentioned in this paper that relate to reinforced concrete box culverts. For all projects, regardless of culvert shape, the soil-pressure versus time curves are approximately linear. That is, from the beginning of construction to the time of fill completion, soil pressures were observed to be proportional to fill height. In addition, a substantial amount of soil friction on the side walls was observed in all of the RCBC projects. This friction generally exhibited a downward drag, thus increasing the pressures on the bottom slab.

After fill completion, however, changes in soil pressure with time varied among the projects. For most of the pipe and arch structures, vertical soil pressures changed only negligibly with time; horizontal pressures, however, did increase with time, especially at the California sites. An exception to this is the twin pipe installation in Kentucky in which vertical pressures increased with time while horizontal pressures remained fairly constant. On two of the box culverts in Kentucky, soil pressures increased significantly after fill completion, by about 25 percent. It should be pointed out that measurements were taken on the Kentucky boxes for more than 2,000 days. This is about twice as long as the period of time for which measurements have been reported for the other installations.

Loads resulting from horizontal and vertical soil pressure were not symmetrical about the culvert vertical centerline at any of the field installations. The amount of asymmetry varied among the different projects, however, and may be related to the asymmetry of the in situ geologic conditions at the individual sites. The Texas researchers believed that the asymmetry of pressure cell readings could be attributed to uneven fill compaction at the low fill heights involved or the questionable reliability of the pressure cells at these low pressures.

Both horizontal and vertical soil pressures were higher than AASHTO design loads at the Kentucky box culvert locations and at the Ohio embankment pipe installation. Observed pressures were lower than AASHTO loads at the Kentucky pipe culvert site and at the Ohio trench pipe location. At the Texas box culvert site, horizontal pressures were higher and the vertical pressures were lower than AASHTO loads at low fill heights. The California research in general showed higher vertical pressures on the arches and lower vertical pressures on the pipes when compared with AASHTO values. For both arches and pipes, observed horizontal soil pressures at the California locations generally fell between the two AASHTO-

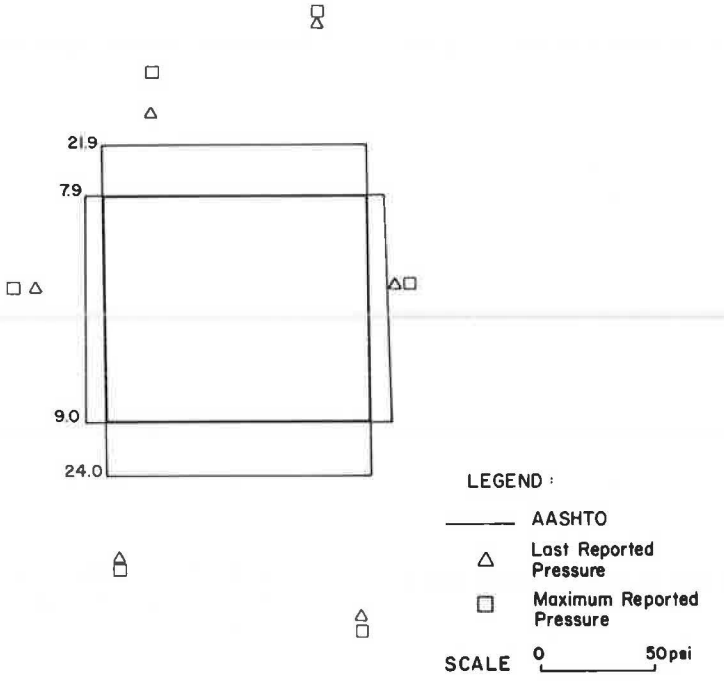

FIGURE 4 Comparison of test and AASHTO results: 5- by 4-ft box culvert (37.5-ft fill), unyielding foundation, Station 268+30, Clark County, Kentucky.

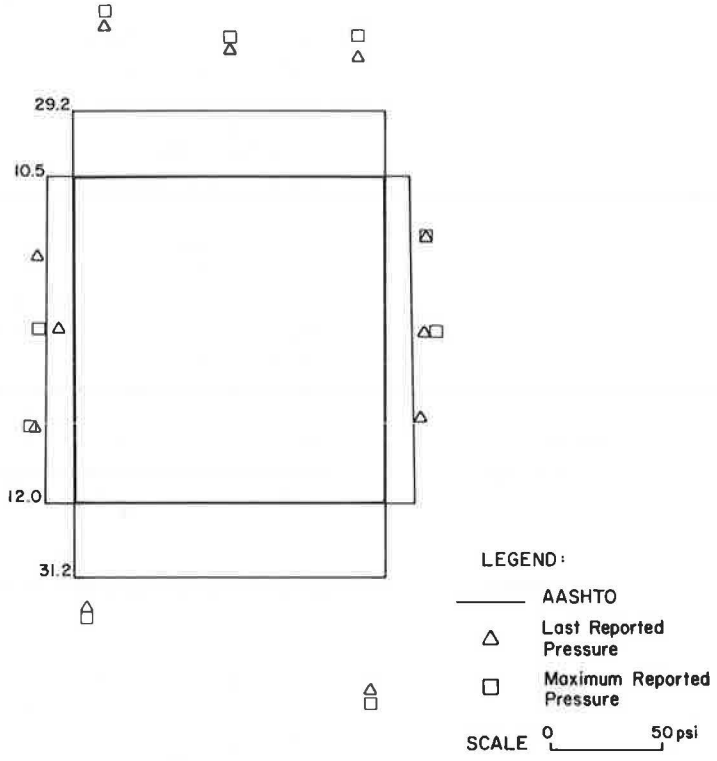

FIGURE 5 Comparison of test and AASHTO results: 6- by 6-ft box culvert (50-ft fill), Station 459+50, Marion County, Kentucky.

specified design loads of 30 lb/ft³ and 120 lb/ft³ equivalent fluid pressure.

CONCLUSIONS

The survey of state highway departments has indicated a diverse interpretation and application of AASHTO specifications relevant to concrete box culvert design. A number of states use higher soil pressures than AASHTO-specified values. Also, there appears to be a trend toward more use of the strength design approach. Only a few cases of structural distress were reported, indicating that current design practices produce safe, but not necessarily economical, box culverts.

Field measurements of culvert behavior have been limited. Most of the testing on pipe culverts was performed in California. Kentucky's work was done on seven box culverts, mostly under deep soil fills. The test program in Texas was somewhat inconclusive. Additional field research would provide a larger data base to compare experimental results with correct design procedures. Any improvement in the culvert design procedures could result in safe, yet more economical, structures.

The analytical work done at the University of Nebraska (*2*) seems to support this belief. That comprehensive study addressed soil pressure distribution, live load distribution, and influence of the design methods used. Research is currently underway to obtain field measurement on a twin cell 12-ft by 12-ft box culvert with 12 ft of soil fill. A report on these field measurements and comparison with analytical values will be given at a later date.

ACKNOWLEDGMENTS

This paper is based on a research project conducted at the University of Nebraska and sponsored by the Federal Highway Administration and the Nebraska Department of Roads (NDOR). The support of members of the Bridge Division, NDOR, under the leadership of James Holmes, bridge engineer, is gratefully acknowledged. Many other individuals contributed to this project. More detailed acknowledgment is given in the final report, Report NE-DOR-R 86-3.

REFERENCES

1. *Standard Specifications for Highway Bridges*, 12th ed. and subsequent interims. American Association of State Highway and Transportation Officials, Washington, D.C., 1978.
2. M. K. Tadros. *Cost-Effective Concrete Box Culvert Design*. Project HRP 83-3, Engineering Research Center, University of Nebraska, Lincoln, 1986.
3. M. G. Katona and J. M. Smith. *CANDE User Manual*. Report FHWA-RD-77-6, Federal Highway Administration, U.S. Department of Transportation, Washington, D.C., 1976.
4. M. G. Katona, P. D. Vittes, C. H. Lee, and H. T. Ho. *CANDE-1980: Box Culverts and Soil Models*. Report FHWA-RD-80/172, Federal Highway Administration, U.S. Department of Transportation, Washington, D.C., 1981.
5. F. J. Heger and K. N. Long. *Structural Design of Precast Concrete Box Sections for Zero to Deep Soil Cover Conditions and Surface Wheel Loads*. Concrete Pipe and Soil-Structure System, ASTM 630, American Society for Testing and Materials, Philadelphia, Pa., 1977, pp. 17–40.
6. F. J. Heger and T. J. McGrath. Radial Tension Strength of Pipe and Other Curved Flexural Members. *ACI Journal*, Vol. 3, No. 1, Jan.–Feb. 1983, pp. 33–39.
7. F. J. Heger and T. J. McGrath. Shear Strength of Pipe, Box Sections, and Other One-Way Flexural Members. *ACI Journal*, Vol. 79, No. 6, Nov.–Dec. 1982, pp. 470–483.
8. M. R. Boring, F. J. Heger, and M. Bealey. Test Program for Evaluating Design Method and Standard Designs for Precast Concrete Box Culverts with Welded Wire Fabric Reinforcing. In *Transportation Research Record 518*, TRB, National Research Council, Washington, D.C., 1974, pp. 49–63.
9. R. W. LaTona, F. J. Heger, and M. Bealey. Computerized Design of Precast Reinforced Concrete Box Culverts. In *Highway Research Record 443*, HRB, National Research Council, Washington, D.C., 1973, pp. 40–51.
10. *Standard Specifications for Precast Concrete Box Sections for Culverts, Storm Drains, and Sewers (ASTM C789-82)*. Annual Book of ASTM Standards, American Society for Testing and Materials, Philadelphia, Pa., 1983.
11. *Standard Specifications for Precast Concrete Box Sections for Cover Subjected to Highway Loadings (ASTM C789-82)*. Annual Book of ASTM Standards, American Society for Testing and Materials, Philadelphia, Pa., 1983.
12. R. E. Davis and A. E. Bacher. Concrete Pipe Culvert Behavior: Part 2. In *Proc., American Society of Civil Engineers*, Vol. 100, No. ST3, March 1974, pp. 615–630.
13. D. L. Allen and R. L. Russ. *Loads on Box Culverts Under High Embankments: Analysis and Design Considerations*. Research Report 491, Kentucky Transportation Cabinet, Frankfort, 1978.
14. D. L. Allen and B. W. Meade. *Analysis of Loads and Settlements for Reinforced Concrete Culverts*. UKTRP-84-22. Kentucky Transportation Cabinet, Frankfort, 1984.
15. H. F. Girdler. *Loads on Box Culverts Under High Embankments*. Research Report 386, Kentucky Transportation Cabinet, Frankfort, 1974.
16. R. L. Russ. *Loads on Box Culverts Under High Embankments: Positive Projection Without Imperfect Trench*. Research Report 431, Kentucky Transportation Cabinet, Frankfort, 1975.
17. Jey K. Jeyapalan. *Soil-Structure Interaction Behavior of Reinforced-Concrete Box Culverts*. Paper presented at the 64th Annual Transportation Research Board Meeting, Washington, D.C., 1985.
18. R. J. Krizek, R. B. Corotis, and T. H. Wenzel. Soil-Structure Interaction of Concrete Pipe Systems. Methods of Structural Analysis, Vol. 2. In *Proc., National Engineering Conference*, 1976, pp. 607–643.
19. R. J. Krizek, R. B. Corotis, and M. H. Farzin. Field Performance of Reinforced Concrete Pipe. In *Transportation Research Record 517*, TRB, National Research Council, Washington, D.C., 1974, pp. 30–47.
20. R. J. Krizek and P. V. McQuade. Behavior of Buried Concrete Pipe. In *Proc., American Society of Civil Engineers*, Vol. 104, GT7, July 1978, pp. 815–836.
21. R. E. Davis and A. E. Bacher. California's Culvert Research Program—Description, Current Status, and Observed Peripheral Pressures. In *Highway Research Record 249*, HRB, National Research Council, Washington, D.C., 1968, pp. 14–23.
22. R. E. Davis and A. E. Bacher. Concrete Arch Culvert Behavior—Phase 2. In *Proc., American Society of Civil Engineers*, Vol. 98, ST11, Nov. 1972, pp. 2329–2350.
23. R. E. Davis, A. E. Bacher, and J. C. Obermuller. Concrete Pipe Culvert Behavior—Part 1. In *Proc.*, American Society of Civil Engineers, Vol. 100, ST3, March 1974, pp. 599–614.
24 R. E. Davis, H. D. Nix, and A. E. Bacher. Arch Culvert Footing Movements. In *Proc.*, American Society of Civil Engineers, Vol. 105, ST4, April 1979, pp. 729–737.
25. R. E. Davis, H. D. Nix, and A. E. Bacher. Arch Culvert Research—Phase 3. In *Proc., American Society of Civil Engineers*, Vol. 105, ST4, April 1979, pp. 739–749.
26 A. E. Bacher and E. G. Klein, Jr. Reinforced-Concrete Arch Culvert Research by the California Department of Transportation. In *Transportation Research Record 785*, TRB, National Research Council, Washington, D.C., 1980, pp. 33–36.
27. A. E. Bacher, A. N. Banke, and D. E. Kirkland. Caltrans Prestressed Concrete Pipe Culvert Research: Design Summary and

Implementation. In *Transportation Research Record 903*, TRB, National Research Council, Washington, D.C., 1983, pp. 95–99.
28. A. E. Bacher, A. N. Banke, and D. E. Kirkland. Reinforced-Concrete Pipe Culverts: Design Summary and Implementation. In *Transportation Research Record 878*, TRB, National Research Council, Washington, D.C., 1982, pp. 83–92.
29. R. E. Davis and F. M. Semans. Rigid Pipe Prooftesting Under Excess Overfills with Varying Backfill Parameters. In *Transportation Research Record 878*, TRB, National Research Council, Washington, D.C., 1982, pp. 60–82.

Publication of this paper sponsored by Committee on Culverts and Hydraulic Structures.

Investigation of the Structural Adequacy of *C* 850 Box Culverts

G. R. FREDERICK, C. V. ARDIS, K. M. TARHINI, AND B. KOO

The structural behavior of American Society for Testing and Materials *C* 850 box culvert sections resulting from live load was investigated using theoretical analyses, field testing, and model testing. The field testing was performed on box culvert sections that were put into service after testing. These box culvert sections were installed on state routes in Ohio using construction crews and normal construction procedures. An overview of these analyses is presented in this paper. The initial purposes were to determine whether shear connector plates are required to transfer the load across a joint between adjacent box culvert sections, and if the recommended maximum spacing of 30 in. was appropriate. Testing at the first site indicated that shear connector plates are not required to transfer the load. The primary purpose of testing at the second site was to verify the results from testing at the first site. For these box culvert sections, there were no provisions for shear connectors, hence the reinforcing steel was not cut because the shear connector attachments were not installed. The results verified those from testing done at the first site. Additionally, it was concluded that *C* 850 box culvert sections are overdesigned structurally. Before testing was undertaken at the third site, a redesign was executed for *C* 850 box culvert sections. The redesigned *C* 850 box culvert section was essentially the same as the *C* 789 design with 4 ft of earth cover and HS 20 loading. Testing at this site demonstrated that the redesigned *C* 850 box culvert section performed satisfactorily. The major conclusions are that shear connectors are not required on American Society for Testing and Materials *C* 850 box culvert sections and that these sections are overdesigned structurally. It was also concluded that the deflection along an edge of the top slab was so low, even with the wheel load applied at that edge, that the American Association of State Highway and Transportation Officials' edge beam requirement need not be enforced.

The design requirements for box culvert sections installed with less than 2 ft of cover and subjected to highway loadings are enumerated in American Society for Testing and Materials (ASTM) Specification *C* 850 (*1*). These requirements generally follow the American Association of State Highway and Transportation Officials (AASHTO) *Standard Specifications for Highway Bridges* (*2*). The requirements of interest in this paper (as applied to box culvert sections) are

1. Use of shear connector plates,
2. AASHTO edge-beam requirement, and
3. Applicability of AASHTO distribution width for wheel loads.

Department of Civil Engineering, The University of Toledo, Toledo, Ohio 43606

Two separate studies were undertaken to investigate these requirements. These studies included theoretical analyses, model testing in a laboratory, and field testing of prototypes.

THEORETICAL ANALYSES

In the theoretical analyses, the structures were idealized into plane frames with a unit width. The corresponding live load was determined using the AASHTO distribution width for a wheel load. The dead load associated with 2 ft of earth cover and the weight of the box culvert, as well as the lateral earth pressure on the side walls, was also considered. The analyses were performed using classical methods of structural analyses and the finite element method.

A three-dimensional stress analysis was also performed using the finite element method. STRUDL was used for this analysis; prismatic elements with triangular cross sections and six nodes were selected. There were three linear degrees of freedom at each node of the element.

In these analyses, deflections, bending moments, shear, and normal forces were calculated. Reinforced concrete design was performed using the ultimate strength method.

FIELD TESTING

During the field testing of prototype structures, deflections of the top slab were observed and recorded along both edges of a joint that was subjected to load. Additionally, electric resistance strain gages had been mounted at selected locations and strain magnitudes were recorded. Primarily, strain values were recorded for the top slab.

All prototype structures were cast by the same manufacturer, Hyway Concrete Pipe Company in Findlay, Ohio, with tongue-and-groove joints. The cylinder strength of the concrete was a minimum of 5,000 lb/in.^{2} and the minimum yield strength of the welded wire fabric reinforcing was 65,000 lb/in.^{2}. Normal construction techniques were followed except that over-reinforcing was minimized. The theoretical steel areas were matched as closely as practicable.

For the first investigation (*3*), strain gauges were mounted on both the welded wire fabric and the concrete. Also, a few strain gauges were mounted on the shear connector plates. Deflection and strain data were recorded for three load conditions:

1. Wheel load applied directly to the top slabs of *C* 850 box culvert sections without shear connector plates installed,

2. Wheel load applied directly to the top slabs with shear connector plates installed, and
3. Wheel load applied to the asphalt pavement placed over the box culvert sections with shear connector plates installed.

For these conditions, a (simulated) wheel load of 20,800 lb (AASHTO HS 20 16,000-lb wheel load plus 30 percent impact) was applied to a simulated tire print (a 10-in. by 20-in. wooden block). Only one wheel load was applied on the structure at a time. The structure was Ohio DOT bridge number MAR-309-09.42 (located in Marion County) and used six box culvert sections with 12-ft span by 6-ft rise and a total laying length of 36 ft. The primary purposes of this investigation were to determine whether shear connectors were required and whether the 30-in. maximum spacing was appropriate. The geometry of an individual box culvert is presented in Figure 1; the overall configuration of the structure is shown in Figure 2. Because this structure was to be placed in highway service after testing, it was decided to limit the magnitude of the loading to 20,800 lb.

For the second investigation (*4*), strain gages were mounted on the concrete only. Two prototype structures were field tested in this investigation: PUT-109-02.67 and CRA-19-17.10. Deflection and strain data were recorded at each site. Based on the results of testing at the Marion County site, it was decided to load these box culvert sections until a hairline crack developed.

At Ohio Department of Transportation (DOT) bridge No. PUT-109-02.67 (located in Putnam County), the primary purpose was to verify the conclusions from MAR-309-09.42 on box culvert sections that did not have the reinforcing steel cut as is necessary when installing the shear connector attachments. This structure consisted of 17 box culvert sections with 12-ft span by 4-ft rise. These sections conformed to ASTM *C* 789 (*5*) for 3 ft of cover; the geometry of an individual box culvert is presented in Figure 3. However, they were subjected to live loading as though they were *C* 850 box culvert sections. After the sides had been backfilled to the elevation of the top slabs, the box culvert sections were loaded directly on the top slabs with a load of at least 20,800 lb before any earth cover

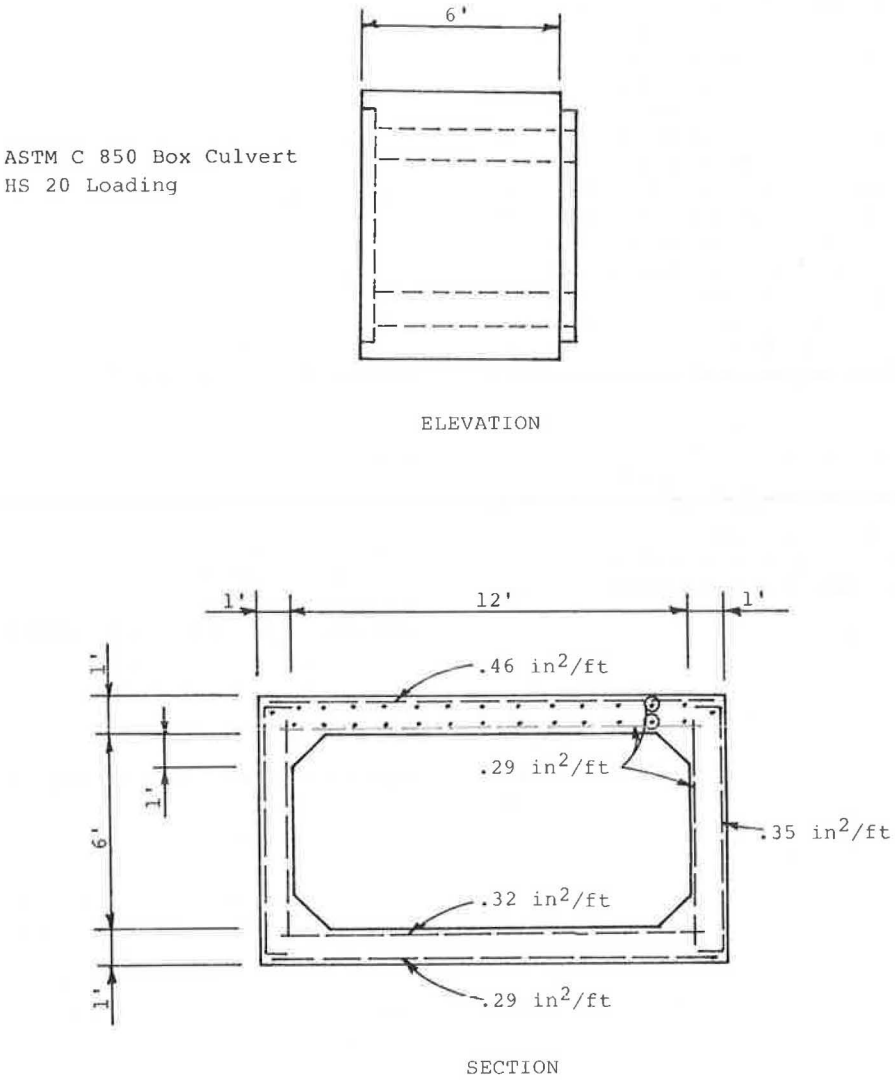

FIGURE 1 Details of 12-ft by 6-ft box culvert (Ohio DOT bridge MAR-309-09.42).

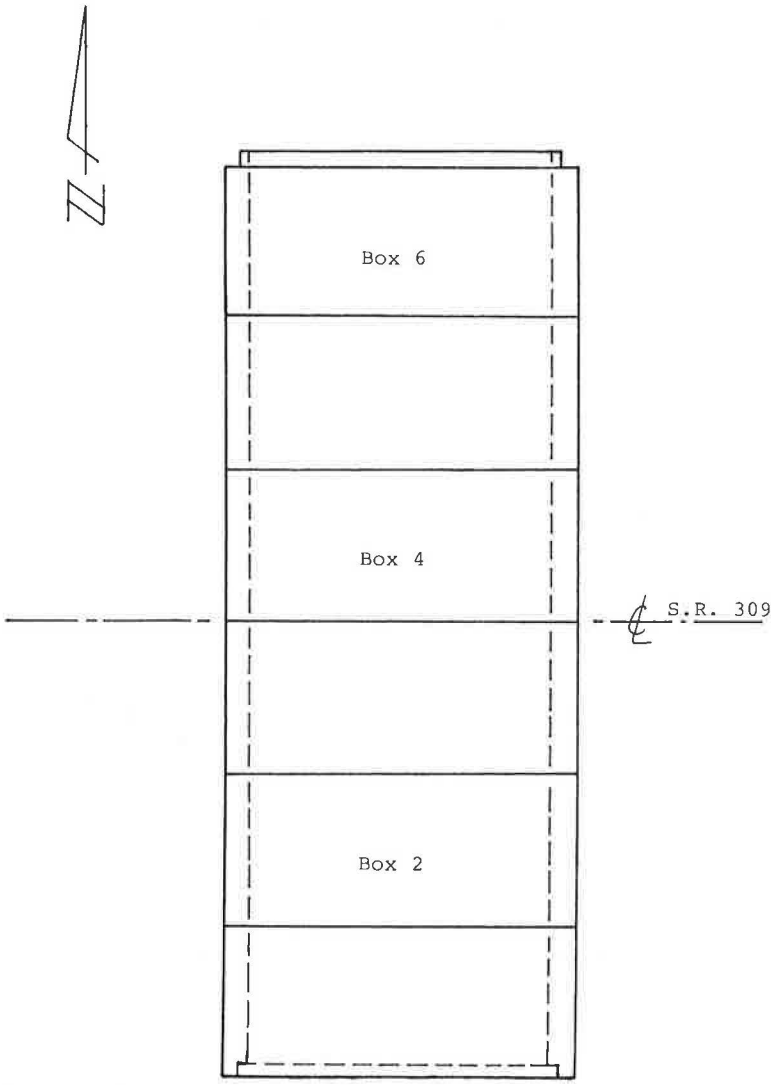

FIGURE 2 Arrangement of box culvert sections (Ohio DOT bridge MAR-309-09.42).

was placed. Four of the box culvert sections in this structure, as indicated in Figure 4, were subjected to single (simulated) wheel loads to produce a hairline flexural crack in the bottom sides of the top slabs.

At Ohio DOT bridge No. CRA-19-17.10 (located in Crawford County), the primary purpose was to verify a redesigned box culvert section that would be subjected to AASHTO HS 20 loading with asphalt pavement placed directly on the top slab. This structure consisted of 10 box culvert sections with 10-ft span by 6-ft rise. All walls of these sections were maintained at thicknesses of 10 in. so that conventional forms could be used in their manufacture. However, the reinforcing steel areas were less than those specified in ASTM *C* 850. The details of the redesigned box culvert are presented in Figure 5; the overall structure is shown in Figure 6.

MODEL TESTING

Model testing (*6*) was performed in a laboratory on ⅛ size scale models of each of the prototypes that were field tested. These models were cast in plywood forms using portland cement concrete and hardware cloth for the reinforcing steel. The concrete was proportioned to provide a 28-day compressive strength of 4,000 lb/in.^{2}. The aggregate used had a maximum particle size of ¼ in. The wires in the hardware cloth were spaced at ⅜ in. in both directions. To achieve the required areas of reinforcing steel, ⅛-in. diameter steel rods were wired to the hardware cloth as necessary. No attempt was made to match the distribution reinforcing or the shrinkage and temperature reinforcing. Each model was subjected to a scaled wheel load. The models were not subjected to lateral earth pressure or dead load (other than the weight of the model).

RESULTS AND CONCLUSIONS

The primary observations (at a wheel load of 20,800 lb) from the investigations of MAR-309-09.42 were as follows:

1. The maximum compressive strain in the concrete in top slabs is very low—of the order of 120 microin./in.

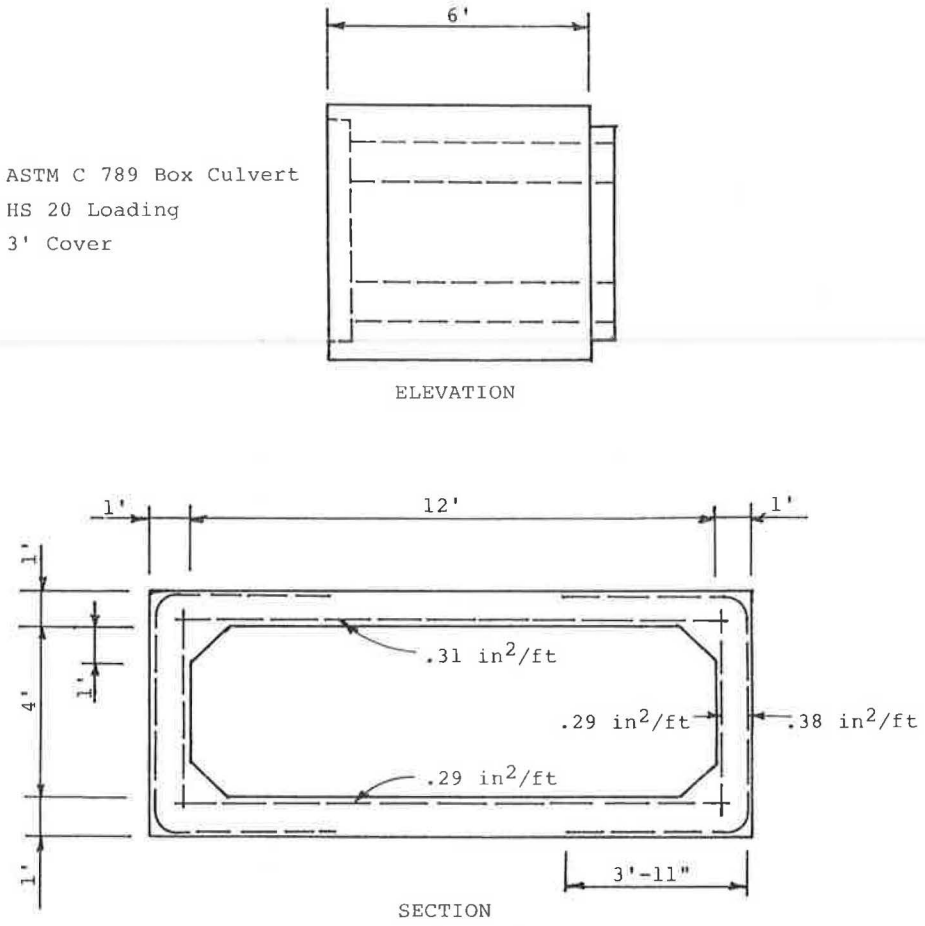

FIGURE 3 Details of 12-ft by 4-ft box culvert (Ohio DOT PUT-109-02.67).

2. The maximum tensile strain in the reinforcing steel is very low—of the order of 120 microin./in. (This is so low that the concrete did not develop tensile flexural cracks.)
3. The maximum deflection along a joint between adjacent box culvert sections was 0.027 in. without shear plates in place.
4. The average values of the deflections without shear plates for the loaded edge and relative deflection across the joint were 0.018 in. and 0.012 in., respectively.
5. The average values of the deflections were 0.014 in. and 0.006 in., respectively, with shear plates and without pavement.
6. The average values remained virtually the same after the pavement was in place.
7. The strain in the shear plates was very low—on the order of 120 microin./in.

Hence, because the deflections and strains were very low, it was concluded that shear connectors are not required to transfer load across a joint. Further, it was concluded that the AASHTO edge-beam requirement does not need to be enforced for box culverts. Note that it was necessary to cut the reinforcing steel to install the anchorages for shear connectors. Often this required cutting the reinforcing steel in locations of greatest bending moments. This did not appear to adversely affect the structural behavior of the box culvert sections. All of the above observations led to the conclusion that ASTM *C* 850 box culvert sections are overdesigned structurally.

The primary observations from the investigations of PUT-109-02.67 were

1. The maximum strain in the concrete was very low at design load plus impact.
2. The average deflection along a joint was very low at design load plus impact—of the order of 0.020 in. The average relative deflection was 0.012 in.
3. The average load required to produce a hairline flexural crack was twice the design wheel load plus impact.

The results of this testing confirmed the results from testing of MAR-309-09.42. It is emphasized that box culvert sections conforming to ASTM *C* 789 for 3 ft of earth cover were tested using *C* 850 live load conditions. Because none of the four box culvert sections subjected to load exhibited a hairline flexural crack at 20,800 lb, it is concluded that a *C* 789 design without shear plates is adequate for *C* 850 live-load conditions. The hairline cracks that developed at twice the design load plus impact virtually closed after the load was removed. This indicated that the reinforcing steel had not yielded. Note that

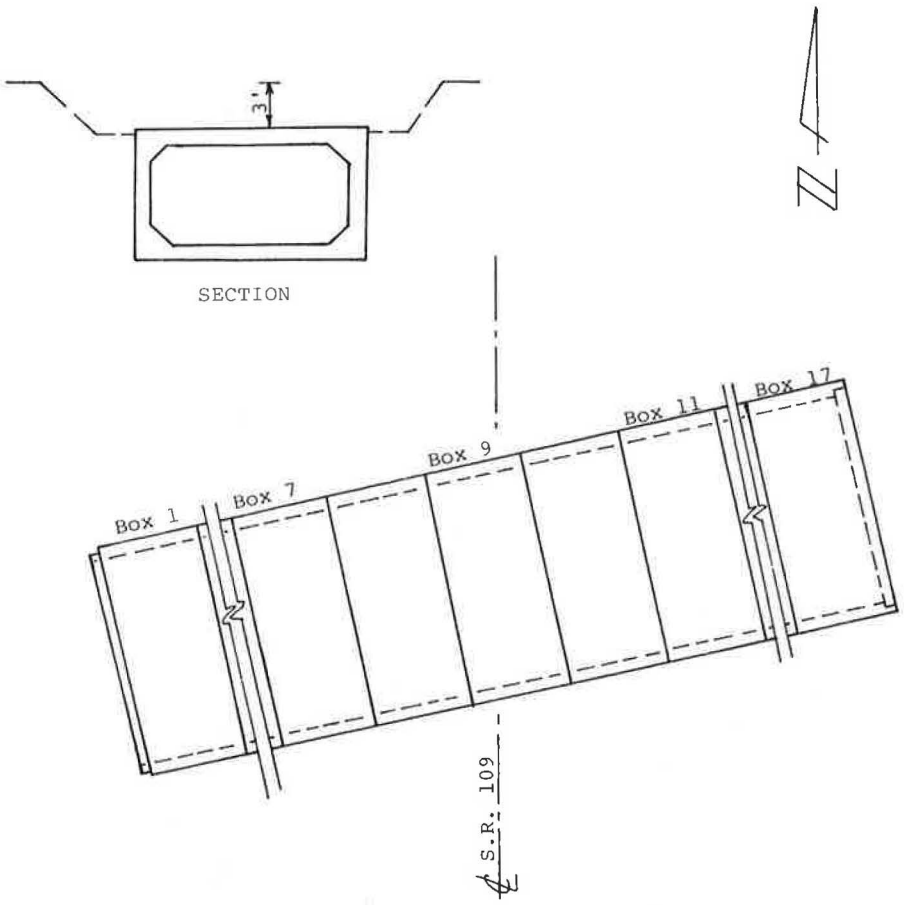

FIGURE 4 Arrangement of box culvert sections (Ohio DOT bridge PUT-109-02.67).

the average cracking load of 41,600 lb is almost equal to the ultimate design load of 45,140 lb (calculated using AASHTO load factors).

The deflection data from both MAR-309-09.42 and PUT-109-02.67 indicated that on the average a moderate amount of load is transferred across a joint between adjacent box culvert sections even when shear connectors are not used. A butyl rubber (ribbon) gasket was installed in each joint. It is believed that this transfer is due primarily to friction in the joint and the presence of the butyl rubber gasket. In many instances the unloaded side of the joint deflected as much as 50 percent of the loaded side. This load transfer appeared to be largely independent of whether the tongue end or the groove end was the loaded side of the joint. As might be suspected, the transfer resulting from friction was sensitive to how tightly the joint was made.

The primary observations (at a wheel load of 20,800 lb) from the investigations of CRA-19-17.10 were

1. The maximum strain in the concrete was very low both with and without the asphalt pavement in place.
2. The average deflection along a joint was very low without the pavement in place—of the order of 0.009 in. The average relative deflection was 0.003 in.
3. The average deflection along a joint was very low with the pavement in place—of the order of 0.013 in. The average relative deflection was 0.006 in.

Additionally, no hairline cracking was observed in the box culvert section subjected to a load of 30,350 lb without the pavement in place.

The results of this testing confirmed the results from testing of MAR-309-09.42 and PUT-109-02.67. It is emphasized that the box culvert sections for CRA-19-17.10 were redesigned box culverts. The redesigned box culverts used for *C* 850 live load conditions were very close to the *C* 789 design for 4 ft of earth cover. Hence, for CRA-19-17.10, the ASTM *C* 789 design for 4 ft of earth cover was used for a redesigned *C* 850 box culvert. It should also be noted that the box culvert sections for CRA-19-17.10 had a 10-ft span by 6-ft rise with wall thicknesses of 10 in.

A visual inspection of the box culvert sections for CRA-19-17.10 performed 21 months after they were installed revealed no signs of distress. Hence, the redesigned box culvert sections appear to be performing satisfactorily.

For the three box culvert sizes indicated, ⅙ size scale models were constructed and tested in a laboratory. These tests were performed on individual sections with the load applied along an edge. The measured strains on the concrete and deflections along the loaded edge agreed well with those quantities measured in the field. The strain values resulting from the application of the design wheel load plus impact on a scale model of the 12-ft by 6-ft box culvert are shown in Figure 7. The models exhibited a hairline flexural crack in the upper slab at approximately 2½ times the scaled design wheel load plus impact.

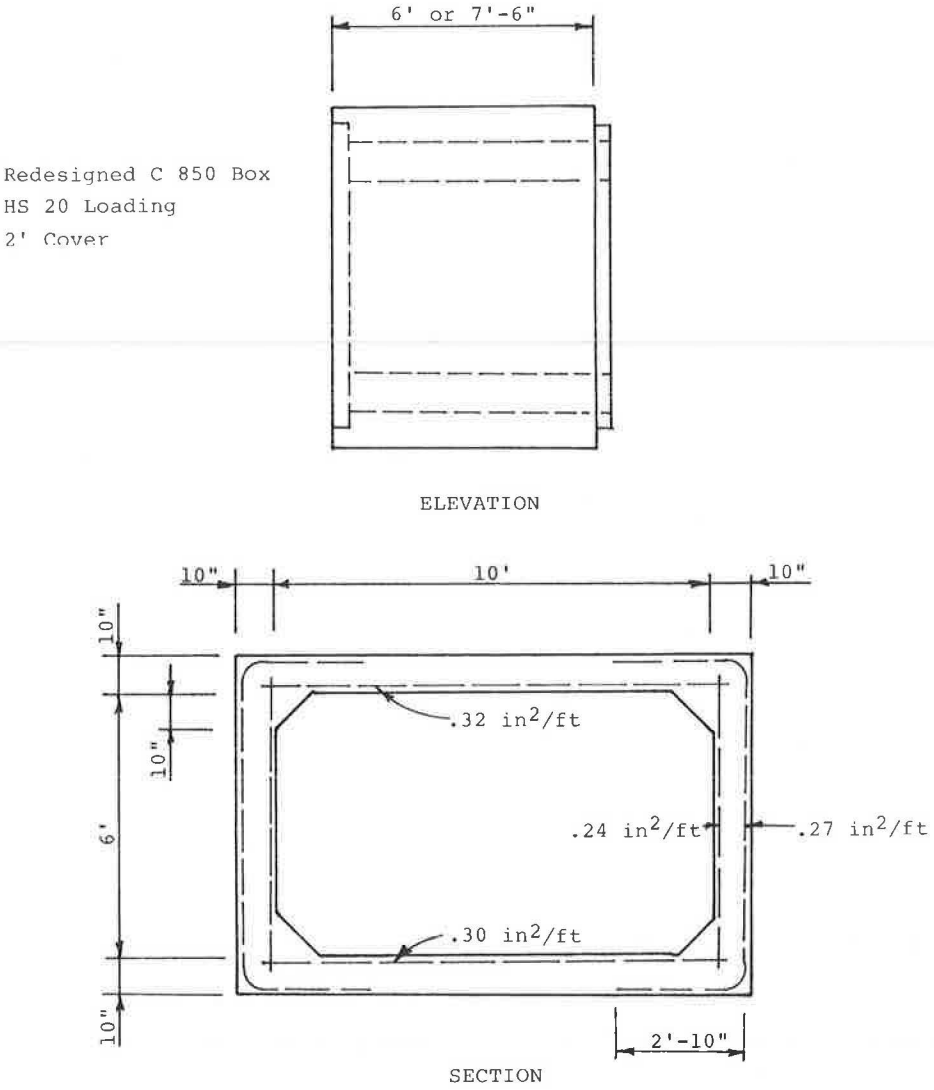

FIGURE 5 Details of redesigned 10-ft by 6-ft box culvert (Ohio DOT bridge CRA-19-17.10).

CLOSURE

Based on the findings described in this paper, the Ohio DOT no longer requires the use of shear connectors on box culvert sections conforming to ASTM *C* 850. The Ohio DOT does not enforce the AASHTO edge-beam requirement for slabs with main reinforcing parallel to traffic in box culverts, even though shear connectors are not used.

Based on the performance of box culvert sections at CRA-19-17.10, it appears that the structural design of ASTM *C* 850 box culvert sections can be economized. In this study only the steel reinforcement areas were changed. However, it is also possible to reduce the wall thicknesses. This may be undesirable because box culvert manufacturers would be required to modify existing forms or to purchase new forms.

It is further concluded that the ASTM *C* 850 specification, as well as the *C* 789 designs for less than 4 ft of cover, can be eliminated. The *C* 789 design for 4 ft of cover is recommended for these cases. For cover depths greater than 4 ft, the *C* 789 designs should be reevaluated.

In the redesigned box culvert section for *C* 850 live load conditions used in this study, the AASHTO distribution width for a wheel load was not used. Accounting for the transfer of load to adjacent sections by friction at a joint, a distribution width somewhat larger than the AASHTO recommendation, was used. Additional research should be undertaken to define a more appropriate expression for distribution width for a wheel load. In this redesign, a distribution width of 7.5 ft was used. This width corresponded to the largest laying length for these box culvert sections.

Note that the results and conclusions relative to MAR-309-09.42 are in agreement with those of James (*7*), who concurrently and independently investigated *C* 850 box culverts. Additionally, at least in Ohio, the authors' recommendation

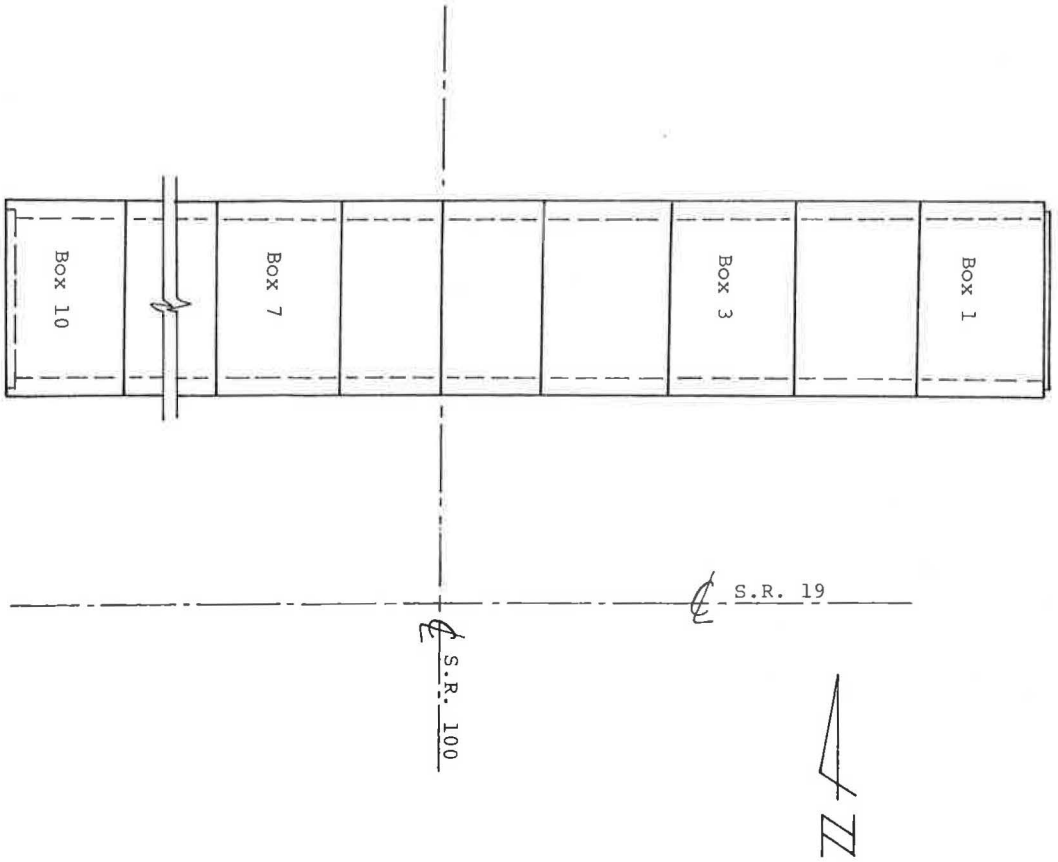

FIGURE 6 Arrangement of box culvert sections (Ohio DOT bridge CRA-19-17.10).

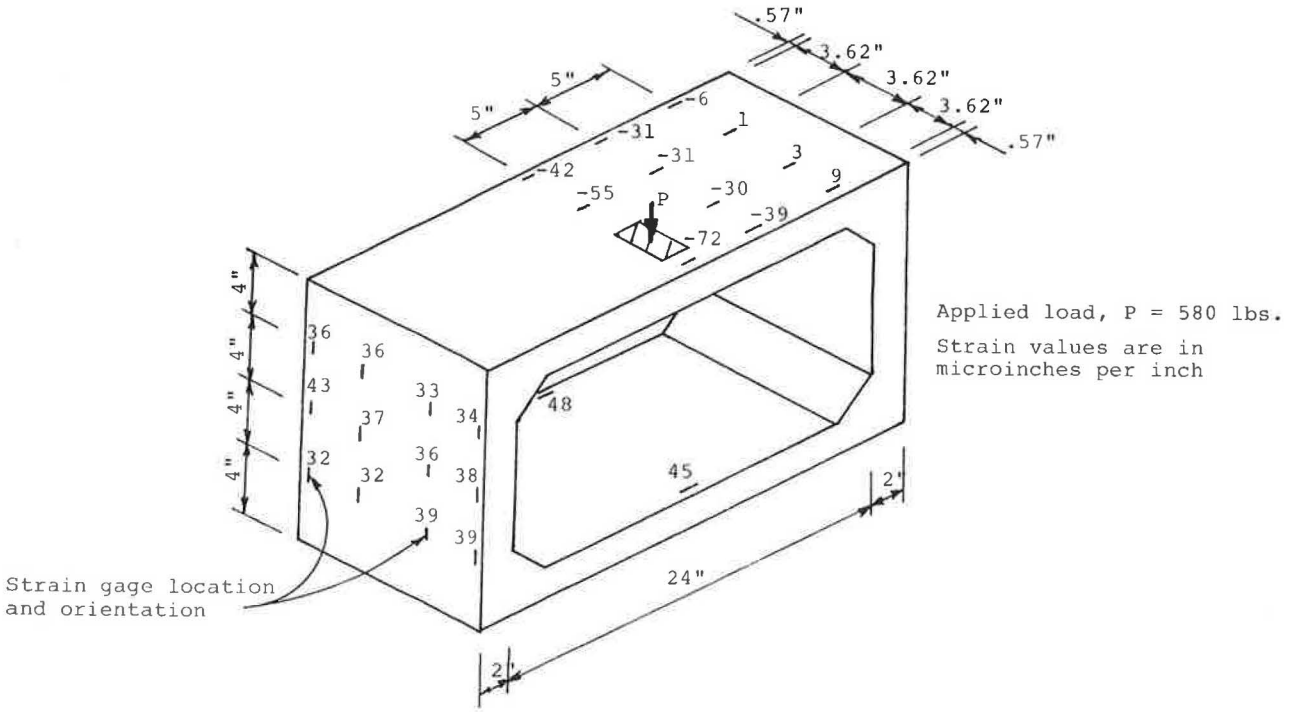

FIGURE 7 Strain data model of 12-ft by 6-ft box culvert.

(as well as that of James) regarding elimination of shear connectors has been implemented. Furthermore, our investigations at all three sites satisfy his second recommendation of field tests of box culverts installed without shear connectors.

ACKNOWLEDGMENTS

The work reported here was jointly funded by the Federal Highway Administration and the Ohio DOT under two separate grants.

The cooperation of personnel at Hyway Concrete Pipe Company in Findlay, Ohio, for providing space and arranging their work schedules for the installation of strain gauges is acknowledged.

The cooperation of the following contractors at the three job sites is also acknowledged:

Wren-Reese Construction Company at Ohio DOT bridge MAR-309-09.42,
Sherburn Construction Company at Ohio DOT bridge PUT-109-02.67, and
Ohio Engineering Company and Crawford Construction Company at Ohio DOT bridge CRA-19-17.10.

Finally, the assistance of several students who helped with the prototype and laboratory testing is acknowledged.

REFERENCES

1. *Standard Specification for Precast Reinforced Concrete Box Sections for Culverts, Storm Drains, and Sewers with Less than 2 Feet of Cover Subjected to Highway Loadings*. Standard C 850-82, American Society for Testing and Materials, 1983 Annual Book of Standards, Vol. 04.05, Philadelphia, Pa., 1983.
2. *Standard Specifications for Highway Bridges*, 12th ed. American Association of State Highway and Transportation Officials, Washington, D.C., 1977.
3. G. R. Frederick, B. Koo, and C. V. Ardis. *Evaluation of Shear Connectors on Precast Reinforced Concrete Box Sections*. Ohio Department of Transportation Project 3612, Department of Civil Engineering, The University of Toledo, Toledo, Ohio, 1984.
4. G. R. Frederick and C. V. Ardis. *Evaluation of Precast Reinforced Box Sections Installed Without Shear Connectors*. Ohio Department of Transportation Project 14370(0), Department of Civil Engineering, University of Toledo, Toledo, Ohio, 1987.
5. *Standard Specification for Precast Reinforced Concrete Box Sections for Culverts, Storm Drains, and Sewers*. Standard C 789-82, 1983 Annual Book of ASTM Standards, Vol. 04.05, American Society for Testing and Materials, Philadelphia, Pa., 1983.
6. G. R. Frederick and K. M. Tarhini. Model Analysis of Box Culverts Subjected to Highway Loading. In *Proc., VI International Congress on Experimental Mechanics*, Society for Experimental Mechanics, Portland, Oreg., June 1988.
7. Ray W. James. Behavior of ASTM C 850 Box Culverts Without Shear Connectors. In *Transportation Research Record 1001*, TRB, National Research Council, Washington, D.C., 1984, pp. 104–111.

Publication of this paper sponsored by Committee on Culverts and Hydraulic Structures.

Optimum Geometric Shapes of Precast Concrete Arch Structures of 24-, 30-, and 40-Ft Spans

PAUL A. ROWEKAMP, JAMES J. HILL, AND THEODOR KRAUTHAMMER

The results of a structural analysis of elliptical-shaped precast concrete arch structures and circular-shaped arches being considered by the Minnesota Department of Transportation are summarized in this paper. These arch structures were analyzed to compare the effect of geometry on structural performance. They were analyzed using the finite element method by placing identical load conditions on each arch. Half of each arch was modeled, based on symmetry, with no rotation allowed at the arch crown. The effects of cracking, critical stresses, and displacements were tabulated. Temperature stresses and shrinkage of the concrete were also introduced into the shape comparisons. Conclusions are included which indicate the optimum geometric shape and considerations for further analysis of different loading combinations.

The application of arch structures in transportation systems is not new. Nevertheless, many aspects of the structures' behavior are not well understood, and therefore studies are being conducted by several researchers to enhance knowledge in this area. In April 1987, an analytical study was initiated to review the differences between an elliptical-shaped arch and several proposed arches being developed by the Minnesota Department of Transportation (Mn/DOT). The circular shapes chosen have rise-span ratios of approximately 1:3 to 1:4 and radii less than 25 ft. The structures were compared by subjecting finite element models of each arch to identical loads and reviewing the resulting stresses and deflections. This study and its conclusions were based on a computer analysis and did not include field testing. However, the results of this study will be used as a basis for the development of future field testing.

The arches vary in span from 24 to 44 ft and have vertical openings from 8 to 14 ft high. They have a constant thickness of 10 in. and support an HS20 loading. The circular shapes were designed for use over small rivers or streams and were not intended for traffic passage through the arch opening. The arches are generally manufactured in 6-ft-wide panels that are placed side by side to form the required roadway width. The circular shapes are presently being designed, but have not yet been built.

P. A. Rowekamp and J. J. Hill, Minnesota Department of Transportation, Transportation Building, St. Paul, Minn. 55155. T. Krauthammer, Department of Civil and Mineral Engineering, University of Minnesota, 500 Pillsbury Drive S.E., Minneapolis, Minn. 55455.

ARCH SHAPES

Included in this paper are the analyses of two different types of 24- and 30-ft elliptical and circular arches (see Figures 1 and 2). The first type is labeled as an arch "without legs." For the 24-ft span the vertical opening for the arch without legs is 8 ft high and for the 30-ft span the opening is 11 ft high. The arches labeled "with legs" have exactly the same geometric shape as the arches without legs except that a portion has been added at the base to obtain a higher vertical clearance.

In the case of the circular arches the added leg is actually an extension of the curve that defines the arch shape. For the elliptical arches the added leg is a vertical strut added at the base. The added leg on the 24-ft elliptical arch increases the vertical opening by 25 in. for a total opening of 10 ft. For the 30-ft arches the leg increases the height by 28 in. for the elliptical arch and 32 in. for the circular arch. This results in a vertical height of 13 ft 8 in. for both structures.

The shape of each arch and geometric comparisons of the structures are shown in Figures 1 and 2.

PROCEDURE

Ten different structures were analyzed using the finite element method. The structures were modeled using a series of beam elements connected end to end to form the geometric shape of the arch. The actual element chosen to model the structures was a two-node beam element that is one of the simplest elements available for use with this method. Nodes or joints are used to define the beginning and ending point of each element (see Figure 3). After defining the material and section properties of each element, a computer program combines this information to form the stiffness matrix. Given the stiffness matrix, the applied loads and the boundary conditions of the structures, the deflections and stresses at each node are calculated (*1*).

Two different computer programs were used: ADINA (*2*), on the IBM 4341 mainframe computer at the Civil Engineering Department of the University of Minnesota, and STAAD3 (*3*), a commercially available program that was run in house at MnDOT. Sample problems run by each program resulted in nearly identical data output.

The thickness and material properties were identical for all the arches. They were all analyzed using 4,000 lb/in.^{2} concrete, which has an elastic modulus of approximately 3605 kips/in.^{2}

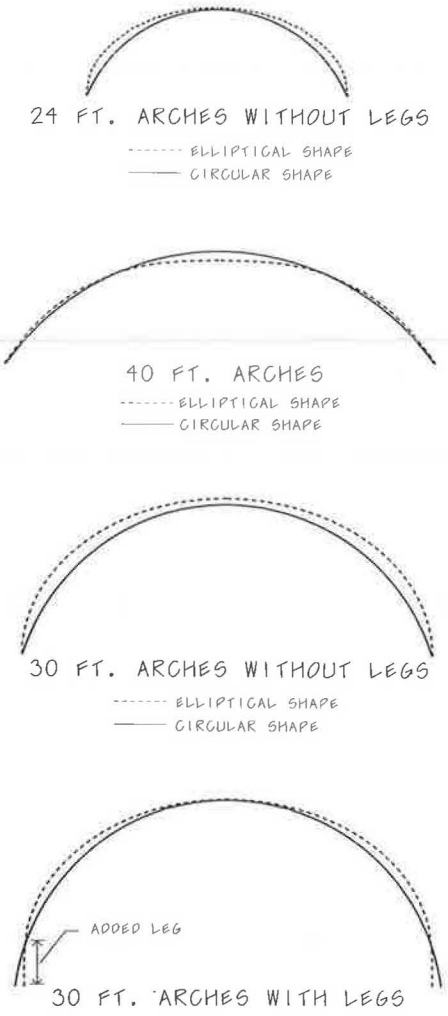

FIGURE 1 Arch profiles.

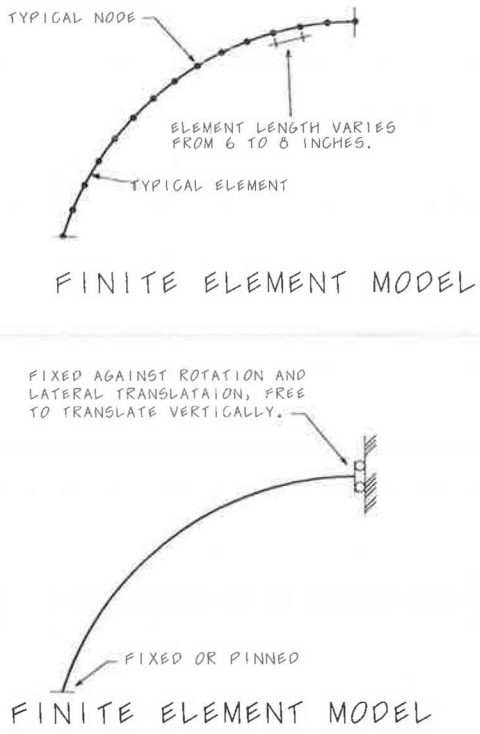

FIGURE 2 Finite element models.

and a Poisson's ratio of 0.2. All arches had a constant thickness of 10 in. and a concrete density of 150 lb/ft³. A 12-in.-wide section was used to compute the cross-sectional area and moment of inertia for each beam element. The 12-in. width was also used for computing the dead weight of the arch and the loads induced by the soil supported by the structure.

LOAD CONDITIONS

A total of eight different load cases were applied to the 24- and 30-ft arches (see Figure 4). They included:

1. Two ft of soil over the entire structure (assumed soil weight = 120 lb/ft³) plus a live load surcharge equivalent to 240 lb/ft².
2. A layer of soil equal in height to half the radius of the arch plus a live load surcharge equivalent to 240 lb/ft².
3. Sixteen in. of soil topped by an 8-in. concrete slab plus a live load surcharge equivalent to 240 lb/ft².
4. Two ft of soil plus a concentrated live load of 3,200 pounds (truck axle load of 32,000 pounds spread laterally over 10 ft) placed at the midspan of the arch. A second set of four

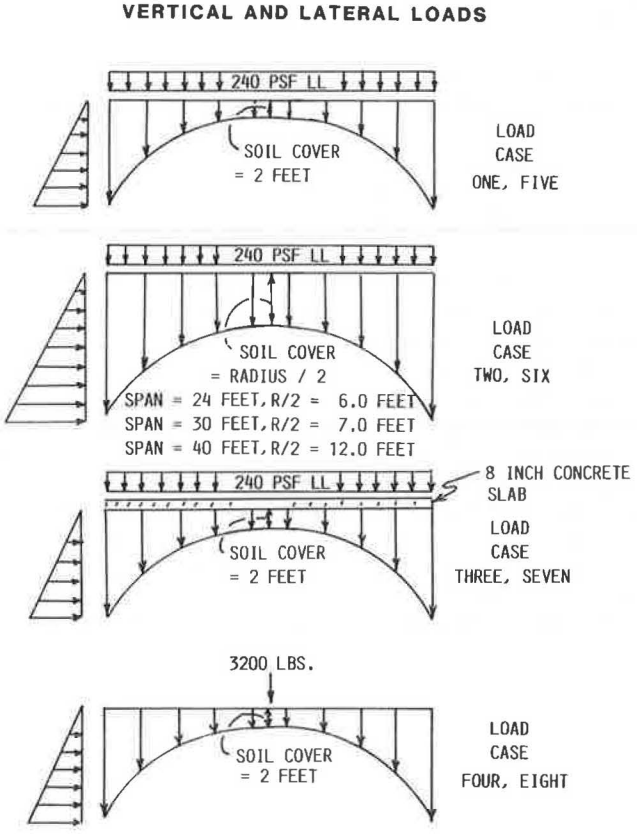

FIGURE 3 Loading conditions.

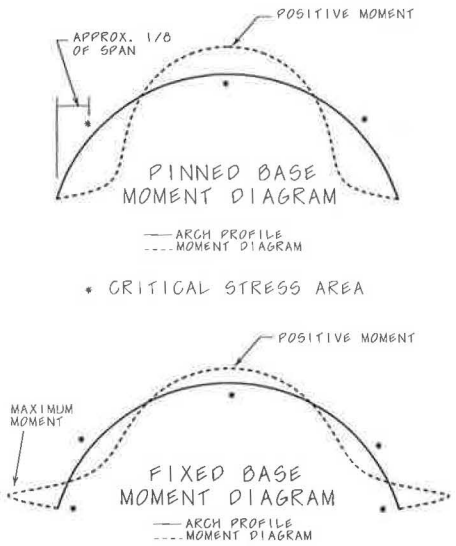

FIGURE 4 Moment diagrams.

load cases included the same vertical loads as previously described plus a hydrostatic lateral load using an equivalent soil weight of 30 lb/ft³ (see Figure 4). These lateral loads were applied to the 24- and 30-ft arches but not to the 40-ft arches. The arches were analyzed using both a fixed and a pinned boundary condition at the base because the true base fixity of each arch is unknown. It should be noted that the load cases applied in this study are an attempt to model conditions that will be encountered in the field. As with any analysis of this type, there is a degree of uncertainty in approximating actual field conditions. However, the load conditions applied are the same for each type of arch and should give valid results when used for comparison purposes.

MODELING TECHNIQUES

Because each arch is symmetric and all loads were applied in a symmetrical fashion, only half the arch needed to be modeled. However, an important boundary condition must be defined before using this shortcut. Specifically, no rotation can be allowed at the crown of the arch and this node must be free to translate vertically and fixed laterally (see Figure 3). The base of the arch is assumed to be fixed or pinned, depending on the actual condition under consideration. For the analysis of the arches in this study, each load case included both the fixed and the pinned base condition.

EFFECT OF CRACKING

The stress at which concrete is assumed to crack in tension is $7.5\sqrt{f_c}$ (*4*), or 474 lb/in.² for 4,000 lb/in.² concrete. Because the exterior face of arches will be in contact with soil and the interior face may be subjected to moisture from stream flow or condensation, a primary design concern is to keep the structure relatively free from cracking. Although all concrete structures are subject to temperature and shrinkage cracking, the main concern is to limit the tensile cracks caused by dead and live loads and temperature effects. By limiting the cracking the chance for moisture to penetrate the concrete will be reduced, which will limit reinforcement deterioration. Cracking will also affect the flow of forces in the structure. Once a portion of a concrete beam is considered a cracked section it is not uncommon for the moment of inertia to decrease by as much as 50 percent. Because the magnitude of the deflection is inversely proportional to the moment of inertia, the deflections may increase substantially if the structure cracks in areas where maximum deflections are likely to occur. The shape of the moment diagram will also shift as a result of cracking.

The analysis carried out in this study neglected the effect of the steel reinforcement and considered the concrete to be a linearly elastic, isotropic, and homogeneous material. This assumption may be valid for an uncracked section but does not hold true once the concrete cracks in tension. In reviewing the results, there are many cases in which the tensile stresses are in excess of the cracking limit and in some cases they are over 2,000 lb/in.². Concrete tensile stresses cannot reach this level but are included here as a means of comparison. If the tabulated stress at a critical point in one arch is 2,000 lb/in.² and in another arch it is 800 lb/in.², the concrete will very likely have cracked in both cases and the load will have been transferred to the tension steel. Because the stresses shown are often above cracking they are not likely to be the actual stresses in the structure, but they do give an indication of the relative stress levels for comparison purposes.

CRITICAL STRESSES

The final stresses included both axial and bending effects and were computed using the equation $P/A + Mc/I$ = final stress. Generally there are three critical areas of each arch that should be checked for maximum tension stresses. These include:

1. The inside face of the arch at the crown;
2. The outside face of the arch, about 45 percent up from the bottom (approximately the eighth point of the arch span); and
3. The stress at the base of the arch (for the arches with a fixed base condition). Figure 4 shows the critical areas where tension stresses are usually at a maximum.

RESULTS

The shape of the moment diagram is fairly similar for all of the load cases (depending on whether the base is fixed or pinned) and for all the arches analyzed. The typical moment diagram for the 30-ft circular arch is shown in Figure 4. As expected, the areas of maximum moment coincide with the locations of maximum tensile stresses. For the 40-ft arches, the maximum moment generally occurs at the crown when the ends of the arch are pinned or fixed. For the 24- and 30-ft arches, the maximum moment occurs near the eighth point of the span for the pinned case, and at the base for the fixed case. A summary, listing the maximum tensile stresses for the exterior face, the interior face, and the base of each arch is provided in Tables 1–4. Load Case 3 produced applied loads and resulting stresses similar to Load Case 2, hence the results for these cases are not included in this paper.

TABLE 1 MAXIMUM TENSION STRESSES, 40-FT ARCHES, VERTICAL LOADS ONLY

	STRESSES IN PSI		
	INTERIOR FACE (CROWN) Maximum Stress	EXTERIOR FACE (1/8 POINT) Maximum Stress	BASE OF ARCH Maximum Stress
ELLIPTICAL			
Load Case No. 1			
Fixed Base Condition	327	213	289
Pinned Base	437	309	-0-
Load Case No. 2			
Fixed	1240	951	1518
Pinned	1696	1464	-0-
Load Case No. 3			
Fixed	340	225	308
Pinned	457	340	-0-
Load Case No. 4			
Fixed	655	285	367
Pinned	777	390	-0-
CIRCULAR			
Load Case No. 1			
Fixed Base Condition	-0-	-0-	-0-
Pinned Base	-0-	-0-	-0-
Load Case No. 2			
Fixed	91	26	434
Pinned	351	404	-0-
Load Case No. 3			
Fixed	-0-	-0-	-0-
Pinned	-0-	-0-	-0-
Load Case No. 4			
Fixed	243	-0-	-0-
Pinned	291	2	-0-

(-0- Indicates no tension)

A summary of the crown deflections and the effect of a 100 degree Farenheit temperature change are provided in Tables 5 and 6. The crown was chosen as a reference point for comparison because it is the area of maximum tensile stress for the 40-ft arches. Other structures also exhibit high stresses in this area. It is also the location of maximum vertical deflection. Deflection data for the pinned base condition is provided in Table 5. These results are approximately two times higher than the results using a fixed base condition.

TEMPERATURE EFFECTS

Stresses resulting from changes in temperature have also been analyzed. The resulting stresses and deflections for a temperature change of 100 degrees Farenheit are included in Table 6. A 100 degree range was used to allow for ease of interpolation of actual temperature changes. An increase in temperature will cause an upward deflection at the crown and this in turn will cause tension stresses on the exterior (top) side at the crown and compression on the interior (bottom) side. A temperature decrease will cause opposite behavior.

A coefficient of thermal expansion of concrete equal to 0.000006 (5) was used for this analysis. The coefficient for shrinkage is 0.0002, which is equal to a temperature drop of 33 degrees Fahrenheit. The effect of shrinkage and a temperature drop of 30 degrees would be similar to a temperature drop of 60 degrees. For a 60 degree temperature drop the stresses and deflections induced would be 60 percent of those listed in Table 6, and are quite substantial for all the arches.

The moments induced by temperature effects for the pinned end case were zero at the base and reached a maximum at the crown. For the fixed end case the maximum moment occurred at the base, then the moment diagram changed sign and reached a second critical point at the crown where the magnitude was approximately 50 percent of the moment at the base. The axial loads induced from temperature changes were very small and were neglected when computing the tensile stresses.

ANALYSIS OF 40-FT ARCH

As seen from Table 1, which summarizes the maximum stresses and their locations, the maximum tension stress for the 40-ft elliptical arch occurred at the underside of the crown of the arch. For Load Cases 2 and 4, the stresses calculated in the analysis far exceeded the cracking stress of 474 lb/in.^{2}. For Load Case 2 with pinned ends, the tension stresses on the outside of the arch also exceeded cracking in an area about 45 percent up from the base of the arch (the eighth point of the arch span). With the base fixed, the stress of 1,500 lb/in.^{2}

TABLE 2 MAXIMUM TENSION STRESSES, 30-FT ARCHES, NO LEGS

	STRESSES IN PSI					
	VERTICAL LOAD ONLY			VERTICAL AND LATERAL LOAD		
	INTERIOR FACE (CROWN)	EXTERIOR FACE (1/8 PT.)	BASE OF ARCH	INTERIOR FACE (CROWN)	EXTERIOR FACE (1/8 PT.)	BASE OF ARCH
ELLIPTICAL						
Load Case 1						
Fixed Base	243	313	992	169	220	685
Pinned Base	516	767	-0-	380	571	-0-
Load Case 2						
Fixed	628	727	1970	481	560	1565
Pinned	1200	1622	-0-	948	1288	-0-
Load Case 4						
Fixed	534	323	910	460	240	673
Pinned	800	731	-0-	664	536	-0-
CIRCULAR						
Load Case 1						
Fixed Base	46	50	252	-24	-32	48
Pinned Base	157	227	-0-	28	54	-0-
Load Case 2						
Fixed	239	228	736	99	77	381
Pinned	516	629	-0-	274	331	-0-
Load Case 4						
Fixed	343	113	336	272	41	132
Pinned	472	275	-0-	343	107	-0-

(-0- Indicates no tension)

TABLE 3 MAXIMUM TENSION STRESSES, 30-FT ARCHES, WITH LEGS

	STRESSES IN PSI					
	VERTICAL LOAD ONLY			VERTICAL AND LATERAL LOAD		
	INTERIOR FACE (CROWN)	EXTERIOR FACE (1/8 PT.)	BASE OF ARCH	INTERIOR FACE (CROWN)	EXTERIOR FACE (1/8 PT.)	BASE OF ARCH
ELLIPTICAL						
Load Case 1						
Fixed Base	438	571	1300	316	415	917
Pinned Base	812	1162	-0-	590	839	-0-
Load Case 2						
Fixed	1026	1213	2653	802	948	2033
Pinned	1779	2344	-0-	1392	1824	-0-
Load Case 4						
Fixed	719	543	1223	597	390	839
Pinned	1068	1065	-0-	846	746	-0-
CIRCULAR						
Load Case 1						
Fixed Base	159	192	623	32	41	249
Pinned Base	376	535	-0-	143	220	-0-
Load Case 2						
Fixed	499	520	1437	265	263	831
Pinned	976	1210	-0-	569	701	-0-
Load Case 4						
Fixed	462	225	646	335	81	272
Pinned	681	530	-0-	448	217	-0-

(-0- Indicates no tension)

TABLE 4 MAXIMUM TENSION STRESSES, 24-FT ARCHES, NO LEGS

	STRESSES IN PSI					
	VERTICAL LOAD ONLY			VERTICAL AND LATERAL LOAD		
	INTERIOR FACE (CROWN)	EXTERIOR FACE (1/8 PT.)	BASE OF ARCH	INTERIOR FACE (CROWN)	EXTERIOR FACE (1/8 PT.)	BASE OF ARCH
ELLIPTICAL						
Load Case 1						
Fixed Base	141	184	566	110	147	470
Pinned Base	313	502	-0-	257	423	-0-
Load Case 2						
Fixed	308	372	1079	247	306	915
Pinned	630	938	-0-	526	804	-0-
Load Case 4						
Fixed	393	220	618	362	183	522
Pinned	575	513	-0-	519	434	-0-
CIRCULAR						
Load Case 1						
Fixed Base	10	-0-	76	-0-	-0-	-0-
Pinned Base	63	78	-0-	6	5	-0-
Load Case 2						
Fixed	77	51	243	15	-0-	95
Pinned	196	222	-0-	92	96	-0-
Load Case 4						
Fixed	255	69	182	223	39	95
Pinned	334	153	-0-	277	85	-0-

(-0- Indicates no tension)

was more than three times higher than the stresses in the circular arch. The 40-ft circular arch also exhibited a maximum stress in the area at the underside of the crown. However, the stresses did not exceed 500 lb/in.^{2} for any of the four Load Cases. It is also important to note that for Load Cases 1 and 3 the entire arch remained in compression. For the fixed base condition, only one of the four load cases caused tensile stress at the base; Load Case 2 produced a stress of 434 lb/in.^{2}.

The maximum deflections for both shapes occurred under Loading 2. With hinged ends, a deflection of 0.72 in. downward occurred for the elliptical shape, with 0.26 in. for the circular shape (see Table 5).

In summary, the stress and deflection data for the 40-ft arches show results that would favor use of the circular arch shape over that of the elliptical shape. After reviewing the geometric profile in Figure 1, it becomes evident why the results turned out as they did. The elliptical arch has a noticeable flat spot near the crown and rises up at a steeper slope from the base than the circular arch. The result was that at the crown the elliptical and circular arches had nearly identical axial loads. The crown moments in the elliptical arch, however, were at least two times higher than they were in the circular. These high moments were induced by the flattening out of the arch and result in high tensile stresses at the underside of the crown.

ANALYSIS OF 30-FT ARCH WITHOUT LEGS

Unlike the 40-ft arches, for Load Cases 1 to 3, the 30-ft arches did not produce a maximum tensile stress at the underside of the crown. For the fixed base condition, the maximum tensile stress occurred at the inside face of the arch at the base and under vertical load, but the magnitude was nearly twice the cracking stress. For the pinned base condition, the maximum stress occurred at the eighth point of the arch span. For the elliptical shape, the tensile stress at this point was approximately 20 percent lower than it was at the base. Under both vertical and lateral load, the tensile stress at the base dropped by 300 lb/in.^{2} but was still nearly 50 percent higher than the cracking stress.

As expected, the addition of lateral load decreased the magnitude of the tensile stresses. However, for the 30-ft elliptical arch without legs, all four load cases still produced tensile stresses above 500 lb/in.^{2} when lateral loads were included in the analysis. Thus all 8 of the load cases (see Figure 4) applied to the elliptical shape induced stresses that exceed the cracking stress. The 30-ft circular arch without legs performed quite well under seven of the eight load conditions applied in this study. The stresses were usually well below the cracking stress and the deflections were quite small. However, Load Case 2, with vertical load only, did produce tensile stresses above 500 lb/in.^{2} for the fixed and the pinned base condition, but these stresses were still two to four times less than those produced by the same load case on the elliptical arch.

The 30-ft circular arch without legs produced maximum moments at the same locations as those of the 30-ft elliptical arch without legs. For the fixed base condition the maximum moment usually occurred at the base and for the pinned base condition the maximum moment usually occurred near the eighth point of the arch span. The major difference between the two arch structure types was the magnitude of the max-

TABLE 5 SUMMARY OF DEFLECTIONS AT CROWN OF ARCHES, PINNED BASE CONDITION

	Deflections in inches					
	VERTICAL LOADS ONLY			VERTICAL AND LATERAL LOADS		
ARCH TYPES	LOAD CASE NO. 1	LOAD CASE NO. 2	LOAD CASE NO. 4	LOAD CASE NO. 1	LOAD CASE NO. 2	LOAD CASE NO. 4
24 FOOT ARCHES						
*ELLIPTICAL WITHOUT LEGS	-0.09	-0.16	-0.10	-0.07	-0.14	-0.09
*CIRCULAR WITHOUT LEGS	-0.02	-0.05	-0.04	-0.02	-0.04	-0.03
30 FOOT ARCHES						
*ELLIPTICAL WITH LEGS	-0.38	-0.79	-0.38	-0.29	-0.64	-0.29
WITHOUT LEGS	-0.21	-0.46	-0.20	-0.17	-0.38	-0.18
*CIRCULAR WITH LEGS	-0.16	-0.37	-0.18	-0.09	-0.24	-0.11
WITHOUT LEGS	-0.07	-0.17	-0.09	-0.04	-0.12	-0.06
40 FOOT ARCHES						
*ELLIPTICAL WITHOUT LEGS	-0.19	-0.72	-0.23	The 40 foot arches were not analyzed for vertical plus lateral load.		
*CIRCULAR WITHOUT LEGS	-0.03	-0.26	-0.08			

(-) Downward Deflection

imum moments. At the base the axial load in the circular arch was approximately 15 percent higher than it was for the elliptical arch, but the moments in the elliptical arch were from two to five times greater than those in the circular arch. At the eighth point the axial load in the elliptical arch was virtually identical to the circular arch, but the elliptical arch exhibited bending moments that were from two to four times greater than they were for the circular arch. At the crown, the circular arch had a slightly higher axial load when compared with the elliptical arch. However, the bending moment produced in the elliptical arch was higher than that of the circular arch.

In summary, the results show that the circular structure acts more like a true arch, with high axial load and low bending moment, when compared with the elliptical shape, which has relatively equal axial load but higher bending stresses.

ANALYSIS OF 30-FT ARCH WITH LEGS

The addition of a leg to the 30-ft arches caused the tensile stresses to increase by about 30 percent for the elliptical shape and nearly a 100 percent increase for the circular shape when compared to the arches without legs (see Table 3).

When only vertical loads were applied, all four of the load cases analyzed caused tensile stresses to exceed the cracking level in both the circular and elliptical arch. This occurred for both the fixed and pinned base condition. However, it should be noted that the tensile stresses in the elliptical shape were approximately twice as high as those of the circular shape.

When vertical and lateral loads were applied, only one of the load cases produced stresses greater than 500 lb/in.^{2} in the circular shape. All four of the load cases resulted in stresses higher than the cracking stress for the elliptical shape, where the tensile stresses were anywhere from 1.5 to 4 times higher than those of the circular arch.

The location on the arch where the maximum tensile stresses occurred changed very little for the arch with legs as compared with the arch without legs. For the fixed base condition the maximum stresses generally occurred at the base of the arch. For the pinned condition the maximum stresses occurred near the eighth point of the span. More precisely, for the arch without legs and a pinned base the maximum moment and maximum tensile stress occurred at a point approximately 57 in. up vertically from the base. For the fixed base condition the maximum tensile stress on the exterior face occurred at a point approximately 72 in. up vertically from the base. This maximum stress occurs at a higher point for the fixed base condition because the moment curve changes sign in moving up from the base to this point of high stress. In the case of a pinned base the moment is zero at the base and the curve does not change sign before reaching this critical stress point (see Figure 4).

The addition of the vertical leg to the arches caused the crown deflection to nearly double for both shapes. The maximum deflection recorded for the circular arch was 0.37 in. downward compared to 0.79 in. for the elliptical.

If a preferred shape must be chosen the circular arch is favored over the elliptical shape for the case of a 30-ft arch with legs. The circular shape produced tensile stresses and deflections that were consistently lower than the elliptical shape. However, it is important to point out that although the circular shape did produce lower stresses, these stresses still exceeded 500 lb/in.^{2} for Load Cases 1 to 4 without lateral load. When the previously defined lateral load was applied to the circular arch the stresses fell to less than the cracking

TABLE 6 SUMMARY OF TEMPERATURE EFFECTS

100 DEGREE TEMPERATURE CHANGE
TENSILE STRESSES AND DEFLECTIONS
Stresses in PSI, Deflections in inches

ARCH TYPES		CROWN DEFLECTION	TENSILE STRESS AT BASE	TENSILE STRESS AT CROWN
24 FOOT ARCHES				
*ELLIPTICAL				
WITH LEGS	HINGED	+/- 0.14	No Tension	+/- 110
	FIXED	+/- 0.18	+/- 435	+/- 215
WITHOUT LEGS	HINGED	+/- 0.15	No Tension	+/- 148
	FIXED	+/- 0.19	+/- 612	+/- 294
*CIRCULAR				
WITHOUT LEGS	HINGED	+/- 0.15	No Tension	+/- 166
	FIXED	+/- 0.18	+/- 603	+/- 324
30 FOOT ARCHES				
*ELLIPTICAL				
WITH LEGS	HINGED	+/- 0.18	No Tension	+/- 79
	FIXED	+/- 0.21	+/- 292	+/- 152
WITHOUT LEGS	HINGED	+/- 0.18	No Tension	+/- 103
	FIXED	+/- 0.22	+/- 403	+/- 203
*CIRCULAR				
WITH LEGS	HINGED	+/- 0.19	No Tension	+/- 88
	FIXED	+/- 0.22	+/- 303	+/- 169
WITHOUT LEGS	HINGED	+/- 0.19	No Tension	+/- 117
	FIXED	+/- 0.22	+/- 420	+/- 229
40 FOOT ARCHES				
*ELLIPTICAL				
WITHOUT LEGS	HINGED	+/- 0.29	No Tension	+/- 137
	FIXED	+/- 0.35	+/- 591	+/- 261
*CIRCULAR				
WITHOUT LEGS	HINGED	+/- 0.28	No Tension	+/- 139
	FIXED	+/- 0.34	+/- 516	+/- 273

(-) Downward Deflection

level for all but one load case ($R/2$ soil cover, Load Case 2). Hence, unless the designer is assured the field conditions will provide a substantial amount of lateral load, the 30-ft arches with legs should be considered very carefully before selection.

Perhaps a more suitable method of acquiring the extra headroom would be to build a short abutment wall that would support the arch. A properly designed wall could provide a base that would not affect the structural integrity of the arch but still allow the required additional vertical clearance. Extra height required for clearance may also be achieved by changing the height of the abutment. If the taller arch section is used, the amount of fill placed above the arch should be limited.

ANALYSIS OF 24-FT ARCH WITHOUT LEGS

The areas of critical tension stress for the 24-ft elliptical arch without legs were the same as those of the 30-ft elliptical arch for the eight loading cases analyzed here. One major difference between the 24- and 30-ft elliptical arches was the magnitude of the stresses. The 24-ft elliptical arches had a maximum stress 33 percent less than those of the 30-ft elliptical arches. However, for the fixed base condition, the tension stresses at the base were equal to or exceeded the cracking stress for all eight load cases and for Load Case 2 they were nearly two times the cracking stress. For the pinned end condition, the stresses at the eighth point of the span exceeded the cracking level for all four load cases for vertical loads only, and were less than 500 lb/in.^{2} for two of four load cases when lateral load was included. A maximum deflection of 0.16 in. was recorded for Load Case 2 with pinned ends. Deflections for the other load cases were less than or equal to 0.14 in., which is negligible for a 24-ft span.

Of all the arches analyzed in this study, the 24-ft circular arch exhibited the best all around structural performance. The highest tension stress was 40 percent less than the theoretical cracking stress, and in most instances was less than 100 lb/in.^{2} (see Table 4). The deflections for this structure were also small.

In summary, a comparison of the 24-ft elliptical arch without legs and the circular arch without legs yielded a result identical to the 40- and 30-ft arches; the circular arch had much lower tension stresses and deflections and performed

better than the elliptical shape for the load cases presented here. It seems that the cause for the higher tension stresses in the elliptical shape was the result of the flatter crown geometry and sharper change in slope along the arch. At the eighth point the elliptical shape developed a moment 3.5 to 5.5 times higher than the circular arch, whereas axial loads were virtually identical. At the crown, the elliptical shape developed a moment two to four times higher than the circular shape, whereas the circular arch had an axial load only 15 percent higher.

ANALYSIS OF 24-FT ELLIPTICAL SHAPE WITH LEGS

The 24-ft elliptical arch with legs has a vertical opening of 10 ft and in this study is noted as a "24-ft elliptical arch with legs." Its shape was derived by adding 24-in. vertical legs to the standard 24-ft elliptical shape. The proposed 24-ft circular arch does not have an added leg and thus has a vertical opening 2-ft shorter than that of the elliptical arch with legs.

For the elliptical shape with legs, the stresses were above the cracking stress for all eight load cases, although they did drop approximately 25 percent when lateral load was added. The tensile stresses at the base were nearly 10 percent higher than those at the eighth point and the deflections were about twice as high as those of the elliptical arch without legs.

Like the 30-ft arches, the preferred method of achieving the extra vertical clearance may be to add a short abutment wall.

CONCLUSIONS AND RECOMMENDATIONS

After reviewing the results of the 24-, 30-, and 40-ft arch data, it is evident that circular arch geometry is preferred over elliptical shapes for the load combinations presented here. The tensile stresses and deflections developed by the circular arches were consistently lower than those of the elliptical shape.

As discussed earlier, the main reason for the difference is related to the geometric shape. A comparison of the 24- and 30-ft shapes, with the crown elevation of each arch being nearly equal, is shown in Figures 1 and 2. This allows for comparison of the curved portions of each arch, showing that the elliptical arch has a steeper slope at the base and is flatter near the crown. A review of the 40-ft arches in Figure 1 shows similar characteristics, including a pronounced flat area at the crown of the elliptical shape.

It should be pointed out, however, that the elliptical shape may prove more effective than a circular shape for other criteria or load cases that were not analyzed by the authors.

The results also show that temperature changes can cause large tensile stresses that cannot be ignored in the design. The present American Association of State Highway and Transportation Officials' code requires similar structures to be analyzed for the effects of a 35 degree temperature rise and a 45 degree temperature fall.

Another important topic that was not investigated in this report is the effect of lateral translation of the footings. In most instances, the thrust from the arch will react on the footing at an angle that may cause outward lateral movement of the footing. If the footings are allowed to translate outward, the tensile stresses at the underside of the crown will greatly increase. The lateral translation can be significantly reduced by using a pile foundation or by anchoring the footings into bedrock.

As mentioned earlier in this paper, the accuracy in idealizing actual field conditions by means of a computer model cannot be easily verified. However, in field measurements of elliptical arch structures the footing translations have been quite low. The effects of soil structure interaction, footing movement, and soil arching are all unknowns that enter the analysis. The only way to validate the effectiveness of the load distributions chosen is to experimentally test small- or full-scale models of each arch. Such testing will provide actual interface pressures, stresses, and deflections and give an indication of the effects of soil structure interaction. However, even though the load distributions and material properties used in this study may not exactly match the actual field conditions, they do provide a good basis for comparing arch geometry and the effects of vertical loads.

Mn/DOT is presently working to fine tune its final selection of arch shapes. This work has included an analysis to optimize the rise-span ratio for each circular shape and computing the effects of moving HS20 live loads over arches with shallow fills. Future work will include the effects of construction loading and the monitoring of full-scale arches to compare the analytical results with actual field data.

REFERENCES

1. K. J. Bathe. *Finite Element Procedures in Engineering Analysis.* Prentice-Hall, Inc., Englewood Cliffs, N.J., 1982.
2. *ADINA Users Manual.* ADINA Engineering, Report AE 81-1, Sept. 1981.
3. Research Engineers. STAAD-III Program User Manual. Marlton, N.J., 1986.
4. *Standard Specification for Highway Bridges*, 13th ed. Section 8.5, American Association of State Highway and Transportation Officials, Washington, D.C., 1983.
5. C. K. Wang and C. G. Salmon. *Reinforced Concrete Design.* Intext Press Inc., New York, 1973.

DISCUSSION

NEAL FITZSIMONS
10408 Montgomery Avenue, Kensington, Md. 20895.

For the practicing engineer, governmental or private, this paper can be too easily misinterpreted. The authors seem to say that field observations of cracking in the soffit of a few arch elements of one or two bridges created great concern for their durability and that this study was undertaken to understand why the cracks occurred and to provide the basis for new geometries that do not have this problem. Several pages of detailed computer printout of maximum tension stresses are provided that show the reader that in a circular geometry the maximum face stresses are less than those in the elliptical geometry for a series of eight static load cases, all of which have an overfill of only 2 ft. From this highly theoretical set of results, the authors seem to imply that a circular arch would be more durable than an elliptical arch.

It is implicitly assumed in this paper that the soffit cracks (in an arch element of an elliptical bridge) that appear to be

the original cause for concern [see Bathe (*1*) in the paper] are caused by tension stresses induced by static loading, not by other causes such as craning during construction or improper backfilling procedures. This is despite the fact that dozens of bridges (involving hundreds of arch elements) built to identical specifications in Australia, Europe, and the United States, are visually crack free. Some of these structures are more than 20 years old. In only one case (other than in Minnesota), soffit cracks in a single arch element very probably caused by craning were observed by inspectors and judged to warrant additional monitoring. Although still under observation, there appears to be little likelihood that the durability of the structure has been compromised.

There also seems to be an implicit assumption in the paper that cracks are to be avoided as a "primary design concern," even those that are less than 0.01 in. in width, which is a widely accepted standard for permissible widths without compromising durability. The ideal of visually crack-free concrete is desirable, but practitioners generally accept that crack control is a reasonable strategy for producing durable structures.

Because the parabola is widely recognized as the ideal geometry for a uniformly arch structure in terms of tension-free stresses, it is strange that this was not studied rather than circular segments. There is no rationale presented for the selection of the circular section, nor is the parabola even mentioned. In his 1937 book on continuous structures and arches, Charles Spofford writes "Segmental arches are seldom used for bridges, but inasmuch as they are susceptible, if of uniform cross section, to precise analysis, they are treated fully in Chapter VI." Of course, the reason for the elliptical section is that it has hydraulic characteristics more desirable than the circular or the parabolic arch. Because the primary design concern is the passage of water under the arch (otherwise there would be no need for the structure), the elliptical geometry has been used for centuries for this purpose.

There are some theoretical questions about this paper. Why was an approximate method such as finite element method (FEM) compared with the "precise" elastic analysis? What were the "errors of closure" in the authors' FEM calculations? I have made more than a few FEM analyses of arches and found that they are sensitive to the number of nodes and that for the spans studied, 50 or more elements were needed to keep the errors of closure within acceptable limits. Also, in one case, the authors used the same number of nodes, 42, for the elliptical geometry as they used for the circular geometry. Because the length of the elliptical arch is greater, this calculation would have a greater error of closure than would the circular.

Neglected in this study is the effect of steel reinforcement and it therefore does not use an interaction diagram to determine stresses at the interior and exterior surfaces. The effect this has on the results is not discussed by the authors. Of course, it is the reinforcement that "liberated" concrete arch bridge design from being a mere copy of the stone arches. Being able to accept some moment-induced tensile stress without significant cracking is the reason that reinforced concrete arch bridges can be designed with geometries that enable the structure to perform its primary function more efficiently.

Instead of using a "tire print" and distributing the wheel load longitudinally, the study uses a load wedge of 3,200 lb. This is unnecessarily unrealistic. Further, the study indicated that the arch elements were 6 ft wide, therefore only one wheel on an arch element would give its maximum load. However, a given wheel load is 16,000 lb, which divided by 6 would give a load of 2,667 lb rather than the 3,200 lb that assumes a 10-ft lane. Also, a moving wheel load would produce only transitory crack openings, giving water little chance to penetrate upward into the soffit.

In the conclusion, the authors write "This allows for comparison of the curved portions of each arch showing that the elliptical arch has a steeper slope at the base and is flatter near the crown." Of course it is! This is the basic difference that makes the elliptical arch preferable to the circular arch for stream crossings.

In summary, although this paper provides some interesting results from applying a highly theoretical set of conditions to a highly theoretical set of arches using FEM, it does not provide a practical basis for selecting arch geometries in real-world situations. Despite technical caveats that are scattered through the paper, readers who are not familiar with short-span arches might receive the erroneous impression that elliptical sections should be avoided in favor of circular segments solely because they are theoretically less durable.

AUTHORS' CLOSURE

The authors would like to thank FitzSimons for his discussion comments. His design work for the manufacturer of elliptical arches has no doubt given him a good background in the design and analysis of such structures.

However the authors would like to clear up several apparent misunderstandings brought forth in the discussion. In the first paragraph, FitzSimons states that all eight load cases had overfill depths of only 2 ft. As shown in Figure 4 of the paper and described in the text, Load Cases 2 and 6 had overfill depths in excess of 12 ft.

The authors were also surprised that the discussion included comments concerning durability. The purpose of the study was to compare the effects of arch geometry on the anticipated state of stress. The issue of durability has not been investigated.

Several other comments in the discussion address crack control and the authors' primary design concern to limit cracking. One particular sentence in the discussion noted that the authors limited cracks, "even those that are less than 0.01 in. in width." In the report the authors actually write "a primary design concern is to keep the structure relatively free from cracking." They go on to say that "Although all concrete structures are subject to temperature and shrinkage cracking, the main concern is to limit the tensile cracks caused by dead and live loads and temperature effects." There is no reference made to not allowing cracks of width less than 0.01 in. or of cracking causing the durability to be compromised.

FitzSimons also poses the question of why a circular shape was used instead of a parabolic shape, which produces a tension-free structure under uniform load. This question is answered by examining an arch with 2 ft of fill at the crown. This results in fill heights of from 8 to 13 ft at the base, depending on the span of the arch. Because of this difference in soil depth, the loads at the base may be from 4 to 6 times higher than the load at the crown, producing a load diagram that is far from uniform and diminishing any advantage of using a parabolic shape.

Arches that have higher curvatures will tend to be in more of a compressive mode than will arches with lower curvatures. A circular shape seems to be an optimum choice between the two groups and was therefore considered in this study. Nevertheless, designers may wish to consider other shapes for particular projects after a careful investigation of their performance.

The discussion also recommends using at least 50 beam elements to model the entire structure and questions the authors' decision in one particular case to use 42 elements to model both the elliptical and circular shape. However, further investigation reveals that the sum of the element lengths for each arch differs by less than ½ of 1 percent for that particular set of arches. Because symmetry was used in the modeling, the shapes were analyzed using 42 elements for half of the arch, which is equivalent to using 84 elements to model the full arch. This is far in excess of the recommended 50 and the very small difference in structure length will produce negligible closure error.

Concerning an elastic analysis, there is no real justification to use an elastic analysis for studying the behavior of reinforced concrete structures beyond the inception of cracking. From that point on this structural behavior enters the nonlinear domain and an approximate analytical method is required.

Steel reinforcement was not included explicitly in the analysis because the major advantage of arch structures is in resisting load through compressive action. The contribution of steel, although important, is a secondary parameter under these conditions. If flexure is taken into consideration, the overall depth of the cross section becomes significantly more important. Increasing the amount of steel has a small effect on the moment of inertia compared with increasing the depth of the cross section. The selection of reinforcement was carried out using conventional techniques, and this has been done in a later phase of the present study.

With regard to the choice of loads, as discussed in the paper, the same loads were consistently applied to each shape and the relative behavior was compared accordingly. As far as transient loads are concerned, dynamic analysis of these systems has not been performed during this phase of the study. It is known that dynamic loads may affect such structures well beyond "transitory crack openings" and it is recommended that such considerations be addressed in the future.

The later part of the discussion highlights the fact that the elliptical shape provides greater area for the flow of water through the opening. Of the structures analyzed in this study, the elliptical shape allowed from 2 to 9 percent more flow. If the required flow area becomes a critical design requirement, the elliptical shape would prove more effective than the circular shape. However, the authors believe that the results of this study show that if a slight reduction in flow area can be permitted, a circular arch shape could be used which, for the load cases analyzed herein, should produce smaller tensile stresses within the structure.

Additional research is needed to address questions related to the ultimate behavior of the structures, soil structure interaction, and dynamic effects. It is also worth noting that in 1987 the California Department of Transportation was granted $600,000 to study arch structures and soil structure interaction. They are currently in the process of finalizing the design of these structures, using circular shapes with thicknesses of less than 10 in.

Again the authors would like to thank FitzSimons for his comments. They hope that the discussion and response clarify the issues with respect to the study. The authors would be happy to provide any further information upon request.

Publication of this paper sponsored by Committee on Culverts and Hydraulic Structures.

Design of Thin Wall Reinforced Concrete Semicircular Arch Using Dimension Ratio

A. E. BACHER, D. E. KIRKLAND, AND M. SEYED

The recent completion of a California Department of Transportation construction evaluated precast thin wall reinforced concrete (semicircular) arch at San Martinez Grande affirmed the application of the dimension ratio design concept to reinforced concrete semicircular arch design. The recent culvert research was further supported by the complete and comprehensive California Department of Transportation reinforced concrete arch culvert research previously reported at Posey Canyon and Cedar Creek. The observed vertical and horizontal pressures observed at Posey Canyon and Cedar Creek are consistent with the application of the dimension ratio concept to reinforced concrete arch design. A significant reduction can be made in the wall thickness of reinforced concrete semicircular arch designs, resulting in substantial future savings.

The California Department of Transportation's (Caltrans) extensive culvert research program included three reinforced concrete (RC) horseshoe arches: San Luis Reservoir, Posey Canyon, and Cedar Creek; and, most recently, one construction evaluated RC semicircular arch, San Martinez Grande, completed in January 1987. Application of the dimension ratio (DR) concept to a RC semicircular arch design is considered to be most logical, and follows the recent successful DR application by Caltrans to circular RC pipe design (*1*). DR is defined as the diameter in inches divided by the wall thickness in inches.

The first consideration in the development of the DR concept application to a semicircular arch is the summary of the RC arch culvert research by Caltrans (*2*). This summary includes the complete and comprehensive research of two horseshoe arches (see Figure 1). It is apparent that the research at Posey Canyon and Cedar Creek are in the rigid range, with DRs ranging between 4.8 and 11.0, whereas San Martinez Grande is in the flexible range, with a DR of 30.0. These initial projected ranges are based on California's extensive culvert research program.

OBSERVED DR: LATERAL PRESSURES ON POSEY CANYON AND CEDAR CREEK

The observed lateral pressures have been plotted (see Figure 2), taken at about 30 degrees from the base line of the horseshoe arch configuration. The initial projected range of loadings is shown as Loading 1 and Loading 2. The two lateral loadings of RC arches provide an envelope that contains most of the observed readings.

Of particular interest is the fact that at Section 2 of Posey Canyon (Figure 3) the lateral pressure readings were observed to increase from 26 to 118 lb/ft³ and from 24 to 136 lb/ft³, and at Section 3 from 24 to 101 lb/ft³ on the right flank (Figure 4) in the 26 months following fill completion. A similar increase was observed on the right flank of Section 10 of Cedar Creek (Figure 5), that is, from 117 to 182 lb/ft³. At the following sections, however, the initial and final lateral pressure readings were virtually the same, that is, at Section 1 of Posey Canyon, 50 lb/ft³ versus 42 lb/ft³; at Section 7 of Posey Canyon the change was from 26 to 22 lb/ft³ and from 84 to 82 lb/ft³; and at Station 4 of Cedar Creek the readings varied from 126 to 119 lb/ft³ and from 180 to 173 lb/ft³. In effect, little change was noted from the initial readings but with lateral pressure ratios varying from 0.2 to 0.6 to 1.3 of the vertical pressure (Figures 6, 7, and 8). Therefore, when the DR is less than 12, the necessity of providing a design for a horseshoe RC arch that must satisfy a range in lateral loadings was amply supported by the RC arch culvert research. Further, of the six test sections using Method A backfill, 80 percent of the 26-month readings exceeded 42 lb/ft³ and 45 percent exceeded 100 lb/ft³. Method A backfill is a minimum of 2-ft structure backfill compacted to 95 percent surrounding the RC arch barrel.

Method A backfill conformed to the following grading:

Sieve Sizes	*Percentage Passing*
3 ft	100
No. 4	35–100
No. 30	20–100

Method *A* backfill required a sand equivalent value of not less than 20.

SAN MARTINEZ GRANDE CONSTRUCTION

The next consideration is the construction of San Martinez Grande and the subsequent H20 live load test.

The intent of a precast design is to use the plant facilities of a nearby concrete precast fabrication facility. This will result in better control of the precast units and higher allowable concrete stresses. However, because only three precast units were required at this site, the contractor, Granite Construction Company, chose to build the precast units at the job site. The inner form with the reinforcement being placed around the periphery are shown in Figure 9. A picture of a completed panel being lifted and subsequently placed is shown in Figure

Department of Transportation, Division of Structures, P. O. Box 942874, Sacramento, Calif. 94274-0001.

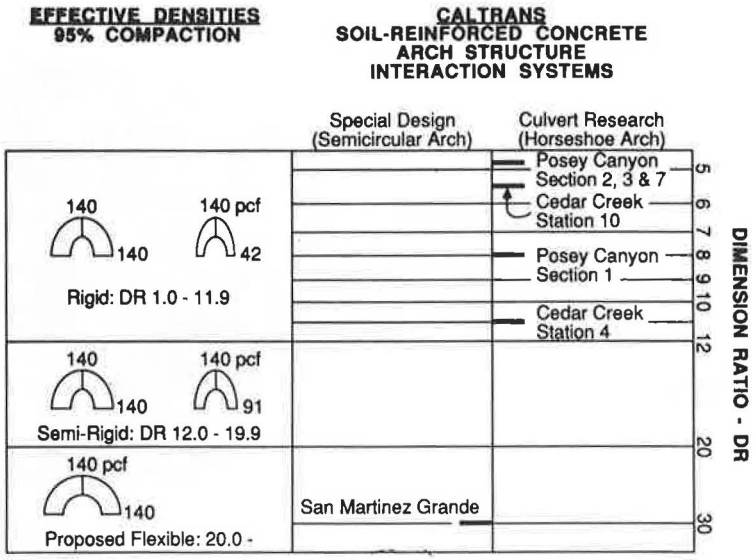

FIGURE 1 California Department of Transportation reinforced concrete arch: dimension ratio.

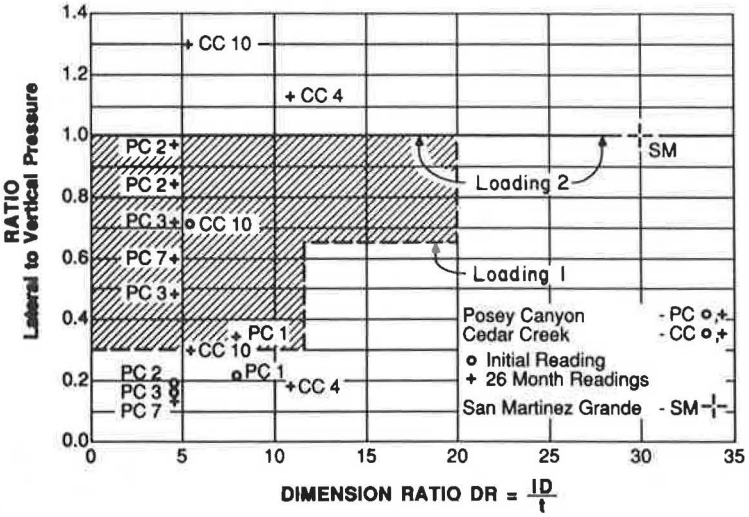

FIGURE 2 Dimension ratio: lateral pressure.

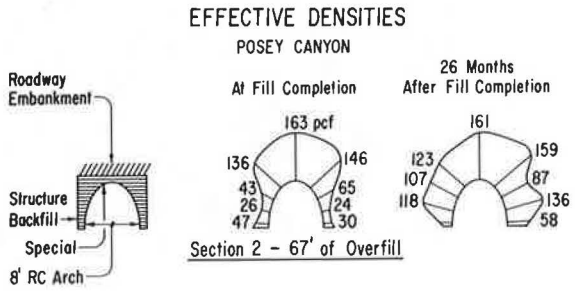

FIGURE 3 Posey Canyon effective densities: Section 2.

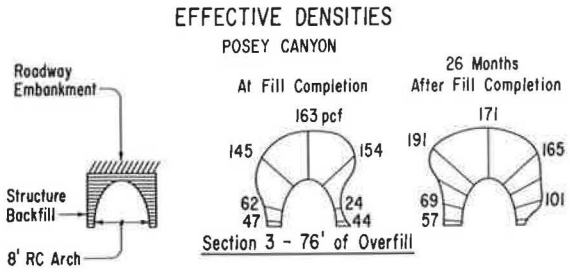

FIGURE 4 Posey Canyon effective densities: Section 3.

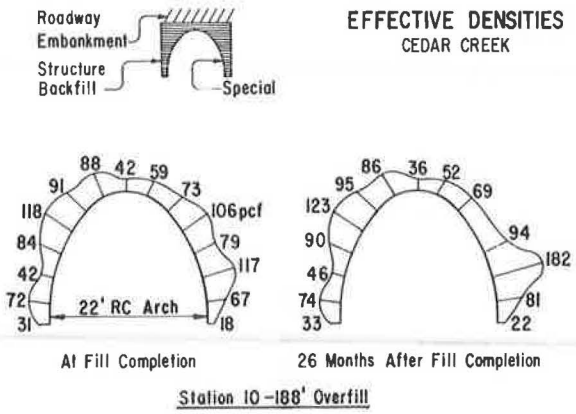

FIGURE 5 Cedar Creek effective densities: Station 10.

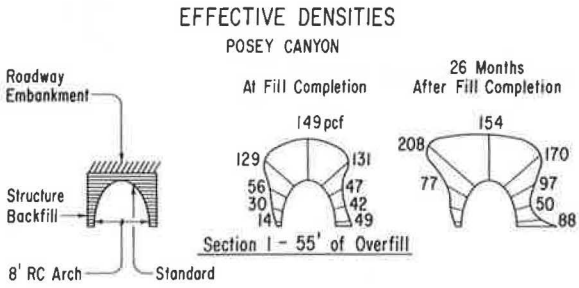

FIGURE 6 Posey Canyon effective densities: Section 1.

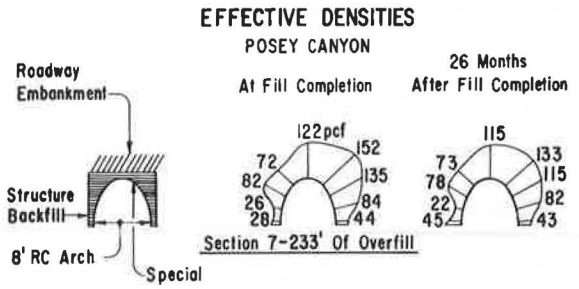

FIGURE 7 Posey Canyon effective densities: Section 7.

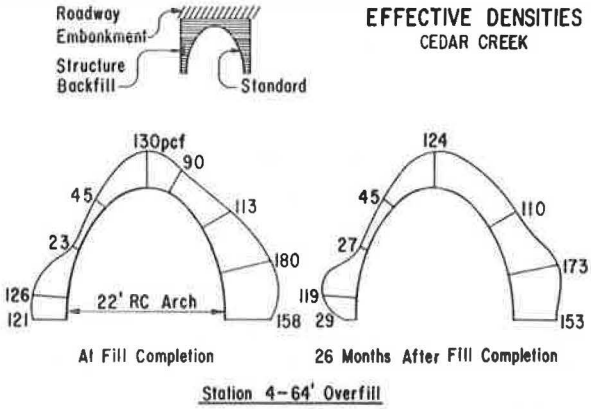

FIGURE 8 Cedar Creek effective densities: Station 4.

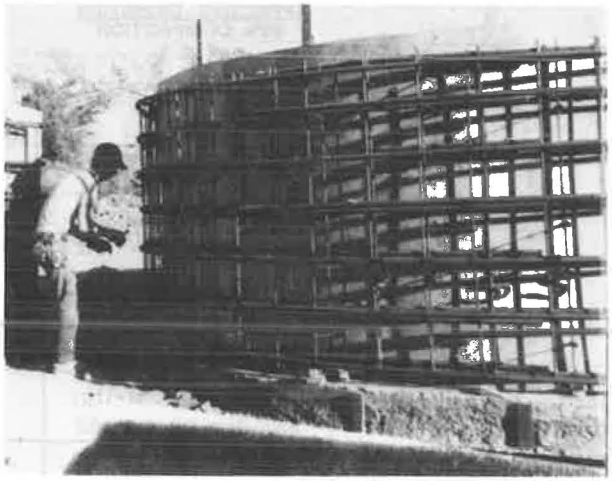

FIGURE 9 San Martinez Grande: bar reinforcing placement in precast form.

10. The existing structure is shown in Figure 11, with the three precast units placed adjacent to the original structure. To ensure independent deformation readings, the center precast unit was placed between the two other precast units with no physical ties to either of them. Peripheral change measurements were made in the center of this center panel. Two sheets of metal were placed over the interfaced precast units (Figure 12) to prevent soil from coming through the joints. Because the space between the original and the widened structure was minimal, portable tampers were used to consolidate the soil (Figure 13).

SAN MARTINEZ GRANDE: STATIC LIVE LOAD TEST

The live load test was made with a Caltrans maintenance vehicle (Figure 14). The live load test was of a static load only (Figure 15) (*3*).

FIGURE 10 San Martinez Grande: lifting precast unit.

FIGURE 11 San Martinez Grande: three precast units in place.

FIGURE 12 San Martinez Grande: backfilling precast units.

SAN MARTINEZ GRANDE: MEASURED PERIPHERAL SHAPE CHANGES

Deformation of the 20-ft semicircular arch was observed during the backfilling stages (Figure 16). Of interest is the fact that the magnitude of these peripheral shape changes during construction was only a maximum of ¼ in. The deformation resulting from a static live load was also observed (Figure 17). The largest live load deformation was only 3/16 in. This confirms previous research that the thin wall semicircular arch design is adequate (*4*) and that a long-term service life of 50 years for RC culverts can be anticipated (*5*). By contrast, the original semicircular arch had a variable thickness of 18 to 13 in. compared with the precast arch uniform thickness of 8 in.

RC ARCH CRITICAL LOADING CONDITIONS

A comparison has been made of the applicability of the two specified Caltrans design loadings with both the horseshoe and semicircular shaped arches (Figures 18 and 19). The moments shown are for an 8-ft RC (horseshoe) arch, with fixed footings and 20 ft of overfill and a 20-ft RC (semicircular) arch, with pinned footings and 20 ft of overfill. It is of interest to note that the optimum loading for the horseshoe arch is Loading 1, 140:42, whereas the optimum loading for the semicircular arch is Loading 2, 140:140. The semicircular arch thin wall moments for Loading 1, 140:42, are theoretical only because the thin wall will deform, reducing the moment, with thrust becoming the significant design consideration.

FIGURE 13 San Martinez Grande: compaction with portable tampers.

FIGURE 14 San Martinez Grande: H20 truck.

FIGURE 15 Static live load test.

COST SAVINGS

A cost comparison was made between the original design at San Martinez Grande and the thin wall design widening for the 20-ft RC semicircular arch. Based on the bid prices at San Martinez Grande, a 100-ft long 20-ft RC semicircular arch would cost approximately the same as the original design (*4*). This design concept, however, will result in future significant savings for semicircular arches from 10 to 30 ft in diameter for longer installations and where construction staging is required and will eventually lead to the use by Caltrans of precast segmented three-hinged RC arches up to 60 ft in diameter (*6*).

STANDARD PLAN: PRECAST REINFORCED CONCRETE SEMICIRCULAR ARCH

A standard drawing is being developed by Caltrans for trial use for precast RC semicircular arches with diameters ranging from 10 to 30 ft. The bedding and backfill will conform with the details shown in Figure 20. Allowable footing foundation pressures will be determined by a soils investigation and must be adequate to support the design pressures; a 2-ft layer of structure backfill compacted to 95 will be placed around the semicircular arch periphery. Designs will be provided for 10 ft and 20 ft of overfill.

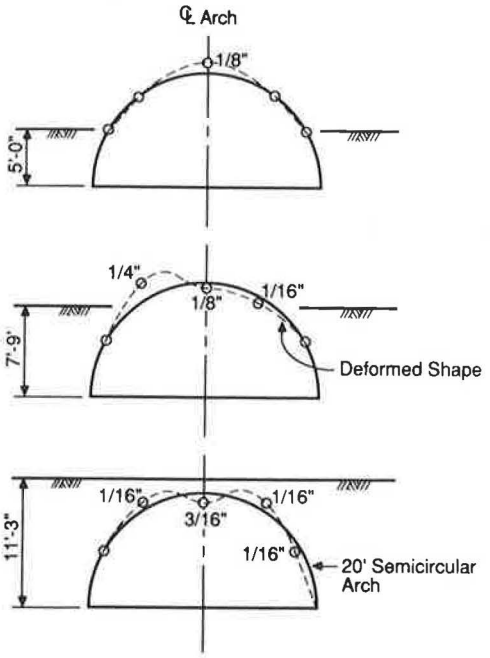

FIGURE 16 Backfilling deformations.

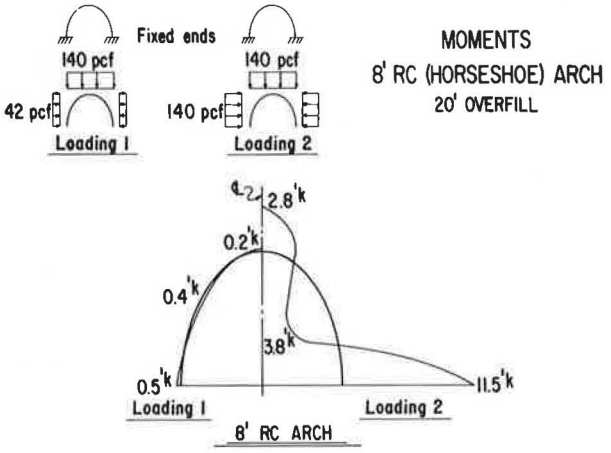

FIGURE 18 Eight-ft reinforced concrete (horseshoe) arch. Theoretical bending moments based on 140:42 and 140:140 loadings.

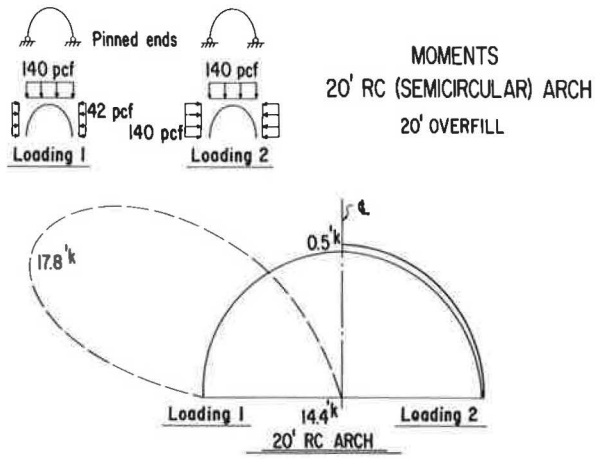

FIGURE 19 Twenty-ft reinforced concrete (semicircular) arch, theoretical bending moments based on 140:42 and 140:140 loadings.

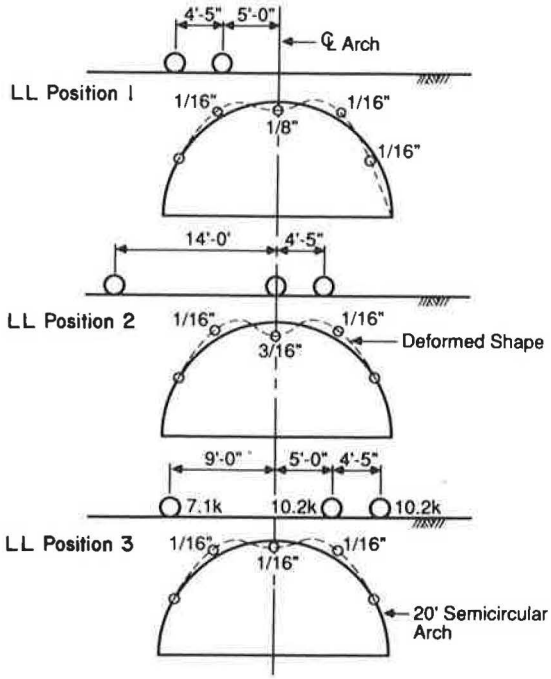

FIGURE 17 Live load deformations.

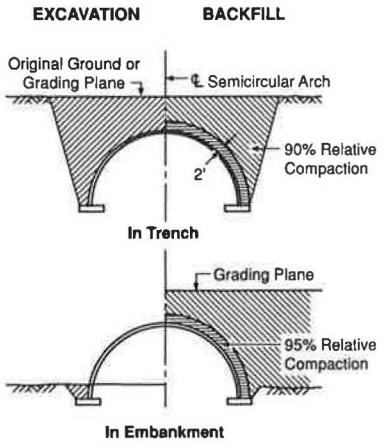

FIGURE 20 Bedding and backfill: semicircular reinforced concrete arch.

REFERENCES

1. A. E. Bacher. Design of Thin Wall Reinforced Concrete Pipe Using Dimension Ratio (DR). *ASCE Pipeline Materials and Design*, American Society of Civil Engineers, New York, Oct. 1984.
2. A. E. Bacher and E. G. Klein. Reinforced-Concrete Arch Culvert Research by the California Department of Transportation. In *Transportation Research Record 785*, TRW, National Research Council, Washington, D.C., 1980, pp. 33–36.
3. W. L. Nielsen and D. E. Kirkland. *Precast Thin-Wall Semicircular Reinforced Concrete Arch Culvert*. Construction Evaluated Experimental Project CA-86-09, California Department of Transportation, Sacramento, July 1987.
4. J. J. Hill and A. M. Shirole. Comparative Evaluation of Precast Concrete Pipe-Arch and Arch Structures. In *Transportation Research Record 1087*, TRB, National Research Council, Washington, D.C., 1986, pp. 32–37.
5. *Highway Design Manual*. California Department of Transportation, Sacramento, Sept. 1982.
6. R. H. Hebden. Giant Segmental Precast Prestressed Concrete Culverts. *PCI Journal*, Nov.–Dec. 1986.

Publication of this paper sponsored by Committee on Culverts and Hydraulic Structures.

PIPECAR and BOXCAR Microcomputer Programs for the Design of Reinforced Concrete Pipe and Box Sections

TIMOTHY J. MCGRATH, DAVID B. TIGUE, AND FRANK J. HEGER

PIPECAR and BOXCAR are structural analysis and design programs for reinforced concrete pipe and box sections that were developed for the Federal Highway Administration in the early 1980s. The programs applied state-of-the-art methods of design but were written for mainframe computers, making them relatively inaccessible to many designers. Reported herein is a description of updated versions of the programs that operate on IBM or IBM-compatible personal computers that have user-friendly input routines with help screens that make access to and operation of the programs very simple, even for a computer novice. Program input is developed from a permanent file of typical or "default" design parameters; thus for a relatively simple design, the user can specify as little information as the diameter (span and rise for a box section) and the depth of fill. The default file can be modified to tailor the program to the particular default configuration needed by any user. For applications with unusual load or installation conditions, the user can modify almost all parameters to produce a suitable design. Structural design is in accordance with current American Association of State Highway and Transportation Officials standards. Reinforcing requirements are output in square inches per foot. If stirrups are required, an additional design routine is automatically invoked to allow the user to determine the size and spacing. Output files are written to computer floppy or hard disks, from which they may be viewed with standard text editor software or printed. Program output level is user controlled. At the maximum levels, the program output is sufficiently detailed to allow independent design review.

In June 1983, the Federal Highway Administration (FHWA) published the *Structural Design Manual for Improved Inlets and Culverts* (*1*). Originally conceived as a specialized project to develop a design rationale for the special geometries of improved inlets, the project resulted in the development of the computer programs PIPECAR and BOXCAR that are applicable to the structural design of circular and horizontal elliptical reinforced concrete pipe and single-cell box sections. The programs incorporate a new state-of-the-art method of design developed by Heger and McGrath (*2*). This design method was later adopted by the American Association of State Highway and Transportation Officials (AASHTO) and is given in Section 17.4 of the AASHTO Specifications for Highway Bridges (*3*). The programs were written for a mainframe computer and, because of their original emphasis on inlet structures, did not include design for wheel loads.

Simpson Gumpertz & Heger Inc., Consulting Engineers, 297 Broadway, Arlington, Mass. 02174.

Reported herein are the capabilities of upgraded versions of the programs that now operate on IBM, or IBM-compatible, personal computers, have user-friendly input-output routines, and include a number of live load options.

GENERAL PROGRAM CAPABILITIES AND LIMITATIONS

Application

PIPECAR and BOXCAR are computer programs that may be used for the structural design and analysis of reinforced concrete pipe and rectangular box sections, respectively. These programs determine the required steel reinforcement for user-specified culvert geometry, material properties, and loading data. PIPECAR is capable of designing any circular or horizontal elliptical pipe-culvert. Pipe-culverts may be designed by the direct method of completing a structural analysis and design for an assumed earth pressure distribution or by the indirect method of design reinforcing for three-edge bearing load conditions (i.e., a specified D-load). BOXCAR is capable of designing any rectangular single cell box culvert with or without haunches. Haunches, it specified, may have any geometry (i.e., the haunch angle may be other than 45 degrees), and haunches at the top may have a different geometry from haunches at the bottom. Steel reinforcing areas are calculated using the design method presented in AASHTO Section 17.4 (*3*). Both programs are capable of analysis and design for truck and railroad live loads in accordance with AASHTO and AREA specifications, respectively. Parameters that may be specified by the user are listed in Table 1.

As an alternative to specifying all the parameters listed in Table 1, the user may rely on a file of preprogrammed "default" parameters. By use of these default parameters, the user need specify only the culvert geometry and depth of fill (or, alternatively for the indirect design method of pipe, the D-load). The default values will be used for any additional parameters not specified by the user. The default file may be reconfigured by the user to meet any particular application such as cast-in-place or precast box sections.

Limitations

PIPECAR and BOXCAR do not optimize designs. That is, they do not process the quantities of reinforcing and concrete

TABLE 1 USER-SPECIFIED INPUT PARAMETERS

CATEGORY	PIPECAR	BOXCAR
Culvert Geometry	Circular or Horizontal Elliptical Inside Radii	Single Cell Inside Span and Rise
	Wall Thickness	Top, Bottom and Sidewall Thicknesses
		Top and Bottom Vertical and Horizontal Haunch Dimensions
Loading Data	Depth of Fill, Density of Fill, Minimum and Maximum Lateral Soil Pressure Ratios, Truck or Railroad Loading, Depth of Fluid, Density of Internal Fluid, Surcharge Loads	
	Uniform or Radial Loading Application (See Fig. 2)	
	Alternatively a D-Load May Be Specified for Pipe	
Material Properties	Type of Reinforcing (Used for Crack Control), Reinforcing Yield Strength, Concrete Compressive Strength, Concrete Density	
Design Data	Live and Dead Load Factors, Strength Reduction Factors for Shear and Flexure, Cover over Reinforcing, Spacing, Size, and Number of Layers of Reinforcing	

and complete successive designs to determine geometries with minimum cost of materials. This can be completed through the use of multiple runs. Other program limitations include the following:

- BOXCAR does not consider the load case of internal pressure,
- The culvert size is limited to spans of 14 ft for box sections and diameters of 12 ft for pipe, and
- Only main flexural reinforcement requirements are fully determined for box and pipe sections.

STRUCTURAL CRITERIA FOR ANALYSIS AND DESIGN

Loadings

PIPECAR and BOXCAR analyze several different load conditions that are typically imposed on culverts. These include loads resulting from culvert self-weight; vertical and lateral soil pressures; internal fluid; and AASHTO truck, railroad locomotives, approaching vehicles (for box culverts only), and vertical and horizontal surcharge pressures. The load conditions are grouped into three categories: permanent dead loads, additional dead loads, and live loads. Permanent dead loads are considered to be always acting on the culvert. These include the culvert self-weight, vertical soil pressure, and a minimum lateral soil pressure that is specified by the user. Additional dead loads are loads that are considered only if they produce higher critical design forces for each of the design sections. These include the additional lateral soil pressure specified by the user and internal fluid load. Live loads include AASHTO HS-20 and Interstate truck wheel loading, railroad loading, or a user-specified live load. BOXCAR analyzes wheel loads at several positions across the top of the box culvert to simulate a truck traversing the culvert. As many as 11 different truck positions are considered to obtain the maximum critical design forces for each design section. Surcharge loads may be considered as either permanent dead load, additional dead load, or live load.

In BOXCAR, loads are applied as linear pressures, as shown in Figure 1. Foundation reactions are assumed to vary linearly across the bottom slab of the box culvert, and it is assumed that the supporting foundation cannot resist tensile forces, as is typically assumed in foundation design. In PIPECAR, loads and reactions can either be applied as a sinusoidally distributed normal pressure or as a linear pressure on the pipe at the option of the user. These two methods, commonly referred to as Olander and Paris pressure distributions, respectively, are shown in Figure 2.

PIPECAR includes the option of designing pipe by the indirect design method. The user may specify a desired D-load capacity for the pipe and the program will complete the analysis and design for the moments, thrusts, and shears of the specialized load condition.

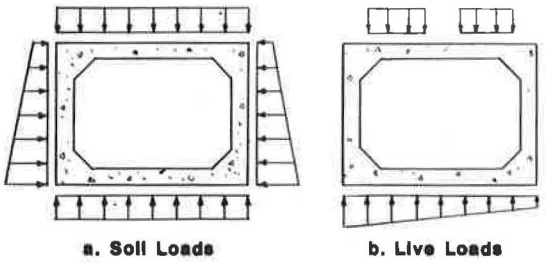

FIGURE 1 Typical pressure distributions used in BOXCAR.

Structural Analysis

PIPECAR and BOXCAR calculate the moments, thrusts, and shears at various design locations using the stiffness method of analysis. BOXCAR models the culvert as a four-member frame having a 1-ft width. For a given frame, member stiffness matrices are assembled into a global stiffness matrix, a joint load matrix is assembled, and conventional methods of matrix analysis are employed. The effect of haunches on the member stiffness is considered by performing a numerical integration across the member. The trapezoidal rule with 50 integration points is used, obtaining a sufficiently high degree of accuracy.

Because PIPECAR considers only symmetrical geometry and loads, the program models only half a pipe. The computer model consists of 36 members with boundary supports at the crown and invert. Each member spans 5 degrees, and nodes are located at the middepths of the pipe wall. For each member, a stiffness matrix is formed and translated into a global coordinate system. Pressures caused by the various loads are converted into normal and tangential nodal loads, which are then assembled into a joint load matrix. A solution is obtained by a recursion algorithm from which member end forces are obtained at each joint.

Design of Reinforcing

PIPECAR and BOXCAR calculate steel reinforcing areas based on the method described in Section 17.4 of the AASHTO specifications (*3*).

BOXCAR calculates steel areas using the maximum governing moments determined at Design Locations 1 through 11, shown in Figure 3. Flexural reinforcing requirements are evaluated at midspan for positive moments and at the tips of haunches and the face of walls for negative moments. The

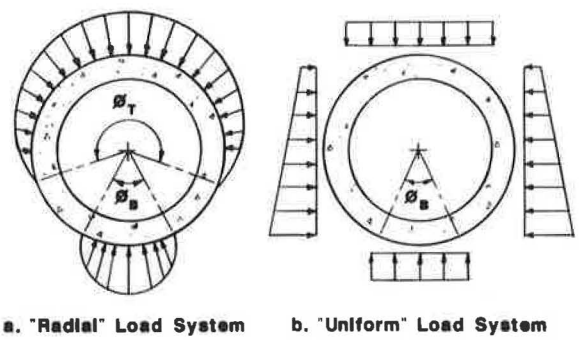

FIGURE 2 Typical pressure distributions used in PIPECAR.

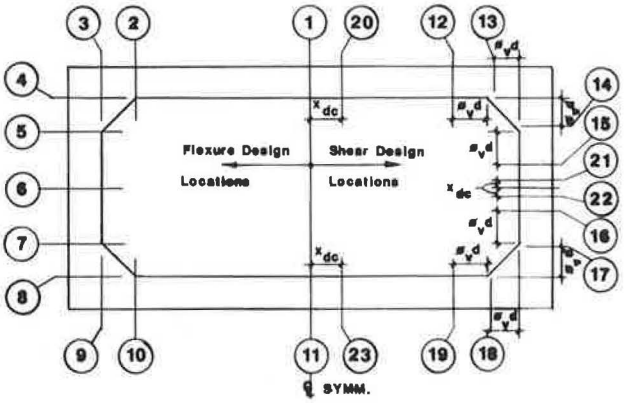

FIGURE 3 Locations of critical sections for shear and flexure design in single-cell box sections.

reinforcing layout consists of six steel areas designated A_{s1}, A_{s2}, A_{s3}, A_{s4}, A_{s7}, and A_{s8}, as shown in Figure 4. The area A_{s1} is the maximum steel area required to resist negative moments at Sections 2 through 10. Areas A_{s2}, A_{s3}, and A_{s4} are provided to resist positive moments at Sections 1, 11, 6; and A_{s7} and A_{s8} are designed to resist negative moments at Sections 1 and 11, respectively. Using the output option (see next section), the reinforcing requirements at all locations may be printed. This allows the designer to use alternate reinforcing layouts. The AASHTO requirement of limiting service load stresses for fatigue is also considered.

Shear stresses are evaluated at Design Locations 12 through 19, which are located at a distance $\phi_v d$ from the face of the haunch or wall and are computed with an allowable shear stress of $3\sqrt{f'_c}$ for boxes with uniform loadings and more than 2 ft of cover. For boxes with less than 2 ft of cover, or for boxes with significant live loads or railroad loads, the allowable shear stress is taken as $2\sqrt{f'_c}$. Shear stresses are evaluated at Design Locations 20 to 23, inclusive, where the value of M/vd equals 3, as required by AASHTO Section 17.4. When shear stresses exceed allowable values, the programs invoke a subroutine to design stirrup reinforcement.

PIPECAR calculates steel areas at three locations; inside crown, inside invert, and outside springline, as shown in Figure 5. These areas are designated as A_{sc}, A_{si}, and A_{so}, respectively. If shear stresses are exceeded at these locations, the program invokes a subroutine to design stirrup reinforcement.

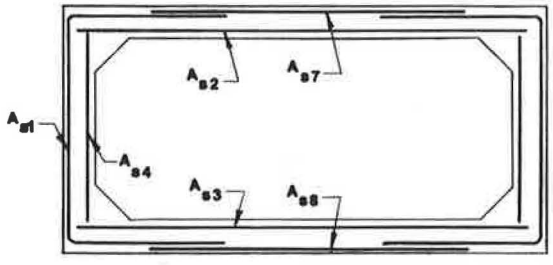

FIGURE 4 Typical reinforcing layout for single-cell box culverts.

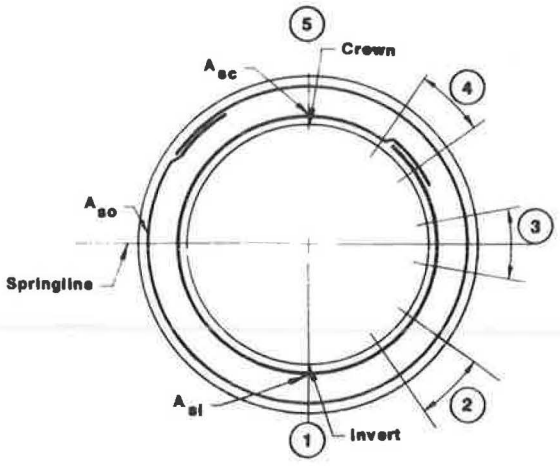

Flexure Design Locations:

1,5 Maximum Positive Moment Locations at Invert and Crown.
3 Maximum Negative Moment Location Near Springline.

Shear Design Locations:

2,4 Locations Near Invert and Crown Where $M/V\phi_v d = 3.0$

FIGURE 5 Typical reinforcing layout and design locations of critical sections for shear and flexure design in pipe sections.

COMPUTER PROGRAM

PIPECAR and BOXCAR run on IBM or IBM-compatible personal computers. Both programs are designed to be user friendly. The programs prompt the user for the various input data through menus. Help screens are available to aid the user in identification of input parameters and their applications. Much of the input is optional in that the program will assume standard default values for those not specified by the user. For BOXCAR, only the span, rise, and depth of fill are required input parameters. PIPECAR requires the user to input the pipe diameter and wall thickness for circular pipe, or the elliptical radii and wall thickness for horizontal elliptical pipe, the depth of fill, and the load system. The user may change the default parameters to gear the program to his or her particular design needs, such as cast-in-place or precast culverts. The programs save the input data for each design on a floppy or hard disk so that they may be retrieved later, and if desired, modified for additional runs.

The amount of output that can be obtained from the programs may be controlled by the user. The minimum amount of output that will be printed is an echo print of the input, any design warnings, and a design summary sheet. Additional available output includes stiffness matrices, displacements, moments, thrust, and shears at each node or design section for each load condition, and a table of design forces. Output files are written to a disk where they may be viewed with standard text editor software, or they may be printed for projects.

The main program routines for PIPECAR and BOXCAR are written in the FORTRAN computer language. User-friendly input and output routines are written in the BASIC language. All programs are compiled, therefore, the user is only required to have operating system software equivalent to PC DOS Version 2.0 or higher to execute the programs. Other hardware and software requirements include

- IBM PC, XT, AT, or a similar IBM-compatible computer and printer. Program output is formatted for 8 ½ × 11-in. paper.
- An 8087 or 80287 math coprocessor.
- A minimum of 640K bytes of memory.
- Two double density disk drives or a single double density disk drive and a hard disk drive.

The programs will be maintained and distributed by McTrans, the Center for Microcomputers in Transportation. Any interested person may obtain copies of the programs at a nominal cost by writing to McTrans, University of Florida, 512 Weil Hall, Gainesville, Florida 32611.

SAMPLE PROBLEMS

BOXCAR

This example problem demonstrates the use of the BOXCAR program for the design of the box culvert shown in Figure 6. For this problem, only the span, rise, and depth of fill were specified. The remaining parameters, listed in the echo print of the input as shown in Table 2, were assumed by the program. The design summary sheet for this example is shown in Table 3. The echo print of the input and the design summary sheet are the minimum amount of output obtained from the programs. More detailed output may be obtained at the option of the user as previously discussed.

PIPECAR

This example problem demonstrates the use of PIPECAR for the pipe shown in Figure 7. The pipe diameter, wall thickness, and depth of fill were specified for this problem. The echo print of the input is similar to that shown for the BOXCAR example problem. The design summary sheet obtained for this example is shown in Table 4.

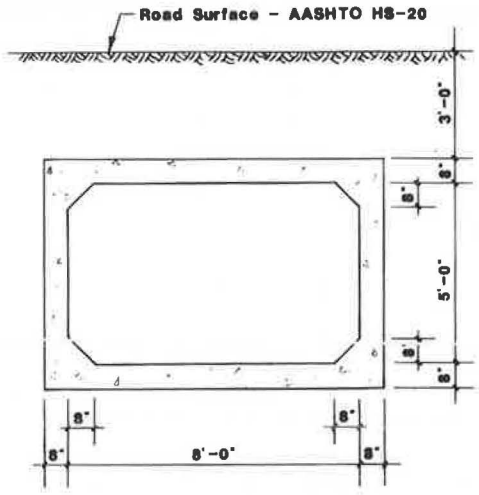

FIGURE 6 Culvert geometry for BOXCAR sample problem.

TABLE 2 ECHO PRINT OF INPUT DATA FOR BOXCAR SAMPLE PROBLEM

Filename	SAMPLE.BOX	
Job Description	Example of Boxcar Execution	
Span	8 ft	
Rise	5 ft	
Depth of Fill to Culvert Top	3 ft	
BOX GEOMETRY		
Top Slab Thickness	8 in.	
Bottom Slab Thickness	8 in.	
Sidewall Thickness	8 in.	
HAUNCH DIMENSIONS		
	Horizontal	Vertical
Top Haunches	8 in.	8 in.
Bottom Haunches	8 in.	8 in.
CONCRETE COVERS		
Top Slab Outside Face	1.5 in.	
Bottom Slab Outside Face	1.5 in.	
Sidewall Outside Face	1.5 in.	
Top Slab Inside Face	1.5 in.	
Sidewall Inside Face	1.5 in.	
MATERIAL PROPERTIES		
Main Reinforcing Yield Stress	60 ksi	
Distribution Reinforcing Yield Stress	60 ksi	
Main Reinforcing Type 2 No. of layers	1	
Design Concrete Strength	4 ksi	
Concrete Density	150 pcf	
LOAD FACTORS		
Dead Load Factor (Shear and Moment)	1.5	
Dead Load Factor (Thrust)	1	
Live Load Factor (Shear and Moment)	2.17	
Live Load Factor (Thrust)	1	
PHI FACTORS		
Shear	.85	
Flexure	.9	
REINFORCING DIAMETERS		
Top Slab Outside Face (AS7)	.4 in.	
Bottom Slab Outside Face (AS8)	.4 in.	
Sidewall Outside Face (AS1)	.4 in.	
Top Slab Inside Face (AS2)	.4 in.	
Bottom Slab Inside face (AS3)	.4 in.	
Sidewall Inside Face (AS4)	.4 in.	
MAXIMUM REINFORCING SPACING		
Top Slab Outside Face (AS7)	8 in.	
Bottom Slab Outside Face (AS8)	8 in.	
Sidewall Outside Face (AS1)	8 in.	
Top Slab Inside Face (AS2)	8 in.	
Bottom Slab Inside Face (AS3)	8 in.	
Sidewall Inside Face (AS4)	8 in.	
SOIL LOAD DATA		
Soil Density	120 pcf	
Minimum Lateral Pressure Coefficient	.25	
Maximum Lateral Pressure Coefficient	.5	
Soil Structure Interaction Factor	1	
LIVE LOAD DATA		
Live Load	HS-20	
Direction of Travel	Transverse to culvert flow	
SURCHARGE LOADS		
UNIFORM VERTICAL LOAD		
Magnitude	0 psf	
VARYING LATERAL LOAD		
Magnitude at Top	0 psf	
Magnitude at Bottom	0 psf	
APPLICATION CODE	PERMANENT DEAD LOAD	
FLUID LOADS		
Depth of Fluid	5 ft.	
Fluid Density	62.5 pcf	

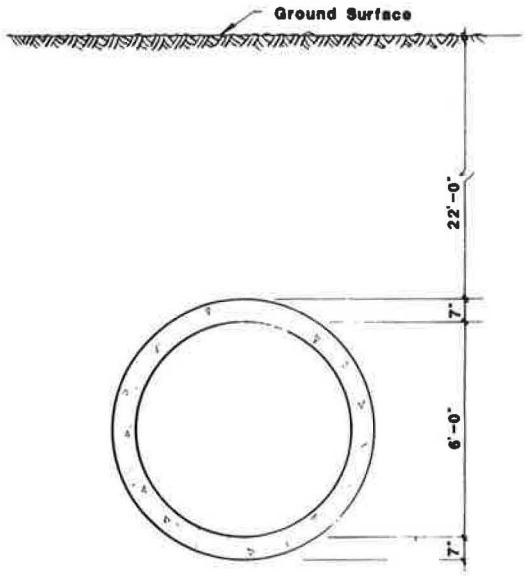

FIGURE 7 Pipe geometry for PIPECAR sample problem.

CONCLUSIONS

Summarized in this paper are the current levels of development of the computer programs PIPECAR and BOXCAR for the structural design and analysis of reinforced concrete pipe and box sections, respectively. The current microcomputer versions of these programs, which were developed for FHWA, are easy to access and operate. With the various live load options that may now be specified by the user, these programs allow users to structurally design reinforced concrete pipe or single-cell rectangular box culverts for almost any given installation condition.

ACKNOWLEDGMENTS

The authors are indebted to Philip Thompson and Thomas Krylowski of FHWA and John Kurdziel of the American Concrete Pipe Association for their support and assistance. The authors also wish to thank cooperative students John E. Moalli and Michael J. Mullaney for the valuable contributions they have made throughout this project.

TABLE 3 DESIGN SUMMARY SHEET FOR BOXCAR SAMPLE PROBLEM

BOX CULVERT DESIGN SUMMARY SHEET
8.0 FT. SPAN X 5.0 FT. RISE

****

INSTALLATION DATA

HEIGHT OF FILL OVER CULVERT, FT	3.000
SOIL UNIT WEIGHT , PCF	120.000
MINIMUM LATERAL SOIL PRESSURE COEFFICIENT	.250
MAXIMUM LATERAL SOIL PRESSURE COEFFICIENT	.500
SOIL - STRUCTURE INTERACTION COEFFICIENT	1.000

LOADING DATA

DEAD LOAD FACTOR - MOMENT AND SHEAR	1.500
DEAD LOAD FACTOR - THRUST	1.000
LIVE LOAD FACTOR - MOMENT AND SHEAR	2.170
LIVE LOAD FACTOR - THRUST	1.000
STRENGTH REDUCTION FACTOR-FLEXURE	.900
STRENGTH REDUCTION FACTOR-DIAGONAL TENSION	.850
LIVE LOAD TYPE	AASHTO HS-20
DIRECTION OF VEHICLE TRAVEL RELATIVE TO CULVERT FLOW	TRANSVERSE

MATERIAL PROPERTIES

MINIMUM SPECIFIED REINFORCING YIELD STRESS, KSI	60.000
CONCRETE - SPECIFIED COMPRESSIVE STRENGTH, KSI	4.000
REINFORCING TYPE	SMOOTH WELDED WIRE FABRIC

GEOMETRY

TOP SLAB THICKNESS, IN.	8.000
SIDE WALL THICKNESS, IN.	8.000
BOTTOM SLAB THICKNESS,IN.	8.000
HORIZONTAL HAUNCH DIMENSION, IN.	8.000
VERTICAL HAUNCH DIMENSION, IN.	8.000
CONCRETE COVER OVER STEEL, IN.	
TOP SLAB-OUTSIDE FACE	1.500
SIDE WALL - OUTSIDE FACE	1.500
BOTTOM SLAB - OUTSIDE FACE	1.500
TOP SLAB - INSIDE FACE	1.500
SIDE WALL - INSIDE FACE	1.500
BOTTOM SLAB - INSIDE FACE	1.500

REINFORCING STEEL DAT A

LOCATION		AREA SQ. IN PER FT	STIRRUPS REQUIRED
TRANSVERSE			
SIDE WALL	- OUTSIDE FACE (As1)	.233	NO
TOP SLAB	- INSIDE FACE (As2)	.316	NO
BOTTOM SLAB	- INSIDE FACE (As3)	.291	NO
SIDE WALL	- INSIDE FACE (As4)	.192	NO
TOP SLAB	- OUTSIDE FACE (As7)	.192	NO
BOTTOM SLAB	- OUTSIDE FACE (As8)	.192	NO

TOP SLAB OUTSIDE FACE STEEL MUST EXTEND COMPLETELY ACROSS THE TOP SLAB.
SIDEWALL OUTSIDE FACE STEEL (As1) MUST BE BENT AT THE CORNER AND EXTENDED ACROSS THE TOP SLAB SUFFICIENTLY TO MEET AASHTO REQUIREMENTS FOR TENSION LAPS.

BOTTOM SLAB OUTSIDE FACE STEEL (As8) MUST EXTEND COMPLETELY ACROSS THE BOTTOM SLAB .
SIDEWALL OUTSIDE FACE STEEL (As1) MUST BE BENT AT THE CORNER AND EXTENDED ACROSS THE BOTTOM SLAB SUFFICIENTLY TO MEET AASHTO REQUIREMENTS FOR TENSION LAPS.

TABLE 4 DESIGN SUMMARY SHEET FOR PIPECAR SAMPLE PROBLEM

PIPECAR PIPE CULVERT DESIGN SUMMARY
72.0 INCH DIAMETER REINFORCED CONCRETE CIRCULAR PIPE

****

INSTALLATION DATA

WEIGHT OF FILL ABOVE CROWN, FT.	22.00
SOIL UNIT WEIGHT , PCF	120.00
SOIL STRUCTURE INTERACTION COEFFICIENT	1.20
LOAD SYSTEM	RADIAL LOAD SYSTEM
LOAD ANGLE DEGREES	240.00
BEDDING ANGLE, DEGREES	120.00
PIPE WEIGHT REACTION BED LENGTH, IN.	.00

MATERIAL PROPERTIES

REINFORCING - MINIMUM SPECIFIED YIELD STRESS, KSI	65.00
REINFORCING TYPE	SMOOTH WELDED WIRE FABRIC
NO. OF LAYERS OF REINFORCING	1.00
CONCRETE - SPECIFIED COMPRESSIVE STRESS, KSI	5.00

LOADING DATA

DEAD LOAD FACTORS - MOMENTS AND SHEAR	1.50
DEAD LOAD FACTOR - THRUST	1.00
LIVE LOAD FACTORS - MOMENT AND SHEAR	2.17
LIVE LOAD FACTOR - THRUST	1.00
STRENGTH REDUCTION FACTOR - FLEXURE	.95
STRENGTH REDUCTION FACTOR - DIAGONAL TENSION	.90
LIMITING CRACK WIDTH FACTOR	.90
RADIAL TENSION PROCESS FACTOR	1.00
DIAGONAL TENSION PROCESS FACTOR	1.00
LIVE LOAD TYPE	AASHTO HS-20

PIPE DATA

WALL THICKNESS, IN.	7.00
INSIDE CONCRETE COVER OVER REINFORCING, IN.	1.00
OUTSIDE CONCRETE COVER OVER REINFORCING, IN.	1.00

FLUID DA TA

WALL THICKNESS, PCF.	62.40
DEPTH OF FLUID, INCHES ABOVE INVERT	72.00

REINFORCING DATA

INVERT - INSIDE REINFORCING, SQ. IN /FT.	.532
SPRINGLINE - OUTSIDE REINFORCING, SQ. IN./ FT.	.345
CROWN - INSIDE REINFORCING, SQ. IN. / FT.	.293

REFERENCES

1. T. J. McGrath and F. J. Heger. *Structural Design Manual for Improved Inlets and Culverts*. Report IP-83-6, FHWA, U.S. Department of Transportation, June 1983.
2. F. J. Heger and T. J. McGrath. *Design Method for Reinforced Concrete Pipe and Box Sections*. A report by Simpson, Gumpertz & Heger, Inc. for the American Concrete Pipe Association, Dec. 1982.
3. *Standard Specifications for Highway Bridges*. Section 17.4, American Association of State Highway and Transportation Officials, Washington, D.C., 1989.

Publication of this paper sponsored by Committee on Culverts and Hydraulic Structures.

Life-Cycle Cost for Design of Army Drainage Structures

JOHN C. POTTER AND LARRY SCHINDLER

Many factors are involved in the design of drainage systems. Although not necessarily overriding, the cost is often one of the most important factors. This cost should be the total, overall cost of the alternative over its projected life, or life-cycle cost. Unless the life-cycle cost is considered over first cost, the owner cannot be assured of receiving maximum value for his construction and maintenance dollars. The importance of the other decision factors are established for Army projects by the minimum functional requirements of the project. Except for determining a service life for the various types (materials) of drainage structures, the procedures for life-cycle cost analysis of such studies are well established. The procedures for economic analysis described in U.S. Army Technical Manual TM 5-802-1 can be used to determine life-cycle cost. U.S Army regulation *Economic Analysis and Program Evaluation for Resource Management* gives the basic criteria and standards for economic studies by and for the Department of the Army. Provided in this paper is the supplemental explanation required to perform life-cycle cost analyses of drainage structures to determine the relative economic rating of design alternatives. The alternatives can then be order ranked by life-cycle cost, and the best design can be rationally and confidently selected.

Many factors are involved in the design of drainage systems. Principal factors are hydrology, soil conditions, material strength, material durability, and cost and type of facility or site being drained. Although not necessarily overriding, the cost is often one of the most important factors. This cost should be the total, overall cost of the alternative over its projected life, or life-cycle cost (LCC). Unless the LCC is considered over first cost, the owner cannot be assured of receiving maximum value for his construction and maintenance dollars. LCC-based economic studies are an integral part of the complete design process and are a requirement specified by Army Technical Manual (TM) 5-802-1(*1*). Department of the Army Regulation (AR) 11-28 *Economic Analysis and Program Evaluation for Resource Management* (*2*) gives the basic criteria and standards for economic studies by and for the Department of the Army. This paper provides the supplemental explanation required to perform LCC analyses of drainage structures to determine the relative economic rating of design alternatives.

J. C. Potter, U.S. Army Corps of Engineers, Waterways Experiment Station, P.O. Box 631, Vicksburg, Miss. 39180-0631. L. Schindler, Headquarters, U.S. Army Corps of Engineers, HQUSACE(CEEC-EG), Washington, D.C. 20314-1000.

GENERAL

The first step in the analysis of design alternatives is to develop a preliminary list of all possible alternatives. This list is then reduced to a group of feasible alternatives by applying the constraints of the particular project, such as availability of materials or equipment, site conditions (e.g., abrasive bed load), or requirements to accommodate large flows or livestock. In other words, the minimum functional requirements must be met. The final design is chosen from this group based on the LCC.

The LCC is the total, overall estimated cost for a particular design alternative. Direct and indirect initial costs plus periodic or continuing costs for operation and maintenance are included. The methods described in TM 5-802-1(*1*) and mentioned subsequently in this paper account for the time value of money and reflect the concepts and procedures used in many economics texts [e.g., Thuesen et al. (*3*)].

Costs incurred over time may be expressed in terms of either constant dollars or current dollars. Constant dollars are costs or savings stated at price levels in effect at some given time, usually the particular time that the analysis is conducted. Current dollars are costs or savings stated at price levels in effect whenever the costs or savings are incurred. Comparison of drainage structure alternatives should be based on constant dollars for all costs, including present and future costs and salvage or retention-residual values.

The LCC is expressed either in terms of present worth (PW) or equivalent uniform annual cost (EUAC). PW is the more common measure of LCCs. It can be thought of as the amount of money, required now, to fund the project for the entire analysis period. The EUAC can be thought of as the amount of money required for each year of the analysis period to fund all project costs.

The same analysis period must be used to compare alternatives using PWs. PWs can be converted to EUACs using a uniform series capital recovery factor. In essence, PW and EUAC are just two ways of expressing the same costs. EUACs can also be calculated from the individual costs for each alternative.

ANALYSIS PERIOD

Economic studies consider projects that have a service life, an economic life, and an analysis period. The service life is the total useful life of the project or time to replacement or rehabilitation. The economic life is the time during which a project is economically profitable or provides the required

service at a lower cost than another facility. For drainage structures, the economic life is usually the same as the service life. The analysis period is the comparison period over which costs are counted in determining the PW or EUAC of an alternative.

The provisions of TM 5-802-1(*1*) on the selection of the analysis period are based on the fact that the Department of Defense (DOD) envisions the economic life of most types of facilities, as well as most major facilities' components and utilities, to be about 25 years for general planning purposes. This is also known as the planning horizon. Accordingly, TM 5-802-1(*1*) specifies that, in general, the analysis period should be considered to end at the end of the economic life of the total facility, or 25 years after the beneficial occupancy date (BOD), whichever occurs first. (In the case of drainage structures, the total facility would be the complete facility or set of facilities encompassing and serviced by the drainage structures.) There are provisions for exceptions to the 25-year limit, however, and it would appear that many, if not most, drainage structure projects would qualify for the exception. The justification for the exception in the case of drainage structures is that infrastructure such as drainage facilities may realistically be expected to provide economical service in its original mission well beyond 25 years. A review of the service lives used by various state and federal government agencies and industry (*4*, *5*) reveals that most agencies expect culverts to provide service longer than 25 years, with a 50-year life used most frequently. This period strikes a balance between the intangible or indirect costs associated with replacement or rehabilitation and the unpredictability of long-term land use. Accordingly, a 50-year analysis period appears to be reasonable and justifiable and should be used. Note that the selection of the analysis period is not influenced by the expected service lives of the design alternatives.

COST

The initial and recurring costs considered in an economic analysis are sometimes categorized as agency costs, user costs, and nonuser costs (*6*). Agency costs include initial capital costs of construction; future capital costs of rehabilitation or replacement; maintenance or operational costs, or both, during the analysis period; salvage or retention-residual value (a negative cost) at the end of the analysis period; and engineering and administrative costs. User costs include travel time, vehicle operating costs, and accident costs and inconvenience (e.g., when a detour is required). Nonuser costs result from the impact of the facility on those not actually using the facility, such as the cost of flood damage occurring downstream from the drainage structure.

Economic analyses frequently include only the initial and future capital costs, maintenance and operation costs, and salvage or retention-residual value. For drainage structures, little error is introduced by omitting the other costs from the computations because the other costs are likely to be similar for all alternatives.

Initial capital costs for drainage structures can generally be estimated from local data, usually obtainable from local vendors. Future capital costs can be estimated from current costs, adjusted as necessary for extraordinary price level changes expected before future construction. As a supplement, or if local data are not available, costs can be estimated using the procedures, unit costs, and adjustment factors given in the following publications:

1. Army Regulation 415-17(*7*),
2. *Engineering News Record*'s Building and Construction Cost Index Histories (*8*),
3. Federal Highway Administration's Highway Maintenance and Operation Cost Trend Index (*9*), and
4. Federal Highway Administration's Price Trends for Federal-Aid Highway Construction (*10*).

A description of these resources and their use is included in Kohn et al.(*11*).

Maintenance and operations costs are best determined from local experience with similar projects. Maintenance and operations costs are highly dependent on both local conditions and the particular maintaining agency.

The salvage or retention-residual value of a drainage structure is its residual value at the end of the analysis period. If the end of the analysis period coincides with the end of the service of the alternative, then the salvage value of that alternative should be taken as zero. When the service life is expected to exceed the length of the analysis period, the retention-residual value must be included, generally as a future income or negative cost.

DISCOUNT RATE

The time value of money is expressed by the discount rate. The discount rate can be viewed as the amount that the value of money in the future is reduced or discounted to reflect its present value. It is considered to be the minimum real or net rate of return, after inflation, to be achieved by public sector investments. Congress has stipulated that diverting investment capital from the private sector (by taxation) for use on public-sector projects can only be justified when that capital earns a real rate of return at least as high as that achievable in the private sector. This rate is 10 percent at the present time (January 1988) (*12*).

COMPUTING PW

The basic method for computing the PW of a given alternative is described in detail in TM 5-802-1(*1*) and summarized here, as follows:

One-Time Costs

Step 1: Estimate the amount of the one-time costs as of the base date (date of the study).
Step 2: Escalate this cost to the time at which it is actually to be incurred, using the differential (from inflation) escalation rate e.
Step 3: Discount the escalated future one-time cost to PW (on the base date), using the discount rate d (10 percent in January 1988).

Recurring Costs

Step 1: Estimate the amount A_o of the annually recurring cost as of the base date and determine the number of costs, k, in the series (i.e., over the analysis period).
Step 2: Escalate A_o to A_i at the time at which the first cost in the series is to be incurred, using the differential escalation rate e.
Step 3: Determine, for the date on which A_i is incurred, the single cost that is equivalent to a series of, k, uniformly escalating annual costs, in which the amount of the first cost is A_i and the differential escalation rate is e.
Step 4: Discount the single equivalent cost, from the time the first annual cost is to be incurred to a PW on the base date, using the discount rate d.

Escalation of any current cost C to a future cost F is accomplished using the relationship

$$F = C\,(1 + e)^n$$

where e is the escalation rate above the rate of inflation and n is the number of years until the future cost is incurred.

The PW P of a future cost F is

$$P = F\,(1/1 + i)^n$$

where i is the discount or net interest rate after inflation. Formulas, tables, and sample calculations are provided in Technical Manual 5-802-1 (*1*).

DECISION CRITERIA

If, in the judgment of the designer or analyst, it is reasonably certain from the results of the LCC analysis that one particular type of drainage structure (material) will have a lower LCC than any of the other feasible alternatives on a certain project, then that type of drainage structure should be selected for the project in question. If, on the other hand, it is clear from the results of the analysis that two (or more) of the alternatives will have equal (or very nearly equal) LCCs (and that the LCCs of all the other feasible alternatives will be greater), then the design selection should be based essentially on initial procurement cost considerations. That is, the particular type of drainage structure with the lowest procurement costs should be selected.

For other situations, when one cannot be reasonably certain from the results of the analysis whether one of the alternatives will be lower in LCC than one (or more) of the other alternatives, it may be necessary to conduct an uncertainty analysis to support the design-selection decision or to allow multiple bid options. The exact criteria are beyond the scope of this paper, but are described in detail in TM 5-802-1 (*1*).

EXAMPLE

Suppose a drainage structure is being selected for construction 2 years after the analysis base data (date of study). The soil-water pH is 6.0, the minimum soil-water resistivity is 6,000 ohm-cm, and a nonabrasive flow of 6 ft/sec is expected. The materials to be considered are reinforced concrete, plain galvanized steel pipe, asphalt-coated and paved corrugated steel pipe (ACPCSP), and polyethylene (PE) pipe. All of these alternatives are structurally adequate for the design load. A 24-in.-diameter, smooth wall pipe will carry the design flow at the design slope of 1 percent. A 27-in.-diameter pipe will be required for the corrugated alternative because of its higher n value. The differential escalation rate is projected to be 0 for installation costs and for the concrete and plain galvanized materials. For illustrative purposes, a rate of 3 percent will be assumed for the asphalt-coated and paved and PE pipes, as their cost is closely tied to the cost of petroleum. Assume that an exception will be granted to allow a 50-year analysis period, that maintenance costs over the analysis period are equal for all alternatives, and that pipe still serviceable at the end of the analysis period will not be recovered for reuse or resale (no salvage value). Uncertainty assessment is omitted for simplicity. Note that costs stated herein are hypothetical costs—they do not apply to any particular project, and are not to be used for an actual LCC analysis.

Suppose the expected service life of reinforced concrete pipe is 100 years. It should therefore last through the entire analysis period. The current cost is \$12.50/ft, delivered, plus \$10.00/ft for installation. Because $e = 0$ percent for both materials and installation, the one-time cost to be incurred in 2 years is simply \$12.50 + \$10.00 = \$22.50, in terms of today's dollars. The PW is \$22.50 $(1/1.1)^2$ = \$18.59/ft.

The California method (*13*) can be used to estimate the service life of the plain galvanized pipe. For a pH of 6.0 and a minimum resistivity of 6,000 ohm-cm, a 16-gauge, plain galvanized corrugated steel pipe (CSP) has an expected life of about 25 years. This alternative will require a replacement at the midpoint of the analysis period. The current cost of 27-in. plain galvanized pipe is \$10.65/ft, delivered, including bands, plus \$8.50/ft installation. In many cases the cost of replacement is much greater than the cost of initial construction, especially considering user costs. However, to simplify this example, assume that the current cost applies to both initial construction and replacement. Because $e = 0$ percent for both materials and installation, the cost to be incurred in 2 years and again in 27 years is \$10.65 + \$8.50 = \$19.15/ft. The PW of the initial installation is \$19.15 $(1/1.1)^2$ = \$15.82/ft. The PW of the replacement is \$19.15 $(1/1.1)^{27}$ = \$1.46/ft. The total PW for this alternative is thus \$15.82 + \$1.46 = \$17.28/ft. All these are expressed in terms of today's dollars.

Asphalt coating and paving can be used to extend the life of plain galvanized pipe. Assume that this coating will add 25 years to the life of the pipe. The service life of an asphalt-coated and paved CSP (ACPCSP) at this site will be 25 years + 25 years = 50 years, and no replacement is anticipated during the analysis period. The current cost for ACPCSP is \$13.90/ft, including bands. Assuming a 3 percent annual differential escalation rate for the cost of the asphalt, the pipe will cost \$13.90 × $(1.03)^2$ = \$14.75/ft at the time of installation. Installation is currently \$9.50/ft. Assuming $e = 0$ percent for installation cost, this cost will remain at \$9.50/ft. The total cost of this alternative will thus be \$14.75 + \$9.50 = \$24.25/ft. The PW is \$24.25$(1/1.1)^2$ = \$20.04/ft.

The proposed American Association of State Highway and Transportation Officials design procedure is structured to provide a 50-year service life. One 24-in. smooth-flow PE pipe

meeting the requirements of this procedure costs \$19.50/ft. An escalation of 3 percent for 2 years yields a cost at time of installation of \$19.50 × $(1.03)^2$ = \$20.69/ft. Installation is and will be (e = 0 percent) \$8.00/ft. At the time of installation, the total cost will be \$20.69 + 8.00 = \$28.69/ft. The PW is \$28.69 × (1/1.1)2 = \$23.71/ft.

The life cycle of these alternatives is summarized in Table 1. In this example, plain galvanized CSP would be chosen for its lowest LCC. If two or three alternatives are to be selected as bid options, the CSP and RCP or CSP, RCP, and ACPCSP would be considered.

SUMMARY

The LCC of drainage structures can be determined in accordance with the provisions of TM 5-802-1(*1*). Because of the nature of drainage structures, an analysis period greater than 25 years may be justified. However, the salvage or retention-residual value beyond the end of the analysis period is 0, except in special cases such as those where the structure will be recovered for reuse or resale. The alternatives are order ranked by LCC, and the alternative with the lowest LCC is selected. The treatment of uncertainty in the input data and the exact criteria to be used in the selection process, when the results of the LCC analysis are not conclusive, are described in detail in TM 5-802-1 (*1*).

CONCLUSIONS

The LCC of a drainage structure design alternative is the estimated, total cost of that design. Except for determining a service life for the various types (materials) of drainage structures, the procedures for LCC cost analysis of such studies are well established. The procedures for economic analysis described in TM 5-802-1 (*1*) can be used to determine LCC. Although the LCC is only one of the decision factors used to select the preferred design alternative from among the feasible alternatives, it is generally the most important. The importance of the other decision factors are established by the minimum functional requirements of the project. The alternatives can then be order ranked by LCC, and the best design can be rationally and confidently selected.

ACKNOWLEDGMENT

The authors are grateful to the U.S. Army Corps of Engineer Waterways Experiment Station for administrative support as well as permission to publish this paper. The views of the authors do not purport to reflect the position of the Department of the Army or the U. S. Department of Defense.

TABLE 1 EXAMPLE LIFE-CYCLE COSTS

Cost (\$)	24-in. RCP	27-in. CSP 1st	27-in. CSP 2nd	27-in. CSP Total	24-in. ACPCSP	24-in. PE
Current material	12.50	10.65	10.65		13.90	19.50
Installation (e = 0)	10.00	8.50	8.50		9.50	8.00
Escalated material	12.50	10.65	10.65		14.75	20.69
PW material	10.33	8.80	0.81	9.61	12.19	17.10
PW installation	8.26	7.02	0.65	7.67	7.85	6.61
Total PW	18.59			17.28	20.04	23.71

REFERENCES

1. *Economic Studies for Military Construction Design—Application*. TM 5-802-1, Headquarters, Department of the Army, Washington, D.C., Dec. 31, 1986.
2. *Economic Analysis and Program Evaluation for Resource Management*. AR 11-28, Headquarters, Department of the Army, Washington, D.C., Dec. 2, 1975.
3. H. G. Thuesen, W. J. Fabrycky, and G. J. Thuesen. *Engineering Economy*, 4th ed. Prentice-Hall, Inc., Englewood Cliffs, N.J., 1971.
4. W. W. Renfro and R. M. Pyskadlo. *National Survey of State Culvert Use and Policies*. New York Department of Transportation Special Report G8, Albany, N.Y., 1980.
5. T. J. Summerson. Corrosion Resistance of Aluminum Drainage Products: The First 25 Years. Symposium on Durability of Culverts and Storm Drains. In *Transportation Research Record 1001*, TRB, National Research Council, Washington, D.C., 1984, pp. 77–87.
6. R. Hass and W. R. Hudson. *Pavement Management Systems*. McGraw-Hill, Inc., New York, N.Y., 1978.
7. *Construction-Cost Estimating for Military Programming*. AR 415-17, Headquarters, Department of the Army, Washington, D.C., Feb. 15, 1980.
8. Building Cost Index History and Construction Cost Index History. *Engineering News Record*, McGraw-Hill, Inc., New York, N.Y., 1987.
9. *Highway Maintenance and Operation Cost Index*. Federal Highway Administration, U.S. Department of Transportation, 1987.
10. *Price Trends for Federal-Aid Highway Construction*. Federal Highway Administration, U. S. Department of Transportation, 1987.
11. S. D. Kohn, J. A. Epps, and T. B. Rosser. *Analysis Procedures for Pavement Life-Cycle Cost*. U.S. Army Engineers Waterways Experiment Station, Vicksburg, Miss., 1987.
12. *Circular A-94*. Executive Office of the President, Office of Management and Budget, Washington, D.C., March 27, 1972.
13. *California Test Method for Estimating Service Life of Metal Culverts*. Test Method California 643-C, California Department of Transportation, Sacramento, Calif., 1972.

DISCUSSION

MIKE BEALEY
American Concrete Pipe Association, 8320 Old Courthouse Road, Vienna, Va. 22180.

The authors have prepared an excellent summary of LCC analysis. However, there are serious errors in application. Potter and Schindler erroneously cite Office of Management and Budget (OMB) Circular *A*-94, dated March 27, 1972 (*12*), as the authority necessitating the use of a high real discount rate of 10 percent to evaluate alternate materials for a construction project. In *A*-94, the purpose is stated as follows: "This Circular prescribes a standard discount rate to be used in evaluating the measurable costs and/or benefits of programs or projects when they are distributed over time."

The scope of *A*-94 is specific on discount rate use:

3. Scope

a. This Circular applies to all agencies of the executive branch of the Federal Government except the U.S. Postal Service. The discount rate prescribed in this Circular applies to the evaluation of Government decisions concerning the initiation, renewal, or expansion of all programs or projects, other than those specifically exempted below, for which the adoption is expected to commit the Government to a series of measurable costs extending over three or more years or which result in a series of benefits that extend three or more years beyond the inception date.

b. Specifically exempted from the scope of this Circular are decisions concerning water resource projects (guidance for which is the approved Water Resources Principles and Standards), the Government of the District of Columbia, and non-Federal recipients of Federal loans or grants.

c. The remaining exemptions derive from the secondary nature of the decisions involved; that is, how to acquire assets or proceed with a program after an affirmative decision to initiate, renew, or expand such a program using this Circular. Thus:

(1) This Circular would not apply to the evaluation of decisions concerning how to obtain the use of real property, such as by lease or purchase.

(2) This Circular would not apply to the evaluation of decisions concerning the acquisition of commercial-type services by Government or contractor operation, guidance for which is OMB Circular *A*-76.

(3) This Circular would not apply to the evaluation of decisions concerning how to select automatic data processing equipment, guidance for which is OMB Circular *A*-54 and OMB Bulletin 60-6.

d. The discount rates prescribed in this Circular are:

(1) Suggested for use in the internal planning documents of the agencies in the executive branch;

(2) Required for use in program analyses submitted to the OMB in support of legislative and budget programs.

In other words, *A*-94 is required to be used in the evaluation of cost-benefit for projects submitted to OMB for approval to determine whether it is beneficial to finance the project with tax dollars rather than private investment. The high discount rate, then, is intended to ensure that the government does not undertake projects that can be even marginally profitable when undertaken by private investment.

After a project is approved by OMB, secondary decisions as to how to proceed with the project are exempt from the requirements of *A*-94 (i.e., the materials to be used).

The evaluation of alternate materials for a project should use realistic inflation and interest rates. There is no company that will guarantee to do a job 25 years, 50 years, or even 2 years in the future for the same price that they would charge today without a government subsidy.

Projecting long-term costs and discount rates requires evaluation of historical records. In "Taking the Guesswork Out of Least-Cost Analysis" (*1*), W. O. Kerr and B. A. Ryan examine the long-term relationships of rates and indices. Kerr and Ryan show that although wide swings occurred in interest and inflation rates, the overall average differential between the rates was relatively stable, and recommend that evaluation of construction projects be based on historical averages of the differential (real discount rate) between the producer price index and treasury bill rate for federal projects, municipal bond rate for state and local projects, and prime rate for private projects.

The future current cost and PW equations can be combined: $P = [(1 + I)/(1 + i)]^n$. Where I is the inflation rate, or escalation rate defined by Potter and Schindler. Kerr and Ryan define the term $[(1 + I)/(1 + i)]$ as the interest-inflation (i/I) factor, which is virtually constant for any specific difference between interest and inflation rates regardless of the absolute values of the rates. Because market factors work to maintain a constant i/I differential, selecting a differential and using the appropriate i/I factor frees the engineer from errors related to short-term volatility of forecasts of absolute rates. Kerr and Ryan show that the average differential between treasury bill rates and the producer price index was 1.66 percent for the years 1954–1983, and the average i/I factor was 0.9853. A differential of 1.66 percent is a more realistic real discount rate for evaluating construction bids by private companies on federal projects than the 10 percent used by Potter and Schindler. Recalculating the example (where RCP = reinforced concrete pipe, CSP = corrugated steel pipe, ACPCSP = asphalt-coated and paved corrugated steel pipe, PE = PE pipe, and PW = PW) using the Kerr and Ryan recommended i/I factor, the results of the same costs as selected by Potter and Schindler, and an escalation factor of 0 for all costs results in:

Cost ($)	*24-in. RCP*	*27-in. CSP*	*24-in. ACPCSP*	*24-in. PE*
PW material	12.14	17.48	13.49	18.93
PW installation	9.71	13.95	9.22	7.77
Total PW	21.85	31.43	22.71	26.70

The cost ranking of the alternates stays the same except for CSP, which moves from lowest to highest PW. This result indicates the sensitivity of LCC analysis to the real discount rate and the importance of using a realistic differential. With a high differential, LCC analysis will always indicate that it is best to use the cheapest possible material and replace it often during the project design life.

Flexible pipe deflects, cannot carry load directly, and relies on surrounding soil to carry loads. Rigid pipe is designed to carry loads without any load transfer into surrounding soil. The more flexible a pipe, the more care, compaction, and select material is required for embedment to ensure that the surrounding soil can carry the load to prevent pipe deflections. The installation costs selected by Potter and Schindler are exactly opposite and indicate that as pipe becomes more flexible, it becomes cheaper to install.

Potter and Schindler selected the same cost for the CSP replacement as for the original installation. Pipe replacement costs are always higher than the original installation because of additional costs associated with removing the installation, traffic, safety procedures, and so on.

The California method for estimating the years to perforation of CSP is applied to the exterior and interior separately and perforation life determined by considering corrosion can proceed from both sides simultaneously. In the example, this

would reduce the service life of CSP to about 13 years. According to the Federal Highway Administration's "Evaluation of Highway Culvert Coating Performance" (*2*), six states discontinued the use of asphalt coatings because it was found to provide insufficient increase in service life to justify the cost. The long service lives selected by Potter and Schindler for CSP and asphalt-coated and paved corrugated steel pipe (ACPCSP) are questionable.

Recalculating the example with realistic service lives and costs would reorder the pipe priorities.

REFERENCES

1. W. O. Kerr and B. A. Ryan. Taking the Guesswork Out of Least-Cost Analysis. *Consulting Engineer*, March, 1986.
2. *Evaluation of Highway Culvert Coating Performance*. Federal Highway Administration, U.S. Department of Transportation, 1980.

AUTHORS' CLOSURE

The discussant takes issue with the authors' use of a 10 percent real discount rate, based on the provisions of Office of Management and Budget (OMB) Circular *A*-94 (*12*), in conducting LCC analyses for design of Army drainage structures. Bealey's discussion consists in essence of three main points:

1. Materials selection for Army drainage structures is an LCC application area exempt from the provisions of OMB Circular *A*-94 (or, more simply, *A*-94), and so *A*-94 should not have been cited as the authority necessitating the use of the 10 percent discount rate;
2. The 10 percent discount rate should not have been used because its use is not mandated by *A*-94 for applications such as this (a point strongly implied, if not explicitly stated); and
3. A more realistic discount rate of 1.66 percent should have been used (instead of the 10 percent rate).

The authors take exception to all of these points, and will address each of them in turn.

Point 1. Bealey appears to have missed the point here. The authors never did, in fact, state that the LCC analysis of Army drainage structures was subject to the requirements of *A*-94, or that the 10 percent discount rate was mandated by *A*-94 for such applications. In our discussion of discount rate, we stated that "Congress has stipulated that diverting investment capital from the private sector (by taxation) for use on public sector projects can only be justified when that capital earns a real rate of return at least as high as that achievable in the private sector," and that "this rate is 10 percent at the present time," with a reference to *A*-94. That rationale is clearly valid regardless of whether or not the analysis is exempt from the provisions of *A*-94.

Point 2. We do not agree with Bealey on this point. Our position was—and remains—that the 10 percent real discount rate was the appropriate rate to use, even if its use is not mandated by *A*-94 in connection with LCC analyses for design of Army drainage structures. The basis for that position was clearly presented in the paper (although it appears that Bealey misinterpreted it). A point we did not make explicitly in the paper, but clearly should have, is that the 10 percent discount rate was the appropriate rate to use in any case. Its use is mandated by the provisions of the Army criteria documents cited in the background section of the paper—Army Regulation (AR) 11-28 (Economic Analysis and Program Evaluation for Resource Management) and Army Technical Manual (TM) 5-802-1 (Economic Studies for Military Construction Design—Applications). Although it could be argued that LCC analyses for design of Army drainage structures are exempt from the provisions of *A*-94 (as Bealey does), and perhaps even from the provisions of AR 11-28 (although this would be more difficult to argue), such analyses are certainly not exempt from the provisions of TM 5-802-1. That document establishes the governing criteria and standards for the conduct of all LCC analyses by and for the Department of the Army in connection with the design of facilities in the military construction program.

Point 3. Although we do not take issue with the fine work of Kerr and Ryan—cited by Bealey as the basis for his assertion that we should have used a real discount rate of 1.66 percent for the analysis—we do not agree that the results of the Kerr and Ryan effort are applicable here (i.e., to the conduct of LCC analyses in support of the design of Army facilities).

In conducting an LCC analysis in support of the design of an Army facility, the designer-analyst is deciding whether it would be more economical, on a total cost-of-ownership basis, to select Alternative *A*—the design alternative that is least expensive in terms of cost to purchase-construct initially—or Alternative *B*—a more expensive design alternative, which will cost less to operate, maintain, and repair over its design life. If Alternative *A* is selected (instead of Alternative *B*), the taxpayer will have to pay less taxes for the year(s) in which the facility is constructed, but will have to pay more taxes for the years that the facility is in use. If Alternative *B* is selected, the reverse will be true. It appears to us, therefore, that—on a conceptual level—the role of the government in this decision process is that of an investor of capital (on behalf of the taxpayer).

The position of the Joint Economic Committee of the Congress' Subcommittee on Economy in Government (Subcommittee on Economy in Government, 1968) is that it is the opportunity cost of displaced private spending—and not the cost to the U.S. Treasury of borrowing—that should serve as the basis for defining the discount rate to be used in public-sector economic analyses. The subcommittee states specifically in the preceding reference that "no public investment be deemed 'economic' or 'efficient' if it fails to yield overall benefits which are at least as great as those which the same resources would have produced if left in the private sector." In a classic work, Stockfisch (*1*) has shown that a real discount rate of 10 percent is the appropriate rate of return to use in this regard.

The 1.66 percent real discount rate recommended by Bealey is calculated from a nominal discount rate that is tied directly to the "treasury bill rate for federal projects" (according to Bealey) (i.e., to the government's cost of borrowing). The Subcommittee on Economy in Government specifically rejects this approach in no uncertain terms (*2*). The subcommittee states specifically in the preceding reference: "In past discussions within the Government . . . an interest rate equal to the cost to the Federal Government of borrowing has been

supported . . . Implicit in this position is the presumption that the Government is an independent organization which should seek the greatest differential between its revenues and outlays as does a private business. The subcommittee rejects this view of the Federal Government when it functions as an investor of capital."

Accordingly, in our view, the 10 percent real discount rate actually used in the analysis is the appropriate one to use, and the 1.66 percent rate urged by Bealey is not appropriate.

As for installation costs, more care, compaction, and select material is required for proper installation of flexible pipes. However, the Corps of Engineers has tailored their compaction specifications to allow the widest possible selection in, and therefore economy of, backfill material. Also, the reduced wall thickness of flexible pipes allows for smaller excavation quantities, lighter pipe sections allow use of less expensive lifting and loading equipment, and longer pipe sections result in less labor for jointing. Rigid pipe may or may not be less expensive to install than flexible pipes. The correct installation costs to use in LCC analyses are those used by local contractors to bid each alternative.

Culvert replacement can be cheaper than initial construction. Detour, delay, and resurfacing costs are insignificant for unsurfaced, tertiary roads, and labor costs may be borne by separately funded maintenance forces, not subject to contract-administration overhead.

The California method is based on actual field performance. Corrosion from both sides is therefore considered, although corrosion from the more aggressive side usually dominates the overall deterioration rate. The National Corrugated Steel Pipe Association points out that a CSP may provide satisfactory service until most of the invert is lost, which can be double the time to first perforation predicted by the California method. This results in a 50-year service life for CSP. Asphalt coating with paving, used in the example, is significantly more durable than plain asphalt coating. The authors used the 25-year coating life suggested by the American Iron and Steel Institute and others in the pipe industry. The design engineer must exercise engineering judgment in selecting design service lives, but these values are reasonable for a hypothetical example.

REFERENCES

1. J. A. Stockfisch. *Measuring the Opportunity Cost of Government Investment*. Research Paper *P*-490, Institute for Defense Analyses, Arlington, Va., March 1968.
2. *Economic Analysis of Public Investment Decisions: Interest Rate Policy and Discounting Analysis*. Report of the Subcommittee of the Joint Economic Committee of the Congress to the Full Committee, Subcommittee on Economy in Government, Government Printing Office, Washington, D.C., 1968.

Publication of this paper sponsored by Committee on Culverts and Hydraulic Structures.

Life Cycle Cost Analysis: Key Assumptions and Sensitivity of Results

THOMAS J. WONSIEWICZ

The growing use of life cycle cost techniques has brought to the surface some misconceptions and apparent conflicting approaches. Examined in this paper is the underlying basis for the two general approaches of selecting discount rates and dealing with inflation. The opportunity cost approach is endorsed as being the most effective in allocating resources. Suggestions are provided on how to evaluate the differential interest-inflation approaches being offered. Sensitivity analyses are used to show the relative insignificance of variations in design life, salvage value, and rehabilitation cost assumptions on results. By clarifying and putting these issues in a commonsense perspective, the reader should be able to use least cost analysis techniques with improved confidence.

Least cost analysis techniques are not new, although their use in the selection of economical project alternatives seems to be increasing. The approach, in general, is reasonably straightforward and provides a way to evaluate competing alternatives that have differing series of expenditures over the life of the project.

As simple as it all sounds, the practitioner can often be left bewildered by what seems to be conflicting information contained in articles on the subject and advice offered by energetic material suppliers.

The objective of this paper is to identify the more critical assumptions and to demonstrate the sensitivity of the results to variations in certain assumptions. This will put some of the more confusing issues into perspective and thereby result in improved confidence in the proper application and use of least cost analysis techniques.

TECHNIQUES

General

Mathematical formulas will not be presented in this paper. They are readily available in numerous texts on the subject. Inexpensive hand-held business or financial calculators are recommended as they readily handle the required computations.

The cost data used are intended to be realistic in their proportions, and represent typical competitive market conditions between corrugated steel pipe (CSP) and reinforced concrete pipe (RCP).

Lane Enterprises, Inc., 3705 Trindle Road, Camp Hill, Pa. 17011.

Base Information

The following data pertain to three alternative drainage structures intended to satisfy a 50-yr design life requirement.

1. Alternative *A*: Galvanized CSP with an initial cost of $195,000 and a projected service life of 40 yr, followed by invert maintenance at 25 percent of initial cost ($48,750) to satisfy required design life.
2. Alternative *B*: Asphalt-coated CSP with initial cost of $214,500.
3. Alternative *C*: Reinforced concrete pipe with an initial cost of $230,000.

Present Value

Of the three choices, only Alternative *A* needs to be analyzed to determine the present worth of the projected maintenance cost in Yr 40. The present value of Alternates *B* and *C* are equal to their first costs because there are no significant future expenditures.

In the case of *A*, at a discount rate of 9 percent, the present value is as shown in Table 1. The simple approach shows, for the assumptions used, that when ranked on a present value basis, Alternative *A* is the lowest cost alternative.

Average Annual Cost

This technique takes the present value calculation one step further. It is sometimes referred to as a sinking fund payment. In a way, it is similar to a mortgage payment. It represents the annual amount that would yield, over the project life, the total present value based on the stated discount rate. Accordingly, based on a 9 percent discount rate and a 50-yr project design life:

Cost ($)	*A*	*B*	*C*
Total current	243,750	214,500	230,000
Present value at 9 percent	196,550	215,500	230,000
Average annual (50 yr @ 9 percent)	17,930	19,660	20,980

Both the present value and average annual cost methods result in the same ranking of alternatives.

A potential error can occur if the material service life for each alternate is used to calculate the average annual cost. For the comparison to be fair, the project design life should

TABLE 1 PRESENT VALUE OF ALTERNATE *A* AT DISCOUNT RATE OF 9 PERCENT

Year	Current Dollars	Present Value at 9 Percent	
		Factor	Amount ($)
0, initial cost	195,000	1.0000	195,000
40, rehabilitation	48,750	.0318	1,550
Total	243,750		196,550

TABLE 2 PRESENT VALUE OF $1.00 EXPENDED AT VARIOUS INTERVALS AND DISCOUNT RATES

Year	Discount Rate (percent)		
	3	6	9
0	1.00	1.00	1.00
25	0.48	0.23	0.12
50	0.23	0.05	0.01
75	0.11	0.01	0.01

always be used so that all competing alternates are on an equal footing.

Differential Cash Flow Comparisons

Although not widely used in engineering assessments, this technique is frequently used in private industry to evaluate capital expenditure decisions. Essentially, it compares the cash flow of competing alternatives, and solves for an interest rate. It is often referred to as a discounted cash flow analysis that results in an internal rate of return. The magnitude of the resulting interest rate is used to judge the relative attractiveness of spending a higher sum initially to avoid future expenditures. Expenditures that do not meet some specified minimum rate of return are usually avoided. Generally, cost of capital is considered to be at least 10 percent.

A comparison of Alternates *A* and *C* results in the following:

Cash Flow ($)	*C*	*A*	*Difference (C–A)*
Year 0	230,000	195,000	35,000
Year 40	–	48,750	(48,750)
Total	230,000	243,750	(13,750)

The internal rate of return in this case is 0.83 percent, or less than 1 percent. This represents the discount rate at which the $48,750 of future expenditures avoided are equal to the $35,000 increased initial cost. Said another way, the added $35,000 investment to avoid a $48,750 future cost results in less than a 1 percent return on investment—by any measure, a poor return.

Because the results of a discounted cash flow comparison can be directly interpreted as a return on investment percentage, it serves as a useful way to gauge the significance of difference in present value amounts.

INTEREST AND INFLATION

General

The method of handling these two components probably contributes to most of the confusion in developing least cost comparisons. There are many articles and texts that go on at length about whether to inflate or not, by how much, and what should be used for interest rates. The logic for each seems coherent and yet, depending on the approach used, the calculations often result in completely different choices appearing to have the lowest cost. How can that be?

Why Are Results So Sensitive?

The answer lies in gaining an understanding of how the results are affected over a range of discount rates. In general, greater significance is given to future spending at low discount rates and less significance at high discount rates, as shown in Table 2 and Figure 1.

In contrast to the three-times increase in discount rates from 3 to 9 percent, there is a 23-times decrease in the significance in the present values of expenditures occurring in Yr 50 (0.23 versus 0.01). Also, because present value factors behave exponentially, a 3 percentage point difference at higher rates (9 percent versus 6 percent) has less of a present value significance than the same 3 percentage point difference at low rates (3 percent versus 6 percent).

In practical terms, if an alternate were to require a future expenditure equal to the initial investment some time between Yrs 25 and 50, that expenditure would represent a much more significant portion of total present value at a 3 percent discount rate, and much less at 9 percent.

	Significance of Future Expenditure as Percent of Total Present Value	
Discount Rate (%)	*Year 25*	*Year 50*
3	32	19
9	11	1

Generally, those who promote the recognition of inflation in least cost analysis wind up using relatively low discount rates, and those who exclude inflation use higher rates. So who is correct?

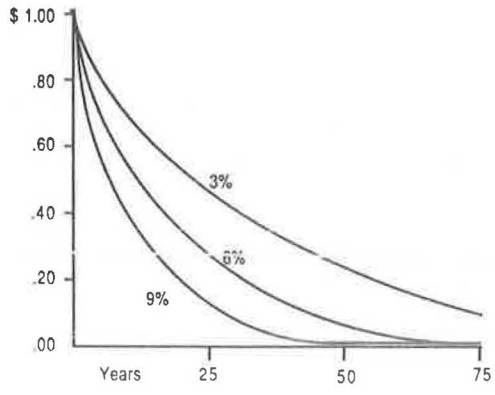

FIGURE 1 Graph of present value of $1.00 expended at various intervals and discount rates.

To Inflate or Not To Inflate

Recognition of inflation is a matter of policy. Strong arguments can be made for both techniques. As will be seen, the results of each approach require different interpretations.

In actual practice, both approaches are used. The Water Resources Council of the U.S. Department of the Interior in a report entitled, *Economic and Environmental Principles and Guidelines for Water and Related Land Resources Implementation Studies* (*1*), established evaluation principles to be followed by the Corps of Engineers, Bureau of Reclamation, Tennessee Valley Authority, and the Soil Conservation Service for water resource project plans. The report states that all costs are to be at a constant price level and at the same price level at the time of the analysis and as used for the computation of benefits [Section XII 2.12.4 (*b*) and (*i*)].

Similarly, Department of the Army Technical Manual, TM 5-802-1, *Economic Studies for Military Design—Applications* (*2*), indicates that the rate of inflation of the economy as a whole will be neglected in all least cost calculations. Although provisions are made to recognize differential cost growth (where particular costs or benefits are expected to change at rates different from the economy as a whole), it concludes that, in general, the differential growth rate will be assumed to be 0 (Chapter 2–2.b.(7)–*C*).

Although the foregoing suggests that inflation is not considered at the federal level, practice at the state level is mixed. Based on the 20 states and provinces that responded to the Transportation Research Board survey, *National Cooperative Highway Research Program Synthesis of Highway Practice 122, Procedures for Selecting Pavement Design Alternatives*, (*3*) and that provided meaningful descriptions of their techniques, eight states recognized inflation in their life cycle cost evaluations.

Opportunity Value or Cost of Money

The previously mentioned Department of the Army Technical Manual describes the "opportunity value" basis for evaluation (*2*). It states: [Chapter 2.–2.b.(4)] "The prescribed annual discount rate of 10 percent should be viewed as the minimum 'real' rate of return—i.e., the net rate of return, over and above the rate of inflation—to be achieved by public sector investments. The Office of Management and Budget, at the recommendation of the Joint Economic Committees of Congress, has determined that withdrawal of investment capital from the private sector by taxation can be justified only when the capital is used to finance public sector investments for which the real rate of return is at least equal to that achievable on the average in the private sector (estimated to be 10 percent)."

This position is fairly close to that commonly used in industry. That is, money has value and the competing demands for its use exceed the supply. Using a minimum rate of return screens out the poorer prospects. At the same time, inflation is not expressly calculated because it is believed that both costs and benefits are similarly influenced.

Another commonly held position is to use a discount rate that is related to the cost of borrowing. Typically, the interest rate associated with long-term federal, state, or municipal securities is used. This approach makes the choice between alternatives only on the basis of the cost of borrowing. However, the cost of borrowing a given sum is not necessarily the best measure to determine whether an additional sum for a higher cost alternate is warranted.

The difference between the concepts of opportunity value and the cost of borrowing is fundamental and requires the user to make a policy choice. As noted earlier, when the discount rates are high enough, there is generally little difference in the resulting answer for most drainage projects. In other words, if an agency has a 9 percent borrowing rate, it would come to the same choice of alternates as it would if it used the Department of the Army's 10 percent discount rate.

Inflation

Those who do recognize inflation in their calculations are generally concerned that the savings from an alternate with a lower initial cost may not be sufficient to cover the actual costs incurred in the future. A common approach is to assume an across-the-board inflation factor, project future costs, and then discount the resulting cash flows to their present value. Some formulas require specific assumptions on inflation and discount rates; others deal only with the differential between the two rates. The end result is aimed at identifying the alternative with the lowest real cost.

Although the concept is sensible, its application can be troublesome, especially for projects with long design lives. The first comes with rate selection. Aside from the basic choices of discount rates (opportunity or borrowing costs) what do you use for inflation? How do you apply it? Should a flat rate be used across the board or should different elements (e.g., labor, materials, energy) be treated independently (*4*, *5*)? How do you predict it? If nothing else, the analysis becomes much more complex.

Another major problem is the determination of an acceptable real rate. Whereas most decision makers would be comfortable accepting a 9 or 10 percent return on their investment, how would they feel about accepting a 2 percent real rate of return? For that matter, how about 2 percent or 3 percent? Simply put, most people do not have a practical feel for using real discount rates.

Rate Selection

For long-life projects, rate selection should be a matter of policy similar to the basic choice between using opportunity costs as compared with borrowing costs. Historical trends are useful, but should be viewed for what they are: a guide. Certainly, recent history and economic projections should be given higher weighting than data from 3 or 4 decades in the past.

Above all, common sense should prevail. Some techniques being promoted sound logical but do not make sense. For example, one published approach recommends that inflation should be recognized, and used the differential rate approach. The calculation was based on the long-term relationship of municipal bond rates to the consumer price index of 0.9953. If a long-term municipal bond rate of 8 percent is used in conjunction with this ratio, it implies a long-term inflation rate of 7.96 percent. By difference, the real value of money is only 0.04 percent. This just does not make sense. No inves-

tor or taxpayer would agree to such a small value, real or otherwise.

Recommendations

The National Corrugated Steel Pipe Association (*6*) agrees with the general approach used by the Department of the Army and, similarly, that of the Department of the Interior. The Association recommends using a 9 percent discount rate and excluding adjustments for future inflation.

For those who, by policy, must specifically identify inflation, a rate of 5 percent in conjunction with the 9 percent discount rate is recommended.

DESIGN LIFE

General

Least cost analysis techniques require that some period of time be selected. However, there is uncertainty as to how long the period should be. In many cases, policy controls. Fifty yr is commonly used for primary state highway culverts.

The choice of design life should be independent of the materials available. Two practical parameters that should be considered are the risk of obsolescence and the availability of funds. The future likelihood of needing increased capacity, the options available to increase capacity in the future, and a risk of complete facility abandonment will serve to place an upper limit on design life. Similarly, fiscal limitations often dictate the limit of spending and therefore influence design life. You cannot spend what you do not have.

In the case of drainage pipe, the exact number of years the pipe is required to perform is less important than a reasonable estimate of the timing and magnitude of future expenditures. For example, even in the situation where invert repair is projected, the resulting extension in service life can normally be expected to go well beyond the 50-yr mark. From the point of view of the calculation, the year of rehabilitation and cost are the only data needed.

Material Life

Some methodologies impose a symmetry of lives position in computing present value. That is, the longest life material governs, and the shorter material life must be replaced as many times as necessary to be equal.

The primary flaw with this approach is that the project design life should determine the calculation period, not the material life. Material life in excess of the design life is immaterial. Materials with shorter life spans need to be either replaced or rehabilitated.

In the case of CSP, invert repairs can extend serviceability for another life cycle at a cost far lower than complete replacement. Prudent inspection programs, even at only a 10-yr frequency, will permit timely repairs while they are still inexpensive.

Residual-Salvage Value

Salvage value is usually taken to mean the benefit of being able to use a given material at the end of a project. In practice, it occurs fairly infrequently with drainage pipe. When it does, the extra cost associated with careful removal has to be weighed against the value of the material. An objective review of current practices on replacement projects shows that the probability of salvage is low.

In contrast, residual value is sometimes taken to mean the calculated value associated with a material that can continue to provide service beyond the project design life. To be valid, either the capacity requirements at the end of the original design life will not need to be changed or, if an increase is necessary, the existing line can continue to provide service without any effect on adding the increased capacity. The mathematics used by some to calculate residual value should be approached with caution. One published example uses a design life of 50 yr, a 100-yr material life, a 7 percent interest rate, and a 5 percent inflation rate. It concludes that the 50 yr of remaining service life at the end of the 50-yr project design life represents an "immediate 19 percent benefit" to the owner that results in a life cycle cost of 81 percent of the actual bid price. Although the mathematics are internally consistent, most owners would not agree with this conclusion. A possible savings 50 yr down the road would not be considered as "immediate".

Whereas salvage or residual values may have significance in short-life projects, which have unusual once-and-done requirements (temporary pumps, generators, etc.), they usually have little significance when applied to long-life drainage projects.

SENSITIVITY EXAMPLES

General

The information contained in this section is intended to provide a perspective on the sensitivity of the present value to variations in certain assumptions. The basic information pertaining to Alternates *A* and *C*, introduced earlier, will be used throughout. Data will be shown using a 9 percent discount rate and no inflation, as recommended in this paper, as well as for an inflation-interest combination of 5 percent and 9 percent, respectively.

Salvage-Residual Value

The information in Table 3 gives an indication of the effect of a broad range of salvage value assumptions. It can be noted from this table that salvage value is not a significant factor. Even under the most extreme condition (30 percent of original cost) it represents a value that is less than 5 percent of the initial cost:

	Sensitivity of Present Value of Salvage as A Percent of Initial Cost		
Interest (%)	*10*	*20*	*30*
9	0.1	0.3	0.4
5/9	1.6	3.1	4.6

TABLE 3 EFFECT OF BROAD RANGE OF SALVAGE VALUE ASSUMPTIONS

Year	Alternate *A* ($)	Alternate *C* Salvage Value ($) at % of Initial Cost		
		10	20	30
0	195,000	230,000	230,000	230,000
40[a]	48,750	–	–	–
50[b]	–	(23,000)	(46,000)	(69,000)
Total	243,750	207,000	184,000	161,000
Present value				
At 9 percent	196,600	229,700	229,400	229,100
At 5 percent/9 percent	205,900	226,400	222,900	219,400

[a] Rehabilitation cost.
[b] Salvage value.

TABLE 4 SIGNIFICANCE OF TIMING OF FUTURE REPAIR COSTS RELATIVE TO INITIAL COST

Year	Alternate *A* Invert Repair Cost ($) at Year	
	40	25
0	195,000	195,000
25	–	48,750
40	48,750	–
Total	243,750	243,750
Present value		
At 9 percent	196,600	200,700
At 5 percent/9 percent	205,900	214,100

Rehabilitation Costs: Timing

The significance of the timing of future repair costs relative to the initial cost is shown in Table 4. It should be noted that, despite a significant acceleration in the assumption about invert repair, the effect on the present value is less than 5 percent:

Interest (%)	*Sensitivity Difference in Present Value as* A *Percent of Initial Cost 25 Versus 40 Yr (%)*
9	2.1
5/9	4.2

Rehabilitation Costs: Magnitude

The example given in Table 5 portrays the significance of an increase in rehabilitation costs from the base assumption of 25 percent of original costs to 40 percent. Similar to the previous example, even this significant increase in rehabilitation cost results in less than a 4 percent increase in present value

TABLE 5 SIGNIFICANCE OF INCREASE IN REHABILITATION COSTS FROM 25 TO 40 PERCENT OF ORIGINAL COSTS

Year	Alternate *A* Invert Repair Costs ($) at % of Initial Cost	
	25	40
0	195,000	195,000
40	48,750	78,000
Total	243,750	273,000
Present value		
At 9 percent	196,600	197,500
At 5 percent/9 percent	205,900	212,500

in relation to the initial cost:

Interest (%)	*Sensitivity Difference in Present Value as* A *Percent of Initial Cost 40 Versus 25 Yr (%)*
9	0.5
5/9	3.4

SUMMARY

Least cost analysis techniques are a front-line tool to aid in the selection of alternatives and to see that limited financial resources are spent prudently. Because some of the approaches being promoted appear to be contradictory, the user must be on guard. The most crucial assumption is the basis for the proposed discount rate. Low rates should be rejected on a commonsense basis. Additionally, the sensitivity calculations show that for long-life drainage projects, variations in design life, salvage value, rehabilitation costs, and timing have only a small effect on total present value.

REFERENCES

1. *Economic and Environmental Principles and Guidelines for Water and Related Land Resources Implementation Studies*. PB 84-199405, U.S. Water Resources Council, U.S. Department of the Interior, Feb. 3, 1983.
2. *Economic Studies for Military Construction Design—Applications*. TM 5-802-1, Department of the Army, Washington, D.C., Dec. 31, 1986.
3. *NCHRP Synthesis of Highway Practice 122. Life Cycle Cost Analysis of Pavements*. Transportation Research Board, National Research Council, Washington, D.C., Dec. 1985.
4. E. L. Grant and W. G. Ireson. *Principles of Engineering Economy*, 5th ed. The Roland Press Company, New York, 1970.
5. H. L. Beenhakker. *Handbook for the Analysis of Capital Investments*. Greenwood Press, Westport, Conn., 1976.
6. J. K. Leason and R. Standley. *Least Cost Analysis*. National Corrugated Steel Pipe Association, Washington, D.C., March 1986.

Publication of this paper sponsored by Committee on Culverts and Hydraulic Structures.

Service Life Model Verification for Concrete Pipe Culverts in Ohio

JOHN OWEN HURD

Separate analyses of reinforced concrete pipe durability data collected by the Ohio Department of Transportation were conducted by the Ohio Department of Transportation and another research agency. There was a large discrepancy in the service life predicted for culverts installed in nonacidic sites between the two models. This study was initiated to establish which model was the most accurate. An inventory of older reinforced concrete pipe installations was compiled. The age of many of these culverts approached the very conservative service life predicted by the linear model developed by the other agency. The total number of 196 culverts inspected included 70 culverts installed before 1940, 89 culverts installed from 1940 to 1949, and 37 culverts installed from 1950 to 1969. The culverts were evaluated using a revised, more detailed rating system and predicted service lives extrapolated from the rating and age at the time of inspection. It was found that the linear model significantly underpredicted service life of reinforced concrete pipe for a flow pH range above 4.5 and that the Ohio Department of Transportation model provided a reasonable estimate of projected service life for the entire pH range studied.

In 1982, the Ohio Department of Transportation (ODOT) published a comprehensive research report (*1*) that provided information on the durability of various culvert materials. As part of this report, predictive equations for the service life of reinforced concrete pipe culverts were presented. These equations were developed from data collected in 1972 at 545 concrete pipe culvert sites throughout Ohio. These sites encompassed a wide range of topography and environmental conditions. The condition of the concrete pipe culverts was evaluated by means of the following visual rating system:

1. Excellent—condition of concrete as constructed.
2. Very Good—discoloration but no loss, corrosion, or softening.
3. Good—slight loss of mortar leaving aggregate exposed.
4. Fair—moderate loss of mortar and aggregate, slight softening of concrete.
5. Poor—significant loss of mortar and aggregate, complete loss of invert, concrete in softened condition.

It is readily apparent that the comparative times required for deterioration between progressive ratings were not equal. For the purpose of analysis, however, arbitrary linear numerical values of 0 to 4 were assigned to the visual ratings. The predictive equations for concrete culvert rating derived from the analysis were for pH less than 7.0

Ohio Department of Transportation, 25 S. Front Street, Columbus, Ohio 43215.

$$\text{Rating} = \frac{10\,(\text{age}^{0.13})(\text{slope})^{0.11}}{(\text{pH})^{1.20}}\left(1 - \frac{\text{sed}}{\text{rise}}\right)^{0.76} \quad (1)$$

and for pH greater than or equal to 7,

$$\text{Rating} = \frac{K(\text{age})^{0.17}(\text{slope})^{0.054}}{(\text{velocity rating})^{0.088}} \quad (2)$$

where

sed = sediment depth in inches,
rise = pipe rise in inches,
slope = pipe slope in percent,
age = culvert age in years,
velocity rating = 1 for rapid, 2 for moderate, 3 for slow, 9 for nil, and
K = 0.9 for nonabrasive flow, 1.2 for abrasive flow.

These equations accounted for the nonlinearity in the time of deterioration between successive ratings by the power on the variable age. The fact that this power of approximately ⅙ to ⅐ is so much less than 1 (power = 1 indicating a linear relationship between rating and age) is indicative of the extreme nonlinearity of the time required for progressive deterioration between successive ratings. The comparative times of deterioration for the various ratings are illustrated in Figure 1. This nonlinearity of the rating system was discussed in detail in the 1982 ODOT report (*1*).

Conservative predictive equations for concrete pipe service life were obtained by setting the numerical rating value equal to 3.5 (between fair and poor) and solving Equations 1 and 2 for age. The resulting service life equations were for pH less than 7.0,

$$\text{Service life} = \frac{[0.349(\text{pH})^{1.2}]^{7.76}}{(\text{slope})^{0.82}}\left(1 - \frac{\text{sed}}{\text{rise}}\right)^{-5.912} \quad (3)$$

and for pH greater than or equal to 7.0,

$$\text{Service life} = \left(\frac{3.5}{K}\right)^{5.9}\frac{(\text{velocity rating})^{0.52}}{(\text{slope})^{0.31}} \quad (4)$$

Because of the rather crude and biased rating system used, questions were raised regarding the possible conservatism of the predictive equations for the acidic pH range. The greatest concern was based on the observation that the fair and poor ratings covered too wide a range of actual material condition ranging from moderate mortar loss to complete loss of invert.

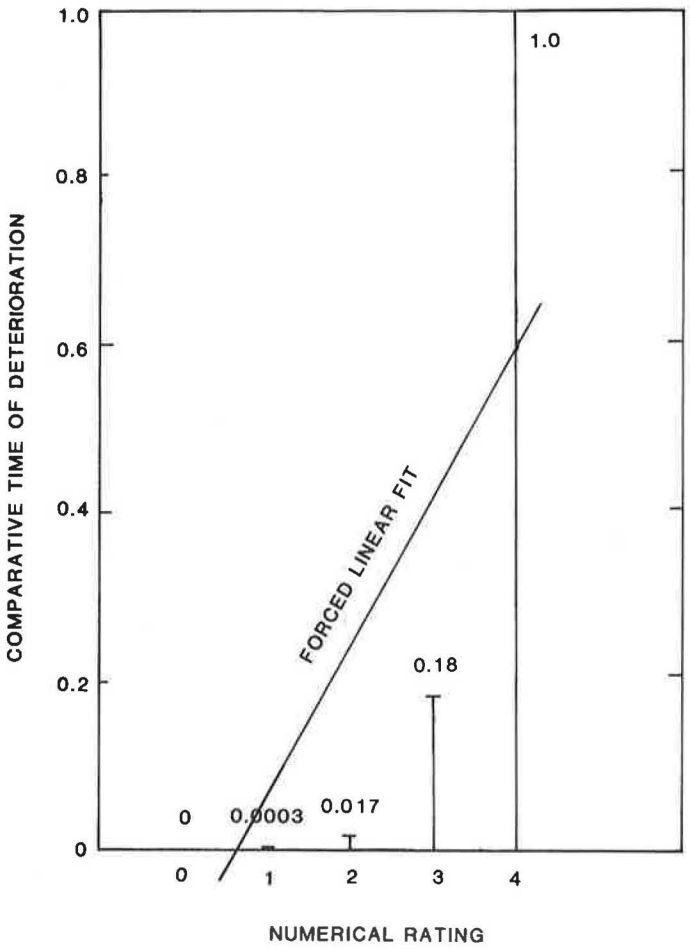

FIGURE 1 Comparative times of deterioration for concrete pipe ratings, ODOT/L&D/82-1.

Pipe with moderate mortar loss could have several decades of useful service still remaining, whereas complete loss of invert would require repair or replacement.

Because of these concerns, a follow-up study (*2*) of culverts at acidic flow sites was conducted in 1984. The original data set for acidic flow was expanded to include additional sites. The sites from the previous work were included with an additional 12 years of service. It should be noted that no culvert rated fair or poor from the initial study had been replaced and all were functioning well with no structural distress at the time of the follow-up study. Except for one culvert installed on an 18 percent slope with a flow pH equal to 3.0, no culverts were observed with complete loss of invert in either the initial or the follow-up study. Otherwise, the worst condition observed was deterioration through the inner reinforcing mesh. This represents about a 1-in. thickness of concrete loss.

The more refined rating system described in Transportation Research Record 1008 (*2*) was used to evaluate the culverts in 1984 as follows:

0 As manufactured,
10 Slight loss of mortar, aggregate exposed,
20 Moderate loss of mortar, aggregate exposed,
30 Significant loss of mortar, slight aggregate loss,
50 Moderate aggregate loss,
60 Significant aggregate loss,
70 Severe aggregate loss,
80 Reinforcing exposed at a few places,
90 Reinforcing exposed throughout the pipe, and
100 Reinforcing gone.

This rating system represented a definite improvement over the 1972 rating system, described earlier in this paper, for two reasons. First, ratings above 95 more accurately describe a pipe with loss of reinforcing that could adversely affect the structural integrity of the pipe. This rating could be defined conservatively as the rating at which end of service life occurs. However, as shown in Figure 2, substantial wall thickness would still remain protecting the pipe foundation from erosion. Second, the number of ratings for culverts with greater degrees of deterioration was expanded.

This 1984 rating system attempted to provide an equal number of ratings for all stages of deterioration. The power of age in the resulting equation for concrete pipe rating indicates a closer approximation of equal times of deterioration between successive numerical ratings.

$$\text{Rating} = \frac{6.5\ (\text{age})^{0.55}(\text{rise})^{1.08}(\text{slope})^{0.23}}{(\text{pH})^{3.08}}\left(1 - \frac{\text{sed}}{\text{rise}}\right)^{1.46} \tag{5}$$

The power on age has been increased from approximately ⅙ to more than ½. However, even with the refined 1984 rating

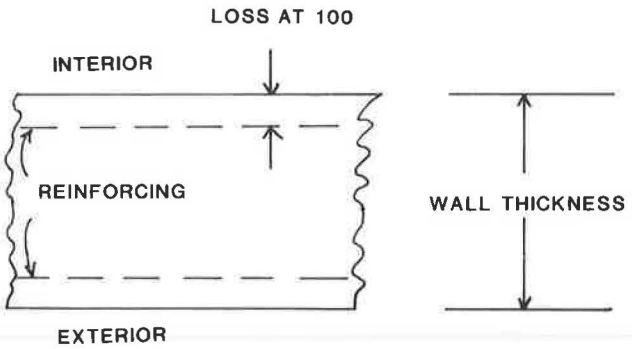

FIGURE 2 Reinforced concrete pipe wall diagram.

system, a true linear relationship between numerical rating and age was not obtained. The comparative times of deterioration for the various ratings are shown in Figure 3. Use of a linear model would result in conservative service life predictions even if the 1984 rating system were used.

A service life equation for concrete pipe at acidic flow sites was obtained by setting rating equal to 95 and solving for age. This equation,

$$\text{Service life} = \frac{123.5(\text{pH})^{5.55}}{(\text{rise})^{1.94}(\text{slope})^{0.42}}\left(1 - \frac{\text{sed}}{\text{rise}}\right)^{-2.64} \quad (6)$$

gave results that compared closely with Equation 3. The range of service life obtained from Equations 4 and 6 are plotted versus pH for various combinations of concrete pipe size, slope, and so on, in Figure 4 for mild, average, and severe conditions. For this plot, sediment depth is set equal to 0, which is a worst-case condition but desirable from a hydraulic design standpoint. It may seem extremely pretentious to extrapolate approximately 50 to 60 years' worth of data out to a four-figure service life for a mild condition. However, the plot indicates the magnitude of service life that could occur for certain installations. There have been documented histories of extremely long service life for concrete pipe at installations throughout the world (*3*).

In 1986, a separate analysis (*4*) of the initial ODOT 1972 data was conducted by others. No field observations were made and no additional data from other states or the ODOT 1985 report were included. Straight-line linear regression analysis of numerical values arbitrarily assigned to ODOT

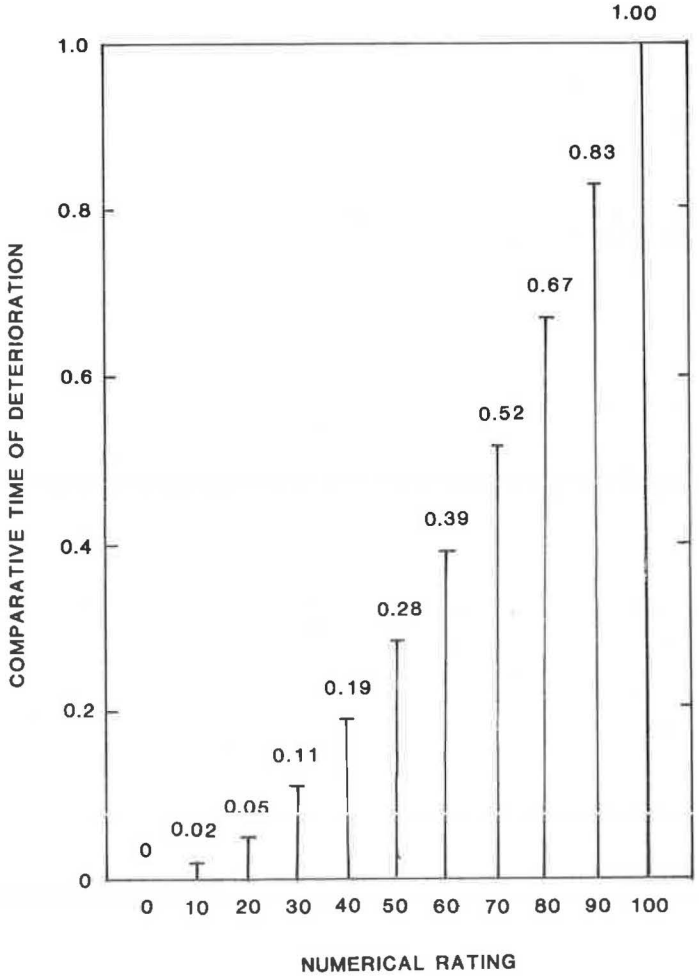

FIGURE 3 Comparative times of deterioration for concrete pipe ratings (*2*).

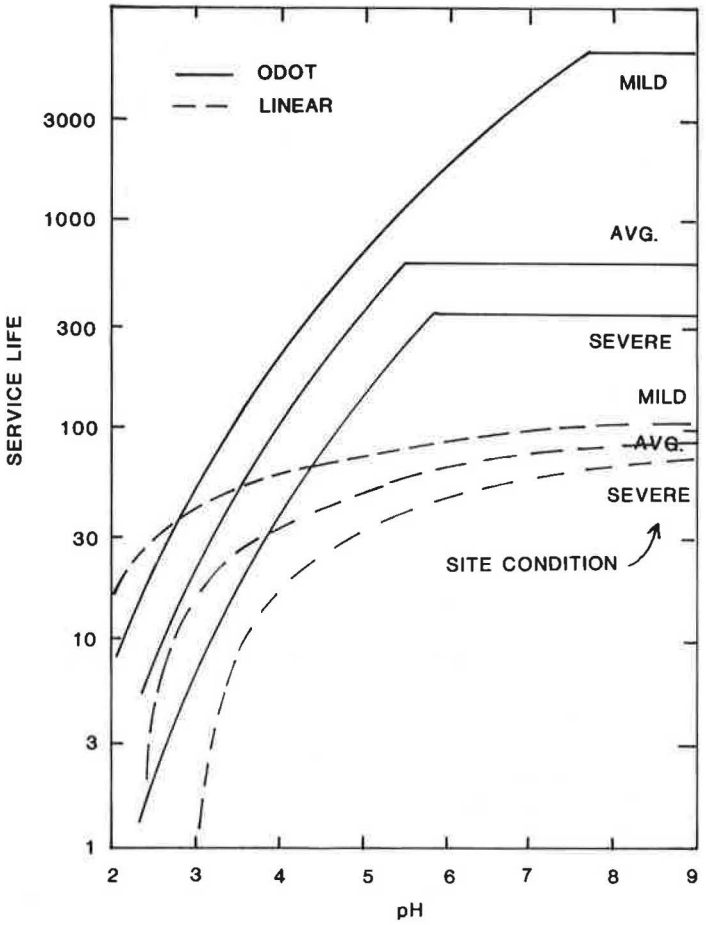

FIGURE 4 Ohio concrete pipe service life models.

ratings versus age and other independent variables were used to develop a predictive linear model for culvert rating.

The problems involved with using a straight linear relationship between arbitrarily assigned numerical ratings and age were explained in detail by both ODOT in previous reports (*1*) and by Stratfull (*5*) in reviewing work by others using a rating system similar to the 1972 ODOT rating system. Any attempt to force a linear regression relationship between age and the arbitrary numerical values assigned to the 1972 ODOT ratings will produce biased service life equations even if the regression statistics, R^2 and standard error, appear reasonable. In the case of the 1972 ODOT rating system, the time required to reach a poor condition would be seriously underpredicted. This can be seen by observing the forced linear regression fit for comparative time of deterioration versus rating in Figure 1. This line is representative of a data set with an equal amount of culverts in each rating. The underestimate would be even more pronounced for a data set dominated by excellent to good ratings, as the 1972 ODOT data set was. In fact, a linear model could have a higher R^2 value than a nonlinear model because of the bias of the data set.

The range of service life (obtained in a way similar to that for the log-linear model) for the linear model for various combinations of pipe size, slope, and so on, is plotted in Figure 4 for mild, average, and severe conditions. There is not much difference between the two models in the extremely acidic range. However, there is clearly a large discrepancy between the ODOT and linear models for slightly acidic to high pH sites. The much lower service life predicted by the linear model for nonacidic sites is contrary to observations made by numerous past researchers (6, 7).

Because of the large difference between the two models based on the same data, this study was initiated to establish which model was more accurate.

SITE SELECTION

In order to evaluate the two predictive models, an inventory of all older reinforced concrete pipe installations over 42-in. diameter or rise was compiled. The 42-in.-diameter cutoff was selected as in the previous studies because this was the smallest-size pipe that could be conveniently inspected by field personnel. The fact that the sizes of pipe inspected were more likely to have dry weather flow would lead to conservative estimates of service life for smaller pipe. This inventory consisted of 495 culverts installed before 1950, of which 173 were installed before 1940. Older culverts were selected to provide a data base population of culverts with ages approaching the very conservative service life predicted by the linear model. This inventory is representative of all precast reinforced concrete pipe culverts installed during that time period, because ODOT has no record of having replaced an in-service precast

reinforced concrete pipe culvert because of invert durability problems.

The intention was to observe the condition of these culverts, which were approaching the service life predicted by the linear model, to determine whether they had reached or were approaching the end of useful service life. If not, a service life for each culvert would be projected based on condition and age at the time of inspection. This projected service life would be compared with that predicted by the ODOT and linear models. It was believed that evaluation of old pipe performance could be used to predict performance of newer installations. Manufacturing methods have been improved in the past 50 years, resulting in greater concrete density. However, the basic material and reinforcing cover requirements have remained similar (8–10).

The 1972 sites used in the data analysis for the 1982 ODOT report (*1*) and the linear model report were not deleted from the inventory because 15 years had passed since they had been inspected. The 1984 sites used in the data analysis for the 1985 ODOT follow-up report (*2*) for acidic sites were not deleted from the inventory because the 1985 report had practically exhausted the population of acidic sites. Without these sites, there would have been almost no acidic sites with which to make comparisons. The 1984 data from acidic sites with installation dates since 1950 were also used to expand the data base for the acidic pH range. This was consistent with the inventory selection criterion of culvert age approaching predicted service life, because predicted service life in the acidic pH range is much less than it is for the nonacidic range.

The initial intention of this study was to inspect as many culverts as possible that were installed before 1940 and a selected number of culverts installed from 1940 to 1949 to assure geographic coverage of the state. Selection of culverts installed in the early 1940s rather than those from the late 1940s was preferred in order to keep the data set as old as possible. The total number of culverts inspected for this study was 196. These included 70 culverts installed before 1940, 89 culverts installed from 1940 to 1949, and 37 acidic-site culverts installed from 1950 to 1969. None of the culverts rated fair or poor in the 1982 report (1972 inspection) that were inspected for this study had been replaced. All were still functioning satisfactorily without signs of structural distress. The locations of the culverts inspected are shown on Figure 5. Although not every county in the state was covered, adequate coverage of areas of the state with common environmental conditions was attained.

In addition to those culverts inspected, 33 sites were visited where reinforced concrete pipe culvert of the age indicated was not found. It appeared that there had never been culverts at 22 of these sites, or the roadway had been built much later and that an inventory coding error in the installation date had been made. At the other 11 sites where culvert replacement had occurred, district personnel were questioned and records checked. In no case had the original culvert (if constructed of reinforced concrete) been replaced because of problems with invert deterioration. In each case, the reinforced concrete pipe culvert removed was salvaged for later use.

DATA COLLECTED

Based on the results of previous research, the data collected in each site were limited to the following:

1. Age of the culvert in years based on the inventory installation date and verified by manufacturers' marks where possible;

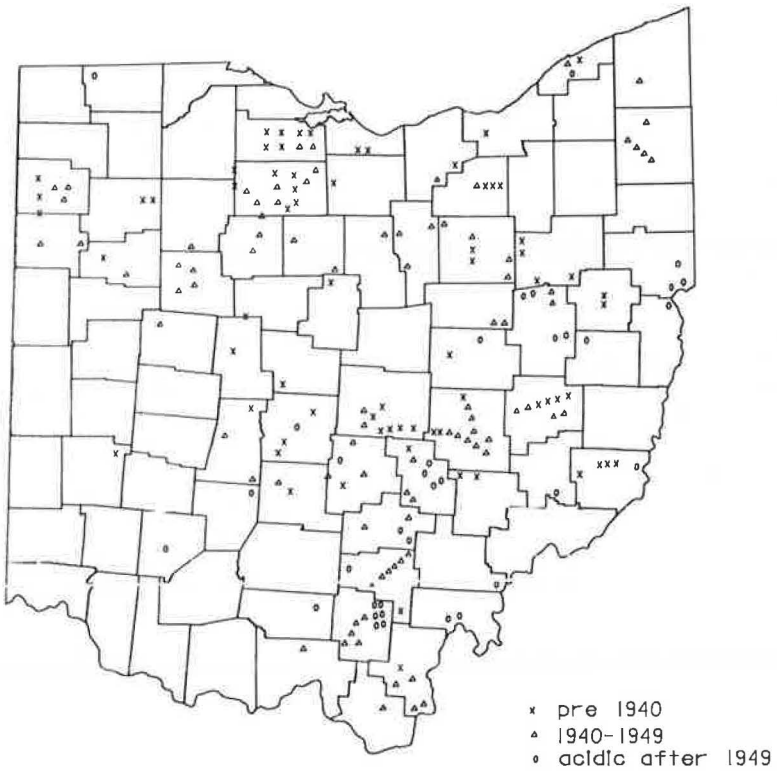

FIGURE 5 Concrete pipe culverts inspected, 1987.

2. Culvert pipe diameter or rise in inches;
3. Flow depth in inches;
4. Flow velocity rating (rapid, moderate, slow, and standing or dry);
5. Sediment depth in inches;
6. Largest frequently occurring bed load particle size in inches;
7. Flow pH;
8. Culvert pipe slope expressed as a percentage; and
9. Culvert pipe rating (*2*) of the culvert invert (shown previously in this paper).

The 1984 ODOT rating system was used to evaluate culvert performance for several reasons. It provides a larger number of ratings for invert conditions approaching that condition defined at end of service life. It comes much closer to representing a linear deterioration rate between successive ratings, demonstrated by Figures 1 and 3. Therefore, projections (either linear or log-linear) of service life based on existing rating and age are less apt to be grossly over- or underpredicted. It specifically defines a culvert condition rating (95 to 100) that can be conservatively used as useful service life (i.e., in cases in which repair should be considered). This rating system is independent of the 1972 ODOT rating system used to evaluate culverts for development of the service life models in the pH range with the greatest discrepancy between models. In general, the condition of the culvert invert was consistent throughout the culvert length and the rating given each culvert was representative of average culvert invert condition.

The data collected is summarized in Table 1 by rating, age range, and pH range. It should be noted that several culverts rated fair or poor on the previous study were reevaluated using revised ratings. Most of those culverts rated fair or poor in 1972 except for extremely acidic sites (pH less than 4.5), were rated between 25 and 65. The age range for these ratings is less than half way to the end of useful service life, as shown in Figure 3. A few culverts had been rated fair or poor because of concrete loss along the haunches caused by shear slabbing, a structural problem caused by improper installation under high fills and unrelated to invert durability. A few others had been rated fair or poor because of concrete spalling on parts of a few pipe sections resulting from lack of adequate cover over reinforcing steel. Although this condition is related to pipe durability, it should not occur with adequate inspection. Inadequate cover over reinforcing steel can be discovered during visual inspection of pipe sections and those sections rejected.

It can be seen from the table that the only culverts, a total of 16, showing serious invert deterioration (rating 75 or greater) are those carrying extremely acidic flow. In fact, only one culvert carrying nonacidic flow showed even moderate deterioration. This particular pipe appeared to have been home made and not in conformance with standard specifications used at the listed time of its manufacture. Wooden form marks were observed, butt joints had been used, the size of large aggregate greatly exceeded allowable limits, and very low cement content mortar appeared to have been used. At the time of inspection, no culvert rated between 90 and 100 showed any structural distress caused by loss of reinforcing steel. In all, 148 (75+ percent) of the 196 culverts whose ages were approaching that service life predicted by the linear model were rated 20 or lower. These ratings represent only surface mortar loss without any aggregate loss, insignificant deterioration compared with that required for end of service life. Twenty-one other culverts (11 percent of the sample) were rated from 25 to 40, experiencing only slight aggregate loss at worst. If the linear model gave accurate estimates of the defined service life, more than 50 percent of the culverts

TABLE 1 SUMMARY OF DATA FROM CULVERTS INSPECTED

Culvert Rating	Age Range	pH Range	No. of Culverts
5, 10	≥50	≥7.0	22
		4.5–6.9	0
		<4.5	0
	40–49	≥7.0	45
		4.5–6.9	4
		<4.5	0
	30–39	≥7.0	18
		4.5–6.9	7
		<4.5	0
	<30	≥7.0	1
		4.5–6.9	8
		<4.5	1
15, 20	≥50	≥7.0	8
		4.5–6.9	2
		<4.5	0
	40–49	≥7.0	12
		4.5–6.9	7
		≥7.0	0
	30–39	≥7.0	4
		4.5–6.9	4
		<4.5	0
	<30	≥7.0	0
		4.5–6.9	3
		<4.5	2
25, 30, 35, 40	≥50	≥7.0	9
		4.5–6.9	0
		<4.5	0
	40–49	≥7.0	4
		4.5–6.9	2
		<4.5	1
	30–39	≥7.0	0
		4.5–6.9	1
		<4.5	1
	<30	≥7.0	0
		4.5–6.9	0
		<4.5	3
45, 50, 55, 60, 65, 70	≥50	≥7.0	0
		4.5–6.9	1
		<4.5	0
	40–49	≥7.0	1
		4.5–6.9	1
		<4.5	1
	30–39	≥7.0	0
		4.5–6.9	1
		<4.5	1
	<30	≥7.0	0
		4.5–6.9	1
		<4.5	3
75, 80, 85, 90, 95, 100	≥50	≥7.0	0
		4.5–6.9	0
		<4.5	0
	40–49	≥7.0	0
		4.5–6.9	1
		<4.5	2
	30–39	≥7.0	0
		4.5–6.9	0
		<4.5	2
	<30	≥7.0	0
		4.5–6.9	0
		<4.5	11

observed should have been rated 70 or greater. This is definitely not the case.

SERVICE LIFE MODEL VERIFICATION

Because it was apparent from these observations that the linear model significantly underpredicted defined service life for concrete pipe, projected service lives for the culverts inspected in this study would have to be developed to compare with the service lives predicted by the ODOT and linear models. The projected service lives of culverts inspected were estimated by both linear and log-linear extrapolation of the culvert age and rating at the time of inspection.

The direct linear extrapolation of culvert age and ratings to project service life is in conformance with the linear model assumption that the actual times required for deterioration between successive arbitrary numerical ratings are equal throughout the range of ratings. Thus, for each culvert

$$\frac{\text{Rating @ Age 2}}{\text{Rating @ Age 1}} = \frac{\text{Age 2}}{\text{Age 1}}, \text{ or} \tag{7}$$

$$\frac{\text{100 (i.e., the rating @ end of service life)}}{\text{Rating @ inspection}} = \frac{\text{Service life}}{\text{Age @ inspection}} \tag{8}$$

As stated previously in discussion of the more refined 1984 rating system, this method of extrapolation will result in very conservative estimates of projected service life.

The log-linear extrapolation of culvert age and rating to project service life is in conformance with the assumption made in the ODOT power equation model that the actual times required for deterioration between successive arbitrary ratings increase, as shown in Figure 3. This increase is related to the power of age in Equation 5 as follows:

$$\frac{\text{Rating @ Age 2}}{\text{Rating @ Age 1}} = \frac{(\text{Age 2})^{0.55}}{(\text{Age 1})^{0.55}}, \text{ or} \tag{9}$$

$$\frac{(\text{Rating @ Age 2})^{1.82}}{(\text{Rating @ Age 1})^{1.82}} = \frac{\text{Age 2}}{\text{Age 1}}, \text{ or} \tag{10}$$

$$\left(\frac{\text{100, i.e., rating @ end of service life}}{\text{rating @ inspection}}\right)^{1.82} = \frac{\text{Service life}}{\text{Age @ inspection}} \tag{11}$$

This method of extrapolation will result in an average estimate of projected service life.

Because both the linear and ODOT log-linear models recognized that increased sediment depths prolonged service life, the projected service lives for the culverts inspected that contained sediment were reduced by an amount equal to that

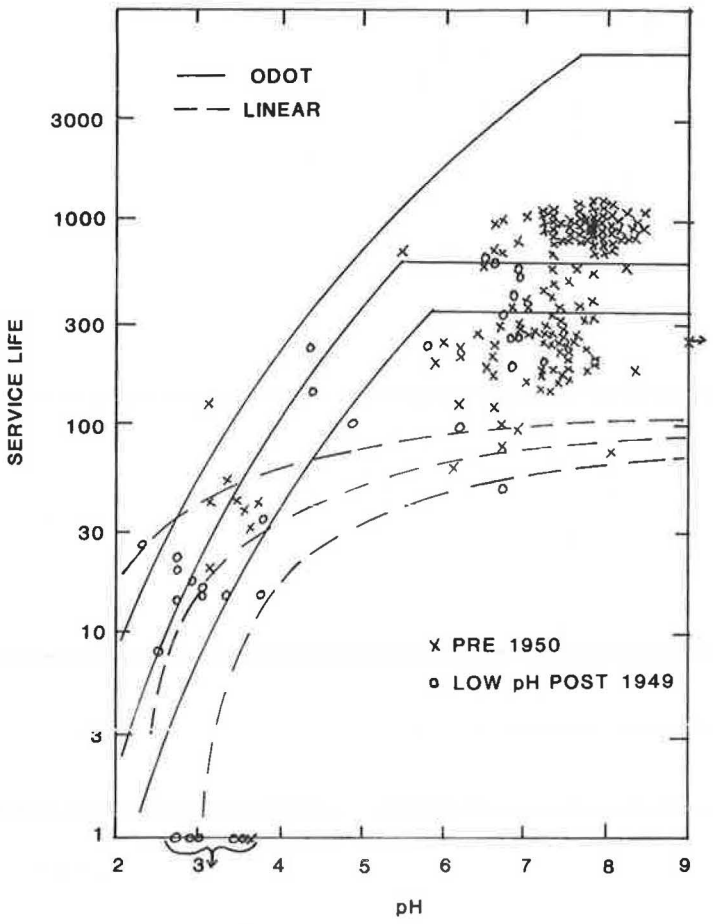

FIGURE 6 Linear projected service life for inspected culverts.

increase in service life attributed to the presence of sediment equal to that observed at the site for each model. The linear projected service life was reduced by subtracting nine times the sediment depth in inches. Although this produces an extreme percentage reduction for short service life at extremely acidic sites, it was applied throughout the range of data for the sake of consistency. The log-linear projected service life was reduced by multiplication by the factor

$$\left(1 - \frac{\text{sed}}{\text{rise}}\right)^{-2.64}$$

from Equation 6.

The sediment-adjusted linear-projected (Equation 8) service lives for the culverts inspected were plotted with the ODOT and with the linear model curves on Figure 6. Even using the conservative linear extrapolation that conforms to the linear theory, only 4 points above a pH of 4.5 fall within the linear model envelope. Approximately 60 percent of the points above a pH of 4.5 fall within the ODOT curves and the rest between the two models. It is demonstrated that the linear model does not represent defined service life but a conservative lower bound. The sediment-adjusted log-linear projected (Equation 11) service lives are plotted in Figure 7. Using the log-linear extrapolation, only 2 points above a pH of 4.5 fall within the linear model envelope. All but a total of 11 points fall within or above the ODOT envelope. It is therefore obvious that the ODOT service life models more accurately estimate the projected service lives for old, in situ reinforced concrete pipe culverts than does the linear model.

CONCLUSIONS

1. ODOT has no record of ever having replaced a reinforced concrete pipe culvert because of invert durability.
2. Both ODOT and linear reinforced concrete pipe service life models reasonably predict service life for concrete pipe installed in extremely acidic environments (pH less than 4.5). The linear model is slightly conservative toward the higher end of this range.
3. The linear reinforced concrete pipe service life model seriously underestimates concrete pipe service life for the pH range 4.5 and above.
4. The ODOT reinforced concrete pipe service life model provides an accurate estimate of concrete pipe service life that conforms well to projected service life of existing older concrete pipe culvert installations.

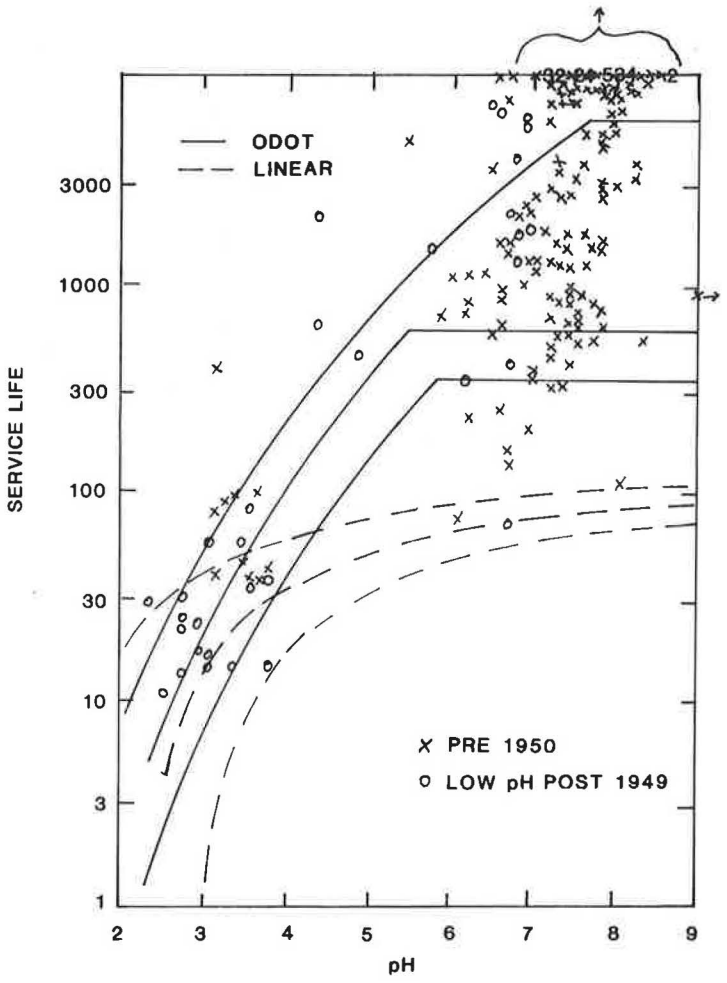

FIGURE 7 Log-linear projected service life for inspected culverts.

5. The ODOT model provides a reasonable estimate of reinforced concrete pipe life expectancy that can be used in life cycle cost analysis. However, the actual average service life of concrete pipe in a pH environment of 6.0 and above is indeterminate at this time because no pipes in this range have had invert deterioration close to that defined as useful service life.

RECOMMENDATIONS

1. The ODOT model should be used in life cycle cost analysis to estimate service life for concrete pipe in culvert installations.
2. The ODOT revised rating system, as given in Transportation Research Record 1008 (*2*), provides an adequate method to evaluate concrete pipe culverts in future studies until an improved rating system is developed.
3. The linear model could be used to estimate a lower bound for concrete pipe service life. If this lower bound value is used in life cycle cost analysis, lower bound service lives must be used for all other materials.
4. Site inspections should be performed at each culvert site to gather data for estimating the service lives of various candidate materials in life cycle cost analysis. This can easily be done during preliminary site surveys.

REFERENCES

1. D. G. Meacham, J. O. Hurd, and W. W. Shisler. *Ohio Culvert Durability Study. ODOT/L&D/82-1*, Ohio Department of Transportation, Columbus, Ohio, 1982.
2. J. O. Hurd. Field Performance of Concrete Pipe Culverts at Acidic Flow Sites in Ohio. In *Transportation Research Record 1008*, TRB, National Research Council, Washington, D.C., 1985, pp. 105–108.
3. *Concrete Pipe Handbook*. American Concrete Pipe Association, Vienna Va., 1980.
4. F. C. Hadipriono. *Durability Study of Concrete Pipe Culverts, Service Life Assessment*. Ohio State University, Columbus, Ohio, 1986.
5. R. F. Stratfull. *A Review of the Maine Department of Transportation Report—Durability of Drainage Structures*. Corrosion Engineering, Inc., Sacramento, Calif., 1983.
6. M. Bealey. Precast Concrete Pipe Durability: State of the Art. Author's Closure. In *Transportation Research Record 1001*, TRB, National Research Council, Washington, D.C., 1984, pp. 93–94.
7. *Study of Use, Durability, and Cost of Corrugated Steel Pipe on the Missouri Highway and Transportation Department's Highway System*. Report MR 87-1, Missouri Department of Highways and Transportation, Springfield, 1987.
8. *Tentative Specification for Reinforced Concrete Culvert Pipe*. ASTM C76- 30T, American Society for Testing and Materials, Philadelphia, Pa., 1930.
9. *Standard Specification for Reinforced Concrete Culvert, Storm Drain, and Sewer Pipe*. ASTM C76-57, American Society for Testing and Materials, Philadelphia, Pa., 1957.
10. *Standard Specification for Reinforced Concrete Culvert, Storm Drain, and Sewer Pipe*. ASTM C76-83, American Society for Testing and Materials, Philadelphia, Pa., 1983.

ACKNOWLEDGMENTS

This study was funded by the Ohio Department of Transportation. The findings and opinions expressed therein are those of the author and do not constitute a standard or specification.

DISCUSSION

FABIAN C. HADIPRIONO, RICHARD L. LAREW, AND BENJAMIN LAWU

Department of Civil Engineering, Ohio State University, Columbus, Ohio 43210.

In the paper, Hurd demonstrates the development of prediction equations for determining the service life of concrete pipe culverts in Ohio. Unfortunately, his paper is erroneous both technically and conceptually.

FATAL CONCEPTUAL ERROR IN SERVICE LIFE PREDICTION

Given Hurd's equation, the estimated pH of the flow, the slope, and the rise of a culvert, an engineer can easily calculate the service life of a culvert. We regret that it is not possible to predict the age of concrete pipe culverts using his equations.

When estimating the parameters for his Equation 5, the regression method used by Hurd assumes that the log of age is independent of the log of sediment depth, the log of rise, the log of pH, and the log of slope. Hurd solves Equation 5 to find an equation for predicting age. Using the age prediction equation, he sets rate = 95 to obtain his Equation 6.

This is a fatal error because in Equation 6 the age of concrete pipe culverts is given as a function of the four variables: sediment depth, rise, pH, and slope. But age cannot depend on these variables in Equation 6 and at the same time be independent of these variables in Equation 5. His service life equation must not be used for predicting a particular culvert, and therefore should be rejected.

RESULTS CANNOT BE REPLICATED

Using Hurd's data for pH less than 7, we tried to replicate his method to obtain his Equation 5 for predicting the pipe rate. However, we are unable to obtain the same results for the parameters of this equation. Our parameter estimates of Equation 5 are compared with Hurd's estimates in the following table:

Parameter Descriptions	*Our Estimates*	*Hurd's Estimates*
Constant or intercept	7.798	6.50
Exponent of age	0.576	0.55
Exponent of rise	0.957	1.08
Exponent of slope	0.173	0.23
Exponent of (1 − sediment/rise)	1.659	1.46
Exponent of pH	−2.885	−3.08

Furthermore, we are unable to reproduce Hurd's Figure 7 (Log-linear projected service life for inspected culverts). Using

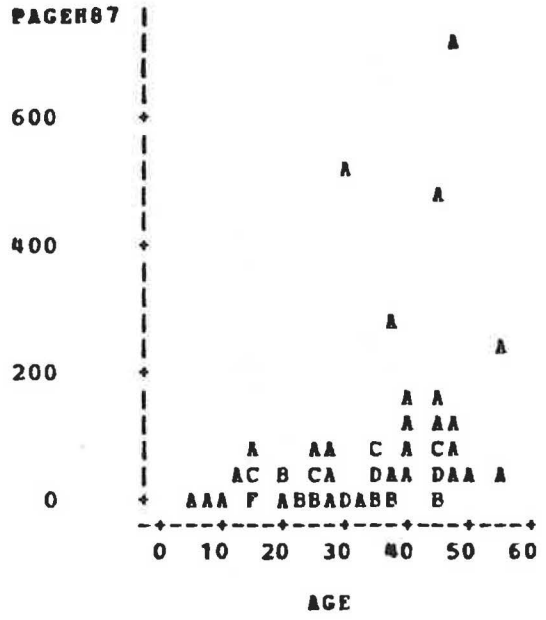

FIGURE 8 Observed sediment depths and rates.

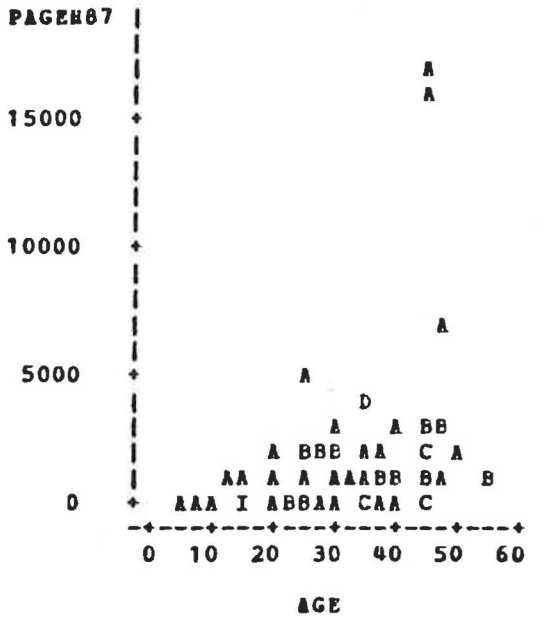

FIGURE 10 Observed sediment depths, rates equal to 95.

his equation for pH values of less than 7, we do not get the same picture. Because he does not find an equation for pH values greater than 7, we have no idea how he plots the service lives in this pH range.

UNACCEPTABLE PREDICTION EQUATION

Replicating Hurd's Equation 6 but using our parameters from the table shown in the preceding section of this discussion, we substituted the observed ratings and sediment depths to plot the relation between the predicted age and the age of the culverts. This relation (PAGEH87 versus Age) for pH less than 7 is shown in Figure 8. Here it can be seen that, despite the fact that none of the culverts in the data set are more than 60 years old, according to Hurd's approach many of these culverts would be predicted to be several hundred years old (about 30 percent of the predicted ages are more than the oldest culverts in the sample). Shown in Figure 9 is the same relation but for sediment depths set to 0 and ratings set to 95. Note that Hurd uses 95 to indicate the terminal condition of the culverts. The results show that the predictions range up to nearly 3,500 years. We also tried to use Hurd's Equation 6 but this results in even larger and unacceptable predicted

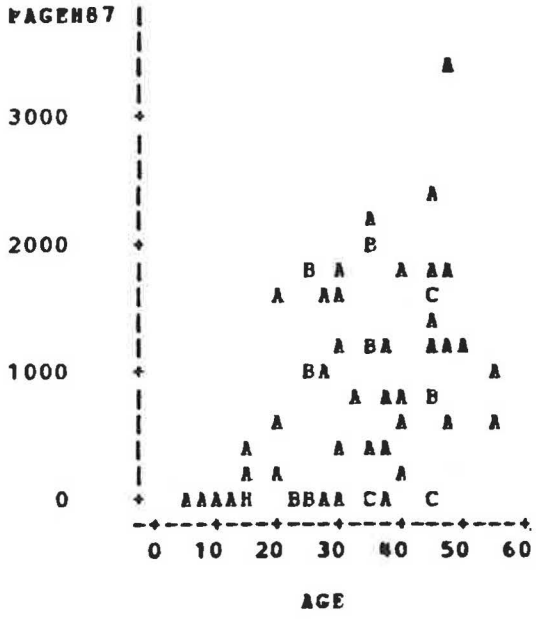

FIGURE 9 Sediment depths equal to 0 and rates equal to 95.

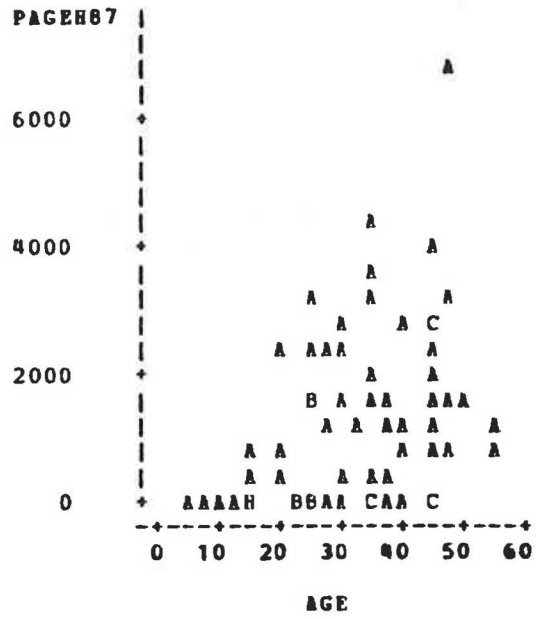

FIGURE 11 Sediment depths equal to 0 and rates equal to 95 (Hurd's Equation 6).

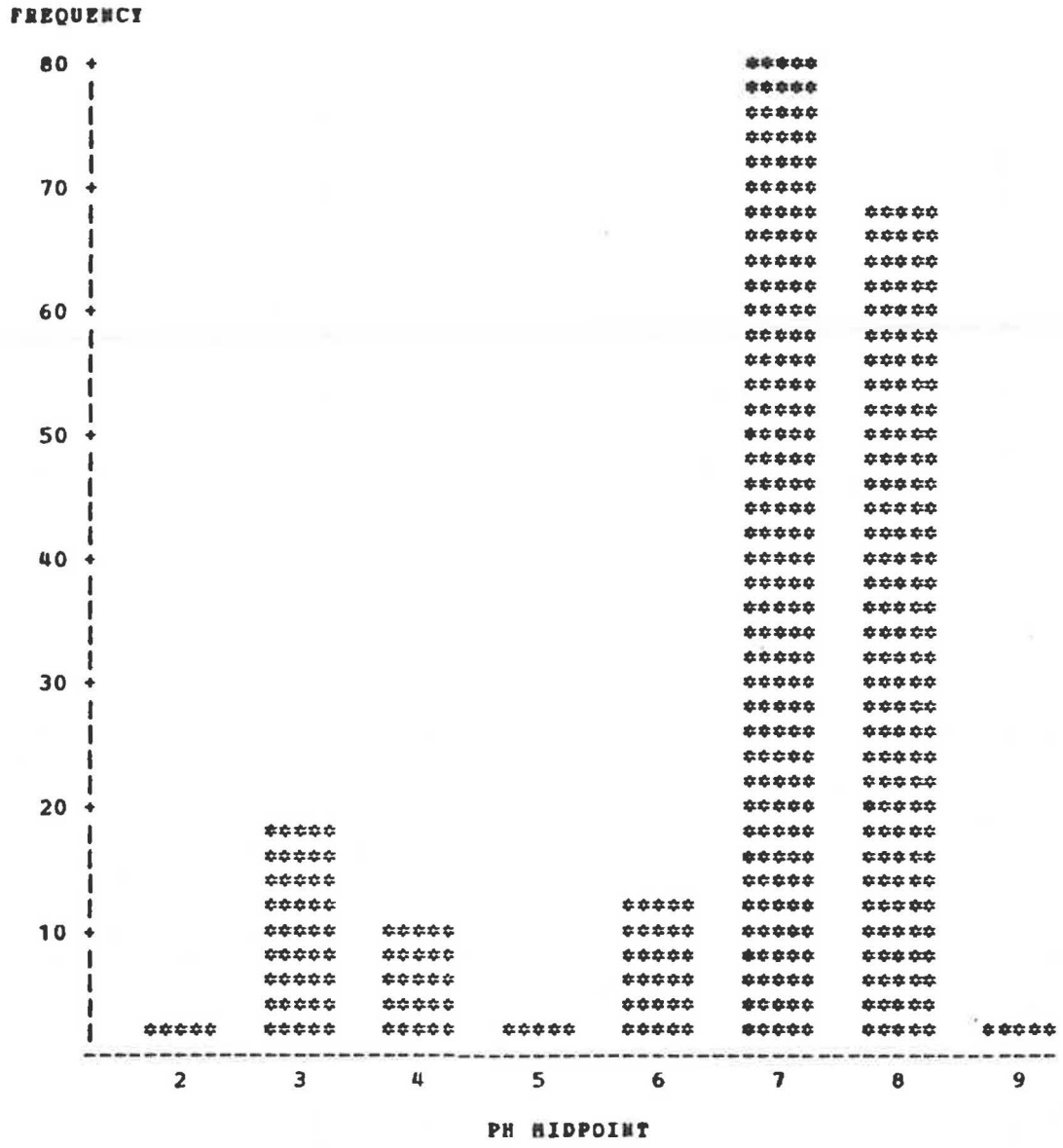

FIGURE 12 Frequency bar chart of pH values.

ages. Predicted ages using observed sediment depths and rate equal to 95 are shown in Figure 10. Sediment depths equal to 0 and rate equal to 95 are used in Figure 11. We reject these predictions.

SAMPLE DATA NOT REPRESENTATIVE

We suspect that another problem in this study is that the sample data are not representative of culverts in Ohio. A binodal sample distribution of pH values of the observations is shown in Figure 12. We expect a continuous uninodal distribution. The relation of age and pH values of the samples are shown in Figure 13, indicating a "boxing" of ages above pH = 7, as well as the lack of observations in the pH = 6 region.

To reduce the variability of prediction errors, we believe that more information is needed about each culvert. This has been addressed in our recent paper (*1*).

REFERENCE

1. F. C. Hadipriono, R. E. Larew, and O-H. Lee. Service Life Assessment of Concrete Pipe Culverts. *Journal of Hydraulic Engineering*, ASCE, Vol. 114, No. 2, 1988, pp. 209–220.

AUTHOR'S CLOSURE

Although the author believes that the commentary presented by the discussants from Ohio State University is not applicable to this paper, he will nonetheless briefly address their concerns.

First, the discussants imply that Equation 6 is not a true valid statistical regression equation. However, nowhere in this

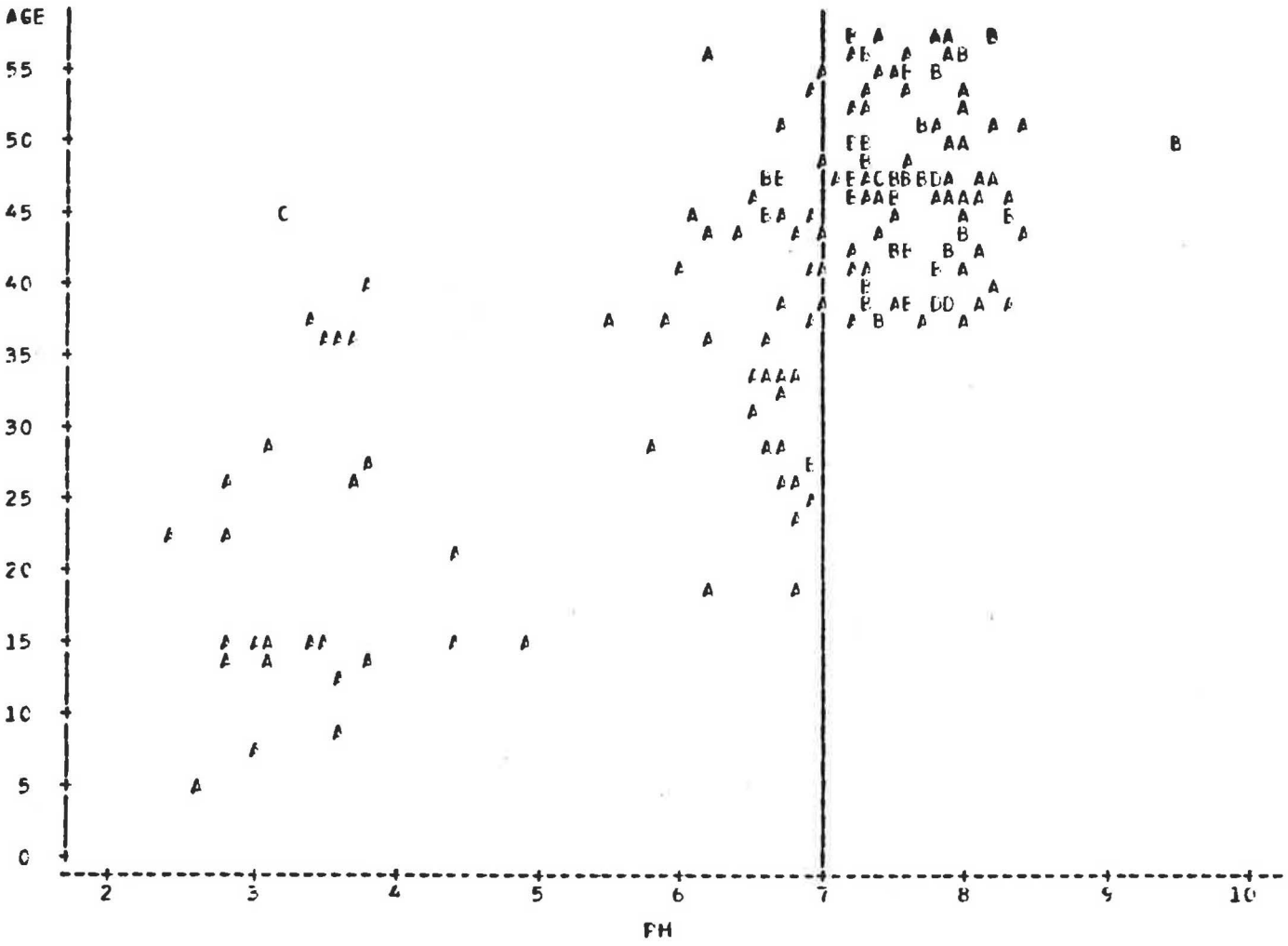

FIGURE 13 Plot of age versus pH.

report or the author's other referenced work was it ever implied that Equation 6 is a statistical regression equation that would produce true average service life for a given set of site conditions. To determine a true average service life for a given set of site conditions, it would be necessary to wait for all concrete culverts installed at sites with those conditions to deteriorate to a specified failure condition, which would not be practical. However, some method of estimating concrete pipe service life is required so that it can be compared with the various available estimates of corrugated metal pipe service life.

Equation 6 is simply a mathematical expression for the mathematical mechanics necessary to produce an estimated median service life value for a given set of environmental conditions. That method is to extrapolate a median deterioration rate from a statistical regression equation containing age and environmental parameters out to a specific failure value and to determine the age required to obtain that value for that set of environmental conditions.

This method is consistent with that used by ODOT to estimate median service life for corrugated metal pipe using the models in "The Ohio Culvert Durability Study" (*1*). These particular models were under review by representatives of the National Corrugated Steel Pipe Association for more than a year before publication without any comment being issued by the Association. The method is also consistent with the methods used to establish the corrugated metal pipe median service life curves from the California report, which is endorsed by the National Corrugated Steel Pipe Association and the American Iron and Steel Institute. In "Durability Study of Concrete Pipe Culverts; Service Life Assessment," Hadipriono indicates that the linear model can be used to estimate median service life by the same methodology ["The service life is determined by obtaining age from Equation 7, given PRate = 4.5 in." (*4*, *p. 36*)].

Second, the discussants claim that they cannot replicate the results. The author does not know why unless there have been transcription errors made in the half dozen or so transcriptions of the data since it was entered in ODOT's computer program. If transcription errors were caused by the action of ODOT, the author apologizes. However, the original coded data set, program, and printout are available at ODOT. To demon-

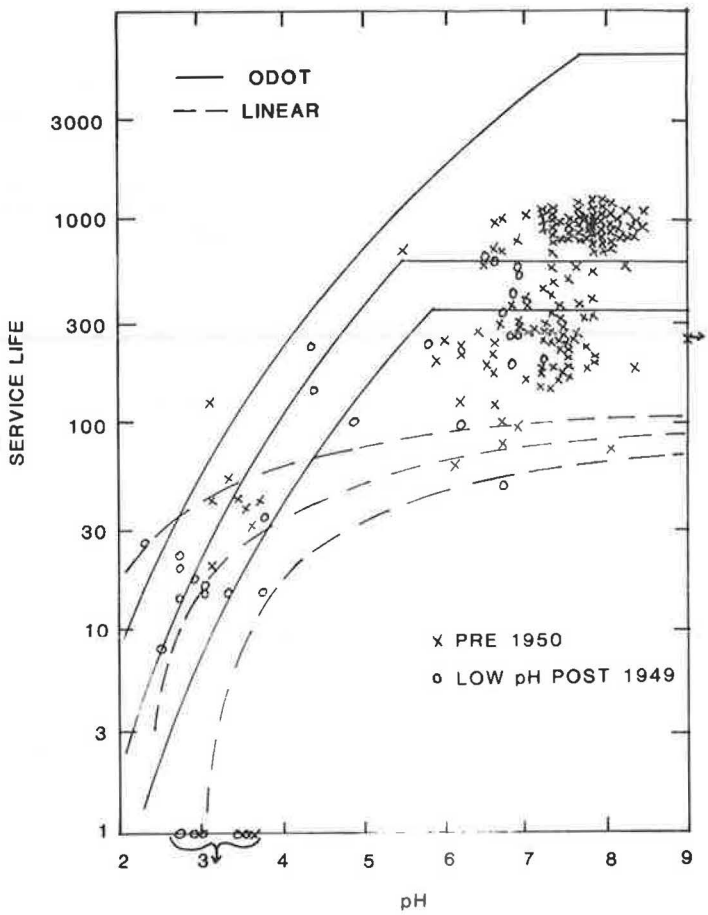

FIGURE 14 Linear projected visual fit service life for inspected culverts.

strate that end results are reproducible, one need only observe the median service life curves in Figures 1 and 3 of Transportation Research Record 1008 (*2*). Here two models developed with different data sets and rating systems produce similar curves. They diverge somewhat at the higher pH values. However, it should be noted that the ODOT service life curves (see Figure 4) cut off this model at higher pH values.

Third, the discussants back calculate estimated values of age using values of rating and other independent variables of the data set to show that the same values of age are not obtained and a large scatter exists outside the original age range of the data. Back calculation to obtain estimated values of any independent variable in any regression equation will produce values outside the original range of values of that independent variable. This is true of both linear and log-linear models. Although log-linear models will tend to produce some rather large outliers from back calculations, median values obtained should still be accurate. Back calculation of the discussants' linear regression model to estimate age will produce negative values of this variable. Back calculation to estimate pH values in the linear model [that uses the log (pH) as an independent variable] produces pH values 2 to 3 units different from actual, which are 100 to 1,000 times more acidic. These results are certainly no less reasonable.

Fourth, the discussants question whether the data sets used in the reports are representative of field conditions in Ohio. This seems presumptuous, because they have never conducted field inspections of any of the culverts used for the data sets. When field data is to be collected, what is there is what is collected, and the researcher does not have the liberty of sitting in an office creating a data set with a perfect distribution of all independent variables.

It appears that the underlying current of all Ohio State University's work in this case is to try to show that because true mean service life values cannot be obtained, life cycle cost analysis or other service life comparisons cannot be made. If that is true, then the designer must specify a minimum guaranteed (bonded) service life for each type of material specified. This service life should be based on the length of time the culvert is to serve drainage needs and not merely the life of the roadway until rehabilitation is needed.

What the discussants have actually done is to take the time to attack a previous work of the author without providing any evidence refuting the logic and findings of this report. That

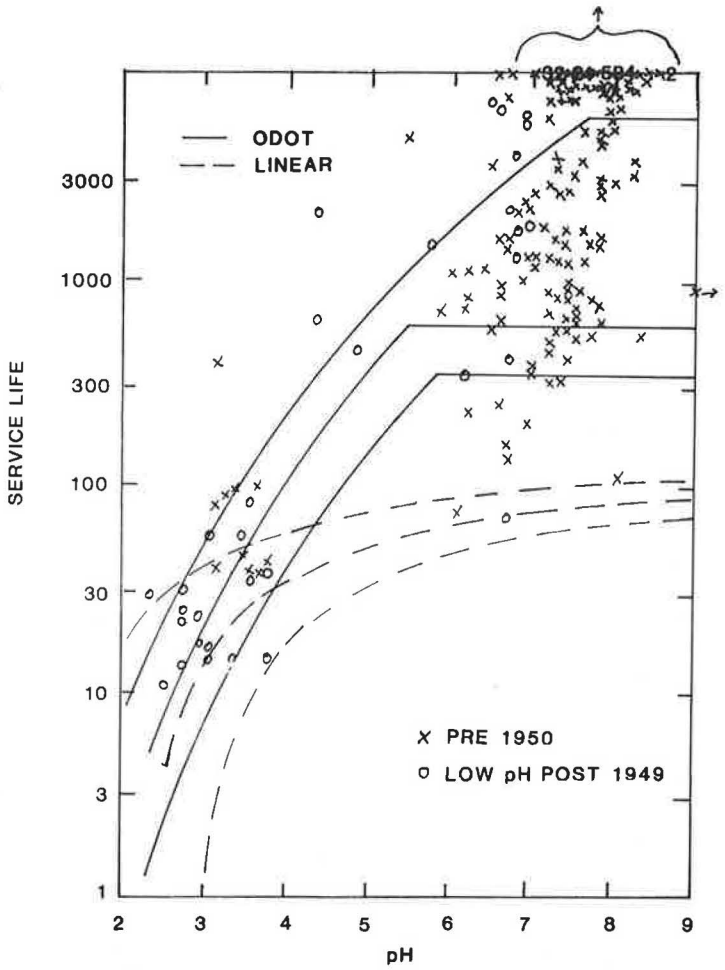

FIGURE 15 Log-linear projected visual fit service life for inspected culverts.

finding is that the data collected at the oldest concrete pipe culvert sites in Ohio clearly indicate that median service life values calculated by using the Ohio State University linear model are gross underestimates.

If the reader does not trust either regression model, the reader may use visual line fitting of a median line on Figure 6 to provide a very conservative estimate of median concrete pipe service life for all conditions (see Figure 14). This is based on the discussants' erroneous assumption of a linear relation of age to the deterioration rating. This was shown in the paper to be extremely conservative. A less conservative estimate could be obtained using Figure 7 (see Figure 15).

Publication of this paper sponsored by Committee on Culverts and Hydraulic Structures.

Culvert Durability Rating Systems

JOHN M. KURDZIEL

The culvert condition rating systems used in durability studies conducted by various private, state, and federal agencies are reviewed in this paper. The rating scales used in these studies were analyzed and compared. A new material durability rating system for both metal and concrete pipe is proposed based on these comparisons. The rating scale corresponds to the one used by the National Bridge Inventory and Inspection Program. The new system will ensure that all types of culvert materials are uniformly rated in every study and will promote the development of a comprehensive data base on the durability of each product material.

The durability of culverts has been studied at great length over the past four decades. Many states at one time or another have conducted at least one study of metal or concrete culverts. Unfortunately, most results have been inconclusive or controversial. Site conditions have an significant effect on how long a facility will last. Product materials react differently in various environments because of inherent strengths and weaknesses. Pipe manufacturers, federal, state, and local government agencies, and consultants all have different opinions on the expected service life of culvert materials and the effects of site conditions.

Durability studies conducted to date have not used a common rating system, instead most have developed their own. This does not present any particular problem to the agency conducting the study but does create problems of correlating information from various studies into a comprehensive assessment of a particular product's qualities and durability in different environments.

Information and ratings from one study seldom correspond directly with those of another, resulting in conflicting data and possible misinterpretation of the information. The answer to these problems is a standard rating system for inspecting and evaluating the condition of the various types of culvert products. A standard rating system would ensure that all culverts were rated identically, end the guess work of correlating studies, eliminate the time and effort of developing rating systems, and eventually provide a comprehensive data basc on the durability of each product material. With a standard rating system, various studies could be analyzed to provide guidance on product service lives.

Evaluated in this paper are current state and federal culvert durability rating systems and clarifications are developed to facilitate the use of the Federal Highway Administration (FHWA) *Culvert Inspection Manual* (*1*).

American Pipe Association, 8320 Old Courthouse Road., Vienna, Va. 22180.

FHWA *CULVERT INSPECTION MANUAL*

The Federal Highway Administration presents standard guidelines in their *Culvert Inspection Manual* (*1*). This publication is a stand-alone supplement to the *Bridge Inspector's Training Manual 70* (*2*). The manual is a unique and valuable tool in that it is the first publication to interrelate reporting procedures, rating systems, and component evaluations. The primary objective of the manual is to provide information that will enable users to do the following tasks:

1. Properly inspect an existing culvert,
2. Evaluate structural adequacy,
3. Evaluate hydraulic adequacy and recognize potential flood hazards,
4. Rate the condition of the culvert,
5. Document the findings of a culvert inspection,
6. Recognize and document traffic safety conditions, and
7. Recommend corrective actions.

To meet these objectives, recommendations are made in the manual for procedures for conducting, reporting, and documenting a culvert inspection, and guidelines for inspecting and rating specific hydraulic and structural culvert components are also provided. Major culvert components, such as shape, joints, seams, footings, and material conditions for metal pipe, and alignment, joint, material, and footing conditions for concrete pipe are described and evaluated to assist the inspector in identifying common types of culvert distress and recognizing their significance. Detailed provisions and guidelines are provided for each type of metal and concrete pipe configuration (Tables 1 and 2).

Recommended in this paper are changes in the assessment and rating of material durability conditions for metal and concrete pipe to improve inspection procedures and evaluation of data. Although distress conditions of both materials are presented in the manual in a systematic and well-structured way, a greater degree of detail is necessary in the condition descriptions to ensure that unique characteristics and features are associated with each rating number in order to eliminate subjective interpretation by an inspector.

Slight modifications to the culvert rating system will be based on the information contained in the durability studies from the various states analyzed. The proposed rating of material evaluations, based on the system used in the *Bridge Inspectors Training Manual 70* (*2*), is as follows:

Rating	*Description*
9	New condition.
8	Good condition–no repairs necessary.
7	Generally good condition–potential exists for maintenance
6	Fair condition–potential exists for major maintenance.
5	Generally fair condition–potential exists for minor rehabilitation.
4	Marginal condition–potential exists for major rehabilitation.
3	Poor condition–repair or rehabilitation required immediately.
2	Critical condition–the need for repair or rehabilitation is urgent. Facility should be closed until the indicated repair is complete.
1	Critical condition–facility is closed. Study should determine the feasibility for repair.
0	Critical condition–facility is closed and is beyond repair.

RATING SYSTEMS

Culvert rating systems included in available state durability reports and federal agency publications, as well as pertinent Transportation Research Board papers, were examined. A list of the 151 references resulting from the literature search is available from the author. Discussion in this paper is limited to those studies that reflect current practices in each region of the country (Figure 1).

There are a number of methods used for analyzing culvert durability. Studies based on percent of metal or concrete loss provide documentation on the actual pipe wall thickness and the rate of deterioration, but may not present an accurate assessment of the culvert's overall condition. Concrete and metal loss cannot be rated in a linear fashion. Once abrasion and corrosion forces start to pit the surface of the metal, the area exposed to corrosion is increased and the rate of metal loss accelerates. Ratings of 20 to 30 percent metal loss do not portray the actual severity of the installation's condition (Table 3). A culvert with its zinc coating lost, metal heavily corroded and pitted, and a quarter of its thickness gone was not considered indicative of a facility in good condition by any of the other studies examined. Similarly, if 50 percent of a concrete pipe wall had deteriorated, it could represent a much more serious problem than a linear rating would indicate. A rating system should take these effects into consideration.

TABLE 1 FEDERAL HIGHWAY ADMINISTRATION'S CULVERT INSPECTION RATING GUIDELINES FOR CORRUGATED METAL CULVERT BARRELS (*1*)

Rating Guidelines for Round or Vertical Elongated Corrugated Metal Pipe Barrels

Rating	Condition
9	• New Condition
8	• *Shape*: good, smooth curvature in barrel - *Horizontal*: within 10 percent of design • *Seams and Joints*: tight, no openings • *Metal*: - *Aluminum*: superficial corrosion, slight pitting - *Steel*: superficial rust, no pitting
7	• *Shape*: generally good, top half of pipe smooth but minor flattening of bottom - *Horizontal Diameter*: within 10 percent of design • *Seams or Joints*: minor cracking at a few bolt holes, minor joint or seam openings, potential for backfill infiltration • *Metal*: - *Aluminum*: moderate corrosion, no attack of core alloy - *Steel*: moderate rust, slight pitting
6	• *Shape*: fair, top half has smooth curvature but bottom half has flattened significantly - *Horizontal Diameter*: within 10 percent of design. • *Seams or Joints*: minor cracking at bolts is prevalent in one seam in lower half of pipe. Evidence of backfill infiltration through seams or joints. • *Metal*: - *Aluminum*: significant corrosion, minor attack of core alloy - *Steel*: fairly heavy rust, moderate pitting
5	• *Shape*: generally fair, significant distortion at isolated locations in top half and extreme flattening of invert - *Horizontal Diameter*: 10 percent to 15 percent greater than design • *Seams or Joints*: moderate cracking at bolt holes along one seam near bottom of pipe, deflection of pipe caused by backfill infiltration through seams or joints. • *Metal*: - *Aluminum*: significant corrosion, moderate attack of core alloy - *Steel*: scattered heavy rust, deep pitting
4	• *Shape*: marginal significant distortion throughout length of pipe, lower third may be kinked - *Horizontal Diameter*: 10 percent to 15 percent greater than design • *Seams or Joints*: Moderate cracking at bolt holes on one seam near top of pipe, deflection caused by loss of backfill through open joints • *Metal*: - *Aluminum*: extensive corrosion, significant attack of core alloy - *Steel*: extensive heavy rust, deep pitting
3	• *Shape*: poor with extreme deflection at isolated locations, flattening of crown, crown radius 20 to 30 feet - *Horizontal Diameter*: in excess if 15 percent greater than design • 3 in. long cracks at bolt holes on one seam • *Metal*: - *Aluminum*: extensive corrosion, attack of core alloy, scattered perforations - *Steel*: extensive heavy rust, deep pitting, scattered perforations
2	• *Shape*: critical, extreme distortion and deflection throughout pipe, flattening of crown, crown radius over 30 feet - *Horizontal Diameter*: More than 20 percent greater than design • *Seams*: plate cracked from bolt to bolt on one seam • *Metal*: - *Aluminum*: extensive perforations due to corrosion - *Steel*: extensive perforations due to rust
1	• *Shape*: partially collapsed with crown in reverse curve • Seams: failed • *Road*: closed to traffic
0	• *Pipe*: totally failed • *Road*: closed to traffic

NOTE: See Coding Guide for description of Rating Scale. As a starting point, select the lowest rating that matches actual conditions.

TABLE 2 FEDERAL HIGHWAY ADMINISTRATION'S CULVERT INSPECTION RATING GUIDELINES FOR CONCRETE CULVERT BARRELS (*1*)

Rating Guidelines for Precast Concrete Pipe Culvert Barrels			
Rating	Condition	Rating	Condition
9	• New condition		
8	• *Alignment*: good, no settlement or misalignment • *Joints*: tight with no defects apparent • *Concrete*: no cracking, spalling, or scaling present; surface in good condition	4	• *Alignment*: marginal; significant settlement and misalignment of pipe; evidence of piping; end sections dislocated about to drop off • *Joints*: differential movement and separation of joints, significant infiltration or exfiltration at joints • *Concrete*: cracks open more than 0.12 in. with efflorescence and spalling at numerous locations; spalls have exposed rebars which are heavily corroded; extensive surface scaling on invert greater than 0.5 in.
7	• *Alignment*: generally good; minor misalignment at joints; no settlement • *Joints*: minor openings, possible infiltration/exfiltration • *Concrete*: minor hairline cracking at isolated locations; slight spalling or scaling present on invert		
6	• *Alignment*: fair, minor misalignment and settlement at isolated locations • *Joints*: minor backfill infiltration due to slight opening at joints; minor cracking or spalling at joints allowing exfiltration • *Concrete*: extensive hairline cracks, some with minor delaminations or spalling; invert scaling less than 0.25 in. deep or small spalls present.	3	• *Alignment*: poor with significant ponding of water due to sagging or misalignment pipes; end section drop off has occurred • *Joints*: significant openings, dislocated joints in several locations exposing fill materials; infiltration or exfiltration causing misalignment of pipe and settlement or depressions in roadway. • *Concrete*: extensive cracking, spalling, and minor slabbing; invert scaling has exposed reinforcing steel
5	• *Alignment*: generally fair; minor misalignment or settlement throughout pipe; possible piping • *Joints*: open and allowing backfill to infiltrate; significant cracking or joint spalling • *Concrete*: cracking open greater than 0.12 in. with moderate delamination and moderate spalling exposing reinforcing steel at isolated locations; large areas of invert with surface scaling or spalls greater than 0.25 in. deep	2	• *Alignment*: critical; culvert not functioning due to alignment problems throughout • *Concrete*: severe slabbing has occurrerd in culvert wall, invert concrete completely deteriorated in isolated locations
		1	• *Culvert*: partially collapsed • *Road*: closed to traffic
		0	• *Culvert*: total failure of culvert and fill • *Road*: closed to traffic

NOTE: See Coding Guide for description of Rating Scale. As a starting point, select the lowest rating that matches actual conditions.

FIGURE 1 Location of study reports, indicated by shaded areas.

TABLE 3 CALIFORNIA STATE RATING SYSTEM (*3*)

Rating	Metal Loss (%)	Water	Air Splash	I (inside)	O (outside)	Soil	Abrasion
0	0						
1	10						
2	20						
3	30						
4	40						
5	50	Designates metal loss in the culvert due to the various corrosion components.					
6	60						
7	70						
8	80						
9	90						
10	100						

In some studies, sample coupons from field installations were used to determine the metal thickness and were the main basis on which the condition of the facility was rated (Table 4). A major problem with ratings systems based on coupons is the lack of correlation between coupons and field ratings. Coupons may not include perforations, or coating blisters, or thickness loss that may otherwise be observed in field inspections.

Rating systems based on visual observations are more subjective than the precise techniques used for measuring the pipe wall thickness, however they are more indicative of a culvert's overall performance. Visual condition ratings should be based on the worst area observed in the culvert because this will be the most likely point of failure. A uniform rating system should, therefore, be based on visual ratings with detailed descriptions of the culvert's conditions and should include measurements where appropriate.

The first step in developing a comprehensive durability rating system is to examine available studies, analyze the rating systems, and prepare a rating table that most closely reflects the conditions considered by the majority. On the surface this may appear to be a straightforward task, but most studies have a unique goal that is reflected in the rating table. Rating tables also vary in evaluation of condition ratings. What one study considers a poor rating may be a fair or critical rating for another. The range of ratings may also be restricted by the numbering system used. More broad numbering systems provide more latitude in rating a structure but they may, however, prove to be cumbersome if too large. A 0 to 100 scale, although allowing the rater more room for assessment than a 1 to 5 scale, is meaningless to the rater and reviewer if evaluations are other than increments of 10. A scale of 1 to 10 seems to provide the best compromise between maximum flexibility in rating and maintenance of a distinct significance in each number.

Although a scale based on 10 allows easy conversion of many studies and direct correlation to percentages, it does not correspond to the most widely used and accepted rating scale based on 9, which is used in the National Bridge Inspection Program. By using the bridge program's 0 to 9 scale, culvert inspections will follow a national program already in force. The use of an established rating system would make adoption and use of culvert guidelines easier, because no changes to the current bridge system would be necessary and inspectors would already be familiar with the rating scale. A common system would help promote more culvert reviews and result in larger data bases on pipe products.

METAL CONDITION RATING SYSTEMS

The condition rating scales for corrugated metal pipe from the various state studies are presented in Table 5. There is no distinction made between steel and aluminum in the tables because, regardless of actual durability characteristics, the distress conditions are essentially identical. All state rating scales have been adjusted to conform to the 0 to 9 scale. For comparison purposes, the studies were arranged on the scale according to their original condition guidelines. State condition ratings for metal culverts were similar in the top values of 9 and 8. Once a metal culvert had deteriorated past superficial rust, there was little agreement on the rating, and most studies did not show a uniform systematic progression of deterioration. Rating conditions jumped dramatically from "pinpoint rust" to "heavy pitting rust," with very little, if any, guidance given to evaluate conditions between these extremes. Rating descriptions were also not quantitative. Describing a condition as simply "moderate signs of deterioration" does not adequately explain the condition. Specific degrees of deterioration should be listed such as depth of rust, degree of pitting, and amount of thinning of the metal.

The severity placed on the first sign of perforation was somewhat uniform and represented a critical rating: 1 or 0,

TABLE 4 COUPON RATINGS SYSTEMS

Rating Scale	Idaho (*4*)[a] Metal	Colorado (*5*)[b] Metal	Concrete
5	Like new	No visible corrosion	No apparent change except slight staining
4	Dull: age weathered to the point all zinc luster gone	Light salt deposit or rusting, blistering near edges	Light pitting and/or salt deposits
3	Pinpoint rust: evidence of rust in very small areas	Mild salt deposit or rusting, blistering near edges	Moderate loss of surface mortar and salt accumulation
2	Scale rust: large areas of rust wherein scale can be seen	Extensive rusting and formation of blisters	Moderate loss of aggregate
1	Pitting: rusted to the extent base metal is pitted	Severe corrosion or rusting	Extensive aggregate loss, swelling and/or warping of coupon
0		Very severe rusting or loss of adhesion of protective coating	Total failure of coupon

[a] From field installations, used reverse scale in report.
[b] Based on coupons exposed to environmental conditions.

TABLE 5 STUDIES ON METAL CONDITION RATINGS

RATING	FLORIDA (6)	KANSAS (7)	CALIFORNIA (LA COUNTY) (8)	LOUISIANA (9)	MAINE (10)	MICHIGAN (11)	MINNESOTA (12)	MISSISSIPPI (13)
9		No corrosion - Galvanizing intact.	No corrosion.	No signs of deterioration.	Approaching Original Condition (Galvanizing intact)			
8	Galvanizing intact.		Superficial corrosion. Discoloration of surface, red or black scale lightly adhering to surface.			Galvanizing intact.	Spelter entirely intact.	Spelter entirely intact.
7		Superficial rust (edges and bolt heads) - No pitting; weathered to point all zinc luster gone.	Slight corrosion. Some loss of zinc coating, thin flaking and shallow pitting of surface.	Very slight signs of deterioration and pitting.	Superficial Rust (no pitting).			
6	(+) Galvanizing partly gone, some surface rust.					(+) Galvanizing partly gone, some rust.	(+) General pinpoint rust.	(+) Spelter just gone and thin rust beginning to form in places, no abrasion and no pitting.
5		Moderate rust - Rust flakes light, minor pitting.	Moderate corrosion. Deep pitting of surface.	Moderate signs of deterioration and pitting.	Moderate Rust (minor pitting).			
4	(+) Galvanizing gone. Significant metal loss (about 25%).					Galvanizing gone, significant metal loss.	Heavy pitting rust.	Complete loss of spelter and considerable loss of metal in invert. Pitting and some abrasion.
3		(+) Fairly heaving rusting - Rust flakes light, moderate pitting, but metal is sound.	Heavy corrosion. Build-up of laminations of rust scale.		(+) Fairly Heavy Rust (moderate pitting, metal sound).			
2	Deep pitting, heavy metal loss, first perforation visual or under blows of spike (at least 50% metal loss).			Extreme signs of deterioration and pitting.		Deep pitting, heavy metal loss, metal can be perforated with a sharp metal probe.	Heavy pitting rust and loss of metal in invert.	Decided pitting and abrasion. Heavy loss of metal in invert.
1	Complete metal loss in about 1/2 area of maximum corrosion in invert.	(+) Heavy rusting - Rust flakes easily removed - Deep pitting into base metal.	Heavy corrosion. Beginning to perforate.		(+) Heavy Rust (deep pitting and some perforation).		Start of perforations.	Metal corroded and abraded through invert in small spots. Very heavy rust and deep pitting in general over invert.
0	Metal gone, full width of area of maximum corrosion.	Heavy rust - Deep pitting and unsound or perforated areas. Unsound areas easily perforated with pick end of geologist hammer.	Perforated.	Signs of complete deterioration, and the pipe is no longer useful as a drainage tool.	Unsound Areas (extensive perforation to bottom completely deteriorated).	Metal perforated.	Entire invert gone.	Entire invert gone.

(+) Indicates intermediate rating - condition may also correspond to the next highest rating.
* National Corrugated Steel Pipe Association.

in all cases. The exact uniform and represented a critical rating: 1 or 0, in all cases. The exact point of failure, however, varied for each study. Some considered this point to be the first perforation, others considered it the deterioration of the entire invert or the collapse of the facility.

Each study concentrated on a unique durability feature, with most increasing the number of rating descriptions as the facility neared failure. One notable exception was the Ohio report. The upper half of the ratings are very distinct and clear for conditions representing "excellent" to "fair" facilities. The "poor" rating, however, constitutes one condition description and dominates the entire lower half of its rating system. There is a great deal of deterioration that must take place for a facility to go from a "fair" condition, which constitutes heavy rust and scale with no penetration, to a "poor" condition, which has the invert gone. The poor rating in this case is too large to be of benefit to an evaluator interested in the lower range of conditions approaching failure. The Ohio report, however, recognized the limitations of the rating system used. The predictive equations developed were based solely on measured metal loss.

The use of the broad "poor" category was reasonable in this case because they were not concentrating on predicting failure by means of evaluating metal ratings but only on identifying those installations that were considered in poor condition. The Ohio report is noteworthy because it illustrates the importance of understanding the concentration and scope of the study before reviewing its data.

The Ohio study also highlights another problem with ratings systems that are skewed heavily in one direction. Reviewers of a rating scale may assume that there is a linear relationship for each of the rated conditions. In the case of the Ohio report and many other studies, this observation would lead to estimation of deterioration to failure sooner than it would actually occur. Care must be taken to review the rating scale and conditions before using and comparing data from a particular study.

The proposed metal rating system in Table 6 provides a detailed and unique description for each rating from new to failure. Incorporated in this table are all changes and additions to the metal rating descriptions in the FHWA *Culvert Inspection Manual* (*1*). The intent was to provide a rating system that is easy to understand and has logical increments of deterioration. Major conditional features identified include galvanizing, level of rust, depth of pitting, metal thinning, and degree of perforations. The ratings in the state studies were adjusted to reflect the facility condition ratings described in the bridge rating scale. The effect was the consolidation of

TABLE 5 *continued*

RATING	OHIO (14)	OKLAHOMA (15)	OREGON (16)	TENNESSEE (17)	WASHINGTON (18)	NCSPA (19)
9	Condition as constructed, no apparent loss of galvanizing (Excellent).	Culvert shows absence of only minor amounts of thin rust coatings present as spots or patches of less than one inch diameters. Spelter intact, even in the invert area. Geology Hammer: hard blows will not penetrate (Excellent).	Zinc like new.		Spelter like new	
8	Discoloration but no scaling or corrosion (Very Good).		Zinc dull to very dull.	Spelter entirely intact	Spelter dull to very dull	Spelter intact - spangles visible
7	Slight to and scale, pitting just started, isolated spots of moderate corrosion (Good).	Thin continuous coatings of rust in invert area. Spelter absent in invert area. Some small blisters (scale) occasionally present. Geology Hammer Hard blow will not penetrate (Good)	Pinpoint rust spots, zinc entirely gone		Pinpoint rust spots spelter entirely gone	
6	Moderate to heavy scale and rust, no geologist's hammer penetration, no perforation (Fair).		Light rust film, shallow pitting	(+) General pinpoint rust	Light rust film, shallow pitting	(+) General pinpoint rust
5		Thick and scaling rust coatings, pitting of culvert surface noticeable. Geology Hammer Penetrates with 2-3 hard blows in same area (Fair)	Rust or pits not halfway through core metal.		Rust or pits not halfway through core metal.	
4				Heavy pitting rust.		(+) Heavy pitting rust.
3		Scaling pronounced, pitting of metal surface obvious and widespread. Geology Hammer Perforates with one moderate blow (Poor).	Rust or pits halfway through core metal.		Rust or pits halfway through core metal.	
2	Penetration with geologist's hammer, perforation, loss of invert (Poor).		Rust or pits over halfway through core metal.	Heavy pitting rust and loss of metal in invert.	Rust or pits three-quarters through core metal.	Rust scaling loose.
1		(+) Severe scaling, pitting progresses to perforation. Holes may be any size. The rating of (Pf) will be used until such deterioration has taken place in order to cause failure (Perforation).	Few holes through metal.	Start of perforation.	Few holes through metal.	First small perforation.
0		Culvert is bent, warped, sagged, broken, etc., to such an extent as to cause the culvert not to function as intended (Failure).	Large area of metal gone.	Entire invert gone.	Large areas of metal gone.	Perforations large or beginning to connect so small strip removed.

(+) Indicates intermediate rating - condition may also correspond to the next highest rating.
* National Corrugated Steel Pipe Association.

TABLE 6 METAL CONDITION RATINGS

Rating	Condition	Description
9	Excellent	New condition, galvanizing intact, no corrosion.
8	Very good	Discoloration of surface, galvanizing partially gone.
7	Good	Superficial or pinpoint rust spots, no pitting.
6	Fair	Moderate rust, rust flakes tight, shallow pitting of surface galvanizing gone.
5	Fair—marginal	Heavy rust and scale, moderate pitting and slight thinning of core metal.
4	Marginal	Extensive heavy rust, thick and scaling rust coatings, deep pitting and significant metal loss (approximately 25 percent).
3	Poor	Rust and pitting halfway through core metal (some deflection or penetration when struck with pick or geology hammer).
2	Very poor	Extreme deterioration and pitting, three quarters of core metal gone, first perforations.
1	Critical	Extensive or large perforations.
0	Failure	Invert completely deteriorated, culvert beginning to bend, warp or sag, collapse of the culvert is imminent.

some of the less significant upper ratings and an expansion of the ratings of the more critical factors. The degree of perforations now span over three ratings instead of one or two, as was the case in many of the state scales. They are still considered poor or critical items, but now correspond closer to the depth of rust and pitting, and thinning of the metal.

CONCRETE COALITION RATING SYSTEMS

The concrete condition rating scales from the state studies are illustrated in Table 7. One observation immediately apparent upon reviewing the table is the lack of reports. There have been very few studies on the durability of concrete pipe. Durability problems are rare with highway concrete culverts, and normally the only problem encountered is concrete loss in the invert resulting from acidic effluents such as those in mine drainage areas. The state of Ohio has conducted the most studies on concrete culverts, with concentration on the effects of acid environments on the pipe.

The conditional rating scales for concrete pipe were similar, considering the small data base available for analysis. Deterioration concentrated on the degree of scaling and softness of the concrete. In all but one case, deterioration was described in a distinct and systematic progression. Failure was uniformly

TABLE 7 STUDIES ON CONCRETE CONDITION RATINGS

RATING	KANSAS (7)	MAINE (10)	MISSISSIPPI (13)	OHIO (I) (14)	OHIO (II) (20)
9	Intact - no deterioration.	Approaching original condition.		Condition of concrete as constructed (Excellent)	As manufactured.
8			No weathering or disintegration and no softening from acid or alkali or other causes	Discoloration but no loss corrosion, or softening (Very Good)	Slight loss of mortar, aggregate not exposed.
7	Light scaling - 0-1/8" in depth.	Discoloration, slight (scaling) of mortar, no softening of concrete.		Slight loss of mortar leaving aggregate exposed (Good)	Moderate loss of mortar, aggregate exposed.
6			(+) Some weathering or (scaling) and disintegration. Slight erosion of invert.	Moderate loss of mortar and aggregate, slight softening of concrete (Fair).	Significant loss of mortar around aggregate.
5	Medium scaling - 1/8"-1/4" depth.	Slight scaling of smaller aggregate, no softening.			Significant loss of mortar, slight aggregte loss.
4			(+) Decided disintegration or erosion in invert. General weathering and (scaling). Softening due to alkali or acid.		Moderate aggregate loss (part of first layer).
3	(+) Heavy scaling - Scaling over 1/4" depth.	(+) Moderate (scaling) (loss of mortar and aggregate minor amounts of softening).			Aggregate loss (all of first layer into second layer).
2			(+) Decided disintegration throughout the pipe. Considerable weathering and (scaling). Softening due to alkali or acid.	Significant loss of mortar and aggregates, complete loss of invert, concrete in softened condition (Poor).	Reinforcing exposed at a few places.
1	(+) Heavy scaling - Exposed mesh or rust showing on surface.	(+) Extensive (scaling) of mortar and aggregate plus softening of concrete.	Extreme disintegration and (scaling). Material very soft due to acid or alkali.		Reinforcing exposed throughout pipe.
0	Heavy scaling - Total thickness of pipe deteriorated.	Invert completely deteriorated.	Disintegration through pipe. Reinforcing exposed.		Reinforcing gone.

(+) Indicates intermediate rating - condition may also correspond to the next highest rating.

considered to be complete disintegration of the invert at a rating of 0.

Table 7 contains two Ohio studies and is a good example of the differences between rating systems. The first, Ohio (I), was developed from the same study as the metal rating system. The rating systems were consistent for both metal and concrete in that there was a strong concentration on the conditional ratings for the upper range of the scale and only one for the lower half. A follow-up study, Ohio (II), conducted 3 years later, provided a much more detailed rating system for concrete pipe. Unfortunately, this study did not cover metal pipe and, therefore, no comparable rating scale is available. This scale proved to be one of the most comprehensive rating systems found for concrete pipe.

The proposed concrete rating system in Table 8 provides a detailed and unique description for each rating from new to failure. Changes and additions to the concrete rating descriptions in the FHWA *Culvert Inspection Manual* (*1*) are shown in bold type. The rating system provides logical and progressive increments of deterioration for mortar and aggregate scaling, concrete hardness, and reinforcement condition. As in the case of the metal rating scale, the conditional ratings in the state studies had to be modified and consolidated to conform to the facility condition rating system used in the bridge inspection program.

One major change that was made to the concrete rating scale was the addition of a new intermediate rating condition. Most rating scales reviewed went from first exposure of reinforcing to total deterioration of the invert in one step. This increment is too large for one rating step. Considering concrete pipe's inherent strength from its reinforcing and wall thickness, and that the 1-in. cover of concrete over the reinforcement is protective rather than structural, a condition rating inserted between the two existing evaluations seems appropriate. The intermediate rating condition will be classified as a 2 rating and described as "invert scaling below first layer of reinforcing, 50 percent loss of wall thickness at invert, concrete very soft."

Analytically, the inclusion of an intermediate concrete rating is supported by the rating equations contained in the Ohio (I) and Ohio (II) reports. In both studies, the major variable in the log-linear rating equations was age. The Ohio (I) age function, $age^{0.17}$, was definitely not linear as the rating scale indicated. The updated rating evaluations in the Ohio (II)

TABLE 8 CONCRETE CONDITIONAL RATINGS

Rating	Condition	Description
9	Excellent	New condition.
8	Very good	*Discoloration of concrete*, no cracking, spalling, scaling *or softening of concrete* present, surface in good condition.
7	Good	Minor hairline cracking at isolated locations, slight spalling, *light scaling (0 to ⅛ in. in depth) on invert, slight loss of mortar, aggregate not exposed, no softening of concrete.*
6	Fair	Extensive hairline cracks, some with minor delaminations or spalling, *moderate loss of mortar around aggregate, invert scaling ⅛ to ¼ in. deep.*
5	Fair—marginal	Cracking open greater than 0.12 in. with moderate delamination and moderate spalling exposing reinforcing steel at isolated locations, large areas of invert with spalls greater than 0.25 in. deep, *significant loss of mortar and slight loss of smaller aggregates due to surface scaling (¼ to ½ in. depth).*
4	Marginal	Cracks open more than 0.12 in. with effluence and spalling at numerous locations, spalls have exposed rebars that are heavily corroded, *heavy invert surface scaling greater than ½ in., moderate aggregate loss, concrete softening.*
3	Poor	Extensive cracking, spalling, and minor slabbing, invert scaling has exposed reinforcing steel *at isolated locations, moderate amount of concrete softening.*
2	Very poor	Severe slabbing has occurred in culvert wall, *invert scaling below first layer of reinforcing, 50 percent loss of wall thickness at invert, concrete very soft.*
1	Critical	*Holes through in concrete at isolated locations, 75 percent loss of wall thickness at invert, reinforcing exposed throughout invert.*
0	Failure	*Invert completely deteriorated, reinforcing steel gone, collapse of the culvert is imminent.*

NOTE: Condition descriptions in italic reflect additions to those contained in the FHWA Culvert Inspection Manual (*1*).

report, however, presented a more linear approach using an age function, age$^{0.55}$. An examination of the Ohio data and rating systems indicates that as the length of service life of the concrete pipe in these studies increases, there will be an expansion of ratings within the "marginal" to "poor" range and a consolidation of the "fair" ratings. These conditions would necessitate an increase in the age function of the Ohio equation. The proposed scale broadens the number of "poor" ratings for concrete pipe, increasing the Ohio age exponential to a value closer to 1 or a linear relationship. The incorporation of this condition corresponds to the trend apparent in the Ohio data and allows for an equitable direct comparison between metal and concrete ratings.

SUMMARY

The proposed condition rating systems for metal and concrete pipe provide an orderly progression for determining durability conditions in a culvert. Detailed descriptions of the levels of material distress present unique characteristics and features for each rating number. The development of the systems based on the operational evaluations used under the bridge rating scale permits the two systems to be directly compared. The severity of the conditions in a metal culvert can now be related directly to those for a concrete culvert with the same rating. It also allows for cross comparison with bridge structures, an option that is becoming more important as the number of inspections of bridge length culverts increases.

RECOMMENDATIONS

There should be state and federal programs for inspection of all culverts based on the FHWA *Culvert Inspection Manual* (*1*). The assessment and rating of material durability evaluations for culverts should be revised to eliminate subjective interpretation, thereby creating a uniform evaluation system.

REFERENCES

1. *Culvert Inspection Manual*. Federal Highway Administration, U.S. Department of Transportation, May 1985.
2. *Bridge Inspector's Training Manual 70*. Federal Highway Administration, U.S. Department of Transportation, 1979.
3. J. L. Beaton and R. F. Stratfull. *The Corrosion of Corrugated Metal Culverts in California*. Presented at 38th Annual Meeting of the Highway Research Board, National Research Council, Washington, D.C., Jan. 1959.
4. *A Study of the Durability of Metal Pipe Culverts*. Division of Highways, Surveys and Plans Division, Idaho Transportation Department, Boise, April 1965.
5. *Performance of Culvert Materials in Various Colorado Environments*. Report CDDH-PP&R-R-77-7, Colorado Department of Highways, Denver, Sept. 1977.
6. R. P. Brown and R. J. Kessler. *Performance Evaluation of Corrugated Metal Culverts in Florida*. Florida Department of Transportation, Tallahassee, Nov. 1975.
7. H. E. Worley. *Corrosion of Corrugated Metal Pipe*. State Highway Commission of Kansas, Kansas Department of Transportation, Topeka, 1971.
8. *Corrugated Steel Pipe for Storm Drains*. Los Angeles County Flood Control District, Calif., Jan. 1973.
9. *Evaluation of Drainage Pipe by Field Experimentation and Supplemental Laboratory Experimentation*. Final Report. Louisiana Department of Transportation and Development, Baton Rouge, March 1985.
10. K. M. Jacobs. *Culvert Life Study*. Maine Department of Transportation, Augusta, Jan. 1974.
11. R. W. Noyce and J. M. Ritchie. *The Michigan Galvanized Metal Culvert Corrosion Study*. Michigan Department of Transportation, Lansing, Jan. 1979.
12. D. L. Kill. *Serviceability of Corrugated Metal Culverts*. Minnesota Department of Transportation, St. Paul, 1969.
13. *Pipe Evaluation Survey*. Mississippi State Highway Department, Jackson, 1964.
14. P. F. Meacham, J. O. Hurd, and W. W. Shislen. *Ohio Culvert Durability Study*. Ohio Department of Transportation, Columbus, Jan. 1982.
15. C. J. Hayes. *A Study of the Durability of Corrugated Steel Culverts in Oklahoma*. Oklahoma Department of Highways, Oklahoma City, 1971.
16. V. D. Wolfe et al. *Corrugated Metal Pipe Comparison Study*. Oregon Department of Transportation, Salem, July 1976.
17. E. F. Kelley. *Engineering News Record*. June 5, 1930.

18. V. E. Berg. *A Culvert Material Performance Evaluation*. Washington State Highway Commission, Department of Transportation, Olympia, April 1, 1965.
19. A. R. Holt. *Durability Design Method for Galvanized Steel Pipe in Minnesota*. National Corrugated Steel Pipe Association, Washington, D.C., 1967.
20. J. O. Hurd. *Field Performance of Concrete Pipe Culverts at Acidic Flow Sites in Ohio*. Ohio Department of Transportation, Columbus, Jan. 1985.

Publication of this paper sponsored by Committee on Culverts and Hydraulic Structures.

Least Cost (Life Cycle) Analysis Microcomputer Program

JOHN M. KURDZIEL

This paper covers the contents and operation of the American Concrete Pipe Association's Least Cost (Life Cycle) Analysis microcomputer program. The program evaluates the costs associated with each alternate pipe material based on their design components and project requirements. The program has a multiple screen format similar to spreadsheet software and will operate on any IBM compatible system with MS-DOS operating system of version 2.0 or greater. The Least Cost Analysis program's versatility and ease of use will decrease the time and costs for conducting economic analysis and promote more cost-effective project designs.

Least cost (life cycle) analysis is the selection of a product, or material, based not on its initial cost, but on its total cost over the life of the project. Many articles and papers have been written on this subject, but only a few have provided tools for easily comparing complex alternates. The American Concrete Pipe Association's Least Cost Analysis (LCA) microcomputer program performs multiple economic analyses that enable evaluation of different pipe materials bid as alternates for a project to be carried out.

The program incorporates into the analysis the project design life, material service life, economic factors, and other project-related items such as traffic costs. Total costs are calculated using present worth (PW), annualized costs, or future value methods. Ample help screens are provided throughout the program to assist users in creating the data base. Hard copy documentation of all or part of the analysis may be obtained on execution of the program.

Presented in this paper are the program's functions and capabilities and a discussion of each screen from a design as well as an operational standpoint.

PROGRAM OPERATION

The LCA program has a multiple screen format similar to commercially developed spreadsheet software. It is written in *C* language and targeted for the IBM-XT or compatible microcomputer systems with a minimum of 256 K random access memory using the MS-DOS operating system of version 2.0 or greater.

All input and analysis sections are in front of users at all times. Subscreens assist users in creating and modifying the data set. Help screens are provided for every decision making step. Although default values are provided, the actual input values must be selected by users. The default values are only recommended values and are not automatically defaulted by the program. Copy commands are provided where appropriate to minimize repetitive entering.

Most operations within the subscreens may be selected using the scroll and enter keys. The function keys provide the means for moving from one subscreen to another, calling up help screens, or using the copy commands. This dual operation allows users access to file commands while still maintaining their place in the specific input screen.

The main screen is divided into seven major sections (Figure 1). The main menu provides seven alternatives. These include Project, Design, Economic, Material, Analysis, Files, and Quit. As users scroll through these alternatives, the short help screen, which is located just below the main menu, will change, reflecting descriptive information pertinent to the particular main menu alternative. Once a specific alternative is chosen, users will either enter one of the subscreens or a submenu for further selection. Once in a subscreen or submenu, the short help screen will reflect the descriptive information pertinent to the new screen.

Large help screens are available in these subsections (Figure 2). The help screens provide detailed technical information on the specific item highlighted at the time help is requested. The help information replaces the entire existing menu and screen. Text displayed in this way allows maximum use of screen space and enhances reading without displaying any distracting material. Many of the help screens are over a page in length, but easy review can be accomplished by scrolling up or down through the material. Once users have completed their review of the help screen, the same function key is used to return to the work screen.

After the data for a particular section have been entered, users return to the main menu to enter or modify any additional data, execute the program, request printed output, or manipulate the files.

Program execution is accomplished in the same way as is data input. The only difference is that once the type of analysis has been selected, users must request the execution of the program by entering return when "analyze" is highlighted. This provides users with the option of preselecting the type of analysis without executing the program. Once the program is executed, a comparison of the alternate products analyzed is displayed on the large screen. Total program running time is less than 5 sec.

Hardcopy printouts of either the final design summary or the comparison summary, with comprehensive documentation of all the input and analysis, may be obtained. Documentation printouts are requested under a submenu of the "file" alternative.

American Concrete Pipe Association, 8320 Old Courthouse Road, Vienna, Va. 22180.

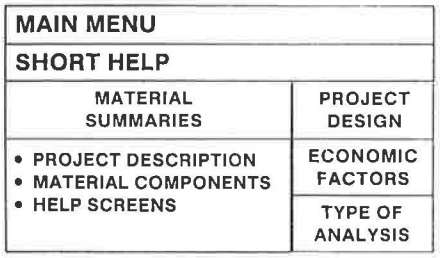

FIGURE 1 Main screen format.

PROJECT DESCRIPTION

The project description window provides the means for identifying the data base. The information in the project description also appears in the heading of the hard-copy documentation of the project design. Project description includes the project title, project location, designer's name, and the date of the design (Figure 3). Thirty-five spaces are provided for each of the first three headings with eight additional spaces for the date.

PROJECT DESIGN

The program provides the project design alternatives of storm sewer, sanitary sewer, and culverts, which are further classified as Interstate, state primary, state secondary, or local/rural projects.

Once the type of facility is selected, users are requested to enter its design service life. Guidance is provided in both the short help screen and long help screens for selecting this value but the final decision is left to the designer, who must manually enter the number of years. By not hardwiring the input, users maintain complete control over their design and this reduces the risk of the acceptance of erroneous information.

The project design service life is the length of time a specific roadway facility is expected to be in service. Figure 4 is an example of a culvert Interstate project with a 100-year project design life. The service life is normally set by the owner or authority responsible for the project. In cases in which a roadway or facility cannot be disrupted for replacement of the pipe, a project design life of 100 years or greater should be considered. This is typical of heavily traveled urban roadways, Interstate highways, stormwater systems, or sanitary sewers. Special consideration should also be given to installations under high fills or in remote areas with poor access. The selection of an appropriate project design life should reflect the transportation and commercial importance of the roadway, its effect on traffic, and the difficulty of replacement with inherent construction hazards to the traveling public.

As guidelines, ranges for the project design lives of the various types of facilities are provided in the program. Minimum design lives are provided as recommended values in the program's short help screens (Table 1).

ECONOMIC FACTORS

Least cost (life cycle) analysis provides the best means for considering and comparing alternate materials with different service lives. The problem with any economic analysis has always been forecasting interest and inflation rates. Short-term rates vary on a daily basis and are impossible to predict. For long-term rates, however, this problem can be avoided by using the relatively constant long-term ratio between interest and inflation rates.

The differential recommended is that between the producer price index (PPI) and the cost of funds for the borrower in question. The PPI represents the producer prices for materials such as steel mill and concrete products. The historical differential between the PPI and the municipal bonds, prime rate, and treasury bonds is appropriate to use when funding is provided by state and local governments, private firms, and

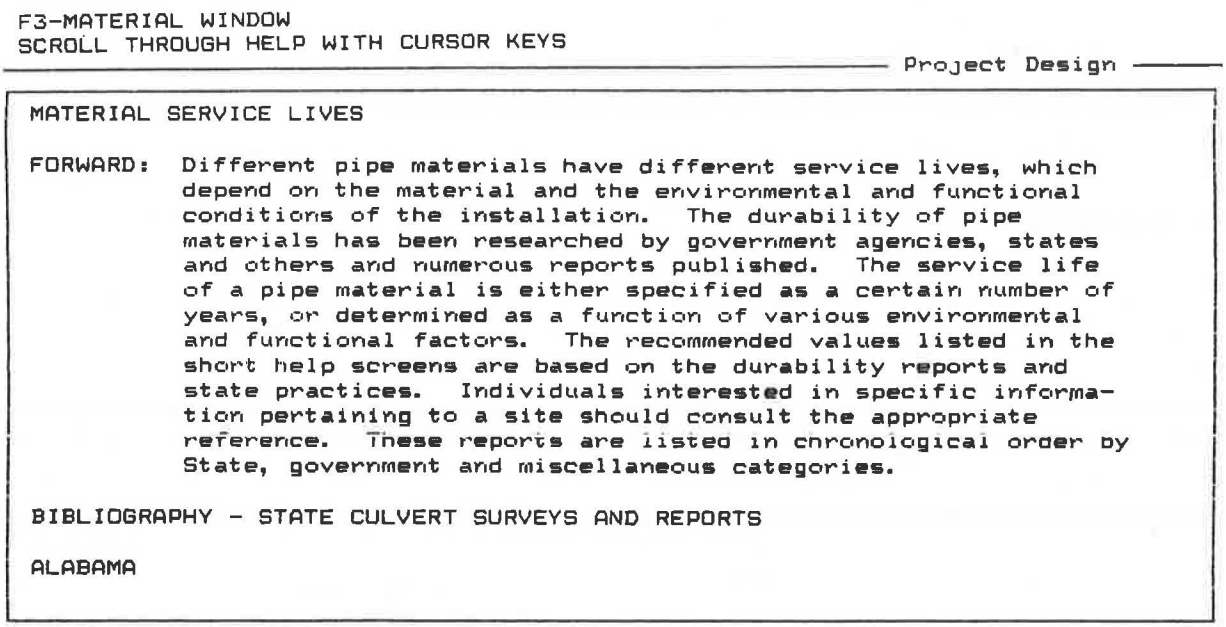

FIGURE 2 Section of a large help screen from material service life window.

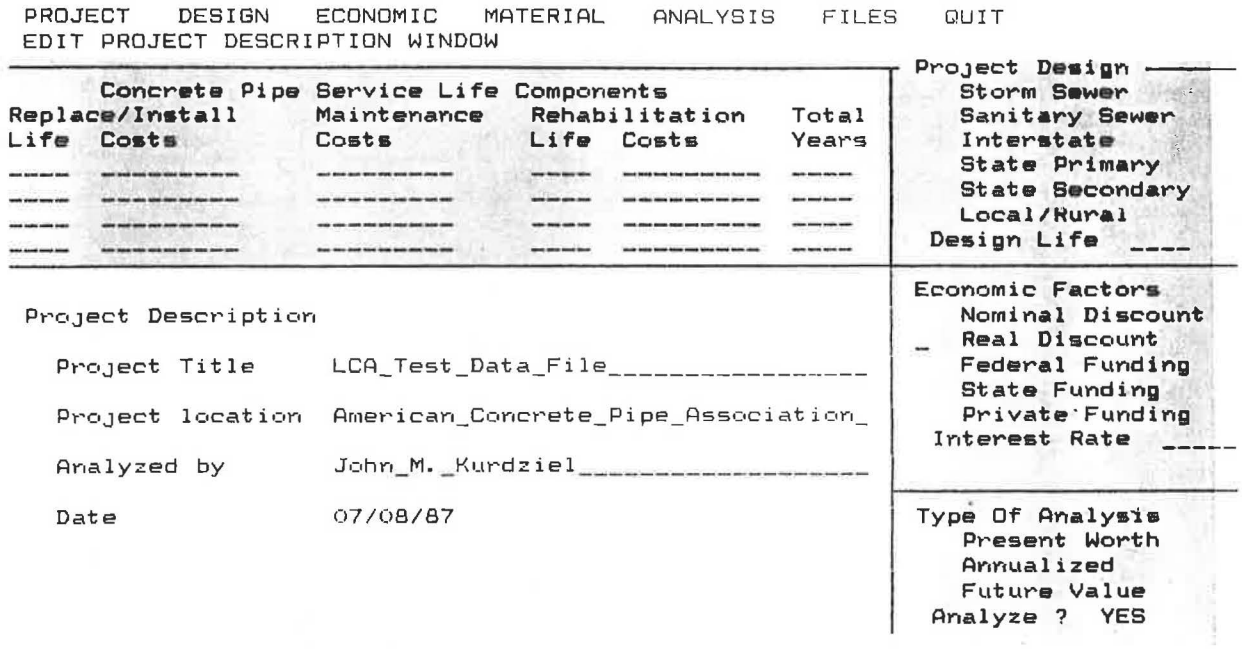

FIGURE 3 Project description window.

GIVEN: Culvert, interstate project with a 100 year project design life.

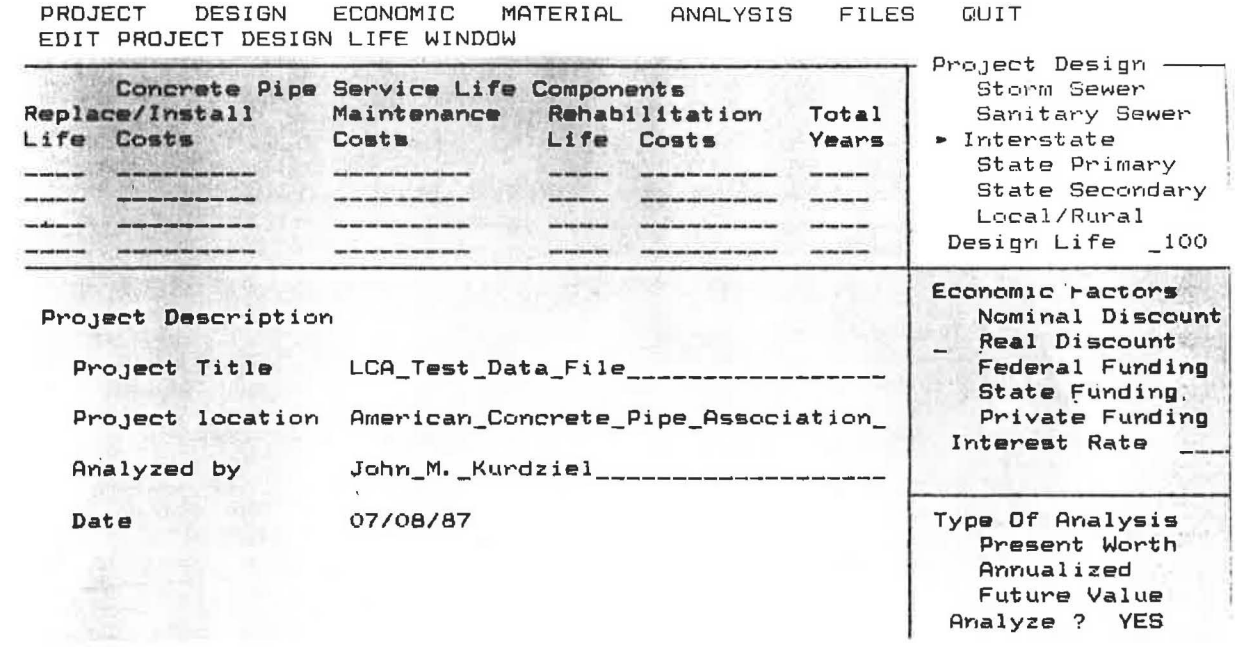

FIGURE 4 Project design window.

federal agencies, respectively (Table 2). Although the economic factor section is based on these assumptions, as with other parts of the program, users completely control the input.

The economic factor section is broken into three steps. The designers first choose whether to use the nominal or real discount rate for the analysis. The nominal discount rate uses current dollars and directly includes an inflation value in its analysis. The real discount rate uses constant dollars and, although it takes inflation into account, a value for inflation does not directly enter into the calculations. For example, if the interest rate was 6 percent and inflation was 4 percent, the nominal discount rate would use the specific values for the interest and inflation rates, whereas the real discount rate would be the differential between the two rates or 2 percent. Choosing one method over another does not affect the final analysis because both yield essentially the same results.

TABLE 1 DESIGN LIFE GUIDELINES

Project	Design Life
Storm sewer system	100 years or greater
Sanitary sewer system	100 years or greater
Interstate culverts	75 to 100 years
Urban culverts	75 to 100 years
State primary culverts	50 to 75 years
State secondary culverts	50 to 75 years
Local/rural culverts	50 years or greater

TABLE 2 HISTORICAL INTEREST-INFLATION RELATIONSHIP

Time Period	Municipal Bonds (%)	Prime Rate (%)	Treasury Bonds (%)
1954–1963	2.08	3.29	2.74
1964–1973	0.81	2.48	1.69
1974–1983	−1.32	2.81	0.55
Average Inflation-interest differential (1954–1983)	0.52	2.86	1.66

NOTE: Differentials represent differences between stated interest rates and the Producer Price Index for the year. All figures are based on annual averages.

EXAMPLE

Given: Interest (i) = 6 percent
Inflation (I) = 4 percent

Nominal Discount Rate

$$\frac{\text{Inflation}}{\text{Interest factor}} = \frac{1 + I}{1 + i}$$

Where $i = 0.06$
$I = 0.04$

$$I/i = \frac{1 + 0.04}{1 + 0.06}$$

$$= 0.9811$$

Real Discount Rate

$$\frac{\text{Inflation}}{\text{Interest factor}} = \frac{1 + I}{1 + i}$$

Where $i = 0.02$
$I = 0$

$$I/i = \frac{1 + 0}{1 + 0.02}$$

$$= 0.9804$$

There is less than 0.1 percent difference between the two methods.

The second step is to select the type of funding the borrower will use to finance the project. Generally funding can be classified into one of the three categories: federal, state, or private. If multiple types of funding are used on the project, the institution providing the majority of funding will normally control the analysis. The purpose for providing the type of funding is to assist users in selecting the discount rates associated with their specific type of project (i.e., a municipal project is less costly to finance than a privately funded one).

In the final step, the program provides recommended interest and inflation rates based on the type of discount method and funding selected by the designers. These values are provided as guidance; users must select and input all values to be used in the analysis. The example in Figure 5 shows a project design using a nominal discount rate with federal fund-

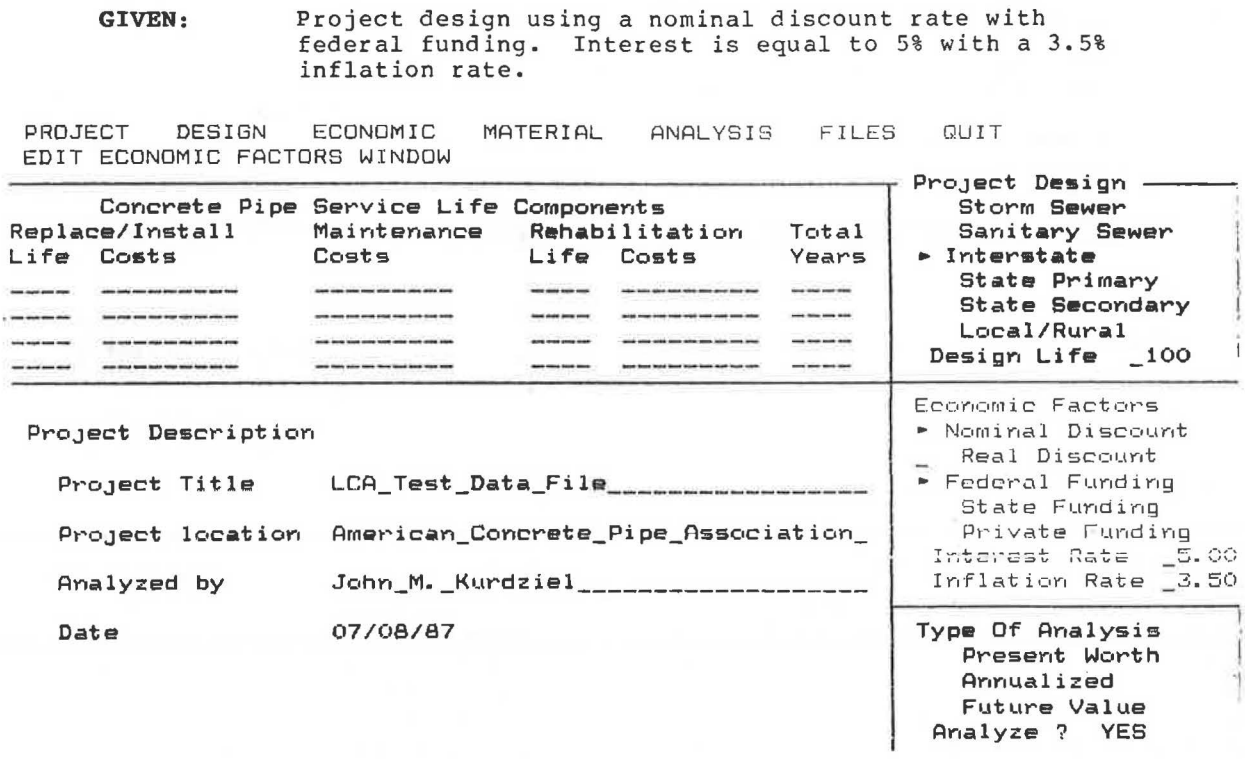

FIGURE 5 Economical factors window.

ing. Interest is equal to 5 percent with a 3.5 percent inflation rate.

MATERIAL SERVICE LIFE

Different pipe materials have different service lives, which depend on the material and the environmental and functional conditions of the installation. The durability of pipe materials has been researched by government agencies, states, and others, and numerous reports have been published. The service life of a pipe material is either specified as a certain number of years or determined as a function of various environmental and operational factors.

The LCA program allows for the analysis of three different product materials simultaneously. Assistance in the form of recommended service lives is provided for concrete and corrugated steel pipes in the short help screens. These values are supplemented with a large help screen, which contains a bibliography of pipe durability studies by various state and governmental agencies. Individuals interested in specific information pertaining to a site should consult the appropriate reference. These reports are listed in chronological order by state, government, and miscellaneous categories. The third alternative, other materials, is used to analyze any other product.

For each material, service life components are listed to assist in calculating the cost and number of rehabilitation and replacement actions necessary for the structure to reach the desired project design life. The service life components are divided into initial installation, maintenance, rehabilitation, and replacement.

Initial installation requires the input of a material service life and the cost of installing the facility. Because a pipe installation normally represents only one part of a project, this cost is usually the project bid price. In the example shown in Figure 6, concrete pipe installation has a bid price of $500,000 and a material service life of 100 years. Any alternative materials will have similar engineering, mobilization, and traffic control costs, and analysis using the bid prices will yield comparative results. If the material service life at this time, or if subsequent input, equals or exceeds the project design life, the program will inform users that the design life has been met and will not accept any further input for the installation. As with other parts of the program, this restriction can be overridden.

Maintenance is any action taken periodically to ensure that the facility functions as originally intended. Typical maintenance activities for pipe installations include removal of debris, flushing, deposition or silt removal, and repair of localized damage. Actions to maintain or improve the pipe's structural integrity are not considered maintenance activities but are addressed as either rehabilitation or replacement projects.

Maintenance costs in the program are handled as an expense per period or cost per number of years (see Figure 7, in which corrugated pipe installation has a $400,000 bid cost, a 30-year material service life, and a maintenance cost of $500 every 5 years). For example, if routine maintenance costs $1,000 every 5 years, the input would be an expense of $1,000 for a period equal to 5 years. To consider maintenance as an annual expense, the input would be the annual cost for a period equal to 1 year.

Rehabilitation entails any remedial action taken on a pipe facility to upgrade its structure condition. Rehabilitation actions cannot restore the pipe to its original condition, but may extend its service life by a number of years depending on the type and amount of deterioration. The years the material life is extended should be judged based on the condition of the pipe and the current rate of deterioration. Costs associated

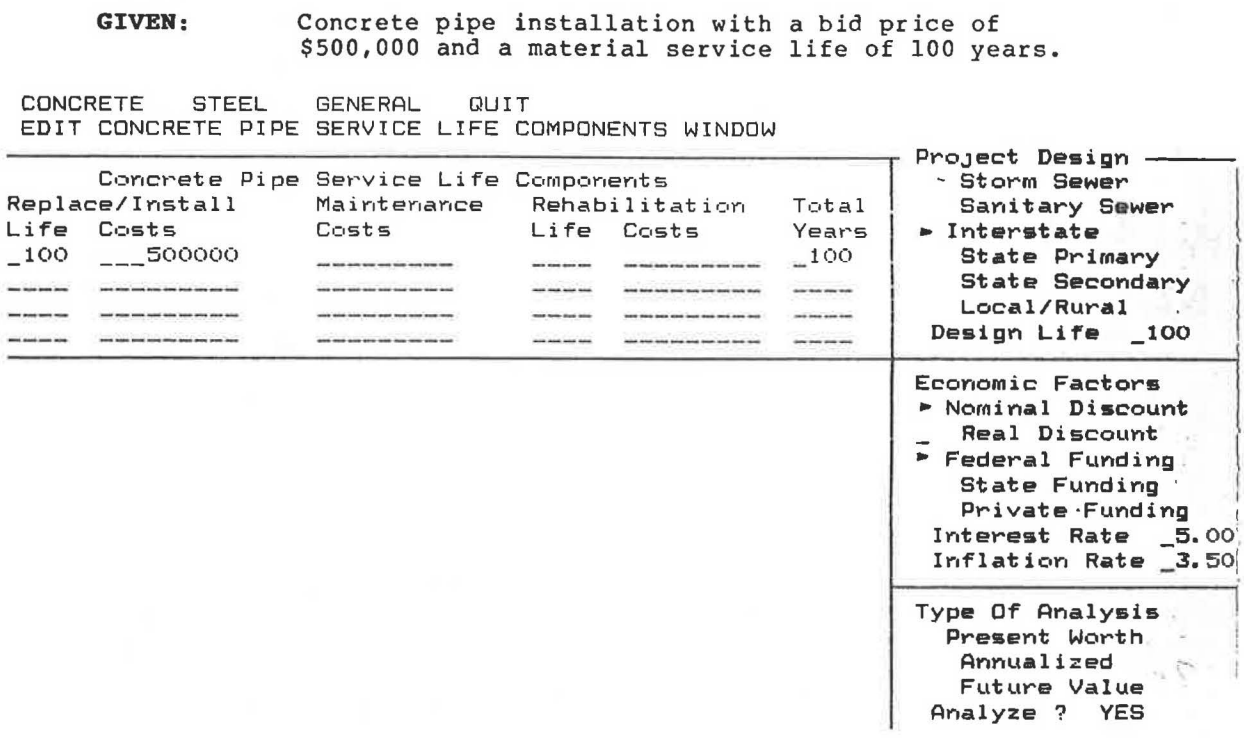

FIGURE 6 Material service life window.

GIVEN: Corrugated pipe installation with a $400,000 bid cost, 30 year material service life and maintenance cost of $500 every 5 years.

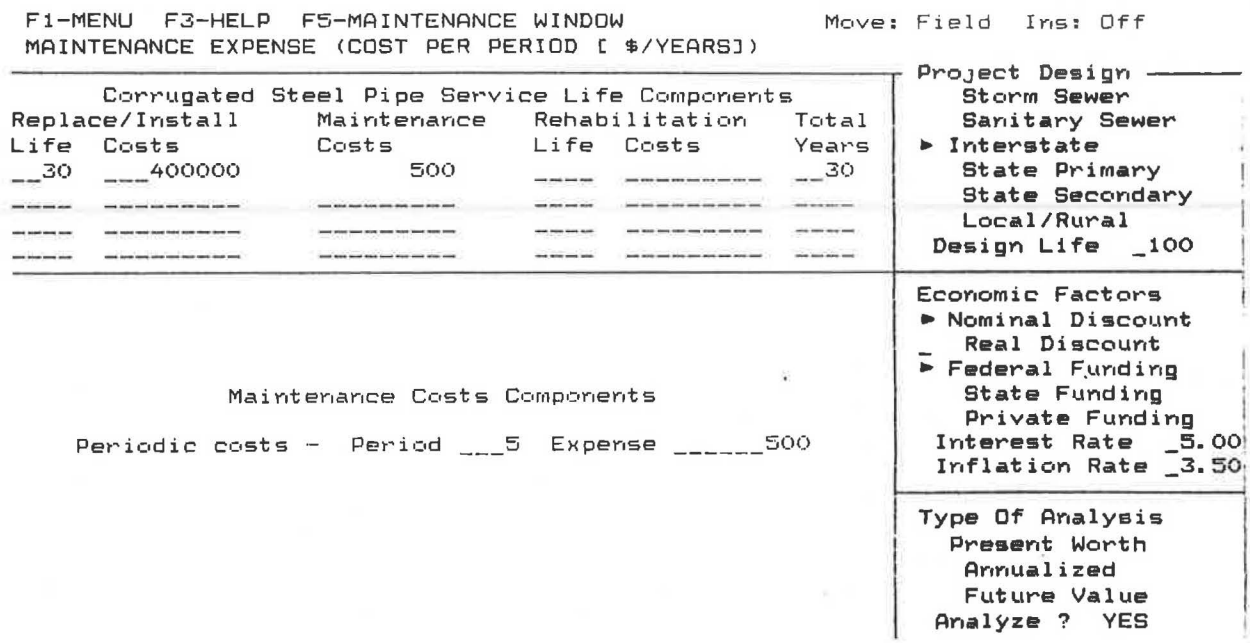

FIGURE 7 Maintenance cost components.

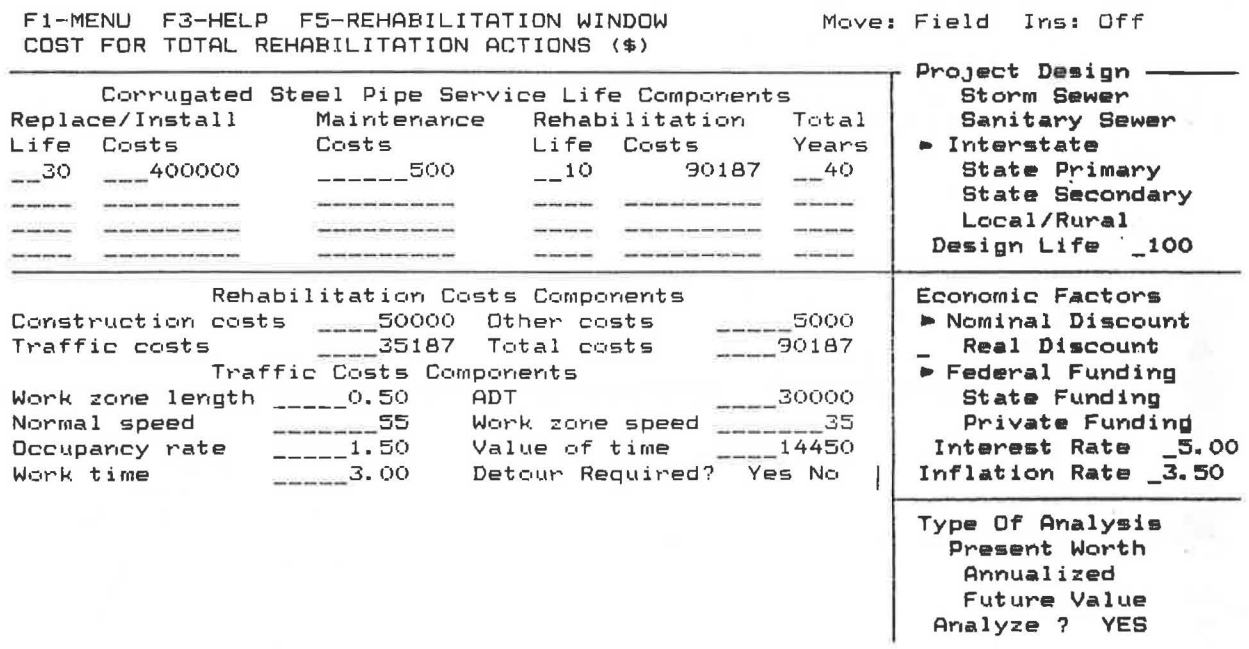

FIGURE 8 Rehabilitation cost components.

with rehabilitation actions not only include the construction and material costs for the work but any other directly or indirectly related costs, such as easements, engineering, safety, detour roadway deterioration, and traffic-related costs. The example in Figure 8 shows corrugated steel pipe with rehabilitation costs of $50,000 for construction and $5,000 for engineering, safety, and so on. The project roadway has an average daily traffic count of 30,000 vehicles with 1.5 people/vehicle and a normal speed limit of 55 mph, which is reduced to 35 mph during the 3-month construction time and construction zone length of 0.5 mi. The value of time is based on the U.S. Department of Commerce 1986 statistics for per capita income (default value).

Provisions have been made within the program to incorporate traffic-related costs into the analysis. Costs associated with vehicle deterioration, passenger time, and construction-

related accidents have been included. Inclusion of these items in the project costs are in accordance with similar analysis procedures such as those presented in the Federal Highway Administration's publication "The Design of Encroachments on Flood Plains Using Risk Analysis" (*2*). Cost of passenger's time is based on the loss of time for the decrease in speed through the construction zone. Vehicle deterioration costs reflect the wear on vehicles from the extra traveling distance for detours. Costs associated with construction-related accidents reflect the number and cost of vehicle accidents through the construction zone, and include property damage, injuries, and fatalities.

Replacement entails the removal of an existing facility and the installation of a new structure. The material life of the replaced facility should equal that of the original material life. Costs associated with replacement actions include all construction and material costs as well as all the direct and indirect costs illustrated under rehabilitation actions. The example in Figure 9 shows a corrugated steel pipe installation with replacement costs as illustrated (see rehabilitation screen for description). In addition, a l-mi detour will be required for the duration of the project. Vehicle operating costs are $0.21/mi (default value). Three accidents are expected with an average cost of $2,500/vehicle in damage. No injuries or fatalities are expected.

Rehabilitation and replacement actions are taken until the project design life is met or exceeded. In the event that the material service life exceeds the required number of years, a residual value will be determined. The residual cost represents the value of extended service. This value appears in the final analysis and hard copy documentation and is subtracted from the overall cost of the particular material.

ANALYSIS

The LCA program allows the economic analysis to be conducted using three different methods: PW, annualized costs, and future value. PW is calculated based on the equivalent costs at the current or present time (see Figure 10, in which analysis is to be conducted using the PW method). In other words, this would be the amount of money needed to be set aside today to meet the desired project design life.

When using the nominal discount rate, present value calculations are made by first inflating estimates of cost expenditures, made in original dollar terms, into the future, to the time that they will be made. These inflated costs are then discounted to present value terms using an appropriate interest rate. The inflation and discount of each future cost or value is done by the equation:

$$PV = A(F)^n$$

where

PV = present value,
A = amount of original cost,
F = inflation (I)/interest (i), $F = [(1 + I)/(1 + i)]$, and
n = period or number of years.

If a real discount rate is used, the future costs are discounted to the present value using the same equation in which the value for inflation is zero and the interest rate represents the difference between the actual interest and inflation rate [i.e., $(i - I)$].

Annualized costs are annual yearly costs or what an agency would have to outlay every year for the life of the project. This may also be computed on a period basis as an outlay every number of months or years by modifying the value of n in the equation:

$$AC = PV\,[i'\,(1 + i')^n/(1 + i')^n - 1]$$

where AC is annualized cost and i' is discount rate.

Future value is simply the cost of the project at a future

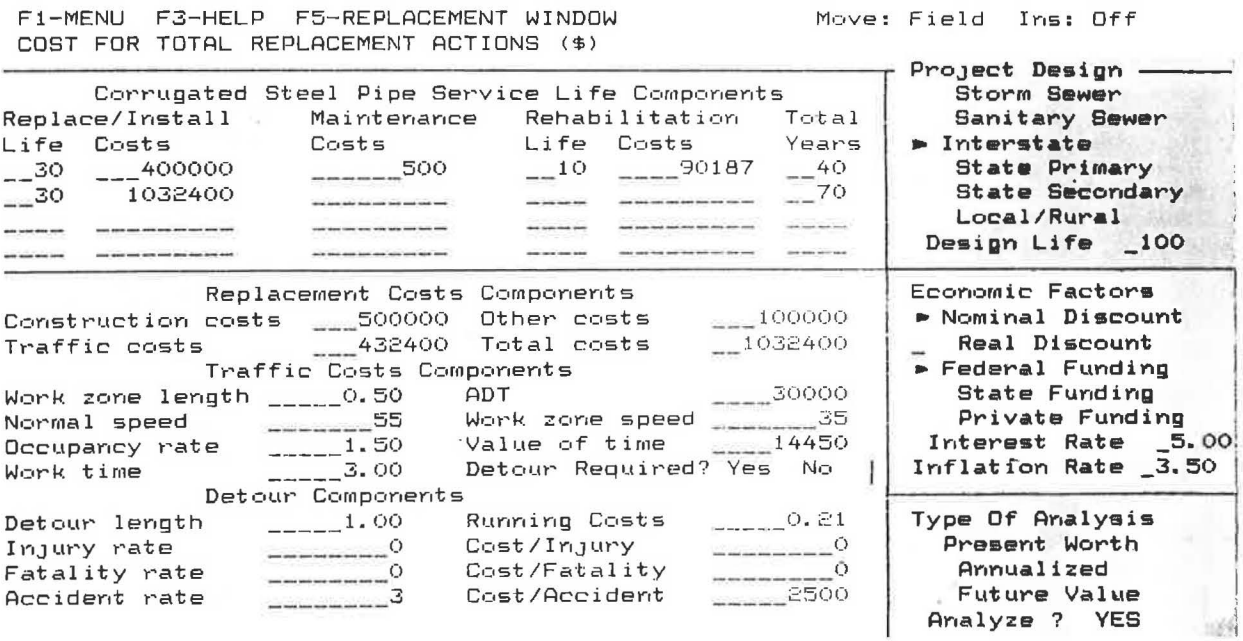

FIGURE 9 Replacement cost components.

date. Costs can be discounted to a future value with the following equation:

$$FV = PV\,(1 + i')^n$$

where FV is future value.

FILES

The file section of the program allows data to be stored and retrieved on either the working diskette or any external directory or subdirectory. The file section has four main functions: retrieve, save, print, and disk/path (Figure 11).

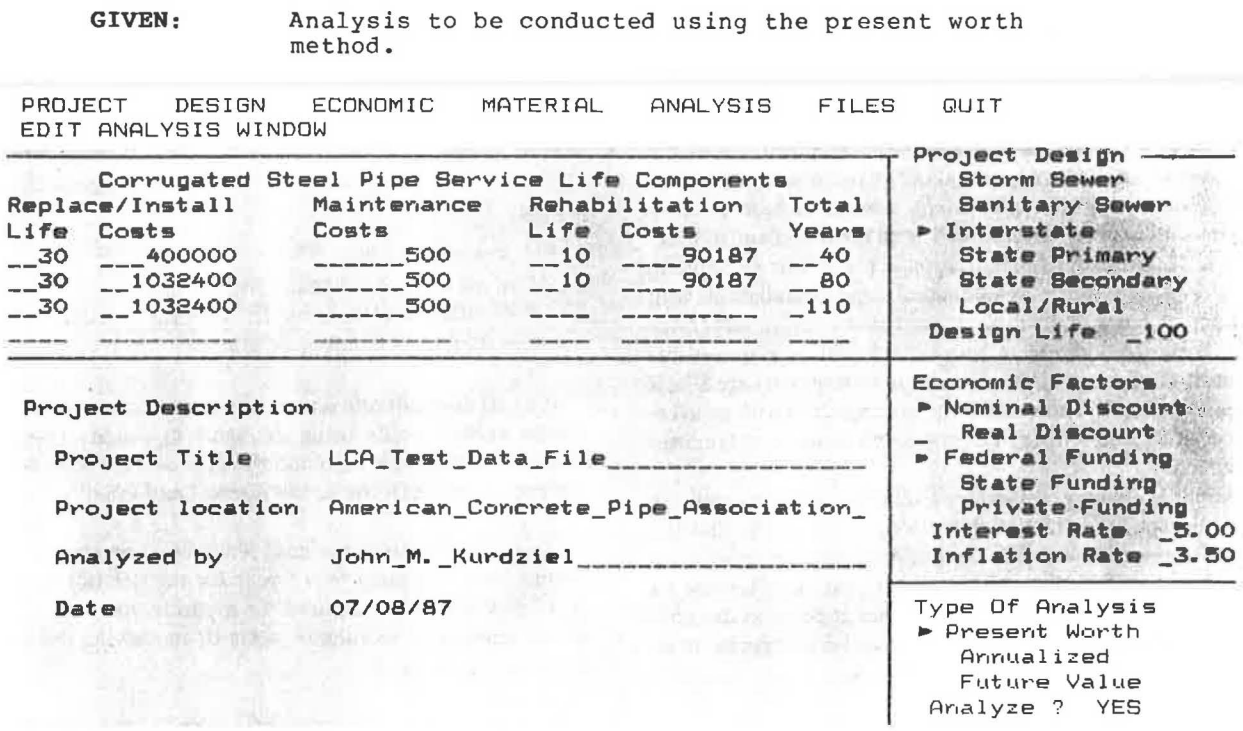

FIGURE 10 Type of analysis window.

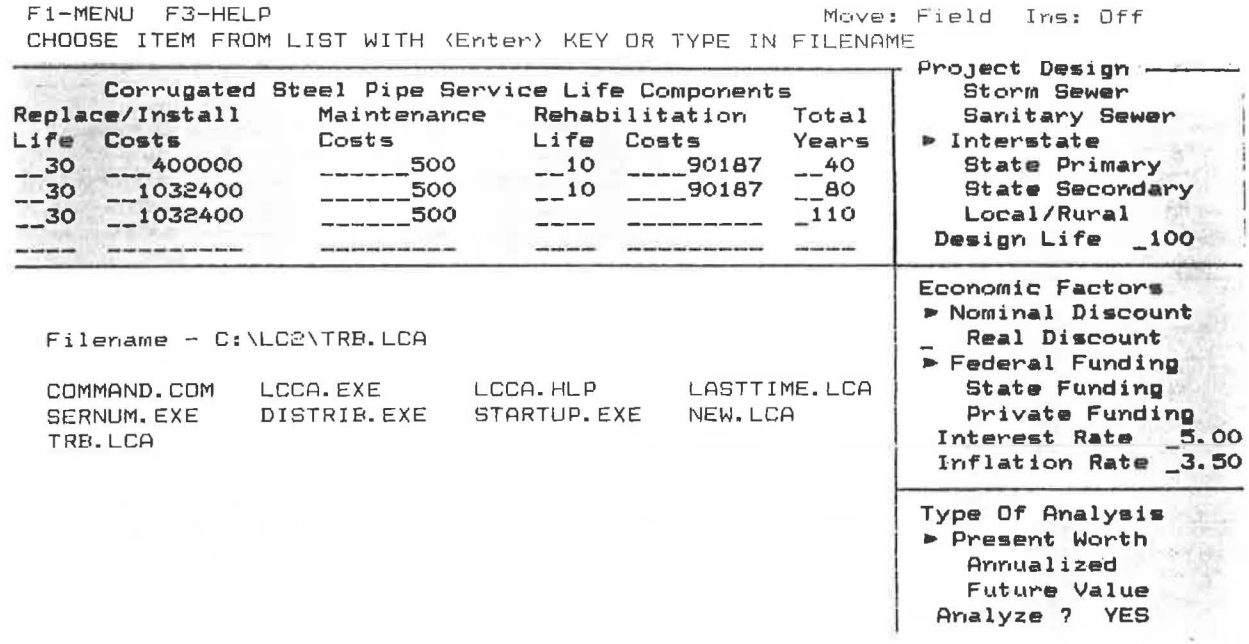

FIGURE 11 File window.

The save and retrieve commands provide access to the directory of the operating diskette or subdirectory. All the files on the directory are listed and an existing file can be either saved or retrieved by highlighting the desired file and entering. New files may be created by storing the data under a new file name, which is simply typed in over the file name prompt.

Printing of any program runs is done by selecting the print command for a complete hard copy printout or the print screen for a final design summary (Figure 12). All tabs and spacings have been preselected and arranged so that the hard copy documentation conforms to the standard 8½-in. by 11-in. sheet size for easy inclusion into plans and files. Figure 13 contains a complete hard copy printout of the analysis developed in this paper. Values used in developing the analysis were only intended to illustrate the computational aspects of the program and do not represent any particular project.

The disk/path command allows users to change or specify a specific default drive or subdirectory. If the program is being executed on the hard disk drive and all the data files are being

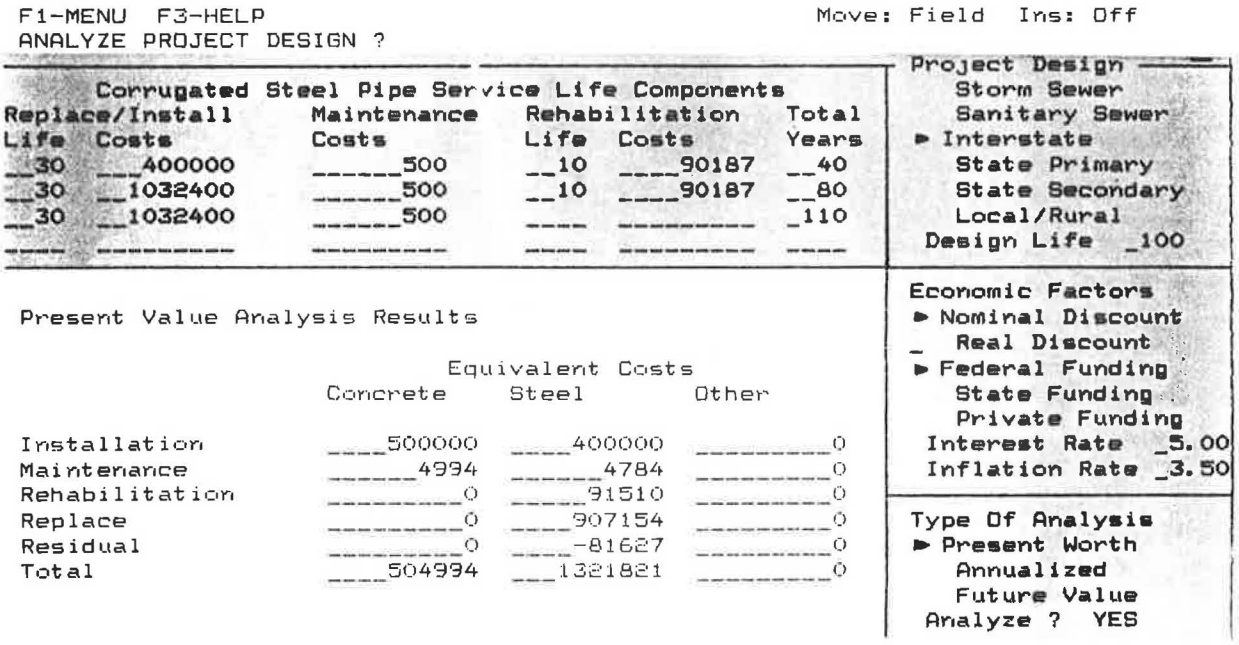

FIGURE 12 Final design.

```
LEAST COST ANALYSIS ANOTATED LISTING
PAGE 1 OF GENERAL PARAMETERS
PREPARED BY : JOHN M. KURDZIEL


Project Description

   Project Title        - LCA Test Data File
   Project Location     - American Concrete Pipe Association
   Analyzed By          - John M. Kurdziel
   Date                 - 07/08/87

Project Design Parameters

   Type of Facility     - Interstate Culvert
   Project Design Life  = 100 (years)

Economic Factors

   Discount Rate Type   - Nominal Discount Rate
   Type of Funding      - Federal Funding
   Interest Rate        = 5.00 (%)
   Inflation Rate       = 3.50 (%)
```

FIGURE 13 Printout of LCA program.

```
LEAST COST ANALYSIS ANOTATED LISTING
PAGE 1 OF CONCRETE PIPE MATERIAL SERVICE LIFE
PREPARED BY : JOHN M. KURDZIEL

Start of Period (years) =    0
End of Period (years)   =  100

Installation       Life (years) =  100          Costs ($) =    500000
Maintenance                                     Costs ($) =       500
Rehabilitation     Life (years) = Undefined     Costs ($) = Undefined

Maintenance Costs Components

   Period (years) =    5                Costs ($) =       500

Rehabilitation Costs Components

   Construction Costs ($) = Undefined   Other Costs ($)          = Undefined
   Traffic Costs ($)      = Undefined   Total Costs ($)          = Undefined

   Traffic Costs Components

   Work Zone Length (mi)  = Undefined   ADT (veh/day)            = Undefined
   Normal Speed (mph)     = Undefined   Work Zone Speed (mph)    = Undefined
   Occupancy Rate (#/veh) = Undefined   Value of Time ($/year)   = Undefined
   Work Time (months)     = Undefined

   Detour Is Undefined


Start of Period (years) =    0
End of Period (years)   =   40

Installation       Life (years) =   30          Costs ($) =    400000
Maintenance                                     Costs ($) =       500
Rehabilitation     Life (years) =   10          Costs ($) =     90187

Maintenance Costs Components

   Period (years) =    5                Costs ($) =       500

Rehabilitation Costs Components

   Construction Costs ($) =     50000   Other Costs ($)          =      5000
   Traffic Costs ($)      =     35187   Total Costs ($)          =     90187

   Traffic Costs Components

   Work Zone Length (mi)  =      0.50   ADT (veh/day)            =     30000
   Normal Speed (mph)     =        55   Work Zone Speed (mph)    =        35
   Occupancy Rate (#/veh) =      1.50   Value of Time ($/year)   =     14450
   Work Time (months)     =      3.00

   Detour Is Not Required


Start of Period (years) =   40
End of Period (years)   =   80

Replacement        Life (years) =   30          Costs ($) =   1032400
Maintenance                                     Costs ($) =       500
Rehabilitation     Life (years) =   10          Costs ($) =     90187
```

FIGURE 13 *continued.*

```
LEAST COST ANALYSIS ANOTATED LISTING
PAGE 2 OF CORRUGATED STEEL PIPE MATERIAL SERVICE LIFE
PREPARED BY : JOHN M. KURDZIEL

Replacement Costs Components

   Construction Costs ($) =     500000   Other Costs ($)          =     100000
   Traffic Costs ($)      =     432400   Total Costs ($)          =    1032400

   Traffic Costs Components

   Work Zone Length (mi)  =       0.50   ADT (veh/day)            =      30000
   Normal Speed (mph)     =         55   Work Zone Speed (mph)    =         35
   Occupancy Rate (#/veh) =       1.50   Value of Time ($/year)   =      14450
   Work Time (months)     =       3.00

   Detour Is Required -- Costs Components

   Detour Length (mi)     =       1.00   Running Costs ($/mile)   =       0.21
   Injury Rate (#)        =          0   Cost/Injury ($/#)        =          0
   Fatality Rate (#)      =          0   Cost/Fatality ($/#)      =          0
   Accident Rate (#)      =          3   Cost/Accident ($/#)      =       2500


Maintenance Costs Components

   Period (years) =    5                Costs ($) =        500


Rehabilitation Costs Components

   Construction Costs ($) =      50000   Other Costs ($)          =       5000
   Traffic Costs ($)      =      35187   Total Costs ($)          =      90187

   Traffic Costs Components

   Work Zone Length (mi)  =       0.50   ADT (veh/day)            =      30000
   Normal Speed (mph)     =         55   Work Zone Speed (mph)    =         35
   Occupancy Rate (#/veh) =       1.50   Value of Time ($/year)   =      14450
   Work Time (months)     =       3.00

   Detour Is Not Required

Start of Period (years) =   80
End of Period (years)   =  110

Replacement       Life (years) =   30          Costs ($) =   1032400
Maintenance                                    Costs ($) =        500
Rehabilitation    Life (years) = Undefined     Costs ($) = Undefined


Replacement Costs Components

   Construction Costs ($) =     500000   Other Costs ($)          =     100000
   Traffic Costs ($)      =     432400   Total Costs ($)          =    1032400

   Traffic Costs Components

   Work Zone Length (mi)  =       0.50   ADT (veh/day)            =      30000
   Normal Speed (mph)     =         55   Work Zone Speed (mph)    =         35
   Occupancy Rate (#/veh) =       1.50   Value of Time ($/year)   =      14450
   Work Time (months)     =       3.00

   Detour Is Required -- Costs Components

   Detour Length (mi)     =       1.00   Running Costs ($/mile)   =       0.21
   Injury Rate (#)        =          0   Cost/Injury ($/#)        =          0
   Fatality Rate (#)      =          0   Cost/Fatality ($/#)      =          0
   Accident Rate (#)      =          3   Cost/Accident ($/#)      =       2500
```

FIGURE 13 *continued.*

LEAST COST ANALYSIS ANOTATED LISTING
PAGE 3 OF CORRUGATED STEEL PIPE MATERIAL SERVICE LIFE
PREPARED BY : JOHN M. KURDZIEL

Maintenance Costs Components

Period (years) = 5 Costs ($) = 500

Rehabilitation Costs Components

Construction Costs ($) = Undefined Other Costs ($) = Undefined
Traffic Costs ($) = Undefined Total Costs ($) = Undefined

Traffic Costs Components

Work Zone Length (mi) = Undefined ADT (veh/day) = Undefined
Normal Speed (mph) = Undefined Work Zone Speed (mph) = Undefined
Occupancy Rate (#/veh) = Undefined Value of Time ($/year) = Undefined
Work Time (months) = Undefined

Detour Is Undefined

Present Value Analysis — Equivalent Costs ($)

	Concrete	Steel	Other
Installation	500000	400000	0
Maintenance	4994	4784	0
Rehabilitation	0	91510	0
Replacement	0	907154	0
Residual	0	-81627	0
Total	504994	1321821	0

Annualized Value Analysis — Equivalent Costs ($)

	Concrete	Steel	Other
Installation	25192	20153	0
Maintenance	252	241	0
Rehabilitation	0	4611	0
Replacement	0	45705	0
Residual	0	-4113	0
Total	25443	66597	0

Future Value Analysis — Equivalent Costs ($) (X1000)

	Concrete	Steel	Other
Installation	65751	52601	0
Maintenance	657	629	0
Rehabilitation	0	12034	0
Replacement	0	119292	0
Residual	0	-10734	0
Total	66407	173821	0

FIGURE 13 *continued.*

stored on a floppy drive or subdirectory, users can specify these parameters using the disk/path command and minimize misplacement of files and excessive inputs.

AVAILABILITY

The LCA program will be made available as a public domain program through the distribution facilities of McTrans, Center for Microcomputers in Transportation. McTrans is the official software distributor and user support center for the Federal Highway Administration. The center provides support to microcomputer users through technical assistance of the software distributed. Costs for public domain programs distributed by McTrans are nominal, covering only their administrative, reproduction, and overhead costs. The LCA program will be only one of a number of programs developed by the American Concrete Pipe Association to be distributed in this way.

SUMMARY

The LCA program evaluates costs associated with each alternate pipe material based on their design components and project requirements. The program allows the maximum amount of freedom in selecting design parameters while providing detailed guidance at every decision making step. Because data entry requires little typing, complex designs may be entered in less than 5 minutes, and multiple runs for parameter studies or sensitivity analysis in a fraction of that time. The LCA program's versatility and ease of use will make life cycle economic analysis easier, decrease government agencies' and consultants' time and costs for analysis, and promote more cost-effective project designs.

REFERENCES

1. W. O. Kerr and B. A. Ryan. Taking the Guesswork Out of Least Cost Analysis. *Consulting Engineer*, March, 1986.
2. *The Design of Encroachments on Flood Plains Using Risk Analysis*. Hydraulics Engineering Circular 17, Office of Hydraulics, Federal Highway Administration, U.S. Department of Transportation, 1980.

DISCUSSION

WAHEED UDDIN
Texas Research and Development Foundation, 6811 Kenilworth Avenue, Riverdale, Md. 20737.

The LCA microcomputer program for pipe type selection is a useful addition to the limited number of user-friendly microcomputer programs for the life cycle cost analysis of highway components. The LCC1 microcomputer program (*1*,*2*) offers a user-friendly approach to analyze life cycle costs for pavement management considering multiple reconstruction, maintenance and rehabilitation treatments, material salvage and extended service life, and different economic scenarios.

The author offers the users both PW and annualized value methods as well as future value analysis to compare the life cycle costs of different pipe material alternatives. It should be recognized that, if correctly performed, PW provides the bench mark against which other methods of evaluation must be judged. The annual equivalent annuity (AE) method will give answers consistent with a bench-mark PW in the absence of inflation and when a uniform inflation is expected over time. The validity of PW and AE are demonstrated when actual (nominal) cash flow and actual (nominal) discount rates are used. Decisions based on real discount rates will be correct only if they are consistent with those obtained using nominal rates. A real rate can be used only with cash flows expressed in base-year prices (i.e., uninflated costs). Similarly, a nominal rate can be used only in conjunction with the actual cash flow expected. There should be no mixing of real and nominal values.

Salvage values are unlikely to have any significant impact on the economic evaluation of alternative strategies. First, they will be similar in value (e.g., similar haulage, labor, and residual value of materials). Second, the cost, when discounted back to present value, is likely to be small, even for modest discount rates. Consideration of the extended value of service life is important for proper life cycle cost comparisons. Both salvage values are provided in the LCA program.

The outputs show a summary of all cost streams and total cost for each alternative. However, it is apparently up to the users to select the least cost alternative based on the total life cycle costs. It will be useful if another output screen is added that rank orders the alternatives on the least cost basis using the following options:

1. All costs.
2. All costs (excluding maintenance, rehabilitation, and replacement costs). This will present a "do-nothing" policy.
3. All costs except road user costs (traffic detour and accident costs). This option can be used to ignore these traffic cost components in the least cost analysis because the program user may not have reliable estimates of the traffic cost components during the service life of the facility.
4. All costs except salvage values.
5. All costs except road user costs and salvage value.

The ranking costs should be provided when using any of these options, along with the option and rank.

REFERENCES

1. W. Uddin, R. F. Carmichael III, and W. R. Hudson. *Life-Cycle Analysis for Pavement Management Decision Making—Final Report*. Report FHWA-PA-85-028, Pennsylvania Department of Transportation, Harrisburg, March 1986.
2. W. Uddin, R. F. Carmichael III, and W. R. Hudson. A Microcomputer Program To Evaluate Cost-Effective Alternatives for Concrete Pavement Restoration. In *Transportation Research Record 1109*, TRB, National Research Council, Washington, D.C., 1987, pp. 60–68.

AUTHOR'S CLOSURE

The discussant raised a very important question about real and nominal discount rates that deserves further discussion.

The LCA program will not permit the mixing of real and nominal values. An amalgamation of the discount rates would present a totally erroneous analysis. Using either the nominal or real discount rate will yield the same results as long as they are used consistently. Problems occur when they are mixed. For example, if an interest rate is 8 percent and an inflation rate is 6 percent, a real discount rate of 2 percent should be used, or for a nominal discount analysis both the stated inflation and interest rates would be used directly. Mixing the discount rates by inflating a cost out to a future time using an inflation rate of 6 percent and then discounting back to PW using the real discount rate of 2 percent would effectively create a debtor's dream, as the following analysis demonstrates.

$$FV = PV/(1 + I/1 + i)^n$$

where

FV = future value,
PV = present value,
I = inflation rate,
i = interest, and
n = period or number of years.

Substituting $I = 6$ percent, $i = 2$ percent
Yields $FV = PV/(1.039)^n$

In this case, the larger the period, the smaller the future value of money. An investor under these conditions would be much better off to borrow all their funds today and simply pay them back at a future date at a cost less than the face value of the original loan. The opposite of this condition, of course, creates a money-generating machine. In either case, the analysis is a distortion of the actual conditions. If a nominal discount rate is used for the analysis, i and I equal 0.08 and 0.06, respectively. For a real discount rate analysis, the inflation rate is not included directly in the analysis and is equal to zero. The corresponding real discount rate, however, takes the inflation rate into consideration because it is the differential between interest and inflation, or 0.02. As long as the consistent factors are used in the analysis, either the nominal or real discount rate may be used. The program includes both methods to allow for maximum flexibility.

The salvage values in the program are based not on the actual salvage value of the material but on the residual service life the product provides for the facility. It is unrealistic to assume that there would be any net salvage value for a product material once the costs for removing and hauling it away are considered. The embankment and all the drainage structures within it must serve far longer than the roadway itself. Pavements may be replaced relatively easily compared with the disruption and cost associated with removing a pipe. Roadways are also seldom abandoned because of the high cost of right-of-way, and most are required to serve longer than their original project design life. Many states design their roadways with these considerations in mind. In their May 1987 durability study, the Missouri Highway and Transportation Department states that "roadbeds and highway corridors are selected and designed with no foreseeable intent to relocate." Even if a roadway is relocated, the old embankment remains intact and efficient movement of water through it must be maintained. It is, therefore, more reasonable to assume a residual value for a material based on the extended project design life of the facility and not on the salvage value of the product material.

There are a number of input options in the program that can yield the results listed in the discussant's comments. The only option that currently cannot be fulfilled within the actual computational routines of the program is the exclusion of salvage values. Salvage values or residual costs are calculated on the last material action that exceeds the project design life. A user, however, could obtain a design void of salvage value costs by adding the residual cost listed in the output to the total costs, but unfortunately this calculation must be done outside the program.

A computer program should be a dynamic entity, constantly evolving and improving. Enhancements such as ranking of alternatives have benefits in documenting the analysis and will be worthwhile additions to the program. Other enhancements and updates will surface as the program is being used. Those revisions that represent a benefit to designers and planners within the engineering community will be included in any future versions of the program.

REFERENCE

1. *Study of Use, Durability, and Cost of Corrugated Steel Pipe on the Missouri Highway and Transportation Department's Highway System.* Missouri Highway and Transportation Department, Jefferson City, May 1987.

Publication of this paper sponsored by Committee on Culverts and Hydraulic Structures.

Laterally Loaded Cast-in-Drilled-Hole Piles

C. K. SHEN, S. BANG, M. DESALVATORE, AND C. J. PORAN

The behavior of cast-in-drilled-hole pile has been investigated in detail with an instrumented model test pile embedded in either level or sloping ground of sand or silty clay soil. Upslope and downslope as well as parallel directional lateral loads were applied to the model test pile to measure the lateral resistance and the load-deflection relationship. Parameters such as the embedment length, the slope of the ground, the distance from the edge of the slope, and the cyclic loading were included in the study.

A large number of subsurface structures are designed mainly to resist the lateral or overturning loads applied above the ground level. These subsurface structures derive their bearing capacity from the passive earth resistance against lateral movements (translation or rotation). One of the widely used types of foundation in this category is the cast-in-drilled-hole (CIDH) pile. Piles of this type are normally less than 12 ft long and have a length-to-diameter ratio ranging from 2 to 1 for short piles to about 10 for longer piles. Because of their relatively low slenderness ratios and high rigidity with respect to the surrounding soils, they are conventionally considered as rigid members in design and analysis. Structures supported by CIDH piles are numerous, notably posts for large road and commercial signs and sound barrier walls for noise control along urban freeways.

A comprehensive investigation conducted more than 15 years ago by the Texas Department of Highways (*1–3*) concluded that the conventional design of CIDH piles appeared to be conservative. This study proposed a rigorous but simple-to-use alternative design method for calculating ultimate lateral loads. The formulation includes the development of shear stresses and the circumferential variation of normal stresses around a pile. The formulation, however, does not completely satisfy all the stress boundary conditions and the failure criterion; most importantly it does not include a provision for sloping ground conditions. In practice, for instance, sound barrier walls are frequently placed near the edge of roadway embankments. In light of the above, there appears to be a need to conduct a study to evaluate the lateral resistance of CIDH piles placed in level or sloping ground with the final objective of establishing an improved design methodology as applied to highway-related structures.

C. K. Shen, Department of Civil Engineering, University of California, Davis, Calif. 95616. S. Bang, Department of Civil Engineering, South Dakota School of Mines and Technology, Rapid City, S. Dak. 57701-3995. M. DeSalvatore, Geotechnical Branch, California Department of Transportation Laboratory, 5900 Folsom Boulevard, Sacramento, Calif. 95819. C. J. Poran, Department of Civil Engineering, Polytechnique Institute of New York, Brooklyn, N.Y. 11201.

LITERATURE REVIEW

The usual approach to treat the problem of a laterally loaded pile is first to categorize the pile as either rigid or flexible. A clear distinction between those two, however, does not exist. It has been suggested that the rigidity of a pile can be related to the ratio of the flexural stiffness of the pile and the foundation soil modulus. Taking into consideration a wide range of soil stiffness, Kasch et al. (*4*) concluded that in order to ensure rigid pile behavior, the length-to-diameter ratio of a pile should not exceed about 6, but could be as high as 10 under certain conditions, such as in weak soils; also that a ratio of 20 or more ensures flexible pile behavior. Accordingly, the CIDH pile can be considered as a relatively rigid pile.

One of the first attempts to calculate the ultimate lateral resistance of a short rigid pile in cohesionless soil was made by Broms (*5*). He assumed that the active earth pressure acting on the back of a pile is negligible, that the distribution of passive earth pressure along the front of a pile is equal to three times the Rankine's passive pressure, and that the shape of a pile section has no influence on the distribution of ultimate soil pressure.

Based on the equilibrium of a tetrahedron-shaped soil failure wedge under lateral load, Reese et al. (*6*) formulated the ultimate soil resistance for a short rigid pile. The total ultimate lateral resistance of the pile is equal to the passive force minus the active force. The active force is computed from Rankine's theory and the passive force from the geometry of the wedge with boundary forces following the Mohr-Coulomb failure criterion.

Broms (*7*) also developed a theory to calculate the ultimate lateral resistance of a short rigid pile in cohesive soil. He suggested a simplified lateral soil resistance distribution: zero from the ground surface to a depth of 1.5 times the pile diameter, and a constant value of 9 times the undrained shear strength below this depth.

Using a failure wedge similar to the one used in cohesionless soils, Reese (*8*) formulated an expression for the ultimate resistance of a laterally loaded pile in soft clay. The resulting ultimate resistance per unit length of pile consists of three terms. The first indicates the resistance at the ground surface, the second relates to the increase in resistance with depth resulting from overburden pressure, and the third is a geometrically related restraint term. Matlock (*9*) later found that the third term in Reese's expression did not agree with experimental observations and suggested an alternative expression.

Ivey (*1*) studied the ultimate resistance of drilled piles in level ground and proposed a comprehensive design method. In his approach, unlike the conventional ones, both normal and shear stresses acting on all faces of the pile were considered. Distributions of these stresses resulting from a rotation

of the pile were assumed to vary along the circumferential direction by cosine and sine functions. The point of rotation and the resulting ultimate lateral resistance of the pile were then calculated from the equilibrium equations. The proposed method was later modified based on model test results (*3*). Although the theory includes most of the essential characteristics of rigid pile behavior under lateral loads, the application may be limited because (a) fully active and passive conditions based on Rankine's theory were used, (b) shear stresses did not totally satisfy the Mohr-Coulomb failure criterion, and (c) most of the test results used to verify the theory, particularly those in sands, were obtained from scaled model piles of limited range.

Other design methods available for short rigid piles are by Hays et al. (*10*), Ivey and Dunlap (*2*), Ivey and Hawkins (*11*), Davidson et al. (*12*), Lytton (*13*), Ivey et al. (*3*), Seiler (*14*), Hansen (*15*), and others. In general, the Ivey and Dunlap and the Ivey and Hawkins methods yield conservative values (*4*); whereas Hansen's and Lytton's methods yield consistently unconservative values for larger piles (*16*). Broms' method yields conservative results in stiff clays but unconservative results in soft clays (*16*).

There have also been many experimental studies on the load-deflection relationships (*2, 4, 10, 17, 18*) and the earth pressure measurements (*4, 16, 17, 19–21*) along laterally loaded rigid piles. In general the measured lateral earth pressure distributions are parabolic shaped. Based on the measured earth pressure distribution, Biershwale et al. (*16*) reported that the point of rotation or the point of zero lateral stress is located at approximately 0.7 times the embedment length of a pile as measured from the ground surface. This generally coincides with results reported by other studies (*1, 4, 10, 17, 19*) stating that the rotation point lies in the vicinity of two-thirds of the embedment length. However, studies (*2, 4, 10, 18, 22*) also indicated that the point of rotation does not remain at a constant depth below the ground surface, rather it moves to lower depths as the lateral load is increased. The point of rotation could also move upward if the strength of the soil decreases with depth (*2*). In general, the point of rotation shifts downward from some point below the middle of the embedded pile for lighter loads to a point approximately three-quarters of the embedment depth for maximum loads.

As indicated in this brief literature review, considerable research has been conducted on the ultimate soil resistance and pile capacity of laterally loaded piles. Most of the solutions, however, are based on the ultimate or limiting equilibrium conditions, and thus cannot be used to compute lateral earth pressures at conditions other than failure. In order to understand the soil-rigid pile interaction more clearly, a comprehensive investigation including a laboratory model study was conducted. Considerations were given to both the working stress and ultimate stress states in level and sloping ground. The pile model study is described in detail in this study.

MODEL TESTING

Testing Facility

The testing facility included a large test bin, an instrumented pile, a loading system, and a data-acquisition system. The wooden test bin (12 ft × 4 ft × 4 ft) was composed of ¾-in.-thick plywood sidewalls, two sets of perimeter steel box beams to reinforce the walls, and a plywood bottom. A 2024-T4 aluminum tube pipe 0.25 in. thick, and 40 in. long, with an outside diameter of 3.5 in., was selected to represent the model pile. To instrument the model pile, the pipe was cut into two half-circular sections with shear pins installed along both sides of one of the half pipe sections.

Eleven lateral pressure gauge mounts were installed in each of the two half pipe sections at a spacing of 3 in./mount. The large number of pressure gauge mounts allowed the locations of the pressure gauges to be changed from test to test. Finally, a thin coat of medium sand was glued to the outer surface of the model pile to produce the typical concrete-soil interface friction. Ten Kulite model KHM-375-series pressure gauges were installed in the gauge mounts along the front and back sides of the model pile, with the pressure-sensitive diaphragm placed flush with the surface of the model pile and in alignment with its length.

A set of electric circuit boards was designed and mounted inside the model pile to perform the multiplexing and signal-conditioning functions so that all the signals could be transmitted from the model pile to the data-acquisition system by a single set of wires. A picture of the fully instrumented model pile is shown in Figure 1.

An electrohydraulic closed-loop testing system was modified to apply the lateral load to the instrumented model pile. The hydraulic actuator was programmed to pull or push the

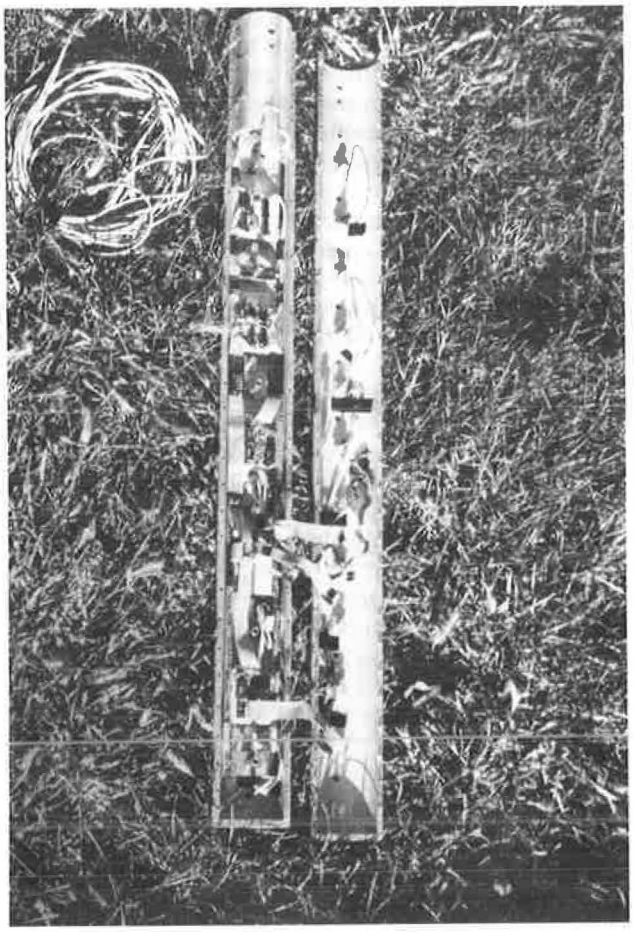

FIGURE 1 Model test pile with instrumentation.

TABLE 1 SOIL PROPERTIES

	Yolo Loam	Cache Creek Sand
Cohesion (psf)	1,800 - 2,750	0
Friction Angle	24° - 26°	40° - 43°
Maximum Dry Density (pcf) (Modified AASHTO Method T-180-57)	116	114.3
Liquid Limit	27	--
Plasticity Index	12	--
Water Content	15.3 - 17.4%	--
Unified Classification	CL	SP

model pile laterally at a rate of 0.2 in./min. A lateral displacement of 3 in. was applied to the top of the model pile that corresponds approximately to a 5° angular rotation assuming no tip movement.

The load applied to the model pile was measured by a load cell connected between the hydraulic actuator and the loading rod. The lateral displacement and angular rotation of the model pile were measured by two linear variable differential transformers (LVDTs) attached to the top of the pile. The angular rotation and lateral displacement (much less than 3 in.) at ground level were calculated from the difference between LVDT readings and the geometry of the setup. Movements of the LVDTs were monitored and recorded by the data-acquisition system.

A microcomputer-based data-acquisition system was used for recording and processing data. Signals from various sensors picked up by the signal conditioners were filtered, converted, and then channeled through a multiplexer to a digitally programmable amplifier-attenuator that adjusted the output signal level. The adjusted analog signals were then fed through an analog-to-digital converter that digitized the signals that were to be processed by the computer.

Testing Program

The model pile testing program required the construction of either level ground or sloping ground embankments made of pit-run, air-dried river sand or silty clay. For each type of the embankment material studies, parameters such as embankment geometry and loading direction were varied to evaluate the load-versus-displacement response of the pile-soil system and the corresponding measurements of lateral earth pressure distribution in longitudinal and circumferential directions.

The testing program involved a sequence of events composed of sample preparation, placement of pile, and testing and data collection. Locally available silty clay (Yolo Loam) and sand (Cache Creek sand) were chosen as embankment materials. Their pertinent properties are described in Table 1.

A brief description of cohesive soil sample preparation is given as follows. The bin was initially treated with a waterproofing seal to help retain moisture in the soil. For each lift of compaction, approximately 1,500 lb of soil was placed in the test bin to make a 4- to 5-in.-thick loose layer. The soil layer was then compacted, first with a vibratory plate compactor and then with a pneumatic hammer. A uniform amount of compaction effort was applied to each layer during compaction to achieve uniformity in shear strength and dry unit weight. The specification for compaction control of the cohesive soil was for each layer to be compacted at 3.5 percent above the optimum moisture content and to a minimum of 95 percent of the maximum dry density obtained by the modified AASHTO method T-180-57. Compaction was carried out on the wet side of optimum in an effort to avoid overcompaction of the layers.

When preparation of a soil sample was completed, damp burlap was placed on the surface of the soil sample and then the entire bin was covered with a sheet of plastic to prevent evaporation of moisture from the soil sample. In an effort to obtain a more uniform moisture content, the soil sample was permitted to sit covered overnight.

After allowing the soil sample to set overnight, a posthole driller was used to drill a 9-in. diameter hole to the desired depth in the embankment soil. The model test pile was then lowered into the hole, aligned vertically and then clamped into place. The material removed during drilling was broken up and placed back around the model pile in 1-in. layers and compacted with a slide hammer compactor.

The method of compaction used in cohesionless soil consisted of compacting 4- to 5-in.-thick loose layers of sand in the test bin with a vibratory sled. To place the test pile in the compacted sand, a vibratory-pneumatic driving system was developed. The pile was lowered into the embankment by a combined action of vibrating the pile and removing the sand directly below the pile with vacuum. The base of the test pile was modified to channel the sand directly below the test pile toward the holes in the base. A large capacity vacuum source was used to remove the sand directly below the pile through two ½-in.-diameter holes in the base. The sand was removed through the pile via two ½-in.-diameter copper tubes that ran from the base, through the center of the pile, and out at the sides of the pile near the top. To keep the sand flowing up the vacuum tubes, compressed air was fed to the base through four ¼-in.-diameter feeder tubes. The feeder tubes ran from the top of the pile, down through the center, and out through the four ¼-in.-diameter holes in the base. The modified pile tip and the plumbing inside the pile, are shown in Figures 2 and 3, respectively.

The installation of the instrumented test pile does not simulate the actual field practice of CIDH pile; disturbance in the surrounding soil and the nonuniformity in density resulting from recompaction should be recognized. Once the instrumented model pile was placed in the soil, the loading arm

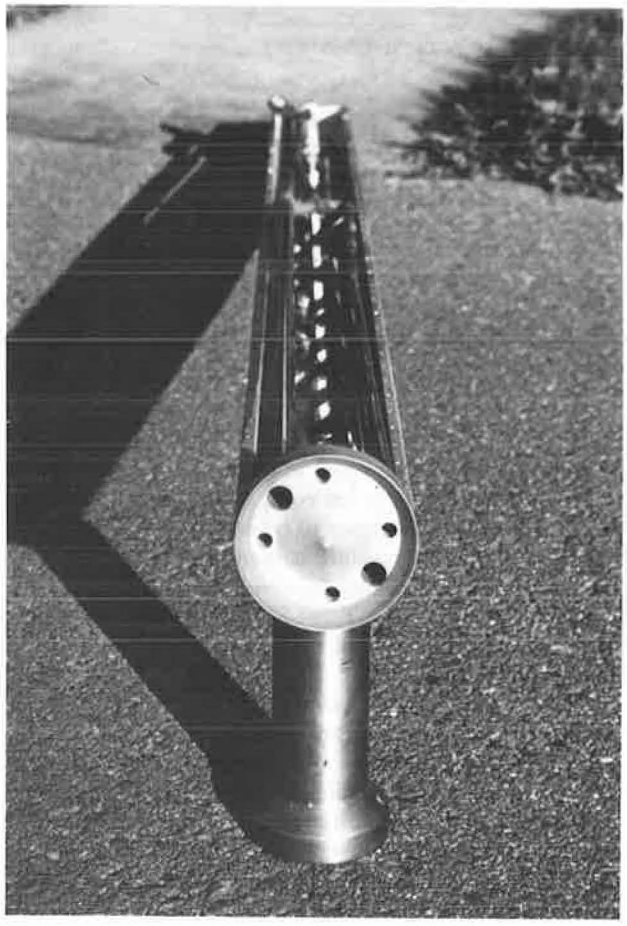

FIGURE 2 Modified pile tip.

was connected to the top of the pile at a predetermined loading height. The photograph in Figure 4 illustrates a typical test setup.

Test Results

A total of 17 tests on sand and 27 tests on silty clay were carried out. Parameters covered in this study were the embedment length (with a slight variation in silty clay soil), the type of loading (monotonic or cyclic), the direction of loading, the sloping nature of the ground, and the distance of the pile from the edge of the slope. Detailed description of each test is given in Tables 2 and 3. The cyclic loading tests were performed on silty clay samples. Different numbers of cycles of low-level loading were applied (Table 3, Tests 29 to 34, inclusive). It was indeed difficult to maintain compaction control when large size test samples were prepared in the model box; thus from sample to sample a substantial amount of scatter existed in the data. However, the results of tests carried out for each individual sample were generally well-behaved and consistent with the loading directions.

One observation that was most apparent during testing was the surface character of the failure zone exhibited in the soil around the pile. A fan-shaped failure zone extending radially from both sides of the pile at 45 degrees or greater to the direction of loading was observed in both level and sloping grounds. A typical ground surface failure pattern can be recognized, as shown in Figure 5.

The typical response of measured lateral load versus displacement in clay embankment and sand embankment can be seen in Figures 6 and 7, respectively. The lateral resistance of the model test piles are given in Table 4. They are recorded as either the maximum lateral load obtained from the load-displacement curves or the lateral load corresponding to approximately 5 degrees of angular rotation of the pile. Because the load cell has a 3,000-lb capacity, a number of tests performed in clay embankments were prematurely terminated at approximately 3,000 lb of lateral load.

When lateral load is applied in the downslope direction on the pile (Figure 8) for both the silty clay and the sand embankments, the placement of the test pile on either the slope or the edge of the slope results in lower lateral resistance than is the case when it is placed with upslope or horizontal loading directions. When the test pile is placed on the edge of a slope and the loading direction is upslope, the resulting load versus displacement curve is approximately the same as the corresponding curve obtained for horizontal loading. Differences, however, can be observed consistently from the test results that show that in clay embankment the lateral resist-

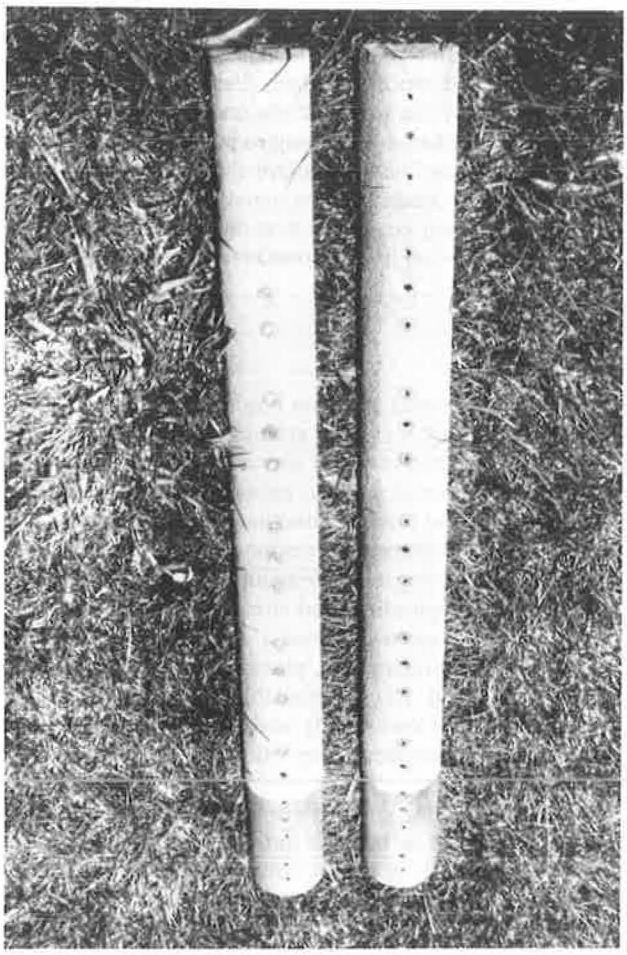

FIGURE 3 Plumbing inside the model test pile.

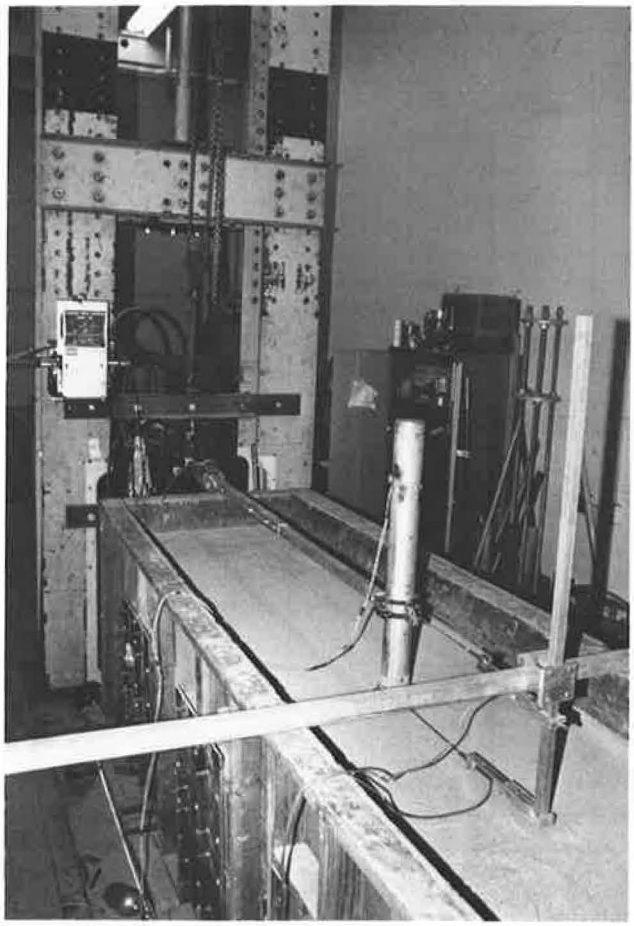

FIGURE 4 Typical test setup.

ance is slightly greater for upslope loading than for horizontal loading, and vice versa for sandy embankment.

For cyclically loaded (push and pull) model pile tests in silty clay (the number of cycles varying from 500 to 2,500 and the low level cyclic loads from approximately 200 to 900 lb at 3 sec/cycle), the results in Figure 9 indicate that the number of loading cycles greater than 500 appears to have little effect on the load-displacement behavior of the model pile. Because the model test condition in the laboratory does not simulate the field cyclic loading environment and does not take into consideration the possible disturbance and weakening of in situ soil, the findings do not agree with the current design concept of reduced pile capacity for cyclic loading applications.

In an effort to develop a three-dimensional picture of the passive earth pressure distributions along the test pile, interface pressure transducers were placed at different locations along the pile circumference from test to test to gather a set of comprehensive data. In Tables 2 and 3, the various θ values represent the angles of transducer locations with respect to the direction of loading: that is, $\theta = 0$ degrees when the transducer is placed in line with the loading direction and $\theta = 90$ degrees when it is placed perpendicular to the loading direction (Figure 8). The data obtained from sandy soil were later normalized and combined to show the radial passive earth pressure distributions against the pile at different depths for various load levels. A typical lateral earth pressure distribution along the depth of a pile in sand under different loading increments is shown in Figure 10. The pressure distributions are nonuniform both circumferentially and longitudinally. In general, the circumferential distribution has its maximum at $\theta = 0$ degrees, and decreases to at-rest pressure at $\theta = 90$ degrees. The longitudinal distribution of pressure

TABLE 2 DESCRIPTION OF TESTS IN CACHE CREEK SAND

Sample#	γ_d (pcf)	Relative Density (%)	Test #	θ_1	θ_2	Slope (%)	Loading Direction	Distance from Edge of Slope or Bin (in)
1	109.8	84.8	1	0	N/A	N/A	Horizontal	52" from edge of bin
			2	35	N/A	N/A	Horizontal	76" from edge of bin
			3	70	N/A	N/A	Horizontal	107" from edge of bin
2	108.6	80.1	4	0	45	N/A	Horizontal	47" from edge of bin
			5	0	45	N/A	Horizontal	78" from edge of bin
			6	20	65	N/A	Horizontal	108" from edge of bin
3	109.8	84.8	7	0	45	56	Down Slope	Pile 1 in. from edge of slope
			8	0	45	N/A	Horizontal	108 in. from edge of bin
4	107.9	77.7	9	20	25	59	Down Slope	Pile 1.3 in. from edge of slope
			10	20	65	N/A	Horizontal	109" from edge of bin
5	109.1	82.4	11	0	45	60	Down Slope	Pile 1.3 in. from edge of slope
			12	0	45	57	Up Slope	Pile 0.8 in. from edge of slope
6	109.0	82.0	13	20	65	58	Up Slope	Pile 1.8 in. from edge of slope
			14	0	45	60	Up Slope	Pile 1.5 in. from edge of slope
7	109.0	82.0	15	0	45	56	Cross Slope	46" from edge of bin
			16	20	65	56	Cross Slope	81" from edge of bin
			17	0	45	56	Cross Slope	108" from edge of bin

Note: The height of loading for all tests in sand was 12 inches.
The embedment length for all tests in sand was 32.75 inches.

TABLE 3 DESCRIPTION OF TESTS IN YOLO LOAM

Sample#	W/C (%)	γ_d (pcf)	Test#	θ	Load Height (in)	Embedment Length (in)	Type of Loading	# of Cycles	Loads low/high (lb)	Slope	Loading Direction	Distance From Edge of Slope (in)
2	17.4	115.2	7	0	10.6	33.1	Monotonic	N/A	N/A	Level	Horizontal	40" From edge of bin
			8	20	10.9	33.9						81"
			9	50	10.6	33.9						113"
3	17.2	113.6	10	0	11.4	33.2	Monotonic	N/A	N/A	1:1.5	Down Slope	Pile on edge of slope
			11	0	11.8	33.0				1:1.5	Up	Pile on edge of slope
			12	0	10.8	33.0				Level	Horizontal	Level ground between slopes
4	16.5	109.1	13	0	12.0	31.8	Monotonic	N/A	N/A	1:1.5	Down Slope	Pile on edge of slope
			14	0	11.8	31.9				1:1.5	Up	Pile on edge of slope
			15	0	10.8	33.0				Level	Horizontal	Level ground between slope
5	16.5	111.3	16	0	10.8	33.0	Monotonic	N/A	N/A	1:1.5	Down Slope	Pile ℄:8in down slope
			17	0	10.7	33.1				1:1.5	Up	Pile ℄:8in down slope
			18	0	10.7	33.1				Level	Horizonral	Level ground between slope
6	17.0	111.3	19	0	10.8	26.9	Monotonic	N/A	N/A	1:1.5	Down Slope	Pile on edge of slope
			20	0	10.5	26.0				1:1.5	Up	Pile on edge of slope
			21	0	10.5	27.1				Level Slope	Horizontal	Level ground between slope
7	16.7	112.1	22	0	10.8	33.4	Monotonic	N/A	N/A	1:2	Down Slope	Pile on edge of slope
			23	0	10.4	33.5				Level	Horizontal	Pile ℄:32in behind slope
			24	70	10.5	33.3				Level	Horizontal	Pile ℄:59in behind slope
8	16.6	113.1	26	0	10.6	32.9	Monotonic	N/A	N/A	1:2	Cross Slope	37in From edge of slope
			27	70	10.5	33.0				1:2	Cross Slope	62in From edge of slope
			28	0	10.5	32.9				1:2	Cross Slope	104in From edge of slope
9	15.3	113.7	29	0	11.0	33.0	Cyclic	500	180/880		Horizontal	39in From edge of slope
			30	0	11.0	33.1		1000	200/890		Horizontal	68in From edge of slope
			31	0	11.0	33.1		2500	170/890		Horizontal	104in From edge of slope
10	16.2	111.2	32	0	11.5	33.4	Cyclic	500	5 /450	1:1.5	Down Slope	Pile on edge of slope
			33	0	11.6	32.8		500	30 /860	1:1.5	Up Slope	Pile on edge of slope
			34	0	11.5	32.9		500	50 /810		Horizontal	Level ground between slope

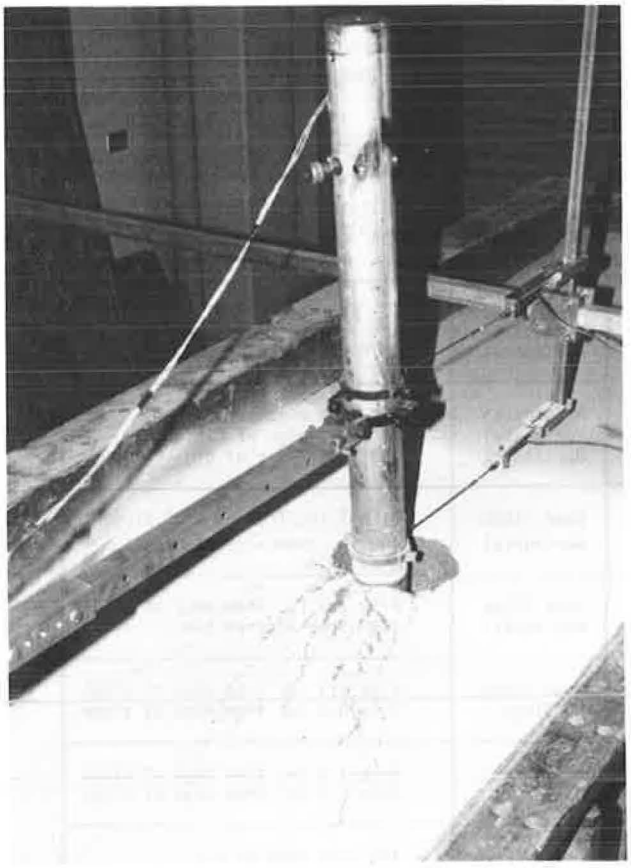

FIGURE 5 Ground surface failure pattern.

is related to both the later displacement and rotation of the pile and the soil depth at the point considered.

CONCLUSIONS

Described in this paper is a laboratory model study of the loading capacity of laterally loaded CIDH piles placed in both level and sloping grounds. Tests were performed in sand as well as in silty clay embankments. Parameters such as the embedment length, the type and direction of loading, the slope of the ground, and the distance from the edge of the slope were included in the study. An instrumented aluminum pipe pile was used to measure the circumferential as well as the longitudinal distributions of lateral earth pressures acting on the pile at different loading levels. Lateral load versus displacement curves for each test were also recorded. Because of difficulties in controlling many of the parameters in testing, particularly the placement densities and moisture contents of the clay soil, large scatter of the test results are evident. Data presented in the paper should therefore be interpreted with caution.

The main purpose of the model study was to develop information concerning the failure pattern and the design capacity of laterally loaded rigid pile. The results presented in this paper can be of help in identifying these items so that a more realistic theoretical formulation of the pile-soil system can be established. Observations pertinent to the overall objective of this investigation can be stated as follows:

1. At ground level, the failure in soil in front of a pile shows a fan-shaped zone originating from the pile at an angle of 45 degrees or greater with the direction of loading.

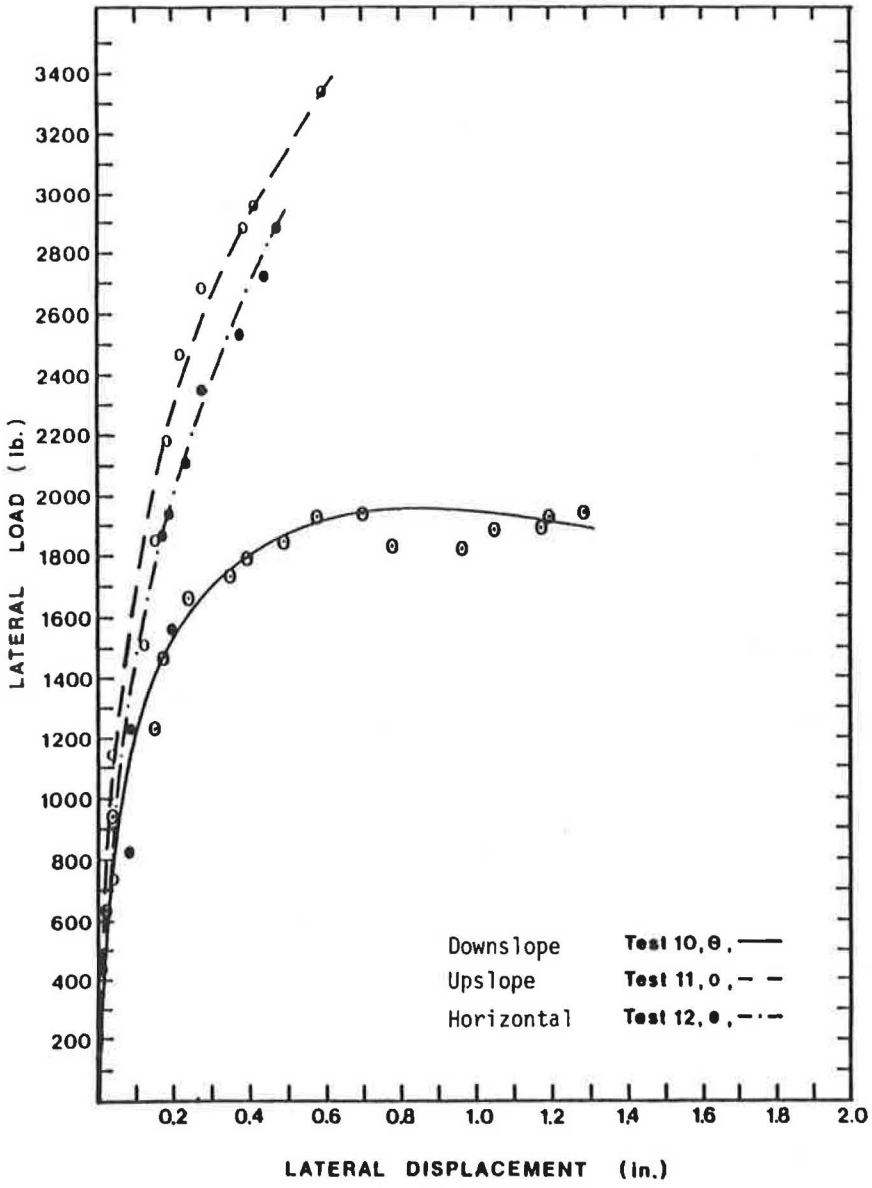

FIGURE 6 Load-deflection at ground line in silty clay.

2. If the pile is placed on a slope and loaded in the downslope direction, its ultimate lateral loading capacity is lower than the capacity produced by a corresponding pile either placed on the slope and loaded in the upslope direction or placed on level ground. Therefore, to be on the safe side, the downslope loading capacity should be used to determine the design lateral resistance for CIDH piles placed on or near an embankment.

3. The passive earth pressure acting on a pile is nonuniform both circumferentially and longitudinally. Furthermore, the magnitudes of earth pressure depend on the movement (displacement or rotation) of the pile with respect to the soil.

ACKNOWLEDGMENTS

The authors are grateful for the support provided by the California Department of Transportation and the Federal Highway Administration.

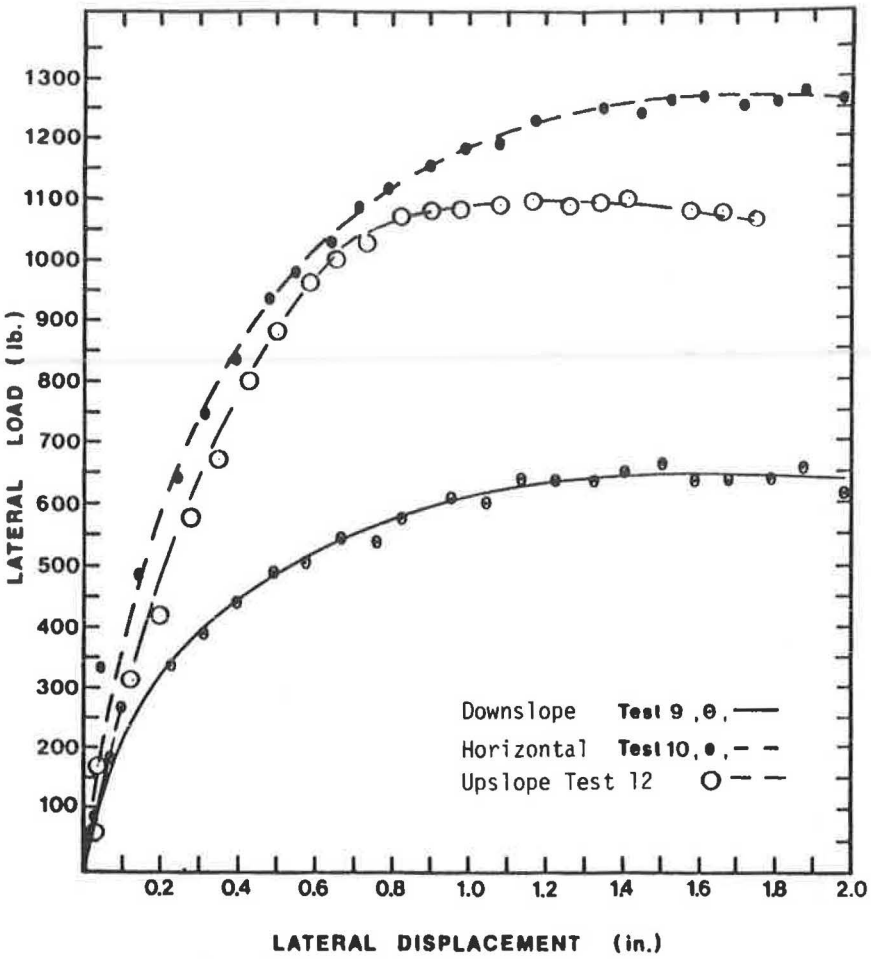

FIGURE 7 Load-deflection at ground line in sand.

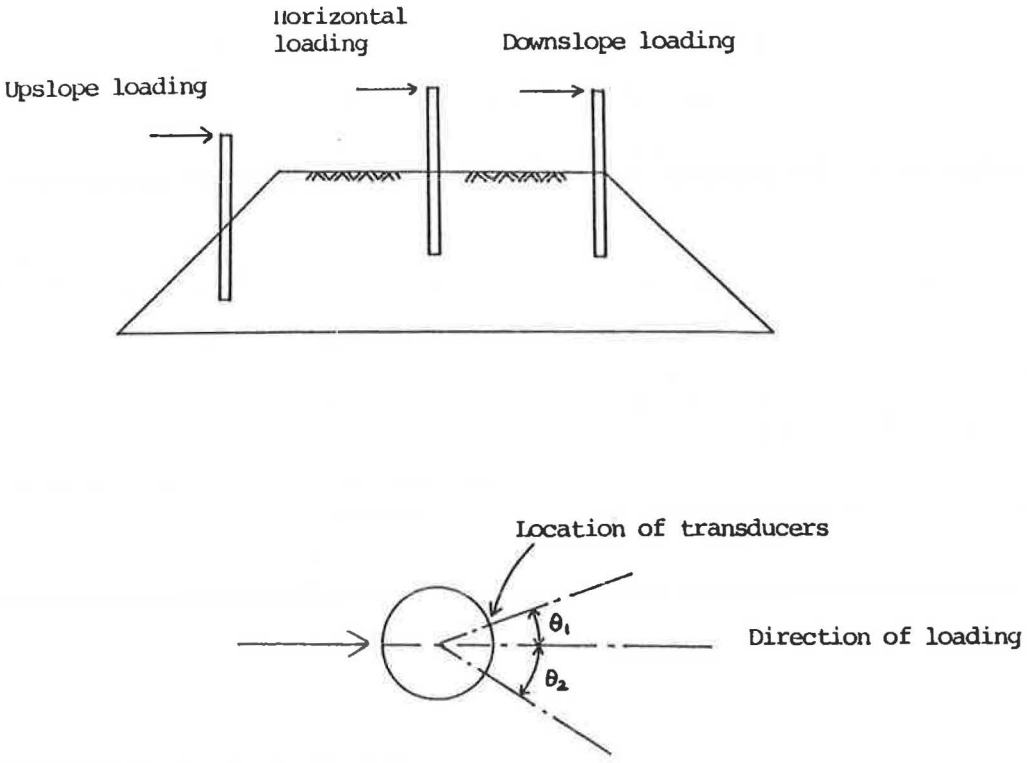

FIGURE 8 Loading direction description.

TABLE 4 LATERAL RESISTANCE OF MODEL TEST PILES

Soil	Test #	Loading direction	Slope (%)	Lateral Resistance (lbs)
Sand	1	Horizontal	N/A	1,040
	2	Horizontal	N/A	1,000
	3	Horizontal	N/A	1,000
	4	Horizontal	N/A	1,040
	5	Horizontal	N/A	970
	6	Horizontal	N/A	960
	7	Downslope	56	450
	8	Horizontal	N/A	1,030
	9	Downslope	59	520
	10	Horizontal	N/A	1,020
	11	Downslope	60	540
	12	Upslope	57	880
	13	Upslope	58	900
	14	Upslope	60	870
	15	Cross-slope	56	970
	16	Cross-slope	56	860
	17	Cross-slope	56	800
Silty Clay	7	Horizontal	N/A	2,650
	8	Horizontal	N/A	2,860
	9	Horizontal	N/A	2,970
	10	Downslope	67	1,900
	11	Upslope	67	2,970
	12	Horizontal	N/A	2,880
	13	Downslope	67	1,480
	14	Upslope	67	2,180
	15	Horizontal	N/A	2,430
	16	Downslope	67	1,390
	17	Upslope	67	3,630
	18	Horizontal	N/A	2,680
	19	Downslope	67	1,050
	20	Upslope	67	2,550
	21	Horizontal	N/A	2,710
	22	Downslope	50	1,820
	23	Horizontal	N/A	2,900
	24	Horizontal	N/A	2,760
	26	Cross-slope	50	2,460
	27	Cross-slope	50	2,550
	28	Cross-slope	50	2,880
	29*	Horizontal	N/A	3,020
	30*	Horizontal	N/A	2,930
	31*	Horizontal	N/A	2,920
	32*	Downslope	67	1,260
	33*	Upslope	67	2,520
	34*	Horizontal	N/A	3,110

* indicates cyclic loading tests

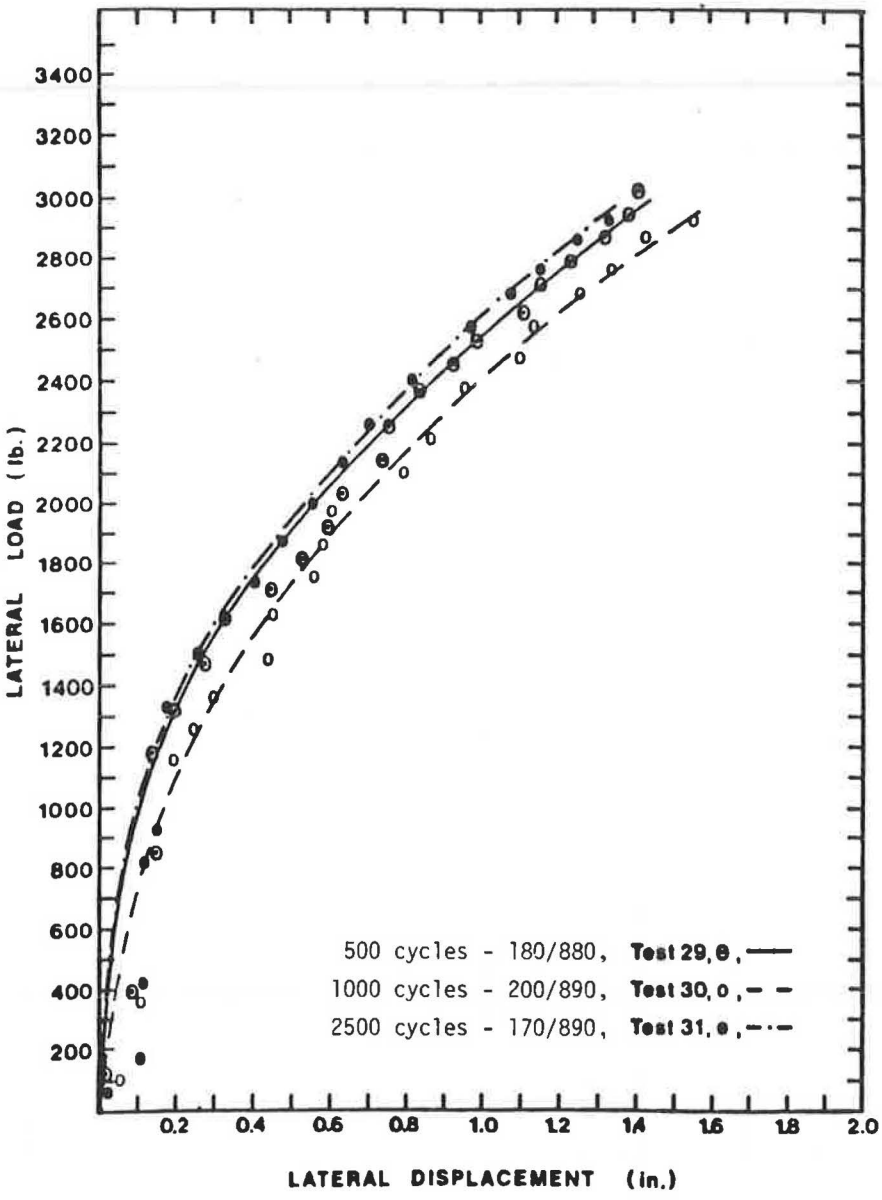

FIGURE 9 Load-deflection at ground line in silty clay—cyclic loading.

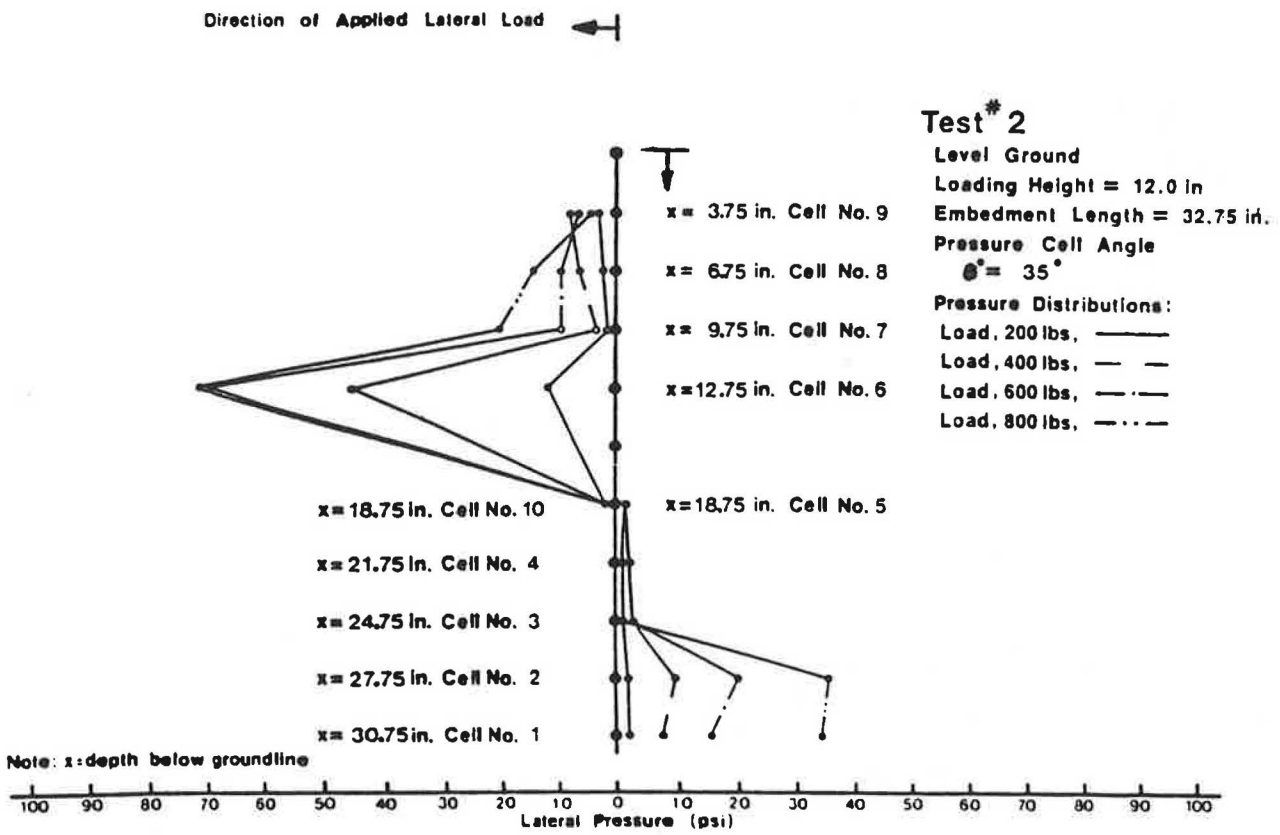

FIGURE 10 Relationship between lateral pressure and depth in sand.

REFERENCES

1. D. L. Ivey. Theory, *Resistance of a Drilled Shaft Footing to Overturning Loads*. Texas Transportation Institute, Texas A&M University, Research Department 105-1, College Station, Feb. 1968.
2. D. L. Ivey and W.A. Dunlap. *Design Procedure Compared to Full-Scale Tests of Drilled Shaft Footings*. Texas Transportation Institute, Texas A&M University, Research Department 105-3, Feb. 1970.
3. D. L. Ivey, K. J. Koch, and C. F. Raba. *Resistance of a Drilled Shaft Footing to Overturning Loads, Model Tests, and Correlation with Theory*. Texas Transportation Institute, Texas A&M University, Research Department 105-2, College Station, July 1968.
4. V. R. Kasch, H. M. Coyle, R. E. Bartoskewitz, and W. G. Sarver. *Lateral Load Test of a Drilled Shaft in Clay*. Texas Transportation Institute, Texas A&M University, Research Department 211-1, College Station, Nov. 1977.
5. B. B. Broms. Lateral Resistance of Piles in Cohesionless Soils. *Journal of Soil Mechanics and Foundation Division*, ASCE, Vol. 90, SM3, 1964.
6. L. C. Reese, W. R. Cox, and F. D. Koop. *Analysis of Laterally Loaded Piles in Sand*. Offshore Technology Conference Paper 2080, Houston, Tex., May 1974.
7. B. B. Broms. Lateral Resistance of Piles in Cohesive Soils. *Journal of Soil Mechanics and Foundation Division*, ASCE, Vol. 90, SM3, 1964.
8. L. C. Reese. *Discussion of Soil Modulus for Laterally Loaded Piles by B. McClelland and J. A. Focht*, ASCE, Vol. 123, 1958.
9. H. Matlock. *Correlations for Design of Laterally Loaded Piles in Soft Clay*. Offshore Technology Conference, Paper No. 1204, Houston, Texas, April, 1970.
10. C. O. Hays, C.O., J. L. Davidson, E. M. Hagan, and R. R. Ristano. *Drilled Shaft Foundation for Highway Sign Structures*. Engineering and Industrial Experiment Station, University of Florida, Research Department D647F, Dec. 1974.
11. D. L. Ivey, and L. Hawkins. Signboard Footings to Resist Wind Loads. *Civil Engineering*, Vol. 36, No. 12, Dec. 1966.
12. J. L. Davidson, C. O. Hays, and E. M. Hagan, Jr. Design of Drilled Shafts Supporting Highway Sign. In *Transportation Research Record 616*, TRB, National Research Council, Washington, D.C., 1976, pp. 62–66.
13. R. L. Lytton. *Design Charts for Minor Service Structure Foundations*. Texas Transportation Institute, Texas A&M University, Research Department 506-IF, Sept. 1971.
14. J. R. Seiler. Effect of Depth of Embedment on Pole Stability. *Wood Preserving News*, Vol. 10, No. 11, Nov. 1932.
15. J. Б. Hansen. *The Ultimate Resistance of Rigid Piles Against Transversal Forces*. The Danish Geotechnical Institute Bulletin, No. 12, Copenhagen, Denmark, 1961.
16. M. W. Bierschwale, H. M. Coyle, and R. E. Bartoskewitz. *Field Tests and Design Procedure for Laterally Loaded Drilled Shafts in Clay*. Texas Transportation Institute, Texas A&M University, Research Department 211-3F, Jan. 1981.
17. G. L. Holloway, H. M. Coyle, R. E. Bartoskewitz, and W. G. Sarver. *Field Test and Preliminary Design Method for Lateral Loaded Drilled Shafts in Clay*. Texas Transportation Institute, Texas A&M University, Research Department 211-2, Sept. 1978.
18. W. L. Shilts, L. D. Graves, and G. G. Driscoll. A Report of Field and Laboratory Tests on the Stability of Posts Against Lateral Loads. In *Proc., 2nd International Conference on Soil Mechanics and Foundation Engineering*, Vol. 5, Rotterdam, The Netherlands, 1948.
19. N. F. Ismael, and T. W. Klym. *Behavior of Rigid Piers in Layered Cohesive Soil*. ASCE, Vol. 104, GTB, Aug. 1978.
20. L. C. Reese. *Design and Construction of Drilled Shafts*. ASCE, Vol. 104, GTI, Jan. 1978.
21. W. V. Wright, H. M. Coyle, R. E. Bartoskewitz, and L. J. Milberger. *New Retaining Wall Design Criteria Based on Lateral Earth Pressure Measurements*. TTI, Texas A&M University, Research Department 169-4F, Aug. 1975.
22. E. Czerniak. Resistance to Overturning of Single Short Piles. *Journal of the Structural Division*, ASCE, Vol. 83, No. ST2, March 1957.

Publication of this paper sponsored by Committee on Subsurface Soil-Structure Interaction.

Seismic Response of Tieback Walls: A Pilot Study

RICHARD J. FRAGASZY, AMJAD ALI, GORDON M. DENBY, AND ALAN P. KILIAN

The results of a study on the seismic response of permanent tieback walls prepared for the Washington State Department of Transportation are presented in this paper. The use of permanent walls in highway construction has expanded greatly during the past decade. The Washington State Department of Transportation has been a pioneer in permanent tieback wall construction, especially along Interstates I-50 and I-90 in western Washington. Because of the high seismicity of this area, it is necessary to evaluate the vulnerability of these walls to earthquake loading. It is current Washington State Department of Transportation design practice to assume that the static design of a tieback wall retaining clayey soils provides an adequate reserve of strength to prevent failure during seismic loading. This is based on the assumption that the soil and the wall move together and significant dynamic loads are not produced. For tieback walls retaining sandy soils, Mononobe-Okabe dynamic soil pressures are added to the static design pressure. The validity of these design practices is evaluated in this paper. The results of a literature review clearly show that very little work has been done on the seismic response of tieback walls and no analysis or design procedures have been proposed. A pilot numerical study was undertaken for this research project. A 40-ft-high wall with three levels of tiebacks was analyzed using the program FLUSH. For this particular example problem it was found that the wall and the soil tend to move in-phase and that only negligible dynamic tie forces are generated. However, the soil above and below the excavation level tends to move out-of-phase, leading to significant dynamic earth pressures on, and bending moments in, the wall near the excavation level. Also, high vertical accelerations are predicted, even though only horizontal accelerations are used as input. The vertical accelerations appear to be caused by rocking of the soil-wall system and lead to high bearing pressures below the wall.

The use of tieback walls as permanent retaining structures along highway right-of-way has grown significantly in popularity during this decade, especially in the state of Washington. The Washington State Department of Transportation (WSDOT) makes extensive use of permanent tieback walls, particularly in the Puget Sound area. In addition to those walls already in service, new portions of I-90 on Mercer Island and on I-5 through Olympia currently being designed and constructed by WSDOT contain several miles of tieback walls. Both cohesive and granular soils are retained by these walls and the ground surface frequently slopes upward behind the walls.

R. J. Fragaszy and A. Ali, Washington Transportation Center, Department of Civil and Environmental Engineering, Washington State University, Pullman, Wash. 99164. G. M. Denby, Geo-Engineers, Inc., 2405-140th Avenue, N.W., Bellevue, Wash. 98005. A. P. Kilian, Materials Laboratory, Washington State Department of Transportation, Olympia, Wash. 98504.

Because the Puget Sound region ranks as one of the more active earthquake areas in the United States, dynamic loading is considered in the design of transportation structures. Current WSDOT design procedure related to seismic analysis of tieback walls retaining cohesive soils is to assume that the wall and retained soil move together and that no significant additional stresses are imposed on the wall or the tiebacks. Although there appears to be a general consensus among geotechnical engineers that this assumption is reasonable, there does not appear to be any information in the literature to support it.

Current WSDOT design procedure for permanent tieback walls retaining cohesionless soils is to use Mononobe-Okabe dynamic soil pressures against the wall. These pressures are then added to the static pressures and the wall is designed to resist the combination. Again, this procedure is not based on any research reported in the literature.

In order to validate and improve this current design methodology, WSDOT and the Federal Highway Administration (FHWA) provided funding for the authors to conduct a pilot study of the response of tieback walls to earthquake loading. This study included a review of literature related to seismic response of tieback walls and a pilot dynamic finite element analysis of the response of a specific model wall to earthquake loading. In this paper the findings of the literature review are summarized and the results of the pilot numerical analyses are presented.

LITERATURE REVIEW

There are several recent books and FHWA reports that address the design and analysis of tieback walls and permanent ground anchors (*1–5*). Of these, only Hanna (*2*) specifically discusses seismic loading of anchors and only two paragraphs are devoted to the topic. The following quote from this book gives a good summary of the current state of knowledge:

> The subject of anchored structures in earthquake regions is not well documented and, in future projects in such regions, anchored structures should be monitored to assess the adequacy of present design methods, load levels in anchors and how the structure behaves under seismic loading. Until this is done there must be some uncertainty about how best to design prestressed anchor systems for these loading conditions.

There have been a few papers that discuss seismic loading of tiebacks and cyclic loading of anchors. These are divided

into numerical, laboratory, and field studies and are discussed in the following paragraphs.

Numerical Studies

In what appears to be the first numerical study of seismic response of tieback walls, Rutledge (*6*) used a pseudo-static force in conjunction with a static finite element method to design tieback walls with sloping ground surface. Anchor forces equal to the dead load and a 0.2g horizontal pseudo-static load were applied to the wall in the finite element analysis. Soil elements were checked for failure and the procedure repeated until a satisfactory stress distribution was obtained. At this point the design load for the anchors was increased by a factor of 1.5 and the soil wall system was reanalyzed using a limit equilibrium analysis to ensure that the wall could withstand a seismic coefficient of at least 0.25g. He also observed that there is no standard method of analysis or literature available on the seismic design of tieback walls.

The only other numerical study located by the search was recently described by Siller et al. (*7*). The authors performed a dynamic finite element analysis of a wall subjected to a vertically propagating half-sine pulse with a frequency of 6.5 Hz and an amplitude of 0.5g. The model wall was 36.4 ft high, including 10.4 ft below the excavation level. Two levels of tieback anchors were used. The tiebacks were modeled by incorporating a spring support for the wall at the tieback locations. The tieback prestress was modeled by applying equal but opposite nodal forces at the two ends of each tieback. The tieback stiffness was 1.0 kip/ft, which models a 50-ft steel tieback, with a diameter of 1.9 in., placed at a spacing of 8 ft longitudinally. It appears from the paper that the tiebacks were horizontal.

The authors used both linear and nonlinear soil models in their study. They concentrated the discussion of their results on the differences in permanent displacements of the wall and total force acting on the wall that are predicted using the two soil models. They concluded that the nonlinear behavior leads to a significantly reduced response and an accumulation of permanent deformations of the wall toward the excavation. They also concluded that the total force acting on the wall is lower for nonlinear soil because of the permanent deformation of the wall.

Laboratory Studies

Murphy (*8*) carried out an experimental study on a model wall in sand. The wall was made of ¾-in. thick solid rubber and the tie rod was made of a strand of round sectioned rubber. After vibrating the wall in a shaking table for 20 sec, it was noted that the wall had translated horizontally while remaining vertical. At this stage the strand was released to simulate anchor failure. Planes of shear failure were observed during vibration and after tie release. Murphy concluded that active stresses under dynamic conditions are higher than those under static conditions. He also found that the planes of shear failure are at a lower angle than Rankine's state both for active failure behind the wall as well as passive conditions at the toe.

Kurata et al. (*9*) performed shaking table tests on flexible anchored model walls in sand. They used a single anchor and densified the sand by an initial stage of vibration before they applied the accelerations. They concluded that the bending moments and the tieback forces consist of two parts: an oscillating part during the vibration and a residual part that remains after the shaking ceases. They showed that the residual stresses were considerably higher than the oscillating stresses. They also showed the effect of soil modulus at the toe of the wall. As expected, the bending moments near the toe increase with an increase in the soil modulus and decrease with a reduction of the soil modulus.

Most anchor studies using cyclic loads have used dead anchors (anchors with zero prestressing). Prestressing the anchor overconsolidates the soil between the wall and the anchor, thereby reducing the rate of deformation under subsequent loading (*10*). Also, the higher confining pressures tend to stabilize sandy backfill materials (*11*). Hanna et al. (*12*) indicate that the general lack of related research may be due to the common belief that preloading negates any adverse effects caused by subsequent cyclic loads. They note the work of Carr (*13*) and Abu Taleb (*14*). Carr (*13*) subjected a plate-shaped anchor to repetitive loads showing that the displacements increased with the application of cyclic loads but the ultimate pullout capacity remained the same. Abu Taleb (*14*) performed tests on prestressed anchors. He showed that repeated loads decrease the prestressing force in the tie and that the higher the initial prestress load, the lower the anchor displacement per load cycle.

Hanna et al. (*12*) performed 46 laboratory tests on plate-shaped anchors, only two of which were preloaded to induce displacement. These two anchors were then unloaded before the cyclic load was applied. Although none of the tests were performed on prestressed anchors, their results show general trends of anchor behavior. They concluded that

1. Dead anchors undergo permanent movements when subjected to repetitive loads.
2. Movements per cycle of load decrease as the number of loading cycles progresses; however, for very large load ranges instability may occur.
3. Alternating loads (positive to negative and vice versa) cause much more severe conditions than repetitive loads (sign remains the same).
4. Alternating loads reduce the life of an anchor tremendously compared with repeated loads.
5. Prestressing does not completely eliminate movement under subsequent loading; a small movement always occurs.
6. It is expected that prestressed anchors will behave similarly to dead anchors, although the fatigue life of dead anchors may be smaller.

In the current codes of practice, little attention is paid to the effects of cyclic loads.

Field Testing

The only reference found that describes field testing deals with the effects of nearby blasting on prestressed anchors, and is reported by Littlejohn et al. (*15*). They concluded that only nominal fluctuations occurred in the prestressing loads even when the anchor heads were only 5 m from the first line

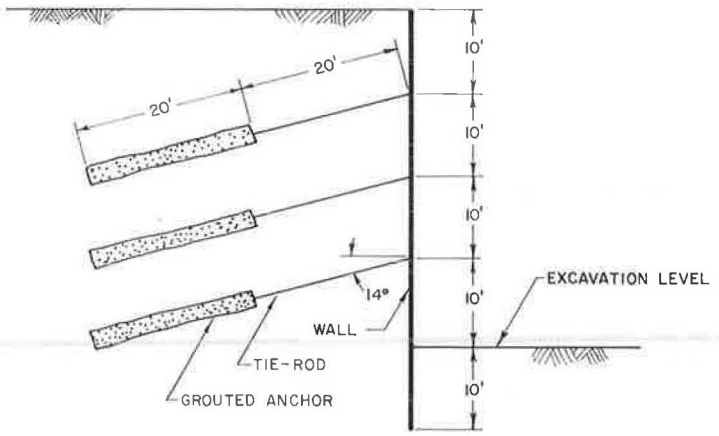

FIGURE 1 Tieback wall used in numerical analyses.

of charge holes. However, the anchors were being used to stabilize a rock slope, so the applicability of the results to tieback walls in soil may be minimal.

PILOT NUMERICAL ANALYSES

As part of the work conducted during this research project, pilot numerical studies have been performed. The intention of this work is to help evaluate the significance of seismic loading on static failure modes and to aid in the identification of other failure modes (if any) created by the dynamic loading. The work is not intended to be comprehensive, but rather to highlight areas that need additional study. Clearly, more sophisticated numerical analyses and physical modeling are required before definite conclusions can be made.

The behavior of tieback retaining walls under earthquake conditions is modeled using the finite element method. For this purpose, a dynamic finite element computer program FLUSH (*16*) is used. The program FLUSH only provides the dynamic increment of stresses; therefore, a static finite element program SOIL-STRUCT (*17*) is also employed to obtain the initial static stresses in the soil and the wall.

Wall-Soil System

A 1-ft-thick concrete wall with three levels of ties is used in all the analyses. Wall height is 40 ft with a penetration of 10 ft below the bottom of the excavation. The ties are spaced vertically at 10-ft centers, horizontally at 7-ft centers, and are inclined at an angle of 14 degrees from the horizontal. The angle was selected to keep the anchors above the bottom of the excavation. The unbonded length of the tie rods is approximately 20 ft and the bond length is 20 ft. The anchor diameter is 12 in. A schematic drawing of the wall is shown in Figure 1.

Static Analysis

Initial stresses in the soil wall system caused by gravity and the static stresses induced by the construction sequence are simulated using SOIL-STRUCT. The state of stress in the soil-wall system, after the final sequence of construction, is used to compute input parameters for FLUSH, in particular the initial shear moduli for the soil elements.

Boundaries on both the left and the right sides of the mesh are fixed in the horizontal directions only, whereas, the bottom boundary is fixed against vertical movement as well. The finite element mesh used with SOIL-STRUCT is shown in Figure 2. It contains 238 elements and 270 node points.

The soil that is modeled in the analysis is a homogeneous silty sand. Its properties are listed in Table 1. Further details of the static input parameters are discussed by Ali (*18*).

Dynamic Analysis

In order to incorporate the stresses obtained from the static analysis into the dynamic analysis, the dynamic finite element mesh was chosen to be as similar as possible to the mesh used in the static analysis. The mesh used for FLUSH, shown in Figure 3, contains 214 elements and 230 node points. Some of the major differences between the two meshes are:

- The ground anchors are modeled by springs in SOIL-STRUCT and by continuum elements in FLUSH;
- Interface elements were not used in the dynamic analyses as they are not available in FLUSH; and
- The right boundary of the dynamic mesh is placed at a greater distance because of certain modeling constraints, as described later.

To determine the importance of interface elements, an analysis was made in which the elements bordering the wall were given negligible strength. Comparison with the analysis reported as follows indicates no significant differences.

Dynamic Model

In the FLUSH mesh, each ground anchor is modeled by two linear elastic solid elements with the properties of concrete. Ties connecting the wall to the ground anchors and the wall itself are both simulated by one-dimensional beam elements.

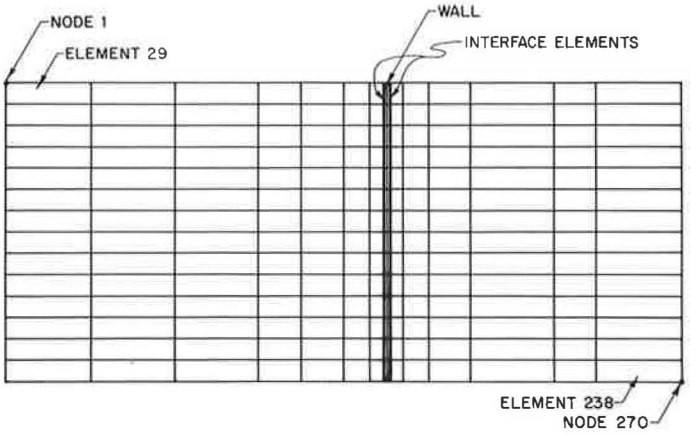

FIGURE 2 SOIL-STRUCT finite element mesh.

TABLE 1 SOIL PARAMETERS USED IN THE NUMERICAL ANALYSES

Parameter	Computer Program	
	SOIL-STRUCT	FLUSH
Unit weight	125 lb/ft³	125 lb/ft³
Poisson's ratio	0.3	0.3
Shear modulus	—	$G = K_2(_m)^{1/3}$
Initial tangent modulus	$E_i = P_a K_m(3/P_a)^n$	—
Unload-reload modulus	$E_{ur} = P_a K_{ur}(3/P_a)^n$	—
At-rest earth pressure coefficient	0.4	—
Friction angle	36δ	—
Cohesion	100 lb/ft²	—

NOTE: $n = 0.5$; $P_a = 2{,}120$ lb/ft² (atmospheric pressure); $K_m = 500$; and $K_{ur} = 700$.

Prestressing of the anchors cannot be simulated in FLUSH. However, the initial stresses calculated by SOIL-STRUCT, which include the effects of prestressing, are used to input initial shear moduli in FLUSH. A transmitting boundary is used on the left side of the mesh. FLUSH, however, does not allow a transmitting boundary on both sides unless both are of equal height. Therefore, the right-side boundary is placed at a distance of 2¼ times the height of the excavation and is free to move in the horizontal direction only. This reduces the effects of the boundary conditions on the area of interest (i.e., the region close to the wall). The horizontal boundary at the bottom represents a rigid base and is the location of the input accelerations.

Dynamic Input Parameters

Input parameters for FLUSH include soil, concrete, and steel properties, and a record of ground motion. Material properties include Poisson's ratio, unit weight, shear modulus at low strain, shear modulus for the first iteration (for soil) and damping ratio for the first iteration.

The earthquake record used in the analyses was provided with the FLUSH program. The time increment of the provided record is 0.02 sec and the duration of the record is 10.24 sec. A number of different time steps were used and finally 0.015 sec was chosen as it produced the maximum dynamic amplification in the soil-wall system. This reduced the duration of the record to 7.68 sec. The maximum input acceleration was set at 0.15g. The predominant period of the record

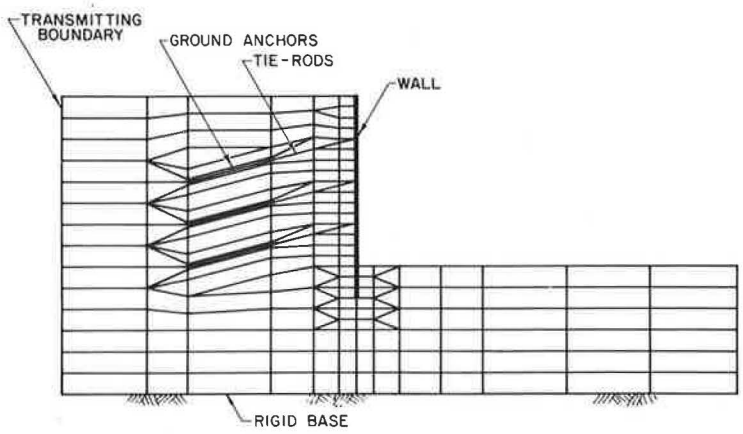

FIGURE 3 FLUSH finite element mesh.

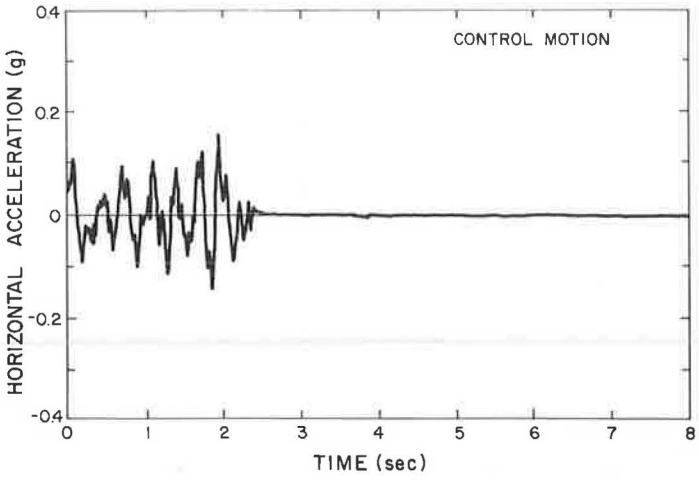

FIGURE 4 Input motion used in numerical analyses.

is 0.32 sec. A time history of the input motion used is shown in Figure 4.

RESULTS

Although the numerical studies conducted to date are preliminary in nature, they do shed considerable light on the problem. Of particular importance is the insight they give to the question of in-phase versus out-of-phase motion. One of the reasons often given for not considering seismic loading separately for tieback walls is the intuition that the wall and the soil backfill are in-phase. This means that the soil and the wall face tend to move together for the given hypothetical conditions and that there is little to no relative movement between them. It is often assumed that this will result in negligible increases in load on the wall. Although this study tends to confirm the in-phase behavior of the wall and the backfill, it clearly points out a second, perhaps more serious, consideration. On the basis of these numerical studies, it appears that the soil above and below the bottom of the excavation may not move in-phase. The analyses show that these two layers of soil move in opposite directions during a significant portion of the shaking. This can be seen in Figure 5, which shows the horizontal acceleration of each node point 1.965 sec after the beginning of shaking. The vertical dashed lines represent zero horizontal acceleration. The soil lines represent the horizontal accelerations of the soil at that location in the mesh. Where the solid line is to the left of the corresponding dashed line, the soil is accelerating to the left; where the solid line is to the right of the dashed line, the soil is accelerating to the right. The magnitude of the acceleration is given by the distance between the solid and the dashed line. Although actual magnitudes of acceleration are difficult to pick out, it is clear from this figure that the upper and lower portions of the soil deposit are accelerating in opposite directions. This out-of-phase behavior leads to the development of high horizontal pressures and bending moments at the excavation level.

It was also found that relatively high vertical accelerations are induced in the wall and the soil, even though the input motion is entirely horizontal. This increases the bearing pressure at the base of the wall and lowers the safety factor against bearing capacity failure.

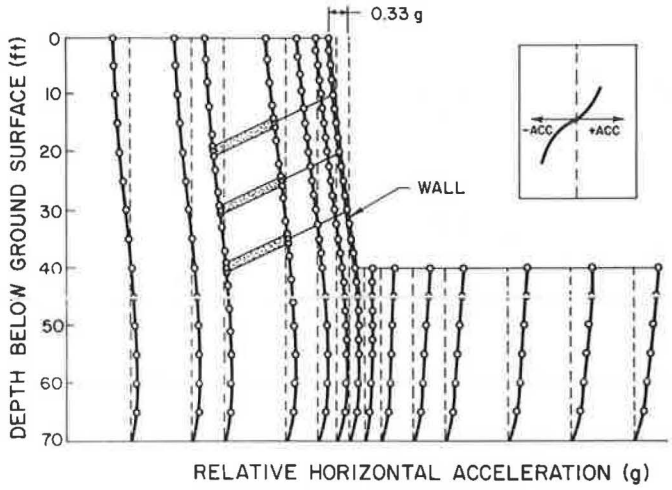

FIGURE 5 Horizontal acceleration at Time = 1.965 sec.

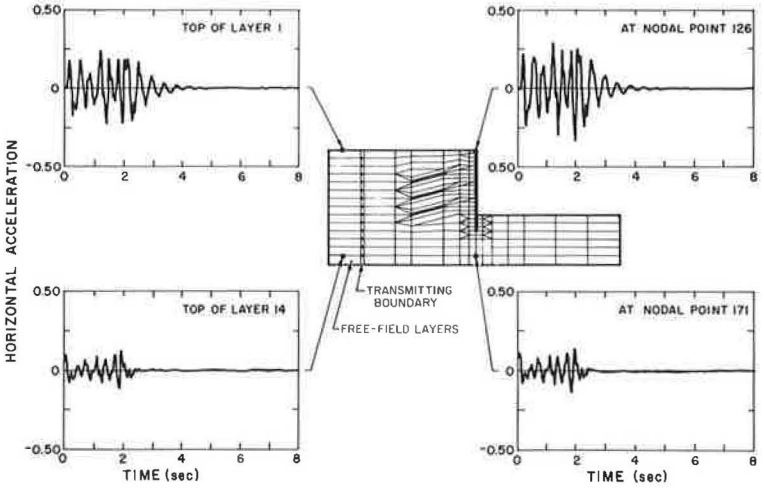

FIGURE 6 Time histories of horizontal ground motion at four locations.

Finally, it was found that dynamic amplification of the base motion was produced, resulting in peak horizontal ground accelerations of 0.33g compared with a peak input acceleration of 0.15g.

The three factors discussed all influence the response of the wall-soil system. More detailed results are presented in the following paragraphs for each of the major parameters of wall behavior: displacements, horizontal accelerations, pressures on the wall, bending moments, vertical accelerations and tie forces.

Wall Displacements

The FLUSH program does not calculate absolute displacements of the system, but rather pseudo-displacements. However, based on these data it is clear that some residual displacement does occur because of shaking. Additional studies will have to be conducted to determine the potential magnitude of these displacements.

Horizontal Acceleration

Maximum horizontal accelerations in the wall occur at the top, where they are slightly more than twice the maximum input motion. The wall acceleration decreases with depth and at the bottom of the wall it is only slightly higher than the peak input acceleration. Amplification of horizontal accelerations in the free field is lower than that observed both in the soil near the wall and in the wall itself. This is illustrated in Figure 6, which shows time histories of horizontal acceleration at various locations.

Soil Pressures on the Wall

Large dynamic horizontal pressures are induced on the wall near the bottom of the excavation. This can be seen in Figure 7, which shows the static pressure and the maximum dynamic pressure on the wall versus the depth below the ground surface. Below the excavation level the net soil pressure on the

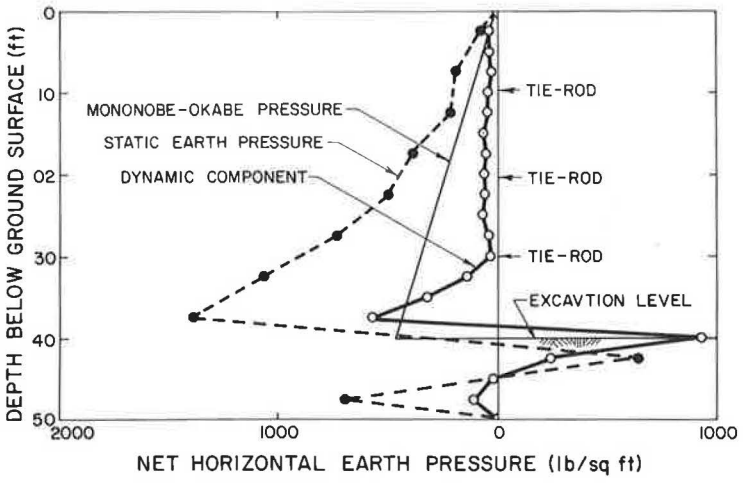

FIGURE 7 Earth pressures acting on wall.

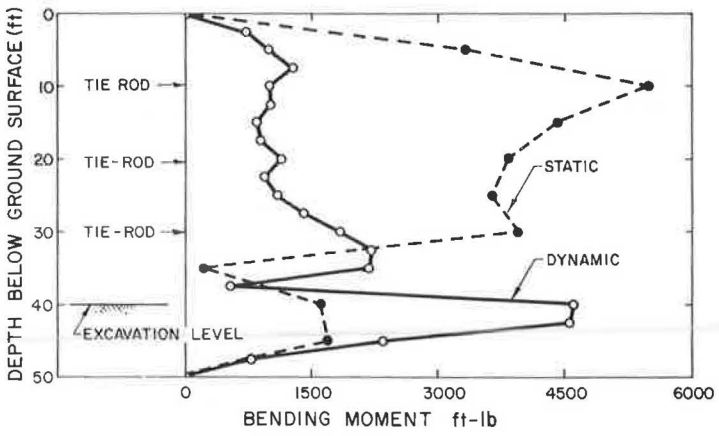

FIGURE 8 Static and peak dynamic moments in wall.

wall is plotted. The upper 30 ft of wall are subjected to only negligible dynamic pressures, but beginning at the level of the lower tieback the pressures increase dramatically to a peak of approximately 600 lb/in.^{2} 2 ft above the excavation. This dynamic increment is approximately 40 percent of the static pressure at this location. The reason for this large increase in pressure is the out-of-phase motion of the upper soil versus the lower soil.

The dynamic earth pressure predicated using the Mononobe-Okabe equations are also plotted on Figure 7. A wall friction angle of 18 degrees and a horizontal ground acceleration of 0.15g were used to obtain this pressure diagram. In this case, the Mononobe-Okabe method overpredicts the dynamic earth pressure by a significant amount except for a small 2-ft interval near the excavation level.

Bending Moments

The movement of the wall and the large dynamic pressures generated by the out-of-phase behavior of the soil above and below the excavation level led to large dynamic bending moments in the wall, as illustrated in Figure 8. In this figure, the dynamic bending moment 1.965 sec after the beginning of shaking is plotted versus location along the wall. These moments are largest at the excavation level, where it is approximately −4,500 lb-ft/ft. This dynamic moment is approximately 10 percent of the static moments at this location and, therefore, represents a reduction in safety factor. Similar dynamic moments are produced at other times during the shaking.

Vertical Accelerations

Very large vertical accelerations, approximately equal to the maximum horizontal input motion, are induced in the region between the wall and the anchors. This is illustrated in Figure 9, which shows the time history of vertical acceleration at Node Point 101, located at the ground surface behind the wall. Sitar and Clough (*19*) also noted high vertical accelerations when analyzing the seismic response of steep slopes in cemented sands. It is believed that these accelerations are real and not caused by difficulties in the numerical procedures. Rocking of the soil-wall system is the most likely cause of the vertical accelerations.

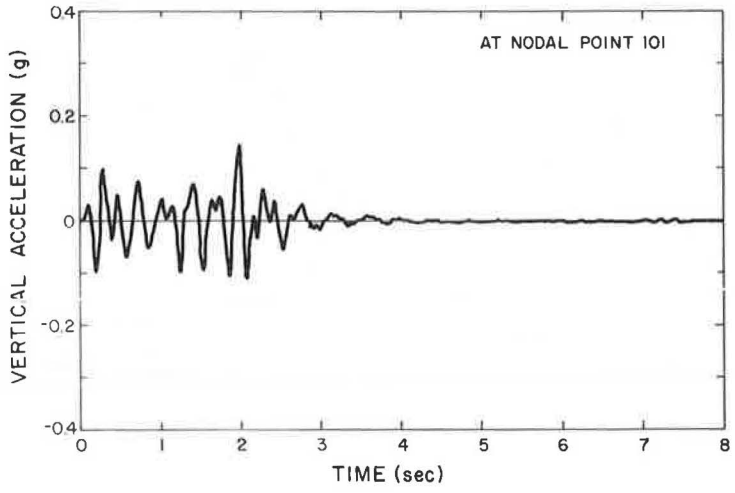

FIGURE 9 Time history of vertical acceleration at Node 101.

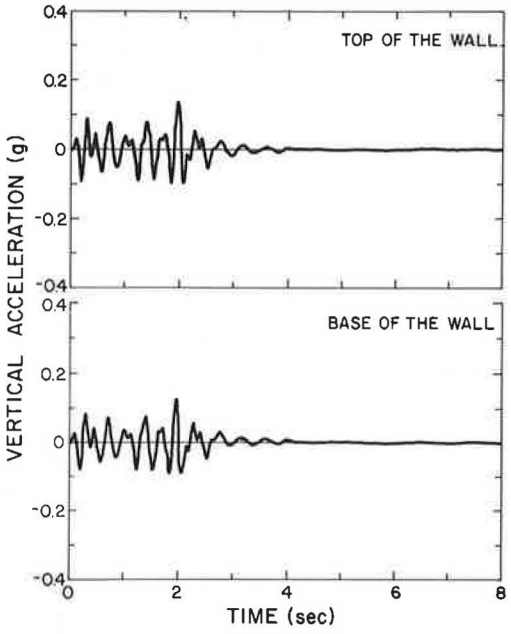

FIGURE 10 Time histories of vertical acceleration at top and bottom of wall.

The wall itself also undergoes significant vertical accelerations, as shown in Figure 10. These accelerations cause large axial stresses to develop in the wall that are transmitted to the ground. This is shown in Figures 11 and 12. Figure 11 is a plot of maximum dynamic axial force in the wall as a function of depth. The peak dynamic vertical stress in the ground immediately below the wall can be seen in Figure 12.

It is possible that the lack of an interface element between the wall and the soil might affect the predicted values of vertical pressures beneath the wall. To estimate the possible effects of slippage between the wall and the soil, an analysis was conducted in which the stiffness of the soil immediately adjacent to the wall was reduced to a negligible value. The results indicate minimal effect, thus indicating that the lack of an interface element does not appear to be a problem.

Tie Forces

In these analyses negligible dynamic load increments are induced in the tie rods. The peak dynamic loads are −428 lb, −434 lb, and 413 lb for the upper, middle, and lower tie rods, respectively. In comparison, the prestressing force applied

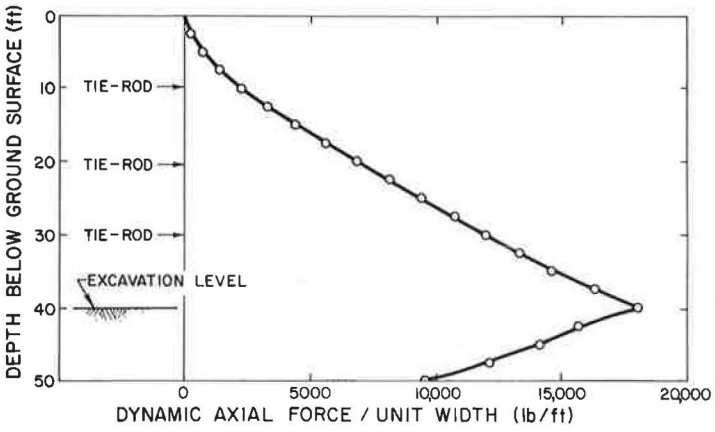

FIGURE 11 Peak dynamic axial force in wall.

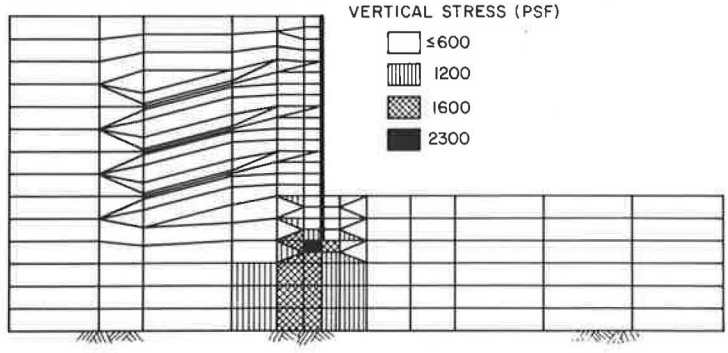

FIGURE 12 Peak dynamic vertical stresses beneath wall.

during construction is 11,000 lb. It should be remembered, however, that all three levels of tie rods are located in the upper layer of soil above the base of the excavation. There is little relative movement between the wall and the soil in this layer. It is probable that significant tie forces would develop in the tie rods in situations in which the anchors are located in the lower soil layer. An even more important consideration in this case is the possibility of load reversals occurring if the anchor is moving out-of-phase with the wall. As discussed by Hanna, significant loss of anchor strength may develop in such a case.

DISCUSSION

It is important to realize the limitations of the numerical study described above. Because the objective was to do pilot work to determine whether a more detailed numerical study was justified, only one wall and soil profile were considered. It is with care, therefore, that general conclusions should be made regarding other wall geometries, input motion, and soil profiles. This study does show that for at least one set of conditions significant dynamic loading can occur.

It is likely that there are less favorable combinations of wall geometry, soil profile, and input motion so the results of this study cannot be taken as an upper bound. An example of a case in which the loads on the wall might be much more severe would be a wall that penetrated through a soft layer into a very stiff one. Considerably lower forces might be generated when the soil deposit was relatively uniform and the wall height was small compared with the depth of the deposit.

Another limitation of this study comes from the selection of a single soil profile. It appears that the major factor in the response of the wall to seismic loading is the out-of-phase behavior of the upper and lower soil layers. The location of the anchors relative to the bottom of the excavation may also be important. In an extreme case, an anchor embedded in a very stiff layer below the excavation might be subjected to load reversals when the upper soil is much softer. As described in the literature review, load reversals significantly affect the capacity of anchors and could lead to failure of the anchor much more quickly than repeated loading without load reversal.

Finally, it should be made clear that the program FLUSH has many limitations that must be recognized when evaluating the results of this study. The inability to include static stresses, lack of an interface element, and inability to provide information on permanent displacements limits its usefulness. However, this study does point out potential problems that should be examined in detail by more sophisticated methods. The authors are continuing this work using a time domain, nonlinear program, FLEX, which is believed to be better suited for the analysis of this type of problem.

SUMMARY AND CONCLUSIONS

The results of a literature review and a pilot numerical study of the seismic response of tieback walls are presented in this paper. The literature review clearly shows that very little research has been conducted on this subject and that there is no recognized analysis-design procedure for seismic loading of tieback walls. The results of the pilot finite element analysis point out at least two possible difficulties associated with dynamic loading. The first is out-of-phase motion of the soil above and below the excavation level. This can cause high dynamic soil pressures on the wall near the excavation level and high dynamic bending moments in the wall. This may also lead to load reversals on anchors located below the excavation level. The second is rocking of the wall-soil system leading to high bearing pressures in the soil below the wall.

Based on this pilot work the conclusion is reached that there are potential problems related to seismic loading of tieback walls and more extensive numerical analyses are required to determine the extent of these problems. The authors are currently engaged in a follow-up numerical study in which a more complete parametric analysis is being conducted. Included in the parameters to be studied in more detail are ground slope, soil properties, anchor location, earthquake record and wall-backfill geometry.

ACKNOWLEDGMENTS

The research described in this paper was supported by the Washington State Department of Transportation and the Federal Highway Administration.

REFERENCES

1. R. S. Cheney. *Ground Anchors*. Federal Highway Administration Report FHWA-DP-68-1, U.S. Department of Transportation, 1984.
2. T. H. Hanna. *Foundations in Tension: Ground Anchors*. McGraw-Hill Book Co., New York, 1982.
3. P. J. Nicholson, D .D. Uranowski, and P. T. Wycliffe-Jones. *Permanent Ground Anchors: Nicholson Design Criteria*. Federal Highway Administration Report FHWA/RD-81/151, U.S. Department of Transportation, 1985.
4. H. Schnabel, Jr. *Tiebacks in Foundation Engineering and Construction*. McGraw-Hill Book Co., New York, 1982.
5. D. E. Weatherby. *Tiebacks*. Federal Highway Administration Report FHWA/RD-82/047, U.S. Department of Transportation, 1982.
6. J. C. Rutledge. Tie-Back Retaining Walls. *New Zealand Engineering*, Vol. 30, No. 8, Aug. 1975, pp. 242–247.
7. T. J. Siller, P. P. Christiano, and J. Bielak. Structures and Stochastic Methods (A.S. Cakmak, ed.). *Developments in Geotechnical Engineering*. Vol. 45, Elsevier Publishing Co., Amsterdam, The Netherlands, 1987, pp. 141–150.
8. V. A. Murphy. The Effect of Ground Characteristics on the Aseismic Design of Structures. In *Proc., Second World Conference on Earthquake Engineering*, Tokyo, Japan, Vol. 1, 1960, pp. 231–248.
9. S. Kurata, H. Arai, and T. Yokoi. On the Earthquake Resistance of Anchored Sheet-Pile Bulkheads. In *Proc., Third World Conference on Earthquake Engineering*, Vol. 2, 1965, pp. 369–383.
10. D. H. Trollope, I. K. Lee, and J. Morris. Stresses and Deformation in Two-Layer Pavement Structures Under Slow Repeated Loading. In *Proc., First Conference Australia Research Board*, Vol. 1, Part 2, 1962, pp. 693–720.
11. J. R. Morgan. The Response of Granular Materials to Repeated Loading. In *Proc., Third Conference Australia Research Board*, Vol. 3, Part 2, 1966, pp. 1178–1193.
12. T. H. Hanna, E. Sivapalan, and A. Senturk. The Behavior of Dead Anchors Subjected to Repeated and Alternating Loads. *Ground Engineering*, Vol. 11, No. 3, 1978, pp. 28–34.
13. R. W. Carr. *An Experimental Investigation of Plate Anchors in Sands*. Thesis, Sheffield University, England, 1971.

14. G. M. A. Abu Taleb. *The Behavior of Anchors in Sand*. Thesis, Sheffield University, England, 11974.
15. G. S. Littlejohn, P. J. Norton, and M. J. Turner. A Study of Slope Reinforcement at Westfield Open Pit and the Effect of Blasting on Prestressed Anchors. In *Proc., Conference on Rock Engineering*, University of Newcastle upon Tyne, England, April 1977.
16. J. Lysmer, T. Udaka, C. F. Tsai, and H. B. Seed. *FLUSH—A Computer Program for Approximate 3-D Analysis of Soil-Structure Interaction Problems*. Report No. 75-30, Earthquake Engineering Research Center, University of California, Berkeley, Calif., 1975.
17. G. W. Clough and Y. Tsui. *User's Guide, Program SOIL-STRUCT*. Duke University, Durham, North Carolina, 1973.
18. A. Ali. *Seismic Response of Tieback Retaining Walls*. M.S. thesis, Washington State University, 1986.
19. N. Sitar and G. W. Clough. Seismic Response of Steep Slopes in Cemented Soils. *Journal of Geotechnical Engineering*, ASCE, Vol. 109, No. 2, 1983, pp. 210–227.

Publication of this paper sponsored by Committee on Subsurface Soil-Structure Interaction.

Analysis of Tieback Slopes and Walls Using STABL5 and PCSTABL5

JAMES R. CARPENTER

The purpose of this study was to develop a convenient method for assessing the stability of tieback structures using the simplified methods of slices. The Load Distribution Method was developed to transmit the load from a row of tiebacks to the potential failure surface for use with the simplified methods of slices. The load from a row of tiebacks is assumed to form a uniform line load that is distributed to the potential failure surface. This distribution is based on Flamant's distribution of stresses through a semi-infinite elastic medium. STABL5 and PCSTABL5 are limiting equilibrium slope stability programs that contain the Load Distribution Method routines. These programs may be used to analyze the stability of tiedback slopes for landslide stabilization, as well as to determine the overall stability of tiedback walls. The programs consider multiple rows of tiebacks, multiple tiedback structures as well as tieback loads, inclination, and length. The method developed was found to give good results and is applicable to those problems in which the application of a semi-infinite elastic half space may be used to model the slope conditions, and which may be modeled using a two-dimensional analysis. This paper is a brief review of some of the previously available methods for analyzing the overall stability of tiedback structures. In addition, a discussion of the capabilities of STABL5 and PCSTABL5 is presented, and the development of the Load Distribution Method is summarized. The assumptions used in the development of the Load Distribution Method are discussed, along with the implications and limitations of using Flamant's distribution. The effect of tieback load on the factor of safety is also presented, along with recommendations concerning factors of safety for overall stability of tiedback slopes and walls.

The use of tiebacks in geotechnical engineering, transportation, construction for support of transportation routes, construction excavations, and landslide control has increased substantially within the last 10 to 15 years. As a result, the need for a reliable and practical method of analyzing the internal and overall (external) stability of slopes and retaining walls subjected to tieback anchor loads has become evident.

Tiebacks are routinely used for both temporary and permanent support of excavated slopes. Tiedback or anchored retaining structures for temporary and permanent support of excavations may consist of soldier piles with wood lagging, sheet piling, drilled concrete pile walls, or concrete diaphragm walls constructed using the slurry trench method. Tiedback retaining structures for stabilization of embankments and slopes may be continuous along the length of a slope, as in soldier piles and wood lagging, or may be discontinuous, as in tiedback drilled piers with concrete bearing pads or buttress elements placed on the face of the slope.

The analysis of the stability of tiedback structures is a complex problem. The stability of these structures is influenced by, but not limited to (a) the lateral earth pressure behind the wall; (b) the deformation of the soil-structure system; (c) tieback characteristics (individual tieback loads, inclination, horizontal spacing, overall length, size of anchor, method of construction); and (d) soil characteristics. The analysis of tiedback structures is further complicated by the fact that a two-dimensional model is used to model a three-dimensional problem. Analysis of the overall stability of tiedback structures is only one of the many considerations in the design of tiedback structures for excavation support or slope stabilization. Because many factors influence the stability of tiedback structures, and because relatively little is known about these factors at the time of design, a conservative approach is often used by geotechnical engineers and design-and-build tieback contractors in the design of tiedback structures.

Previously available methods for determining the internal and overall stability of multiple tiedback structures (*1–3*) often involved errors in the statement of the problem, or required that arbitrary assumptions be made to perform the calculations, usually by hand (*4*). In addition, it was extremely difficult and tedious to take into consideration nonhomogeneous soil conditions and multiple tiebacks with the previously existing methods of stability analysis. Therefore, there existed a need for a convenient and logical method for determining the internal and external stability of multiple tiedback retaining structures considering nonhomogeneous soil conditions.

The purpose of this study was to develop a rational and convenient method of assessing the internal and overall stability of tiedback and anchored retaining structures. As a result, the Load Distribution Method (LDM) was developed for analyzing the stability of tiedback slopes and walls in conjunction with the simplified methods of slices contained in the STABL programs. The LDM was originally programmed in the slope stability programs STABL4 and PCSTABL4 (*5, 6*) and is also contained in STABL5 and PCSTABL5. The STABL5 and PCSTABL5 versions retain all the capabilities and options of STABL4 and PCSTABL4. However, STABL5 and PCSTABL5 are the only versions of STABL with the enhanced capabilities of analyzing potential failure surfaces, including tiedback slopes and walls, using Spencer's method of slices. The focus of this paper will be on the LDM developed by the author because it is this method that is used most frequently.

CAPABILITIES OF STABL5 AND PCSTABL5

The STABL5 and PCSTABL5 programs calculate the factor of safety against slope failure by a two-dimensional limiting

STS Consultants Ltd., 2929-C Eskridge Road, Fairfax, Va. 22031.

equilibrium method. These programs are written in FORTRAN and contain routines for analyzing slopes and walls subjected to tieback loads. PCSTABL5 is the microcomputer version of the mainframe STABL5 program and contains all the options and capabilities of STABL5. The calculation of the factor of safety against slope instability may be performed using (a) the Simplified Bishop method of slices, which is applicable to circular shaped failure surfaces; (b) the Simplified Janbu method of slices, which is applicable to failure surfaces of a general shape, or; (c) Spencer's method of slices, which is applicable to surfaces having a circular or general shape.

The STABL5 and PCSTABL5 slope stability programs feature unique techniques for random generation of potential failure surfaces for subsequent determination of the more critical failure surfaces and their corresponding factors of safety. Circular, irregular, and sliding block surfaces may be generated and analyzed using either a random search technique or specific input of the coordinates of a given potential failure surface.

The programs are capable of handling heterogeneous soil systems, isotropic and anisotropic soil strength parameters, excess pore water pressure caused by shear, static groundwater and surface water, pseudo-static earthquake loading surcharge, and tieback loading. The tieback loading feature provides for the input of horizontal or near-horizontal tieback or line loads for analyzing the internal and overall stability of tiedback or braced slopes and retaining walls.

Plotted output is provided as a visual aid to confirm the correctness of problem input data. Error messages are generated within the program to pinpoint locations where input data are inconsistent with STABL5/PCSTABL5's input requirements. Free-format data input eases the task of input file preparation, which results in a reduction of input mistakes.

Plotting routines are provided for Calcomp-type plotters (STABL5 version) and for Hewlett-Packard plotters for use with the microcomputer version PCSTABL5. The PLOTSTBL program is a BASIC program for plotting the graphical output from PCSTABL5 using either a Hewlett-Packard HP-7470A two-pen plotter or an HP-7475A six-pen plotter. PLOTSTBL reads the plotted output file created by PCSTABL5, which contains commands and coordinates for plotting.

ANALYSIS OF TIEDBACK WALLS AND SLOPES

Tiebacks tie a structure to a stable soil mass through an anchor secured in the earth. The components of a typical tiedback retaining structure are shown in Figure 1. The anchor is attached to a steel tendon, which is also connected to the retaining structure. After installation of the tendon and grouting of the anchor, the tendon is stressed (pulled) to the desired load using hydraulic jacks. This load is then locked off and permanently applied to the structure. The load in the steel tendon applies a stabilizing force to the structure that is developed by the anchor in the stable soil mass. Tiebacks are different from deadman anchors in that the tieback anchor is made through a hole drilled or driven into the soil for installation of the tendon.

Assumptions are made in the design of a tiedback retaining structure concerning the lateral earth pressure distribution behind the proposed wall. On the basis of the assumed lateral earth pressure distribution, the location and magnitude of load applied to each tieback is determined for the internal (local) stability of the wall. The structure-anchor system must be designed to resist the lateral earth pressures with a suitable factor of safety (FOS). The tieback must then be designed to carry the computed load. The length of the tendon and anchor of the tieback must be made long enough so that the tieback is beyond the area that would be disturbed by wall movements and it will not pull out of the soil mass in which it is secured.

Tiebacks tie a structure to a soil mass that must also be

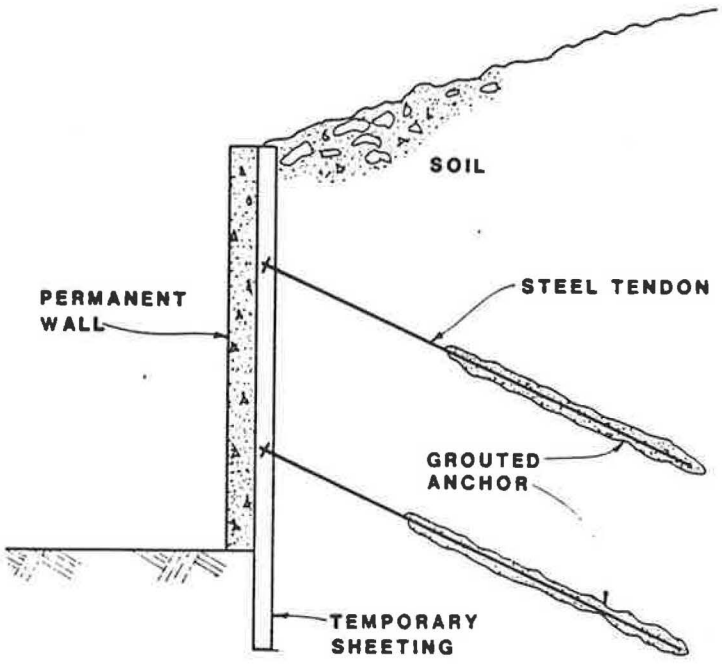

FIGURE 1 Components of a tiedback retaining structure.

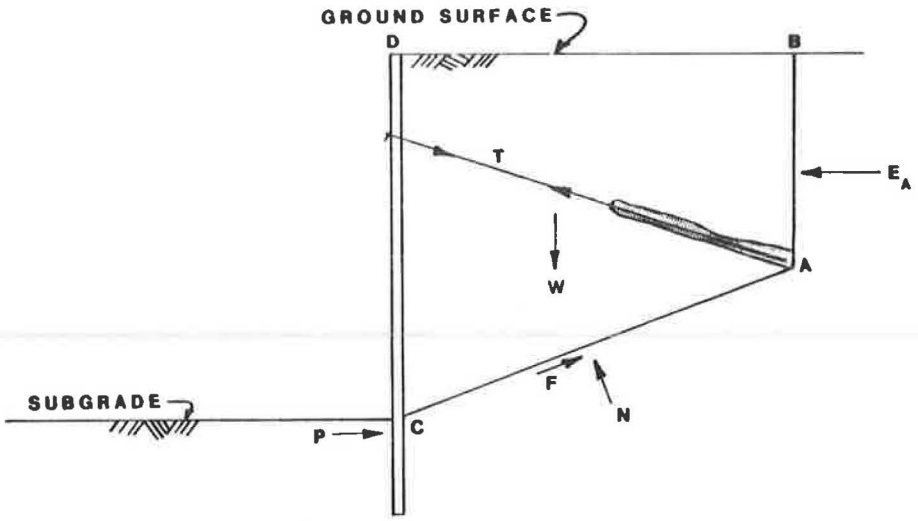

FIGURE 2 Soil mass analyzed for overall stability analysis (*7*).

both internally and externally stable. The shape of the soil mass analyzed for overall stability is often taken to be wedge shaped, as shown in Figure 2. If a tiedback wall is properly designed and the tiebacks have the desired capacity, the pressure on the wall and the tieback will create stabilizing internal forces within this soil mass. The soil-structure-anchor system is then considered to be internally stable.

In addition to ensuring the internal stability of the soil-structure-anchor system, the overall stability of the system must also be checked and a suitable FOS determined. The determination of the FOS for any potential surface that passes behind the ends of the tiebacks is considered a FOS with respect to overall (external) stability (Figure 3*A*), whereas the FOS for any potential failure surface that passes between the ends of the tiebacks and the wall is considered a FOS with respect to internal stability (Figure 3*B*).

If the external stability is insufficient, it may be increased by modifying the tieback geometry. This is usually accomplished by lengthening the tiebacks. Because the loads in the tiebacks are internal forces within the soil mass wedge, they do not increase the overall stability of the system. Increasing the load on the tiebacks or increasing the number of tiebacks will only serve to increase the internal stability of the wedge. Because the cost per tieback increases as the length increases, it is desirable to determine the shortest length of tiebacks, while providing a suitable FOS with respect to external stability.

For the overall stability of the soil-structure-anchor system, the soil mass of Figure 2 is often analyzed. The wedge shape of Figure 2 may be used to expedite hand calculations and is a simplification of the actual conditions. This soil-structure model forms the basis of the Krantz method. The forces tending to displace the soil mass are weight of the soil mass, W, and the earth pressure, E_a, on plane, AB. The earth pressure, E_a, on plane, AB, is usually taken as the active earth pressure, although the at-rest earth pressure condition is sometimes used, (*Z*). The external forces resisting displacement of the soil mass are the tangential and normal forces, F and N, on the failure plane, AC. The failure surface, AC, may not be straight as shown, but may be curved depending on the soil parameters. In addition, if the retaining structure penetrates some distance below the subgrade, passive resistance, P, will be mobilized at the base of the wall. The FOS with respect to overall stability is defined as the ratio of the sum of the resisting forces to the sum of the driving forces. A typical suitable FOS for this type of analysis is 1.5 or greater (*8*).

It is important to stress that the tieback force is an internal force within the wedge and does not affect the external stability of the soil mass. The tieback applies a load to the wall that pushes on the soil. The forces between the wall and the anchor are equal and opposite, which tends to compress the soil.

The Krantz method is based on the soil mass of Figure 2 (*1*). The Krantz method is based on laboratory tests and analyses in which an external pull (force) is applied to the soil wedge. This method requires the calculation of an external force that would be required to displace the soil wedge in which the tiebacks are anchored. The external force is taken as the possible tieback load. This method involves serious errors in the statement of the problem that make it inappropriate for determining the overall stability of anchored structures (*4*). The errors result from the fact that the method assumes that the tiebacks pull on the soil without pushing on the wall. The analysis proposed by Krantz assumes that the tieback force is an external force acting on the soil wedge, whereas the tieback force is actually an internal force in this wedge. The tieback is in tension between the wall and its anchor and is not related to the force required to move the wedge. It is therefore inaccurate to treat the tieback force as an external force acting on the wedge that results in mixing internal and external forces (*4*).

Unfortunately, the Krantz method and others based on this method (*2, 3*) are still used today. In light of the inaccuracies of the methods based on the Krantz method, it is the opinion of the author and of Schnabel (*4*) that this type of analysis should be discontinued in practice because of the errors in the model.

Other Uses and Methods Proposed

Other methods have been proposed *9–11*) that use a wedge-shaped soil mass, but properly consider the tieback force to

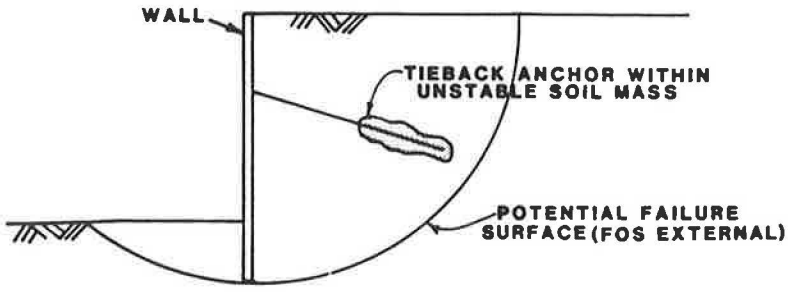

(A) INTERNALLY STABLE BUT EXTERNALLY UNSTABLE SOIL-STRUCTURE-ANCHOR SYSTEM

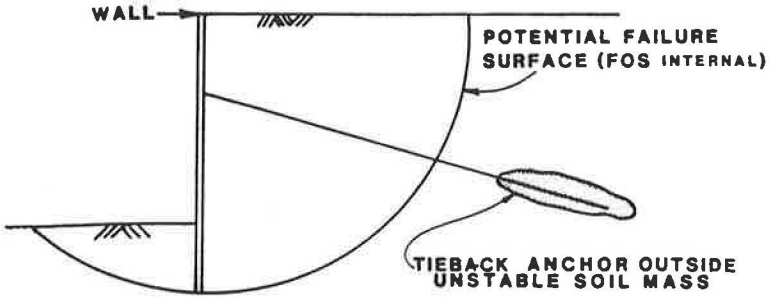

(B) INTERNALLY AND EXTERNALLY STABLE SOIL-STRUCTURE-ANCHOR SYSTEM

FIGURE 3 Modes of tiedback wall stability and instability.

be an internal force within the soil mass. These methods are rather straightforward for homogeneous soil conditions and a single row of tiebacks. However, the hand calculation required for these analyses becomes cumbersome and tedious for multiple rows of tiebacks, layered, or nonhomogeneous soil conditions. In some cases the method is not able to account for these conditions or the definition of the FOS breaks down for purely cohesive soils.

Tiedback retaining structures are frequently used for the control of landslides. These structures, in addition to supporting the soil mass directly behind the structure, must also apply a sufficient resisting force to the sliding mass that it is intended to stabilize. Not only must the tiedback retaining wall, shown in Figure 4, be able to resist the lateral earth-pressure forces produced by the soil mass directly behind the wall (shaded portion), but it must also apply a resisting force sufficient to stabilize the sliding soil mass above the landslide failure surface.

A sliding mass can be stabilized by increasing the resisting forces that act on it, or by decreasing the driving forces.

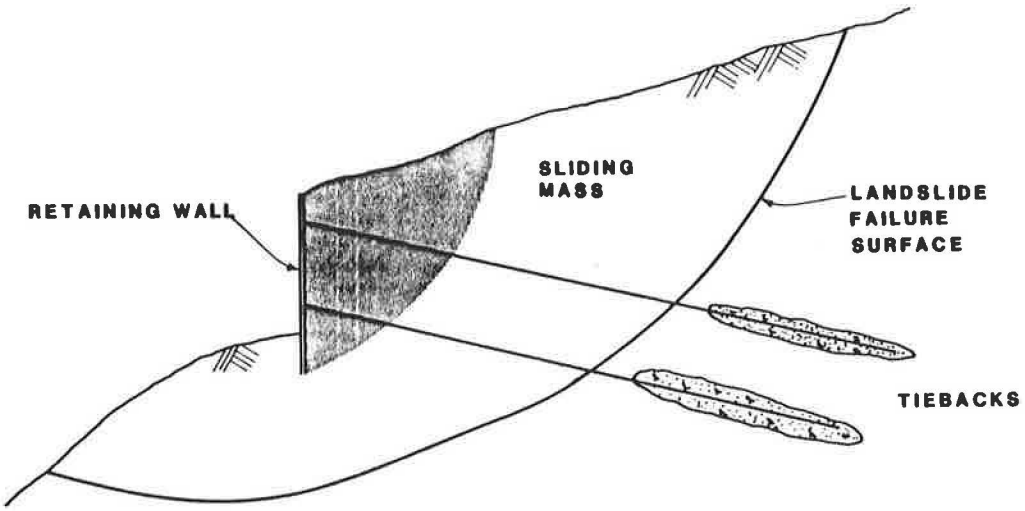

FIGURE 4 Landslide stabilization using tiebacks.

Tiebacks stabilize a sliding soil mass by increasing the resisting forces. Tiebacks can penetrate the sliding surface and apply increased normal and tangential forces to the sliding body. Tiebacks are an excellent tool for stabilizing landslides because they provide a force that acts in nearly an ideal direction for resisting the driving forces, without seriously aggravating the stability of the slope.

It can be seen from Figure 4 that the largest component of the tieback force acts in a horizontal direction. The tiebacks also provide a component of force to the soil mass that increases the normal force on the sliding surface. For soils with frictional characteristics, it can be seen from Equation 1 that by increasing the effective normal force, and hence effective normal stress, N', on the sliding surface, the resistance to sliding at the sliding surface will be increased.

$$S = c' + N' \tan \Phi' \quad (1)$$

where

S = soil shear strength,
c' = effective soil cohesion,
N' = effective normal stress, and
Φ' = effective angle of shearing resistance.

Both components of the tieback force on the failure surface tend to increase the resisting forces on the sliding mass. Any type of stability analysis performed on slopes subjected to tieback loads should consider both components of resistance offered by a tiedback structure for landslide stabilization.

Slope Stability Program Method

Slope stability computer programs based on a limiting equilibrium method of slices are routinely used for determining the stability of slopes and embankments. It is therefore logical to attempt to use such an analysis tool for the determination of the stability of tiedback structures used for landslide control. However, existing limiting equilibrium slope stability computer programs, with the exception of the recent versions of STABL, do not properly account for the presence of tieback loads in the determination of the FOS. This is especially true for the simplified methods of slices, such as the Simplified Bishop method and the Simplified Janbu method, which do not satisfy both force and moment (total) equilibrium (*12, 13*).

When vertical uniform distributed loads are present on the crest of the slope, there are no major drawbacks to using the Simplified Bishop or Janbu methods. However, when using

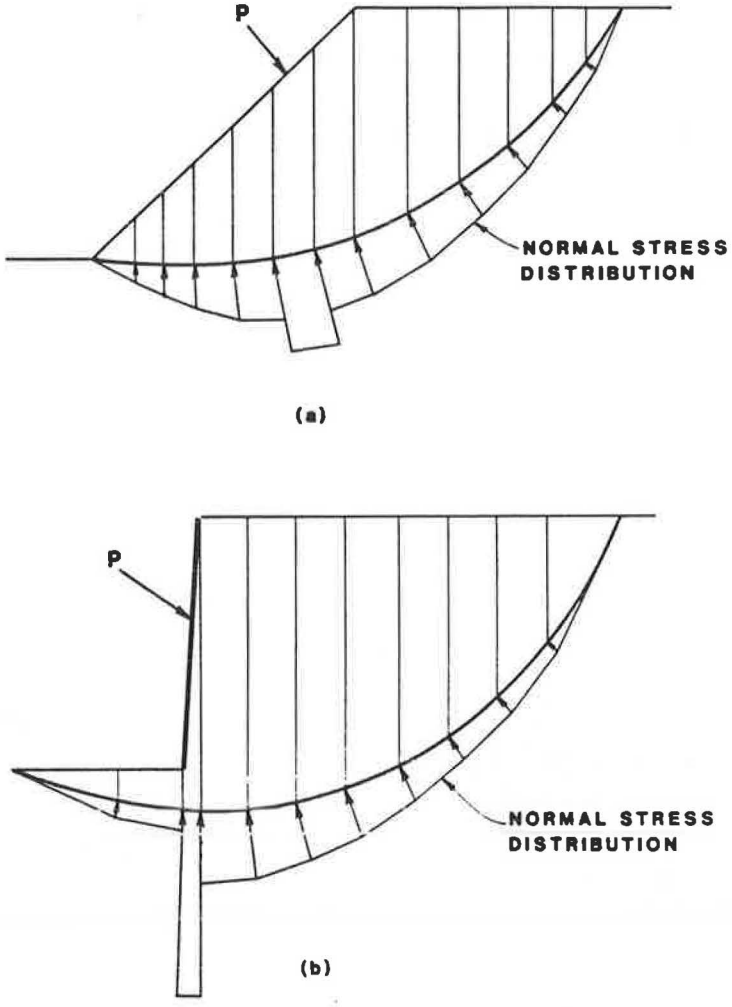

FIGURE 5 Normal stress distribution on failure surface considering a concentrated load.

these methods for near-horizontal and inclined concentrated tieback loads, these methods are inappropriate for the following reasons:

1. The vertical component of an inclined tieback load is taken into account in the numerator of the FOS only on the slice on which it acts. This does not conform to the idea that stresses applied to the ground surface are diffused throughout the soil mass (*14–17*). Shown in Figure 5*A* is the distribution of normal stress on the failure surface caused by the presence of a concentrated load, such as an inclined tieback load, *P*, applied to the face of a slope. It is clear from this figure that the tieback load is only taken into account on the slice on which it acts. The normal stress on this slice is greatly increased, whereas nearby slices remain unaffected. As a result, the soil resistance calculated for the slice on which the tieback load acts (Equation 1) will be extremely high, whereas the soil resistance of nearby slices will remain unchanged by the presence of the tieback load. The result is that the real FOS for the slice on which the tieback load acts will be very high, whereas the FOS of the remaining slices will be unchanged. This problem is especially critical when the width of the slice is small, as is typically true for near-vertical tiedback retaining structures, shown in Figure 5*B*.
2. The horizontal component of a concentrated tieback load is taken into account only in the denominator of the FOS. It will be seen later that the horizontal component of the tieback load produces normal and tangential forces on the base of the slices that contribute to the stability of the slope.
3. A concentrated horizontal load whose line of action passes through the center of rotation will not be taken into account in the FOS determination with the Simplified Bishop method of slices because the moment arm of the load will be zero; hence the resisting moment from such a load will also be zero.

It is apparent from this discussion that the previously available slope stability programs using the simplified methods of slices are not capable of properly accounting for the presence of concentrated loads such as tieback loads. In reality, large compressive stresses, resulting from the presence of a tieback load, are distributed throughout the soil mass to the base of nearly all the slices of the sliding mass. These stresses cause the normal and tangential stresses to be increased on the base of every slice of any failure surface that passes between the tieback anchor and the retaining structure. Any analysis for determining the stability of slopes subjected to tieback loads should consider these increases in stresses at the base of each slice of the sliding mass.

LOAD DISTRIBUTION METHOD: STABL5 AND PCSTABL5

In an attempt to account for the diffusion of compressive stresses throughout a soil mass caused by the presence of tieback loads, the author has developed the LDM, for use with the simplified methods of slices. The LDM was originally programmed in the slope stability computer programs STABL4 and PCSTABL4, and is also contained in the STABL5 and PCSTABL5 programs. The LDM eliminates the drawbacks inherent to computerized slope stability analyses as already discussed. Unlike other slope stability programs, STABL5/PCSTABL5 distributes the force from a concentrated load throughout the soil mass to the whole failure surface and hence to nearly all slices of the sliding mass. STABL5 and PCSTABL5 are the only known limit equilibrium slope stability programs that attempt to account for the distribution of force to the failure surface caused by concentrated boundary loads, such as tieback loads.

The LDM routines in STABL5/PCSTABL5 are applicable to circular and noncircular failure surfaces and are specifically formulated to handle tieback loads, but are also capable of handling other types of loads applied to the ground surface such as strut loads from a braced excavation. A detailed discussion of the derivation of LDM is beyond the scope of this paper. However, the reader may consult Carpenter (*18*) for the complete derivation of the LDM.

Theory

A post-tensioned tieback applies a force to the structure that it supports. This force is developed by the tieback anchor within the soil mass. Because the forces between the wall and the tieback anchor are equal and opposite, they place the soil between the structure and the anchor in compression.

The LDM diffuses the stresses caused by the tieback load to the potential failure surface. This is accomplished by replacing the load applied to the ground surface with a statically equivalent distribution of forces applied to the midpoint of the base of the slices along the potential failure surface. By doing so, the load is distributed to the base of all, or nearly all, of the slices, depending on the slope geometry. The diffusion of stresses within the slope and the increase in forces along the potential failure surface are therefore considered in the determination of the FOS.

The distribution of stresses to the potential failure surface used in the LDM is computed according to Flamant's distribution of stresses through a semi-infinite elastic half-space (*15*), as proposed by Tenier and Morlier (*19*). Flamant's distribution of stresses was adapted to the problem of tiedback slopes and walls because of its simplicity while evaluating and attempting to correct the potential errors associated with applying this method to analysis of tiedback slopes and walls. It is recognized that soils are not necessarily elastic and that tiedback slopes or walls do not necessarily conform to a semi-infinite elastic half space. Although soils do not generally behave as elastic materials, many solutions to the distribution of stresses throughout soils have shown that this approach is practical and reasonable for engineering purposes (*14, 16, 17*). Although Flamant's formula is based on planar stress, it will be seen later that the distribution of stresses obtained using Flamant's distribution of stresses, modified to ensure that the stress distribution obtained is in static equilibrium with the applied tieback load, seems reasonable when compared to finite element studies performed by Tenier and Morlier (*19*).

The primary assumptions used in the formulation of the LDM may be summarized as follows:

1. It is assumed that a linearly elastic half space model may be used to generally describe the slope conditions being analyzed,
2. A uniform line load is assumed to exist horizontally between adjacent tiebacks so that the three-dimensional tieback problem may be analyzed using a two-dimensional analysis, and,

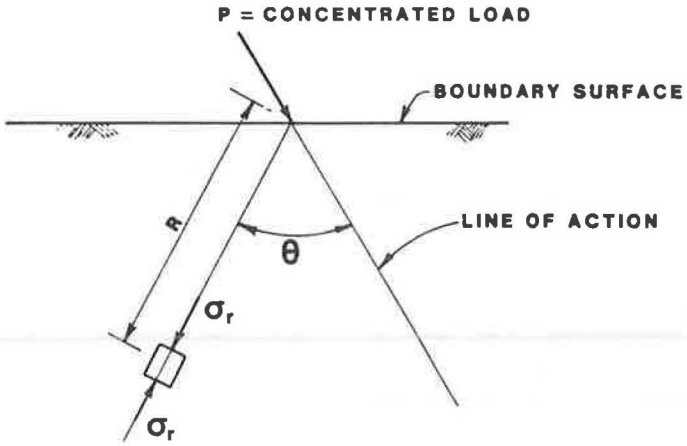

FIGURE 6 Flamant's distribution of stress.

3. The stresses around the grouted anchor are not considered in the analysis.

The significance of these assumptions will be discussed later with respect to the limitations of the analysis.

The distribution of stresses obtained using Flamant's equation is resolved into a distribution of discrete forces acting at the midpoint of the base of the slices. The resulting force distribution is modified so that the distribution of forces along the failure surface is in static equilibrium with the load applied to the ground surface.

According to Flamant (*15*), for a semi-infinite mass subjected to a concentrated load, P, the distribution of stresses is radial and is given (see Figure 6) by:

$$\sigma_r = 2(\mathrm{P})\cos\Phi/(\pi)(R) \times (\text{compression}) \quad (2)$$

where

σ_r = radial stress at a point,
P = concentrated load applied to an elastic half space,
R = distance to the point in question, and
Φ = angle formed by the line of action of the oncentrated load, and the line connecting the point of application of the load on the boundary surface and the point in question.

If the trial failure surface intersects the tendon portion of a row of tiebacks, an equivalent line load is calculated for them. If the trial failure surface passes behind or through the grouted anchor, the tieback load is not considered in the determination of the FOS because the tiebacks are internal to the sliding mass. The individual tieback load, P, for a given row of tiebacks, is divided by the corresponding horizontal spacing, H, between tiebacks. The resulting equivalent line load is designated as TLOAD (Figure 7), and is inclined from the horizontal by an angle, INCLIN.

The author assumes that the replacement of discrete tieback loads by an equivalent line load is valid for tiedback structures because tiebacks are normally closely spaced (horizontally)

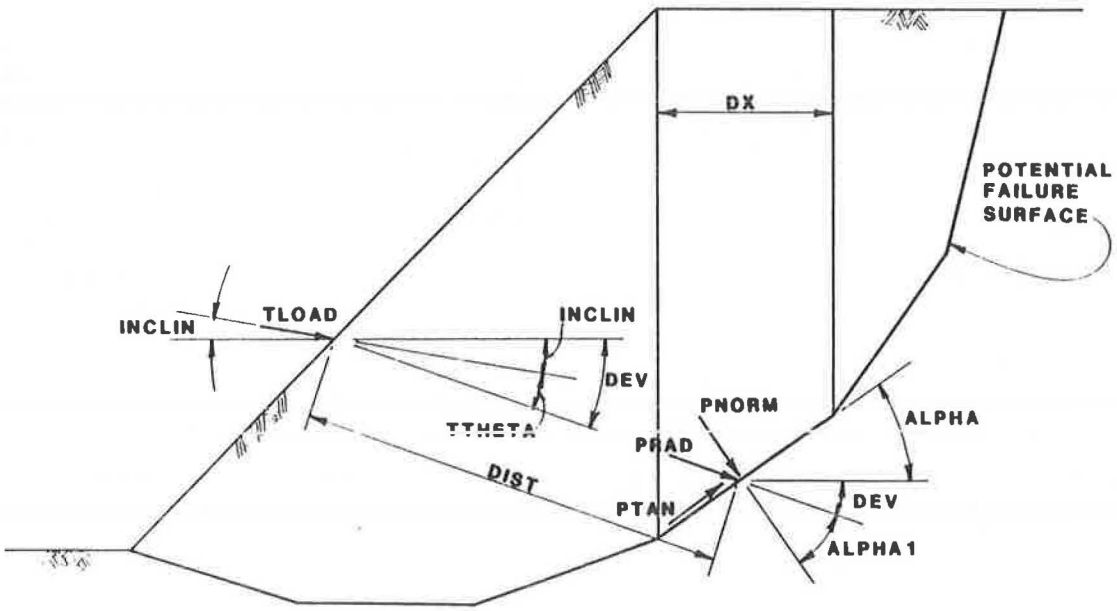

FIGURE 7 Transfer of tieback load to potential failure surface.

and are anchored to horizontal load-bearing elements, such as steel wales that transfer the tieback load to the retaining structure. Based on the assumption of a uniform line load being formed between tiebacks, the LDM neglects any three-dimensional effects that may exist. If horizontal load-bearing members are not present on a tiedback structure, or if the horizontal spacing between tiebacks is large, then this assumption is no longer valid.

The radial stress on the midpoint of the base of a given slice is calculated using Flamant's formula:

$$\sigma_r = 2\,(\text{TLOAD})\cos(\text{TTHETA})/(\pi)\,(\text{DIST}) \qquad (3)$$

where

σ_r = radial stress at the midpoint of the base of the slice,
TLOAD = equivalent tieback line load for a row of tiebacks,
TTHETA = angle formed by the line of action of TLOAD, and the line connecting the point of application of the tieback on the ground surface and the midpoint of the base of the slice,
π = pi, and
DIST = distance between the point of application of TLOAD on the ground surface, and the midpoint of the base of the slice.

The radial force, PRAD, at the midpoint of the base of a slice because of a given tieback load, is calculated by multiplying the radial stress at that point in the soil mass by the length of the base of the slice (*DX*), see Figure 7. Because of slope geometry (i.e., slope is not a semi-infinite half space), location of the tiebacks with respect to the failure surface, and shape of the failure surface, the sum of the radial forces acting at the midpoint of the base of the slices in the direction of the line load is normally not in static equilibrium with the applied load, TLOAD. As a result, a single multiplication factor is applied to the radial forces acting on the base of all the slices so that the sum of these forces is in equilibrium with the applied load. The refined radial force acting on the base of each slice is broken into its components normal and tangential to the base of each slice, PNORM and PTAN, respectively.

The entire process outlined above is repeated for all additional rows of tiebacks. The normal and tangential components of the tieback loads due to all rows of tiebacks are summed on each slice, and it is these forces that are used in the FOS equations.

Distribution of Load to Failure Surface

The distribution of stress (and hence force) to the base of the slices of the sliding mass has been studied in detail to verify the reasonableness of the distributions generated. The following discussion examines the distribution of stresses to the potential failure surface produced by the LDM.

To clearly demonstrate the distribution of normal and tangential stresses (and hence forces) to a failure surface produced by the LDM, a simple 15-ft (4.57-m) high tiedback wall has been chosen as an example (Figure 8). Two different configurations of tiebacks are considered to demonstrate the change in distribution of stress produced along the circular potential failure surface shown with variation in tieback-failure surface geometry.

The wall is shown in Figure 8*A*, subjected to a horizontal tieback load of 25 kips. The 25-kip tieback load is replaced by an equivalent distribution of normal and tangential stresses on the failure surface as computed using the LDM. The distribution of normal stress along the failure surface is smooth and is largest at approximately the midpoint of the failure surface (point *B*).

The same wall is shown in Figure 8*B*, subjected to a tieback load of 25 kips inclined at 30 degrees from the horizontal. The normal stress distribution is similar to that of Figure 8*A*, except that the stress distribution is shifted lower on the failure surface.

Similar distributions are also obtained for tangential stresses. The stresses produced by more than one row of tiebacks are superimposed to produce a combined stress on each slice.

Tenier and Morlier (*19*) obtained similar distributions of normal and tangential stresses. They compared the results of finite element analyses with those obtained using Flamant's distribution of stresses corrected for static equilibrium. The results verified that the distributions of normal and tangential stresses obtained using Flamant's distribution of stresses, corrected for static equilibrium, were in good agreement with those obtained using a finite element model. Tenier and Morlier's analyses were performed on simple slopes subjected to tieback loads with homogeneous elastic soil parameters. The analyses did not consider nonhomogeneous soil conditions, ground water tables, pore pressures, or earthquake loading. STABL5 and PCSTABL5, on the other hand, are capable of handling all the conditions already mentioned.

Load Versus Factor of Safety

One of the prime factors considered in the design of tiedback structures is the determination of the magnitude of the applied load required to ensure stability. The effect of the magnitude of the applied load was investigated for various soil conditions using the soil mass defined by the potential failure surface shown in the simple slope of Figure 9.

The effect of increasing the normal force on the failure surface, through the use of an applied load such as a tieback load, will not increase the mobilized soil resistance for slopes with purely cohesive soil characteristics (Equation 1) because $\Phi = 0$. Therefore, the distribution of the component of an applied load normal to the failure surface will have no effect on the overall stability of the slope. However, the tieback does offer resistance to sliding through the distribution of the component of the tieback load tangential to the potential failure surface.

Demonstrated in Figure 10 is the effect of increasing load on the FOS for three purely cohesive soil strengths for the slope shown in Figure 9. The FOS is observed to increase nearly linearly with an increase in applied load. Note that the increase in FOS is due only to the presence of the components of the load tangential to the potential failure surface.

For slopes with both cohesive and frictional soil strength characteristics, the resistance to sliding will be increased by the distribution of both the normal and tangential components of the applied load acting on the potential failure surface.

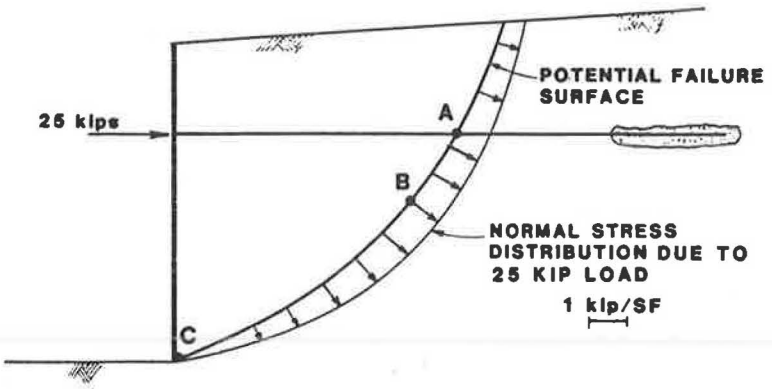

(a) TIEBACK HORIZONTAL

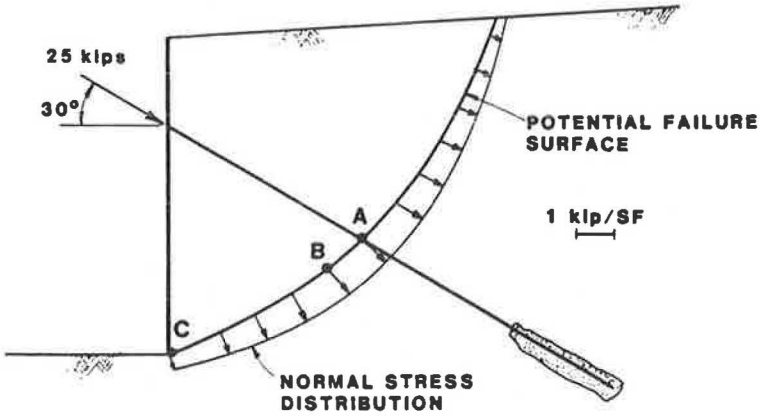

(b) TIEBACK INCLINED AT 30°

FIGURE 8 Slope model for load versus FOS studies.

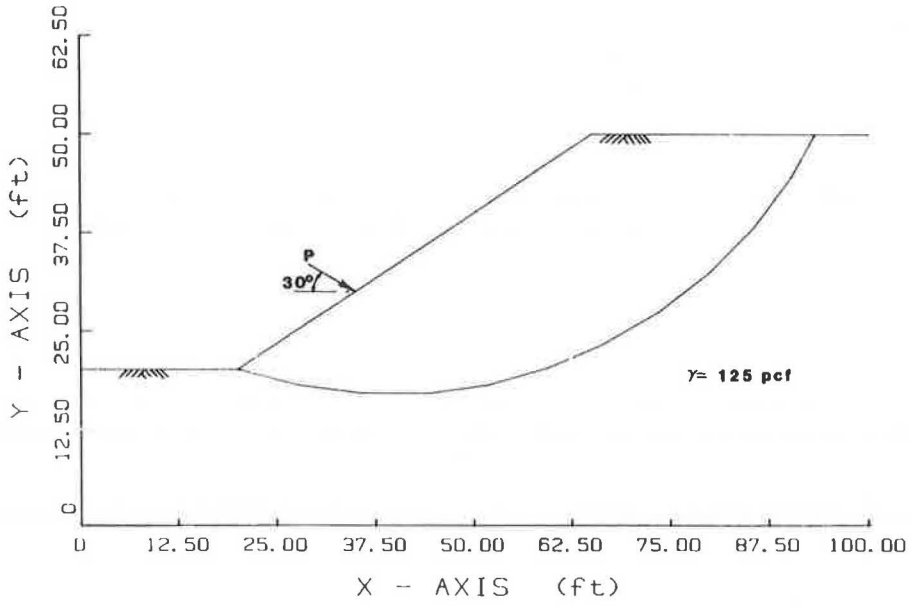

FIGURE 9 Slope model for load versus factor of safety studies.

The results obtained when the slope of Figure 9 was analyzed with three different $c \sim \Phi$ soil strength characteristics are shown in Figure 11.

As with purely cohesive soils, the FOS increases with increasing load. However, the rate of increase (slope of the lines) in FOS with increasing load is greater than that of Figure 10 for purely cohesive soil conditions.

For $c \sim \Phi$ soils, both components of the applied load distributed onto the failure surface act to increase stability. The FOS increases at a faster rate for the slope with $c \sim \Phi$ soil characteristics, because the distribution of the normal component of the load on the failure surface acts to increase the mobilized soil resistance. This resistance is in addition to the resistance offered by the distribution of the tangential component of the load along the failure surface.

Note that at large loads a rather significant increase in FOS is obtained even if the soil has a relatively small Φ value. In addition, inspection of Figures 10 and 11 indicates that the soil strength parameters chosen for stability analysis have a profound effect on the FOS. As in any stability analysis, the choice of soil strength parameters is one of the most critical factors affecting the FOS obtained (*20*).

Limitations

The use of STABL5 and PCSTABL5 for the analysis of the stability of tiedback slopes and walls is limited to those problems that lend themselves to the assumption that a uniform line load may be assumed to exist horizontally between tiebacks. Where this assumption is not valid, other methods of analysis may be more appropriate.

The analysis of the stability of tiedback structures using the LDM is appropriate in cases in which the overall slope may be generally modeled as a semi-infinite half space.

The LDM does not take into account the relative stiffness of individual soil layers because it is based on a solution of stress distribution through a homogeneous elastic half space. Hence, with the LDM, the stresses distributed to the potential failure surface are independent of the deformation characteristics of the soil profile. In other words, the load from a tieback will be distributed to a potential failure surface in the same way for both a homogeneous soil profile and a layered soil profile. This limitation is not significant for most layered soil profiles whose individual soil layers do not have grossly different stiffness characteristics. However, this limitation may be more significant for soil profiles that have grossly different soil layer stiffness characteristics. This topic is worthy of further investigation.

It is important to note that limiting equilibrium slope stability methods, as used in the STABL programs, do not consider displacements of the soil mass or the tiebacks. Displacements may result in increased loads on the tiebacks and reduced soil resistance.

Given the limitations already discussed, along with the assumptions used in the development of the LDM, the reasonableness of any solution provided by STABL or any other computer-generated solution must be judged by the engineer to ensure that the conditions analyzed are modeled properly, and that the solution obtained is reasonable.

The analysis of the stability of a tiedback structure is just one of many design considerations in the design of a tiedback retaining structure. STABL is only one tool for performing the stability calculations. Other considerations in the analysis

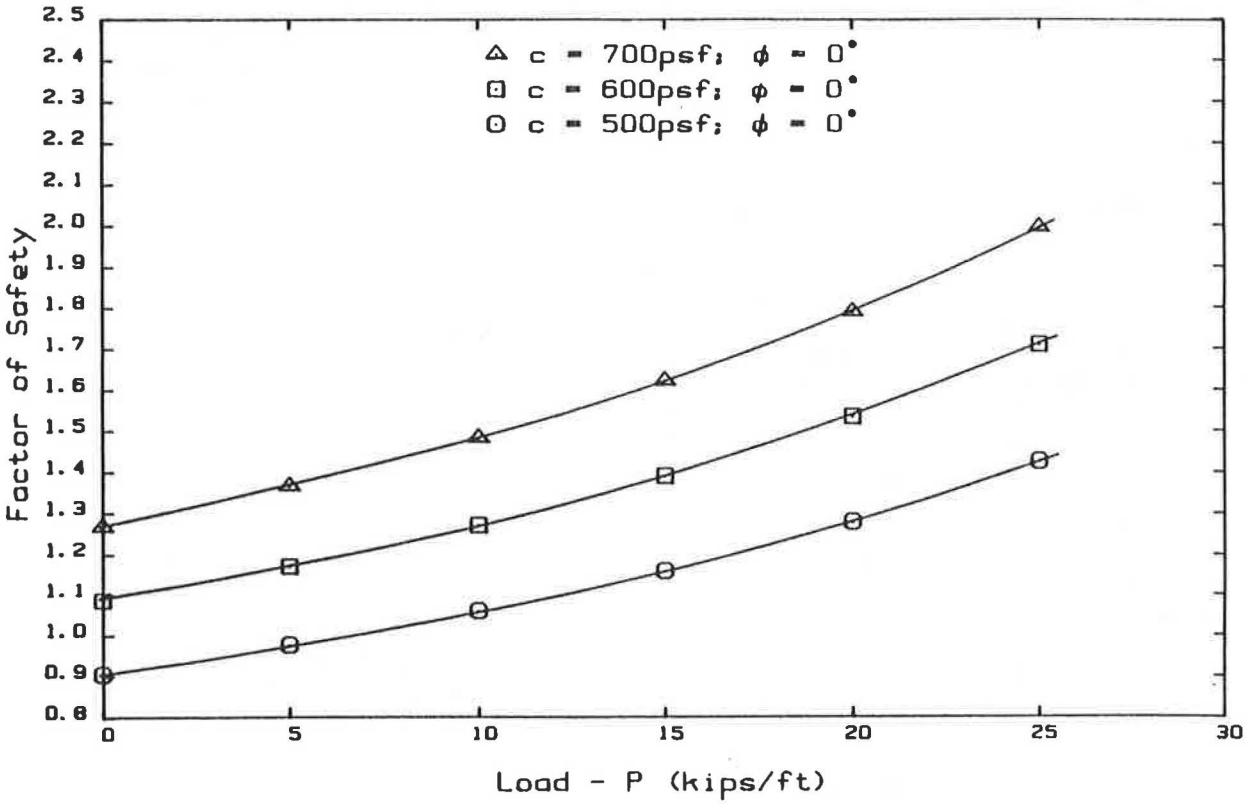

FIGURE 10 Load versus FOS for purely cohesive soil slopes.

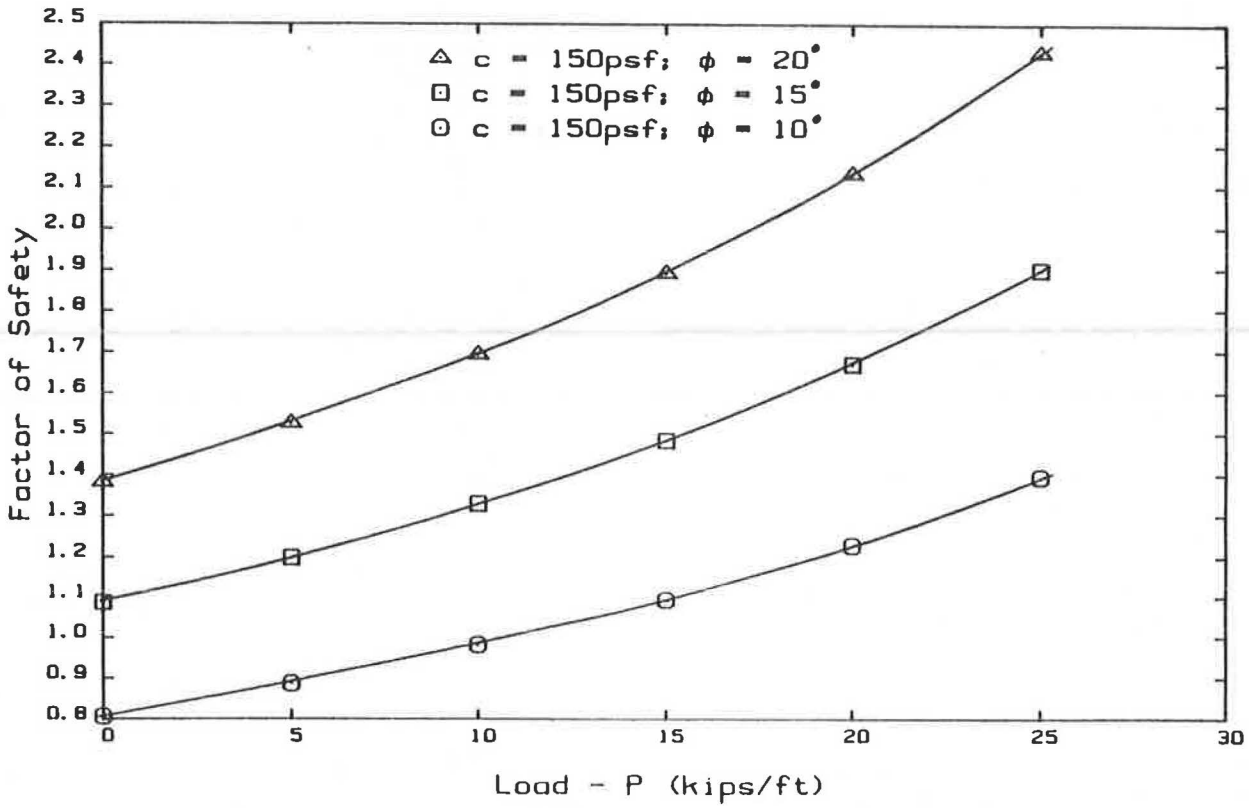

FIGURE 11 Load versus FOS for $c \sim \Phi$ soil slopes.

and design of tiedback structures must be designed and analyzed separately.

For a detailed discussion of the development and limitations of the LDM, the reader is encouraged to consult Carpenter (*18*).

SUMMARY

The purpose of this study was to develop a rational and convenient method of assessing the internal and overall stability of tiedback and anchored retaining structures. Such a method has been developed by the author in the LDM and is contained in the slope stability programs STABL5 and PCSTABL5. The LDM was developed for the analysis of tiedback slopes and walls for use with the simplified methods of slices. The programs contain routines that consider multiple rows of tiebacks, multiple tiedback structures as well as individual tieback loads, tieback inclination, horizontal spacing between tiebacks, and the length of individual tiebacks. The STABL programs are the only known slope stability programs that specifically consider the effect of tiebacks on the stability of tiedback slopes and walls.

Previously available methods for determining the overall stability of tiedback structures were reviewed and the usefulness and limitations of these methods were discussed. Parametric studies were performed during the development of the LDM to determine the reasonableness of applying the assumptions used in the method of solution to tiedback slopes and retaining walls. In addition, the effect of tieback load on the FOS was presented for several different soil conditions. These studies revealed that the method generally gives reasonable results. However, recognizing that a semi-infinite elastic half space model is assumed to generally apply to the problem of tiedback structures, and that a two-dimensional analysis is used to model a three-dimensional problem, a conservative approach should be used in selecting the minimum required FOS for tiedback slopes and walls using the LDM.

CONCLUSIONS

1. The LDM as programmed in STABL5 and PCSTABL5 programs is a useful tool for analyzing the overall stability of tiedback retaining structures for support of excavations or for slope stabilization. The method generally gives good results, but it is important to recognize what assumptions are used in the analysis and how these assumptions relate to the limitations of analyzing the stability of tiedback structures.

2. Analysis of the stability of tiedback structures is a complex problem and the stability of these structures is influenced by, but not limited to (a) the lateral earth pressure behind the wall; (b) the deformation of the soil-structure system; (c) tieback characteristics (individual tieback loads, inclination, horizontal spacing, overall length, size of anchor, method of construction); and (d) soil characteristics. The analysis of tiedback structures is further complicated by the fact that a two-dimensional model is used to model a three-dimensional problem. Recognizing that assumptions concerning these items are required and that assumptions concerning the distribution of loads are introduced into the calculation of the FOS using the LDM for tiedback slopes and walls, a conservative approach

should be used in selecting the minimum required FOS for tiedback slopes and walls.

3. The LDM is preferred over existing methods based on the Krantz method for analysis of the stability of tiedback structures because the LDM does not mix internal and external forces within the soil mass analyzed. It is the author's opinion that methods based on the Krantz method should be discontinued because such methods involve serious errors in the problem statement.

4. The reasonableness of any solution provided by STABL, or any other computer-generated solution, must be judged by the engineer to ensure that the conditions analyzed are modeled properly, and that the solution obtained is reasonable.

5. The soil parameters used in the analysis of the stability of slopes have a profound effect on the FOS. It was found that for a relatively small change in the soil parameters input, a relatively large change in the calculated FOS was obtained. Therefore, the results obtained from any stability analysis are only as reliable as the data input in the analysis.

ACKNOWLEDGMENTS

The author's sincere thanks and appreciation are extended to C. W. Lovell, Jean-Lou Chameau and Milton Harr for their helpful suggestions, guidance, and support during the preparation of this research at Purdue University.

Thanks are also expressed to Thomas C. Anderson and David E. Weatherby of the Schnabel Foundation Company for their practical suggestions concerning tiedback structures and for providing several case histories on the performance of tiedback walls and slopes.

The financial support for this research project was provided by the Federal Highway Administration and the Indiana Department of Highways through the Joint Highway Research Project, Purdue University, West Lafayette, Indiana.

REFERENCES

1. E. Krantz. *Über die Verankerunz von Soundwande*, 2nd ed. Wilhelm Ernst and Son, Berlin, Federal Republic of Germany, 1953.
2. A. Ranke and H. Ostermayer. Beitrag zur Stabilitätsuntersuchung mehrfach verankerter Baugrubenumschliebungen. (A Contribution to the Stability Calculations of Multiple Tiedback Walls.) *Die Bautechnik*, Vol. 45, No. 10, 1968, pp. 341–349.
3. *French Code of Practice*. Recommandation concernant la conception, le calcul, l'exécution, et le control des tirants d'ancrage. Recommandation T.A. 72, Bureau Securitas, lst ed., Paris, France, 1972.
4. H. Schnabel, Jr. Discussion: Overall Stability of Anchored Retaining Walls. *Journal of the Geotechnical Engineering Division*, ASCE, GT Vol. 110, No. 12, Dec. 1984, pp. 1817–1818.
5. J. R. Carpenter. *PCSTABL4 User Manual*. Joint Highway Research Project JHRP-85-7, School of Civil Engineering, Purdue University, West Lafayette, Ind., May 1985.
6. C. W. Lovell, S. S. Sharma, and J. R. Carpenter. *Introduction to Slope Stability Analysis with STABL4*. Internal Report (formerly Joint Highway Research Project JHRP-84-19), Purdue University, West Lafayette, Ind., Jan. 25, 1985.
7. H. Schnabel, Jr. *Tiebacks In Foundation Engineering and Construction*. McGraw-Hill Book Company, New York, 1982.
8. W. F. Anderson, T. H. Hanna, and M. N. Abdel-Malek. Overall Stability of Anchored Retaining Walls, *Journal of the Geotechnical Engineering Division*, ASCE, GT Vol. 109, No. 11, Nov. 1983, pp. 1416–1433.
9. B. B. Broms. Swedish Tie-Back Anchor System for Sheetpile Walls. In *Proc., 3rd Budapest Conference on Soil Mechanics and Foundation Engineering*, Hungary, 1968, pp. 391–403.
10. G. S. Littlejohn. Anchored Diaphragm Walls in Sand-Anchor Design. *Ground Engineering*, Vol. 5, No. 1, 1972, pp. 12–17.
11. H. Ostermayer. *Practice in the Detail Design Applications of Anchorages, A Review of Diaphragm Walls*. Institution of Civil Engineers, London, England, 1977, pp. 55–61.
12. A. W. Bishop. The Use of Slip Circles in the Stability Analysis of Slopes. *Geotechnique*, Vol. 5, No. 1, March 1955, pp. 7–17.
13. N. Janbu. Application of Composite Slip Surfaces for Stability Analysis. In *Proc., European Conference on Stability of Earth Slopes*, Stockholm, Sweden, Vol. 3, 1954, pp. 43–49.
14. M. J. Boussinesq. *Application des potentiels, à l'étude de l'équilibre et du mouvement des solides élastiques*. Gauthier-Villars, Paris, France, 1885.
15. A. Flamant. *Stabilité des constructions: résistance des materiaux*. Paris, France, 1886.
16. N. M. Newmark. Influence Charts for Computation of Stresses in Elastic Foundations. University of Illinois Engineering Experiment Station, Bulletin 338, University of Illinois, Urbana, 1942.
17. G. Y. Baladi. *Distribution of Stresses and Displacements Within and Under Long Elastic and Viscoelastic Embankments*. Ph.D. dissertation, Purdue University, West Lafayette, Ind., 1968.
18. J. R. Carpenter. *Slope Stability Analysis Considering Tiebacks and Other Concentrated Loads*. Joint Highway Research Project JHRP 86-21, Purdue University, West Lafayette, Ind., Dec. 1986.
19. P. Tenier and P. Morlier. Influence des surcharges concentrées sur la stabilité des talus. (Influence of Concentrated Loads on Slope Stability.) *Canadian Geotechnical Journal*, Vol. 19, Feb. 1982, pp. 396–400.
20. E. Boutrup. *Computerized Slope Stability Analysis for Indiana Highways*. Masters thesis, Purdue University, West Lafayette, Ind., 1977.

Publication of this paper sponsored by Committee on Transportation Earthworks.